DEVELOPMENT OF A NOVEL *IN VITRO* 3D OSTEOCYTE-OSTEOBLAST CO-CULTURE MODEL TO INVESTIGATE MECHANICALLY-INDUCED SIGNALLING

MARISOL VAZQUEZ

PhD

2013

DECLARATION

This work has not been submitted in substance for any other degree or award at this or any other university or place of learning, nor is being submitted concurrently in candidature for any degree or other award.

Signed ……(candidate) Date …….

STATEMENT 1

This thesis is being submitted in partial fulfillment of the requirements for the degree of PhD.

Signed ……(candidate) Date …….

STATEMENT 2

This thesis is the result of my own independent work/investigation, except where otherwise stated.
Other sources are acknowledged by explicit references. The views expressed are my own.

Signed ……(candidate) Date …….

STATEMENT 3

I hereby give consent for my thesis, if accepted, to be available for photocopying and for inter-library loan, and for the title and summary to be made available to outside organisations.

Signed ……(candidate) Date …….

STATEMENT 4: PREVIOUSLY APPROVED BAR ON ACCESS

I hereby give consent for my thesis, if accepted, to be available for photocopying and for inter-library loans **after expiry of a bar on access previously approved by the Academic Standards & Quality Committee.**

Signed ……(candidate) Date …….

John Wiley & Sons, Inc. DECLARATION

Permission was granted for the use of figures from (Tortora and Derrickson, 2006) to the usual acknowledgements (author, title, and copyright [year and owner]).

Any third party material is expressly excluded from this permission. If any of the material appears with credit to another source, authorization from that source must be obtained.

This permission does not include the right to grant others permission to photocopy or otherwise reproduce this material except for accessible versions made by non-profit organizations serving the blind, visually impaired and other persons with print disabilities (VIPs).

ACKNOWLEDGEMENTS

Without a doubt completing my PhD has been the biggest challenge of the first 26 years of my life. Many ups and downs occurred along the way which were shared with many people, all of which I will always cherish and be thankful to.

First of all in the long list of 'thank you' are Arthritis Research UK and Cardiff University for funding my PhD, and my three supervisors, or how I like to call them, the three brains. Deborah Mason, my principal supervisor, who provided the vision, encouragement and support I needed to complete my degree. I deeply thank Debbie for pushing me to my limits and out of my comfort zone, and for her unwavering belief that I could take on every challenge no matter how big or small. Bronwen Evans, who stimulated thought provoking critical analysis of the data I produced testing the strength of each experiment. I am very grateful to Bronwen for welcoming me to her lab whenever I needed a chat or carry out experiments, and for teaching me to be critical of my work. Daniela Riccardi, my PhD agony aunt, whose door was always open for me whether it was to share the happiness of my successes or break down in tears when science got the best of me. Dani always provided me with straight forward advice and thanks to her I started believing in myself and what I could achieve. Debbie, Bronwen and Dani have made me the strong and determined person I am today.

My second debt of gratitude goes to Vic Duance, Sophie Gilbert, Emma Blain, Karen Brakspear, Yadan Zhang, Emma Mead and Aisha Al-Sabah, for giving me infinite scientific and personal advice as well as edible treats when I needed them the most. I could not have done it without you. I am especially thankful to Cleo Bonnet, my lab older sister, who has always been there for me. We laughed, cried and argued but we always had each other and I will never forget that. I also thank members of the Evans, Archer and Caterson labs, for the advice, chat and even the odd lab reagent or table-tennis match they have given me throughout my PhD.

Special thanks go to Lynda Bonewald for the provision of the MLO-Y4 cells, Carole Elford for her cell culture expertise, Jim Ralphs for the imaging and immunostaining help, Martin Schepelmann for his CaSR immunostaining skills, Tony Hayes and Marc Isaacs for the confocal imaging support; Sam Evans, John McCrory and Hayley Wyatt for their engineering assistance; Tom Davies, for his contribution to cloning and his witty and warm-hearted friendship; and to Jack Ham, who has been my scientific mentor from the very start, for the provision of the adenosine receptors antibodies.

During my PhD I discovered my love for higher education teaching. I owe this to the support of Beatrix Fahnert and Peter Kille who kindly allowed me to demonstrate in their undergraduate practicals; and to the students, who always made me smile with their questions. In particular, I am thankful to those students who through the turns of life became my friends and made my PhD experience that little bit extra special.

Thanks also go to all the members of Cardiff Institute of Tissue Engineering and Repair for giving me the opportunity to get involved in public engagement; to the Cardiff University Hockey Club, especially my hockey girls, who unknowingly helped me cope with the worries and stresses of my PhD by just playing hockey with me; and to all my family and friends in the UK and in Argentina, who have always encouraged me when I needed it the most, even from the other side of the pond.

Last, but certainly not least, I thank my parents, my step-dad Martin and my mum Isabel, who gave me unconditional love and financial support. My parents, in particular my mum, have been my driving force throughout my PhD making sure I only ever had to focus on my studies by feeding me and exempting me of house chores, being patient with me during the occasional (!) break down, being the practise audience to the talks I prepared, encouraging me to take control of and solve any problems encountered, and most of all by being proud of all my achievements.

If I had to pick one accomplishment from my PhD it would be being resilient when faced with adversity, something I was not when I started and I am still learning to be.

To everyone: I DID IT!!!

ABSTRACT

Normal mechanical loading potently induces bone formation mediated by osteocyte effects on osteoblasts. Current *in vitro* bone models do not reflect these cellular interactions, either focusing on mechanical loading of osteoblasts in monolayers or in 3D and therefore not elucidating the osteocyte-osteoblast interactions that regulate mechanically-induced bone formation. Adenosine, calcium-sensing and glutamate signalling have been shown to influence bone biology, with both adenosine precursors and glutamate having been implicated in mechanotransduction. The aims were to develop a novel *in vitro* 3D co-culture model of bone to investigate mechanically-induced signalling, and to determine the expression of adenosine, calcium-sensing and glutamate signalling components within the 3D model and their contribution to the regulation of mechanically-induced bone formation markers.

A 3D model was developed as a two-phase culture system where MLO-Y4 osteocytes were embedded within type I collagen gels and MC3T3-E1osteoblasts were layered on top. In this model, cells were viable over 7 days (100 % osteoblasts, 87 % osteocytes), maintained appropriate morphology and contacted neighbouring cells through CX43 labelled projections. RT-qPCR revealed Runx2, OCN and E11 mRNA expression in both osteoblasts and osteocytes. COL1A1 mRNA expression was significantly higher in the osteoblasts (*P=0.0001*), whereas ALP mRNA was higher in the osteocytes (*P=0.001*). RT-PCR revealed expression of adenosine receptors A_{2A} and A_{2B} and glutamate transporter GLAST1 in osteoblasts and osteocytes, as well as glutamate receptors AMPAR2 and KA1 in osteocytes. Immunostaining confirmed expression of A_{2A}, GLAST1 and KA1, and revealed expression of CaSR, in both osteoblasts and osteocytes.

A novel mechanical loading device was developed which was used to apply osteogenic loads (5 min, 10 Hz, 2.5 N) to 3D osteocyte mono-cultures and 3D osteocyte-osteoblast co-cultures. A minimum of 48 hr pre-load time was required for a reliable load response. 3D osteocyte mono-cultures cultured for 48-72 hr or 7 days pre-load, remained viable, significantly increased PGE_2 0.5 hr after load (48-72 hr: *P=0.0249*, 7 days: *P=0.041*) and decreased their IL-6 synthesis. RT-qPCR revealed a load-induced decrease in E11 (*P=0.018*) and RANKL (*P=0.0486*) mRNA, in 48-72 hr cultures. In 7 day cultures, E11 mRNA (*P=0.041*) increased as a result of loading. Preliminary data showed that the same loading conditions increased PINP synthesis, a bone formation marker, in 3D co-cultures (*P=0.022*). The AMPA/KA receptors antagonist NBQX increased PINP synthesis by 2-fold over 5 days, similar levels induced by loading in untreated cultures, suggesting that NBQX has similar anabolic effects as mechanical stimuli. Similarly, the A_{2A} receptor antagonist SCH 442416 increased osteoblast ALP mRNA expression by 3.5-fold at day 1 post-load and increased PINP synthesis by 1.9-fold, in co-cultures after 5 days.

This 3D osteocyte-osteoblast co-culture model represents a useful *in vitro* model for the investigation of the osteocyte-osteoblast interactions that lead to mechanically-induced signalling and regulation of bone formation markers. Adenosine, calcium-sensing and glutamate signalling components are expressed within the model, facilitating future investigations of their roles in mechanically-induced signalling. Preliminary experiments indicated that adenosine and glutamate signalling may each contribute individually to the regulation of mechanically-induced bone formation markers.

ABBREVIATIONS

$[Ca^{2+}]_o$	Extracellular calcium concentration
$[cAMP]_i$	Intracellular cyclic adenosine mono-phosphate concentration
$[MgCl_2]$	Magnesium chloride concentration
[Primer]	Primer concentration
18S rRNA	18S ribosomal ribonucleic acid
2D	Two-dimensional
3D	Three-dimensional
A_1	Adenosine receptor 1
A_{2A}	Adenosine receptor 2A
A_{2B}	Adenosine receptor 2B
A_3	Adenosine receptor 3
AC	Adenylate cyclase
ALP	Alkaline phosphatase
AMPA	2-amino-3-(3-hydroxy-5-methyl-isoxazol-4-yl)propanoic acid
ANOVA	Analysis of variance
ASBMR	American Society for Bone and Mineral Research
ATP	Adenosine tri-phosphate
BD	Becton Dickinson
BLAST	Basic Local Alignment Search Tool
BMP2	Bone morphogenetic protein 2
BMSCs	Bone marrow stromal cells
BMU	Basic multicellular unit
bp	Base pair
BRMs	Biological response modifiers
BSA	Bovine serum albumin
BSP	Bone sialoprotein
cAMP	Cyclic adenosine mono-phosphate
CaSR	Calcium sensing receptor
CD44	Cluster of differentiation 44
cDNA	Complementary deoxyribonucleic acid
CH_3COONa	Sodium acetate
CNS	Central nervous system
COL1A1	Type I collagen (mRNA)
ColI	Type I collagen (protein)
COX-2	Cyclooxygenase-2
CREB	Cyclic adenosine mono-phosphate response element-binding
Ct	Cycle threshold
CTS	Contents are trade secret
CV	Caudal vertebra
CX43	Connexin 43
DAB	3,3'-Diaminobenzidine
DAPI	4',6-diamidino-2-phenylindole
DEPC	Diethylpyrocarbonate
DFBS	Dialysed fetal bovine serum
dH_2O	Distilled water
DIC	Digital image correlation
DMARDs	Disease-modifying antirheumatic drugs

DMEM	Dulbecco's Modified Eagle Medium
DMP1	Dentin matrix protein 1
DNA	Deoxyribonucleic acid
Dnase	Deoxyribonuclease
dNTP	Deoxyribonucleotide tri-phosphate
DTT	Dithiothreitol
DZ	Deep zone
E. coli	*Escherichia coli*
EAAC	Excitatory amino acid carrier
EAAT	Excitatory amino acid transporter
ECM	Extracellular matrix
EDTA	Ethylenediaminetetraacetic acid
EIA	Enzyme immunoassay
ELISA	Enzyme-linked immunosorbent assay
$Em_{(max)}$	$Emmision_{(max)}$
ERK	Extracellular signal-regulated kinases
$Ex_{(max)}$	$Excitation_{(max)}$
FBS	Fetal bovine serum
FDA	Food and Drug Administration
FGF23	Fibroblast growth factor 23
GAPDH	Glyceraldehyde 3-phosphate dehydrogenase
GLAST1	Glutamate aspartate transporter 1
GLM	General linear model
GM	Genetically modified
GOI	Gene of interest
H_2SO_4	Sulphuric acid
HCl	Hydrochloric acid
HIFBS	Heat inactivated fetal bovine serum
HINCS	Heat inactivated newborn calf Serum
HPOBs	Human primary osteoblasts
HPRT1	Hypoxanthine-guanine phosphoribosyltransferase 1
hr	Hour(s)
HRP	Horseradish peroxidase
IGF-1	Insulin growth factor 1
IgG	Immunoglobulin G
iGluR	Ionotropic glutamate receptor
IL-1	Interleukin-1
IL-6	Interleukin-6
IP_3	Inositol tri-phosphate
IPTG	Isopropyl β-D-1-thiogalactopyranoside
KA	Kainate
KO	Knockout
LB	Lysogeny broth
LCS	Lacunocanalicular system
LDH	Lactate dehydrogenase
LRP5/6	Low-density lipoprotein receptor-related protein 5
MAPK	Mitogen-activated protein kinase
M-CSF	Macrophage-colony stimulating factor
MEM	Minimum Essential Medium
MEPE	Matrix extracellular phosphoglycoprotein

MES	Minimum effective strain
mGluR	Metabotropic glutamate receptor
min	Minute(s)
MIQE	Minimum Information for Publication of Quantitative Real-Time PCR Experiments
mRNA	Messenger ribonucleic acid
MSC	Mesenchymal stem cells
n	Number of experimental replicates
$NaHCO_3$	Sodium bicarbonate
nBLAST	Nucleotide Basic Local Alignment Search Tool
NBQX	2,3-dihydroxy-6-nitro-7-sulfamoyl-benzo[f]quinoxaline-2,3-dione
NCBI	National Centre for Biotechnology Information
NCS	Newborn calf serum
NFκB	Nuclear factor kappa-light-chain-enhancer of activated B cells
NH_4Cl	Ammonium chloride
NHBCs	Normal human-derived bone cells
NI	Not investigated
NMDA	N-methyl-D-aspartate
NO	Nitric oxide
NSAIDs	Non-steroidal anti-inflammatory drugs
NSB	Non-specific binding
o/n	Overnight
OA	Osteoarthritis
OCN	Osteocalcin
OCT	Optimal cutting temperature
ON	Osteonectin
OPG	Osteoprotegerin
OPN	Osteopontin
PBS	Phosphate buffered saline
PBST	Phosphate buffered saline with tween
PCR	Polymerase chain reaction
PenStrep	Penicillin-streptomycin
PFA	Paraformaldehyde
PGE_2	Prostaglandin E2
Phalloidin-Atto488	Phalloidin conjugated to Atto488
PHEX	Phosphate-regulating gene with homologies to endopeptidases on the X chromosome
PI3K	Phosphoinositide 3-kinase
PINP	Pro-collagen type I N-terminal pro-peptide
PKA	Protein kinase A
PKB/Akt	Protein kinase B
PKC	Protein kinase C
PLC	Phospholipase C
pNPP	p-Nitrophenyl phosphate
PTH	Parathyroid hormone
PVC	Polyvinyl chloride
qPCR	Quantitative polymerase chain reaction
RA	Rheumatoid arthritis
RANKL	Receptor activator of nuclear factor kappa-B ligand

REU	Relative expression units
RG	Reference gene
rhPTH1-34	Recombinant human parathyroid hormone 1-34
RNA	Ribonucleic acid
Rnase	Ribonuclease
rpm	Revolutions per minute
rt	Room temperature
RT	Reverse transcriptase
RT-PCR	Reverse transcriptase - polymerase chain reaction
RT-qPCR	Reverse transcriptase - quantitative polymerase chain reaction
Runx2	Runt-related transcription factor 2
SCH 442416	2-(2-furyl)-7-[3-(4-methoxyphenyl)propyl]-7H-pyrazolo[4,3-e][1,2,4]triazolo[1,5-c]pyrimidin-5-amine
sec	Second(s)
SEM	Standard error of the mean
SERMs	Selective estrogen receptor modulators
SOC	Super optimal broth with catabolite repression
SOST	Sclerostin
STDEV	Standard deviation
SV40	Simian vacuolating virus 40
SZ	Surface zone
TBE	Tris/Borate/EDTA
TGF-β	Transforming growth factor beta
Tm	Temperature
TMB	Tetramethylbenzidine
TNF	Tumour necrosis factor
TRAP	Tartrate resistant acid phosphatase
UK	United Kingdom
UV	Ultraviolet
VGLUT	Vesicular glutamate transporter
VSMCs	Vascular smooth muscle cells
Wnt	Wingless related integration site
X-Gal	X-Galactosidase
αMEM	Alpha minimum essential medium
ΔCt	Delta cycle threshold
ΔΔCt	Delta-delta cycle threshold
με	Microstrain

LIST OF FIGURES

LIST OF TABLES

CHAPTER 1

INTRODUCTION

1. Introduction

1.1 Bone structure

The mature human skeleton has 213 bones, excluding sesamoid bones (bones within a tendon, e.g. patella). Bones are composed of a hard outer-layer of cortical bone (80%) and a spongy inner layer of trabecular bone (20%) (Standring, 2004). Cortical bone is found in external bone surfaces and in the diaphysis (Figure 1.1A), whereas trabecular bone is found in the marrow space and in the epiphysis (Figure 1.1A). However, the molecular and cellular composition of cortical and trabecular bone are the same (White and Folkens, 1999, Clarke, 2008).

Cortical bone contains osteons (Figure 1.1B) (Bourne, 1972), each composed of concentric circles or lamellae of bone matrix (Figure 1.1B). Between lamellae, small cavities called lacunae (Figure 1.1B) contain osteocytes, and minute fluid-filled passageways known as canaliculi (Figure 1.1B), extend from one lacuna to another and from the Harvesian canal to each lacuna. This allows cells in the mineralised matrix to communicate and undergo nutrient/waste exchange (Bourne, 1972, White and Folkens, 1999). Harvesian canals are hollow channels within osteons through which blood and lymph vessels, together with nerve fibres, pass. Smaller Volkmann canals link osteons and supply nutrients to all cells (White and Folkens, 1999), running perpendicular to the sheath of connective tissue covering the outer bone surface (periosteum) (Figure 1.1A and B), and the cellular membrane covering the inner bone surface (endosteum) (Figure 1.1A) (White and Folkens, 1999, Standring, 2004, Clarke, 2008).

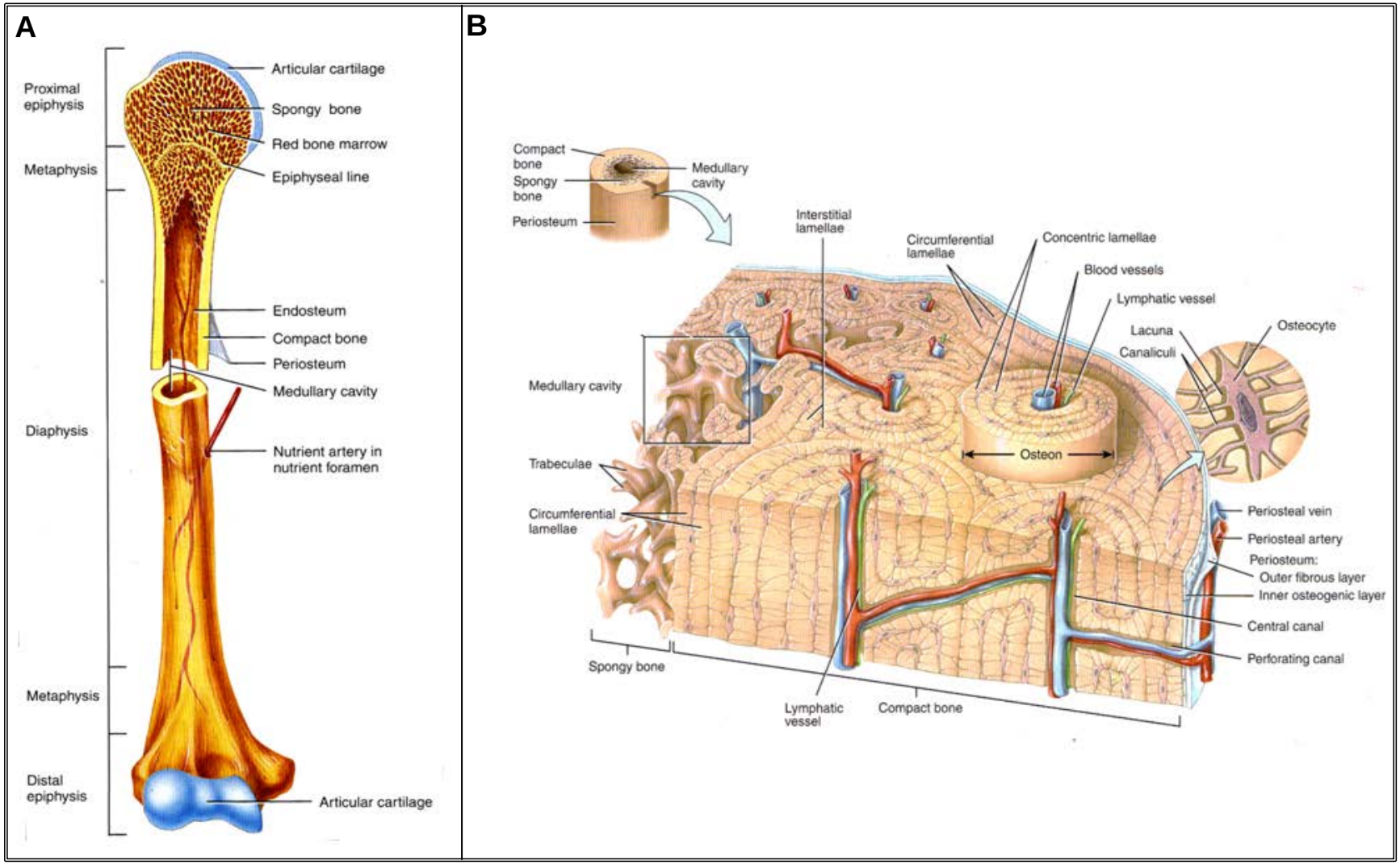

Figure 1.1 *Bone structure.* A) Diagram of a partially sectioned humerus. B) Diagram representing the structure of compact bone (Tortora and Derrickson, 2006). This material is reproduced with permission of John Wiley & Sons, Inc.

1.2 Bone constituents

1.2.1 Bone matrix

The mechanical properties of bone result from the composition of its matrix which has an organic and a mineral component (Currey, 1984, Weiner, 1986, Weiner and Traub, 1986). The mineral component of mature bone consists of inorganic mineral salts (Doty et al., 1976, Glimcher, 1981), with the major component being an analogue of hydroxyapatite: $Ca_{10}(PO_4)_6(OH)_2$, but it also contains calcium carbonate, calcium fluoride and magnesium phosphate (Posner, 1987, Glimcher, 1992, Standring, 2004). It is the mineral phase that gives bone its rigidity and load-bearing strength, making it able to withstand compression but not twisting or bending (Currey, 1984, Landis, 1995). The organic phase of mature bone consists mainly of proteins with type I collagen (ColI) being the major component. However, it also includes lipids, glycoproteins and proteoglycans (Tracy et al., 1987, Robey et al., 1988). Traces of other collagen types such as II, V and XI are also present which may derive from vascular tissues (Leushner, 1983, Robey et al., 1992). Non-collagenous proteins present in bone matrix include osteocalcin (OCN), osteopontin (OPN) and fibronectin (Stevenson and Lindsay, 1998). It is the organic phase that gives bone its elasticity, making it able to withstand twisting and bending, but not compression (Currey, 1984). Mineral and organic phases interact so that collagen fibres provide a scaffold in which mineral crystals can form in between the fibres (Martini et al., 2011).

1.2.2 Bone cells

1.2.2.1 Osteoblasts

Osteoblasts were first identified as large, mononucleated cells situated on the bone surface by Gegenbaur in 1864, who suggested that these cells were responsible for the manufacture of bone matrix (Bourne, 1972) (Figure 1.2).

1.2.2.1.1 Morphology

Osteoblasts range in shape from ovoid to cuboidal (Figure 1.2), being more compact than, for example, connective tissue fibroblasts which are more elongated (Bourne, 1972). Cytoplasmic processes extend out of osteoblast cell bodies connecting them to nearby cells such as other osteoblasts, pre-osteoblasts and osteocytes (Bourne, 1972). Active osteoblasts usually form a single cell layer, laying perpendicular to the bone surface (Bourne, 1972) (Figure 1.2), with their nuclei uppermost and away from the bone surface (Bourne, 1972). However, osteoblasts may also lie with their long axis parallel to the bone surface, diagonally overlapping like roof tiles (Bourne, 1972), or be organised into a rosette fashion, as seen at growing points of trabeculae. Osteoblasts have a large Golgi apparatus and rough endoplasmic reticulum, and numerous mitochondria, typical of high metabolic activity and secretion (Bourne, 1972).

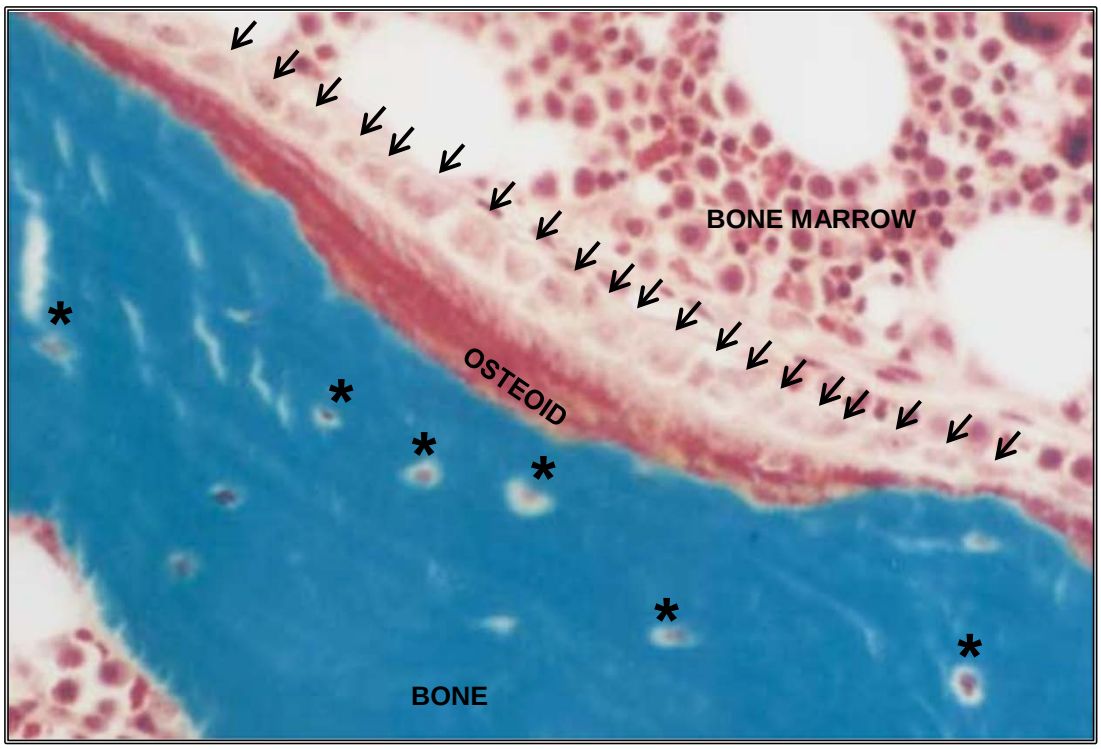

Figure 1.2 *Osteoblasts.* Cuboidal bone forming osteoblasts (arrows) can be seen aligned perpendicular to the bone surface, with a thick layer of newly formed osteoid underneath. *Osteocytes within mineralised bone matrix. Figure adapted from Russ Turner, the American Society for Bone and Mineral Research (ASBMR).

1.2.2.1.2 Function

Osteoblasts are actively involved in bone formation through the synthesis of bone matrix by generating osteoid (unmineralised bone matrix) (Bourne, 1972, Parfitt, 1977). They produce ColI and non-collagenous proteins such as OCN, bone sialoprotein (BSP), OPN and osteonectin (ON) (Lian et al., 1999, Aubin et al., 2006). Osteoblasts also show high alkaline phosphatase (ALP) activity, an enzyme involved in mineralisation, on their plasma membrane suggesting that they not only produce osteoid, but they also mineralise it (Whyte, 1994, Mornet et al., 2001, Nakamura, 2007). These proteins are all highly expressed by osteoblasts compared to other bone cells and are therefore considered osteoblast phenotypic markers (Aubin et al., 2006). Other markers include runt-related transcription factor 2 (Runx2) and osterix, which are essential for osteoblast differentiation (Nakashima et al., 2002, Komori, 2010). Osteoblasts synthesise and secrete proteoglycans and glycoproteins which can bind calcium ions for calcification, and control the growth of hydroxyapatite avoiding excess calcification (Lian et al., 1999). Osteoblasts also regulate the activity of osteoclasts and bone growth through the secretion of various hormones, such as prostaglandins and cytokines. Mature osteoblasts may die, become embedded in the bone matrix and differentiate into osteocytes, or become quiescent bone lining cells (Parfitt, 1987, Miller et al., 1989).

1.2.2.2 Osteoclasts

Osteoclasts were first described by Robin in 1849, who distinguished them from megakaryocytes (Bourne, 1972). However, it was Kölliker in 1873 who suggested that osteoclasts are the main agents in bone resorption (Bourne, 1972) (Figure 1.3).

1.2.2.2.1 Morphology

Osteoclasts are large multinucleated cells (Figure 1.3) which result from the fusion of monocyte macrophage lineage cells (Cormack and Ham, 1987) in the presence of macrophage colony stimulating factor (M-CSF) and receptor activator of nuclear factor κB ligand (RANKL), a member of the tumour necrosis factor (TNF) family (Felix et al., 1990, Kodama et al., 1991, Suda et al., 1992, Nakagawa et al., 1998). Osteoclasts attach to bone to commence resorption. They are motile cells and so their shape varies. They can appear as flattened cells against bone or as a roughly spherical mass (Figure 1.3). Their many nuclei are usually found close together and their cell body may contain processes or be separated into lobes (Bourne, 1972). Active osteoclasts are polarised with an apical plasma membrane in contact with bone and a basolateral membrane opposite to it (Mulari et al., 2003). The apical membrane contains a ruffled or brush border, which increases surface area for resorption (Bourne, 1972); and a sealing zone which anchors the osteoclast to the bone restricting protons and enzymes to the resorption compartment (Vaananen et al., 2000, Nakamura, 2007). The basolateral membrane is involved in cell-cell communication with neighbouring cells through RANKL and osteoprotegerin (OPG) (Bourne, 1972, Vaananen et al., 2000). Osteoclasts contain many mitochondria, indicative of active bone resorption (Bourne, 1972).

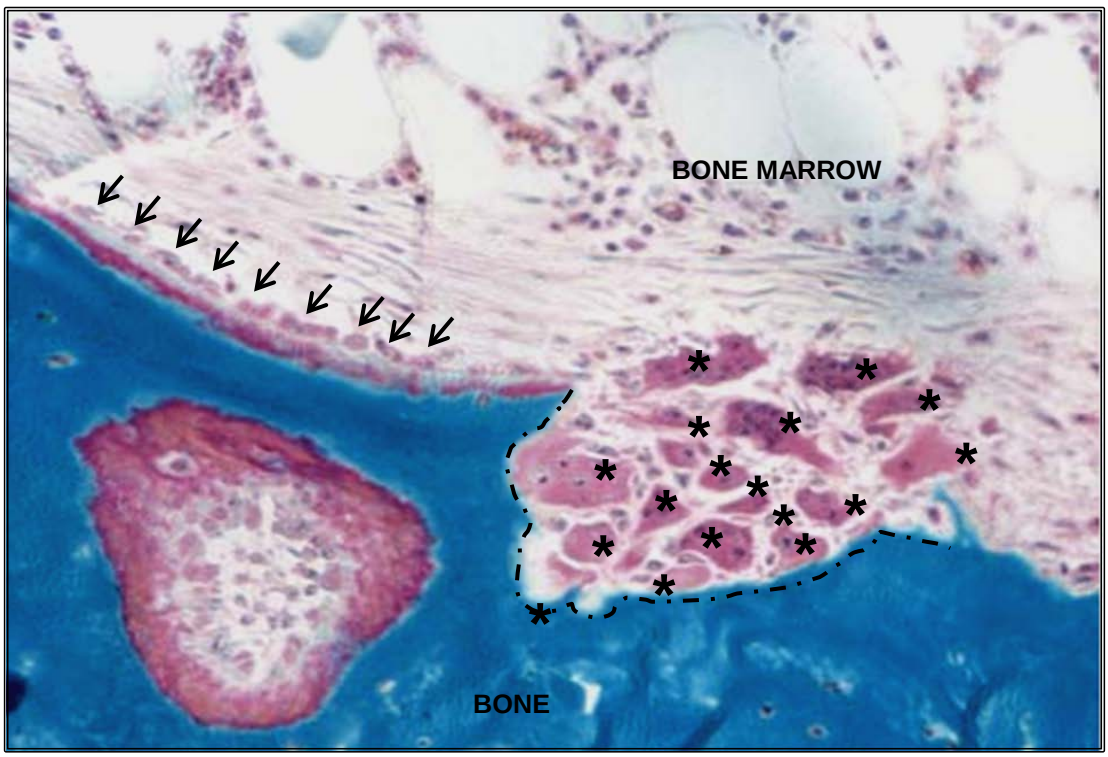

Figure 1.3 *Osteoclasts.* Multinucleated, roughly spherical, bone resorbing osteoclasts (*) can be seen within the erosion cavity (dotted line) on the bone surface. Osteoblasts (arrows) can be seen perpendicular to the bone surface. Figure adapted from Russ Turner, ASBMR.

1.2.2.2.2 Function

Osteoclasts resorb bone (Bourne, 1972) by attaching to the bone matrix and forming a closed compartment. This is where they pump out hydrogen ions, lowering the pH leading to the mobilisation of the mineral component of the bone matrix (Silver et al., 1988, Delaisse et al., 1991, Blair et al., 1993, Delaisse et al., 1993, Goto et al., 1993, Wucherpfennig et al., 1994, Holliday et al., 1997). Osteoclasts then secrete enzymes including tartrate-resistant acid phosphatase (TRAP), cathepsin K and gelatinase, which digest the organic component of the bone matrix forming an erosion cavity (Delaisse et al., 2003). This process of resorption, together with formation and activation of osteoclasts, is induced by RANKL (Boyle et al., 2003, Blair and Athanasou, 2004), a membrane bound protein expressed by osteoblasts (Atkins et al., 2003, Singh et al., 2012) and osteocytes (Zhao et al., 2002, Nakashima et al., 2011). RANKL binds to RANK, a surface membrane receptor present in pre-osteoclasts and osteoclasts (Lacey et al., 1998, Yasuda et al., 1998b). OPG, a soluble decoy receptor for RANKL secreted by osteoblasts and osteocytes, competes with RANK for RANKL binding (Yasuda et al., 1998a, Yasuda et al., 1998b) and therefore inhibits bone resorption and osteoclastogenesis (Mizuno et al., 1998). TRAP, RANK and cathepsin K are osteoclast phenotypic markers; whereas the RANKL/OPG ratio is an indicator of activation of bone resorption (Grimaud et al., 2003).

1.2.2.3 Osteocytes

Osteocytes are the most abundant cell type in mature bone where there are ten times more osteocytes than those of osteoblasts (Parfitt, 1977). They are terminally differentiated, non-proliferative cells derived from mature osteoblasts that are synthesising osteoid (Dudley and Spiro, 1961, Baud, 1968, Palumbo, 1986).

1.2.2.3.1 Morphology

Osteocytes are dendritic cells encased within lacunae in the bone matrix (Figure 1.4). In the adult human, osteocyte cell bodies are smaller than osteoblasts; they have lost many of their organelles (Jande and Belanger, 1973, Irie et al., 2008) and contain a sparse endoplasmic reticulum and an underdeveloped Golgi apparatus, typical of low amounts of synthesis and secretion (Bourne, 1972, Mullender et al., 1996). Osteocytes produce E11, a glycoprotein involved in the formation and maintenance of dendritic processes (Wetterwald et al., 1996, Hadjiargyrou et al., 2001), which extend and retract through canaliculi allowing communication between adjacent osteocytes, bone marrow and surface bone cells (Doty, 1981, Menton et al., 1984, Palumbo et al., 1990) (Figure 1.4). The dendritic processes are able to connect, disconnect and re-connect with neighbouring cells (Zhang et al., 2006). Osteocytes interconnect through gap junctions, for example connexin 43 (CX43), at the ends of their processes which are essential for osteocyte activity, maturation and survival (Baud, 1968, Doty, 1981, Knothe Tate et al., 2004). Osteocytes reside within the lacunocanalicular system (LCS) (Plotkin et al., 2002) which permits metabolic traffic and exchange.

1.2.2.3.2 Function

Osteocytes have many functions in bone, which depend on the maturation state of the cell. Genes that distinguish osteocytes from osteoblasts are those expressed by mature osteocytes, such as fibroblast growth factor 23 (FGF23) and sclerostin (SOST) (Bonewald, 2011) (Figure 1.5).

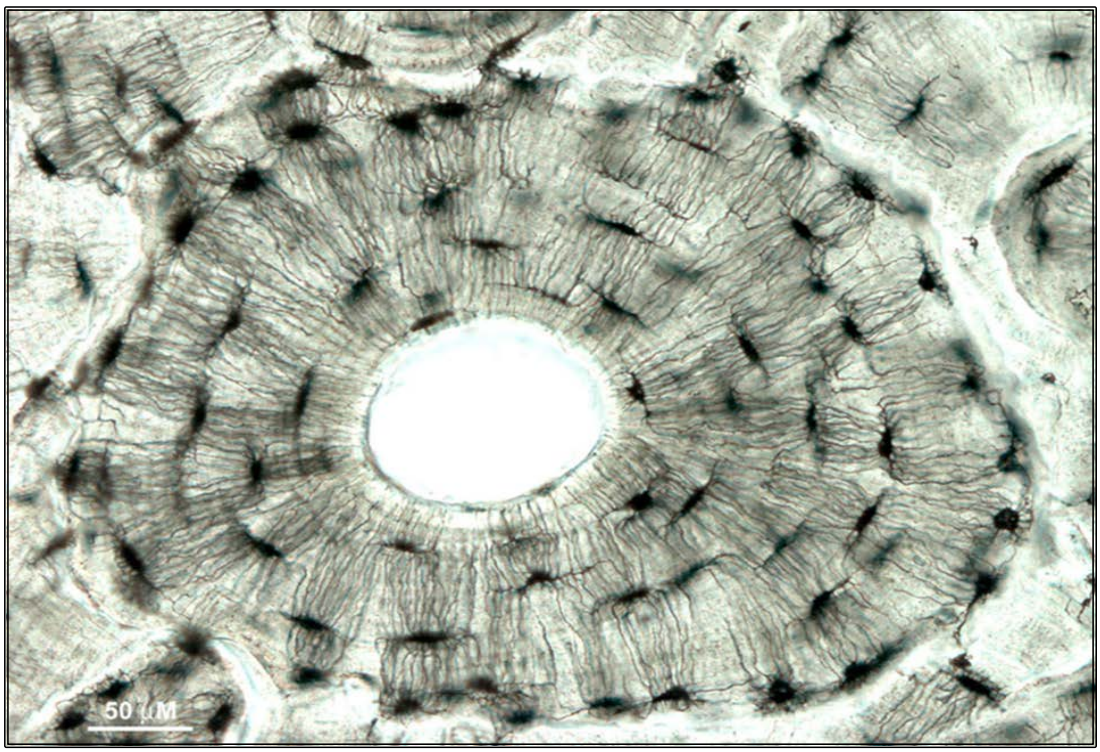

Figure 1.4 *Osteocytes.* Dendritic osteocytes can be seen extending their long processes within the bone matrix forming an osteon. Figure by Tim Arnett, from the Bone Research Society.

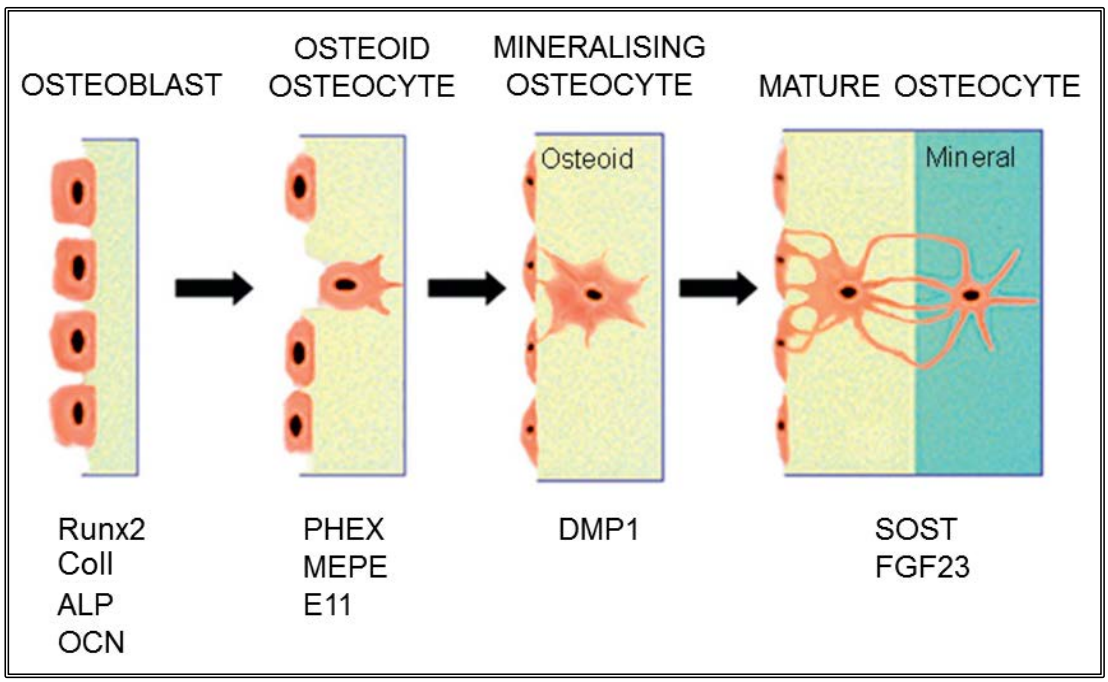

Figure 1.5 *Expression of markers during osteoblast-to-osteocyte differentiation.* Osteoblasts express Runx2 for differentiation, and ColI and ALP for matrix synthesis. OCN is expressed by late osteoblasts and continued to be expressed by osteocytes. Some osteoblasts are then embedded within the osteoid and become osteoid osteocytes where they develop dendritic processes through the expression of E11. At this stage, mineralisation markers phosphate-regulating gene with homologies to endopeptidases on the X chromosome (PHEX) and matrix extracellular phosphoglycoprotein (MEPE) begin to be expressed followed by dentin matrix protein 1 (DMP1). Finally mature osteocytes express FGF23 and SOST. Figure adapted from (Bonewald, 2011).

1.2.2.3.3 Mechanotransduction

Osteocytes are ideal candidate cells within bone to detect and respond to the physical stimuli from forces exerted on bones, because of their abundance, morphology, position within bone and ability to form an extensive network (Mullender and Huiskes, 1997, Nomura and Takano-Yamamoto, 2000, Plotkin et al., 2002, Turner et al., 2002, Klein-Nulend et al., 2013). Furthermore, osteocytic processes are considered the principal structure involved in sensing mechanical stimuli and they are mainly composed of actin filaments which may have an important role in mechanosensing (You et al., 2001, McGarry et al., 2005). Osteocytes also have primary cilia (Xiao et al., 2006, Malone et al., 2007) which, as in other cell types, have been shown to be involved in mechanosensing (Hoey et al., 2011, Xiao et al., 2011, Nguyen and Jacobs, 2013). In addition, proteins involved in the connection of osteocytes to surrounding cells and/or the extracellular matrix (ECM), like focal adhesions, CX43 and integrins, have been found to be involved in osteocyte response to mechanical stimuli (Litzenberger et al., 2010, Zhang et al., 2011). Consequently, osteocytes have been shown to respond to loading *in vivo* and *in vitro* and details of these studies can be found in page 34.

1.2.2.3.4 Regulation of bone remodelling

There are many factors that regulate bone remodelling, including systemic factors such as calcitonin, which inhibits osteoclast resorption (Zaidi et al., 2002); parathyroid hormone (PTH), which not only induces osteoclastic bone resorption and stimulates renal calcium reabsorption to balance serum calcium levels (Talmage and Elliot, 1958), but also induces bone formation (Selye, 1932, Dempster et al., 1993) (page 18), vitamin D_3 which indirectly regulates bone resorption through osteoblasts (Baldock et al., 2006, Crockett et al., 2011) and oestrogen, which regulates osteoclast (Nakamura et al., 2007, Krum et al., 2008) and osteocyte (Tomkinson et al., 1997, Tomkinson et al., 1998, Mann et al., 2007) survival .

Osteocytes are thought to regulate bone formation by orchestrating the formation and activity of osteoblasts and osteoclasts (Klein-Nulend et al., 2013) (page 34). Osteocytes release prostaglandins and bone morphogenetic protein 2 (BMP2), which stimulate osteoblast recruitment and activity (Li et al., 2002, Rawadi et al., 2003). Osteocytes also regulate bone formation through components of the wingless related integration site (Wnt) signalling pathway. SOST is an osteocyte specific protein (Poole et al., 2005) and a Wnt signalling pathway antagonist, which inhibits bone formation by preventing osteoblast differentiation (Winkler et al., 2003, van Bezooijen et al., 2004, Poole et al., 2005, van Bezooijen et al., 2005, Lowik and van Bezooijen, 2006, van Bezooijen et al., 2007). The Wnt signalling pathway stimulates osteoblast differentiation and SOST inhibits this pathway by binding to low density lipoprotein receptor-related protein 5/6 (LRP5/6) (Li et al., 2005c, Semenov et al., 2005, Semenov and He, 2006). SOST expression is responsive to mechanical stimulation (Robling et al., 2008). Inactivating mutations in the SOST gene lead to a high bone mass phenotype in mice (Li et al., 2008) and humans (Balemans et al., 2002) (page 18).

Osteocytes have also been shown to support osteoclast formation and activation as they express large amounts of RANKL, OPG and M-CSF along their processes which come into contact with marrow cells (Kamioka et al., 2001, Zhao et al., 2002, You et al., 2008, Nakashima et al., 2011, Xiong et al., 2011). Furthermore, osteocyte apoptosis is thought to trigger bone resorption signals in defined areas of microdamage (Noble, 2003). Osteocytes undergo apoptosis before osteoclasts start the bone resorption process, suggesting that a signal is generated from dying osteocytes to trigger osteoclastic resorption (Noble et al., 1997, Verborgt et al., 2002, Noble, 2003). It is important to note that osteocyte apoptosis is a common event in both healthy and unhealthy bone (Noble et al., 1997), is age related (Frost, 1960, Dunstan et al., 1990), but it can also be triggered by disruption of cell-cell and cell-matrix interactions (Xing and Boyce, 2005). However, it is reduced by mechanical stimulation (Plotkin et al., 2005).

1.2.2.3.5 Mineralisation

Osteocytes express low levels of ALP. However, they can regulate mineralisation and phosphate metabolism through the expression of phosphate-regulating gene with homologies to endopeptidases on the X chromosome (PHEX), found in osteoid osteocytes (Bonewald, 2011); matrix extracellular phosphoglycoprotein (MEPE), which influences mineralisation through activation of BMP2 (Rowe et al., 2004), also found in osteoid osteocytes (Petersen et al., 2000); dentin matrix protein 1 (DMP1), involved in hydroxyapatite formation and found in mineralising osteocytes (Feng et al., 2003, Feng et al., 2006); and FGF23, a phosphaturic hormone expressed by mature osteocytes (Feng et al., 2006) (Figure 1.5).

1.2.2.4 Bone-lining cells

Bone-lining cells are flattened in shape and cover most of the bone surfaces that are not undergoing remodelling. They have cytoplasmic processes that pass through the osteoid connecting them to mature osteoblasts and early osteocytes (Miller et al., 1989). Bone-lining cells have low amounts of cytoplasm, rough endoplasmic reticulum and free ribosomes, suggesting low metabolic activity. These cells form the endosteum on trabecular surfaces and are present below the periosteum on the cortical bone surface (Parfitt, 1994, Clarke, 2008). Elimination of bone lining cells, leading to exposure of bone matrix, is essential for bone remodelling to occur (Jones and Boyde, 1976, Zambonin Zallone et al., 1984). Bone-lining cells are thought to be quiescent osteoblasts (Nakamura, 2007), but retain the ability to re-differentiate into osteoblasts (Dobnig and Turner, 1995, Leaffer et al., 1995). These cells are joined to mature osteoblasts by adherens junctions (Shin et al., 2000, Shin et al., 2004) and may be involved in regulation of calcium and phosphate movement in bone tissue, thereby acting as a bone-blood barrier (Miller et al., 1989, Dobnig and Turner, 1995). Bone-lining cells also aid resorption by secreting collagenase which removes bone matrix so osteoclasts can attach to bone (Parfitt et al., 1996)

1.2.3 Bone marrow

Bone marrow is present in the cavities of long bones and in the pores of trabecular bone, extending to the blood vessel canals where the blood supply of both bone and bone marrow are directly connected (Brookes, 1961, Standring, 2004). In long bones, marrow is yellow and mainly composed of fat cells, whereas in flat and short bones, marrow is red and is mainly composed of haematopoietic cells, including osteoclasts (Standring, 2004). Red marrow can also be found in the epiphyses of long bones (Figure 1.1A). Bone turnover and marrow composition are directly linked, with a higher turnover rate found in trabecular bone associated with haematopoietic marrow (Krempien et al., 1978, Eventov et al., 1991). Osteoclasts and osteoblasts differentiate from haematopoietic and non-haematopoietic stem cells respectively which are also present in the bone marrow (Compston, 2002). Non-osteogenic marrow cells, such as mononuclear cells of monocyte or macrophage linage, regulate osteoclastogenesis and osteoclast activity through the production of interleukin 1 (IL-1) and TNF-α (Jilka, 1998, Pacifici, 1999, Compston, 2001). Megakaryocytes have also been found to be involved in bone remodelling as they express RANKL (Kartsogiannis et al., 1999), transforming growth factor beta (TGF-β) and its receptors (Bord et al., 2001), as well as glutamate receptors (Genever et al., 1999) and calcium-sensing receptors (House et al., 1997).

1.3 Modelling and remodelling

Bone is a dynamic tissue that undergoes modelling and remodelling.

1.3.1 Bone modelling

The process of modelling, defined by Frost (1990), involves bones altering their overall shape as a result of growth, mechanical loading or physiological effects, adjusting the skeleton to its environment. Modelling may lead to the addition or removal of bone and/or to bones changing their axis. However, bone growth is the major type of modelling (Frost, 1990b, Clarke, 2008).

In 1892, Wolff observed that trabeculae are orientated according to the paths of the mechanical stresses applied to the bone. Therefore, he proposed that long bones adapt their shape to accommodate stresses experienced by them (Wolff, 1986). During modelling, bone formation and resorption are not strongly linked and occur continuously but at different locations in bone (Frost, 1990b, Kobayashi et al., 2003). Modelling is less common than remodelling in the adult human (Kobayashi et al., 2003) but may be enhanced in several pathologies such as hypoparathyroidism (Ubara et al., 2005) and renal osteodystrophy (Ubara et al., 2003). Treatment with anabolic therapies can also increase bone modelling (Lindsay et al., 2006).

1.3.2 Bone remodelling

Bone remodelling is the process by which old bone is replaced with new bone in order to maintain strength and mineral homeostasis. There are no changes in the morphology of the bone, and resorption and formation are balanced and occur in the same site (Frost, 1990a). Bone remodelling takes place in small groups of cells called 'Basic Multicellular Units' (BMUs) (Frost, 1990b). Bone remodelling is initiated by the recruitment of pre-osteoclasts from the circulation (Roodman, 1999). The endosteum and bone lining cells are lifted to reveal the bone surface allowing pre-osteoclasts to fuse and form large multinucleated cells which attach to the bone matrix. Pre-osteoclasts form a resorbing compartment and differentiate into mature osteoclasts (Clarke, 2008) that resorb bone matrix by releasing hydrogen ions and enzymes forming an erosion cavity. Osteoclasts then die and mononuclear cells prepare the bone surface for bone formation (Eriksen, 1986, Reddy, 2004). Bone formation occurs when osteoblasts begin to synthesise new organic matrix and regulate its mineralisation (Anderson, 2003). The new matrix (osteoid) fills in the erosion cavity, 70% of osteoblasts die and the rest are buried within it to differentiate into osteocytes, or convert into bone lining cells, and finally the osteoid is mineralised (Burger et al., 2003). Resorption and formation processes are thought to be coupled, ensuring old bone is removed and restored with new bone, therefore maintaining bone mass (Parfitt, 2000).

1.3.3 Bone diseases

Common diseases occur as a consequence of abnormal bone remodelling. These result from an imbalance between the activities of osteoblasts and osteoclasts and speed of remodelling, leading to disproportionate bone formation and resorption. Many of these pathologies have no or limited treatments and therefore would benefit from alternative therapies.

1.3.3.1 Osteoporosis

Osteoporosis is the most common bone disease (Raisz, 1997) and is characterised by decreased bone mass and weakening of the bone resulting in increased risk of fractures. Osteoporosis leads to accelerated bone remodelling, with increased rates of bone formation which are not sufficient to replace the bone lost by resorption (Raisz, 2005) suggesting a decrease in osteoblast activity which could be due to senescence or the lack of systemic and global growth factors (Raisz, 2005). Osteoporosis can be classified into primary type 1, primary type 2 or secondary osteoporosis (Rosen et al., 2008). Females are more affected than men as bone mass in women is lower and reduced oestrogen production causes female bone mass to abruptly decrease during the menopause (Riggs et al., 1986, Wark, 1993). Menopause-induced osteoporosis is primary type 1 osteoporosis. Primary type 2 osteoporosis is age-related and affects 1 in 2 women and 1 in 5 men over 50 in the United Kingdom (UK) (van Staa et al., 2001). Secondary osteoporosis occurs as a result of other medical conditions, such as hyperparathyroidism, vitamin D deficiency, anorexia and renal disease; or prolonged use of certain medications such as glucocorticoids, immunosuppressants and chemotherapy (Rosen et al., 2008).

Osteoporosis can also be caused by reduced mechanical loading of the skeleton, in which case it is known as disuse osteoporosis and is characterised by increased bone resorption (Weinreb et al., 1989, Bain and Rubin, 1990, Zerwekh et al., 1998, Rantakokko et al., 1999, Li et al., 2005a). It affects bed ridden patients and astronauts, who undergo reduced loading or weightlessness respectively, for long periods of time (Szollar et al., 1998, Kanis et al., 2001, Wang et al., 2001).

Most of the available osteoporosis treatments involve anti-resorptive agents such as oestrogen, selective oestrogen-receptor modulators (SERMs), calcitonin and bisphosphonates. However, none of these cause a great increase in bone mass. Strontium ranelate (PROTELOS®) and PTH (Teriparatide) are the only two available therapies that induce bone formation. Teriparatide is the only food and drug administration (FDA) approved drug, however it was only approved for use of up to 2 years due to safety issues (Dempster et al., 2001, Neer et al., 2001, Rubin and Bilezikian, 2003, Sato et al., 2004).

Oestrogen and SERMs are considered hormone replacement therapy. Oestrogen used to be the only pharmacological approach to osteoporosis, however since other therapies have been approved, it has been proposed that hormones should only be used for treatment of post-menopausal osteoporosis and only after all other treatments have been considered, due to its increased cancer risk (Rosen et al., 2008). SERMs were developed as an alternative to oestrogen. They are molecules that interact with oestrogen receptors producing similar effects to oestrogen itself, however, they have been linked to an increased risk of thrombo-embolic disease (Rosen et al., 2008).

Calcitonin is a peptide secreted by thyroid gland cells which inhibits bone resorption as a result of increased serum calcium levels. It was first used as a treatment for Paget's disease of bone (page 21), but since then it has been used for less severe osteoporosis and in patients who cannot tolerate newer drugs (Rosen et al., 2008).

Bisphosphonates are internalised by osteoclasts and inhibit bone resorption (Russell, 2007), but their retention in bone (Lin, 1996, Khan et al., 1997, Rodan, 1997, Papapoulos and Cremers, 2007) and association with osteonecrosis in the jaw (Marx, 2003, Ruggiero et al., 2004, Marx et al., 2005) have led to concerns about their long term use.

Strontium ranelate (PROTELOS®) is a drug composed of two atoms of strontium (Sr^{2+}) used for post-menopausal osteoporosis. It has been suggested that strontium ranelate triggers bone formation by activating the calcium-sensing receptor (CaSR) to induce osteoblast proliferation (Brown, 2003, Coulombe et al., 2004); and it decreases bone resorption by downregulating RANKL and upregulating OPG (Marie, 2007, Brennan et al., 2009).

Denosumab (Prolia®) is a monoclonal antibody against RANKL, which prevents osteoclast activation and inhibits bone resorption (McClung et al., 2006). It has no major adverse effects (Cummings et al., 2009) and is FDA approved for the treatment of osteoporosis in post-menopausal women (McClung et al., 2006, Cummings et al., 2009) and osteoporotic men.

Teriparatide is a recombinant fragment of human parathyroid hormone (rhPTH1-34), the main regulator of bone and kidney calcium and phosphate metabolism, and is used for the treatment of advanced osteoporosis for a maximum of 18 months. However, its association with increased osteosarcoma risk in animals (Vahle et al., 2004, Schneider et al., 2005, Tashjian and Gagel, 2006) has limited its use.

Rare autosomal recessive inherited bone disorders, such as sclerosteosis and Van Buchem disease, which are caused by loss of function mutations in the SOST gene (Balemans et al., 1999, Balemans et al., 2001, Brunkow et al., 2001, Winkler et al., 2003, van Bezooijen et al., 2004) or SOST enhancer (Balemans et al., 2002, Staehling-Hampton et al., 2002, Loots et al., 2005) respectively, result in increased bone formation without affecting bone resorption. The study of these diseases has led to the development of monoclonal antibodies against sclerostin which mimic its downregulation (Li et al., 2009, Papapoulos, 2011).

1.3.3.2 Paget's disease of bone

Paget's disease of bone is characterised by accelerated and disorganised bone remodelling in localised areas of bone, as a result of highly increased bone resorption and formation (Kanis, 1998, Cundy and Reid, 2012, Ralston and Layfield, 2012). This rapid bone remodelling leads to woven bone formation, which has reduced mechanical strength than normal bone (Ralston and Layfield, 2012). Paget's disease affects one or more bones such as the femur, lumbar spine, skull and tibia, with the pelvis being the most common (Kanis, 1998). It is prevalent in middle-aged and older people with up to 8 % of men and 5 % of women by the age of 80 being affected in the UK (van Staa et al., 2002, Haddaway et al., 2007). Paget's disease can be asymptomatic, or present with bone pain, secondary arthritis, pathological fractures and larger distorted bones. If the skull is affected, it can also cause deafness and increasing hat size (Cundy and Reid, 2012). It is also associated with increased risk of osteoarthritis, back pain and reduced quality of life (Langston et al., 2007). Paget's disease is usually treated with potent bisphosphonates which lead to long-term suppression of the disease (Reid et al., 2005).

It has been suggested that Paget's disease is triggered by environmental factors including vitamin D deficiency (Barker and Gardner, 1974), low calcium intake (Siris, 1994), rural lifestyle (Merlotti et al., 2005) and, more controversially, viral infections such as measles, respiratory syncytial virus (Mills et al., 1984, Friedrichs et al., 2002, Rima et al., 2002), and paramyxovirus (Ralston et al., 2007, Ralston and Layfield, 2012). As reviewed in (Cundy and Reid, 2012), Paget's disease of bone is also inherited as an autosomal dominant trait caused by mutations in the *SQSTM1* gene (Morales-Piga et al., 1995, Hocking et al., 2002, Laurin et al., 2002), which encodes a protein involved in the control of NFκB, extracellular signal regulated kinases (ERK), and mitogen activated protein kinase (MAPK) signalling, as well as transcriptional activation. In addition, common variants of other genes, such as *CSF1*, *TNFRSF11A* and *TM7SF4*, have been linked to increased risk of developing Paget's disease of bone.

1.3.3.3 Osteoarthritis

Osteoarthritis (OA) is the most common degenerative joint disease in the UK, affecting 1 million people per year. OA usually develops in people over the age of 50 and is more common in women than men, however younger people can also be affected. OA is characterised by joint pain and stiffness associated with loss of articular cartilage, the formation of osteophytes (bony outgrowths) and subchondral bone sclerosis (Castaneda et al., 2012). Subchondral bone, underlying the articular cartilage, acts as a shock absorber, provides support (Imhof et al., 2000) and is subject to increased remodelling, microfractures, sclerosis and increased vascularisation in OA (Castaneda et al., 2012). The increased stiffness and thickening of the subchondral bone decreases its shock absorbing capacity, leading to increased mechanical load and breakdown of the articular cartilage (Radin and Rose, 1986, Burr and Radin, 2003).

Current OA treatments, such as painkillers, steroid injections, physiotherapy and joint replacement surgery do not stop the progression of the disease but instead alleviate symptoms such as joint pain, inflammation and stiffness; and so there is a need for disease-halting drugs. Thus, it is unsurprising that anti-osteoporotic drugs have been tested as possible novel OA therapies. From the previously mentioned osteoporosis therapies (page 18), it was found that oestrogens (Turner et al., 1997, Ham et al., 2002, Ho et al., 2011), bisphosphonates (Doschak et al., 2004, Hayami et al., 2004, Karsdal et al., 2008, Kadri et al., 2010, Moreau et al., 2011), anti-RANKL antibodies (Castaneda et al., 2012), Teriparatide (Chang et al., 2009) and strontium ranelate (Tat et al., 2011, Cooper et al., 2012, Reginster et al., 2013) improve the biomechanical properties of subchondral bone.

1.3.3.4 Rheumatoid arthritis

Rheumatoid arthritis (RA) is the second most common degenerative joint disease in the UK, with 580,000 people affected in England and Wales. RA usually develops between 40 and 70 years of age and is more common in women than men, however RA can affect people of any age. RA is an autoimmune disorder characterised by chronic systemic inflammation of various tissues and organs, but mainly of the synovial joints. It is also associated with cardiovascular, pulmonary and psychological disorders. Joint pathology includes destruction of cartilage and subchondral and periarticular bone (Goldring, 2003, McInnes and Schett, 2011). Focal erosions in RA bone are associated with osteoclasts (Bromley and Woolley, 1984, Gravallese et al., 1998) and do not form in RA animal models unable to produce mature osteoclasts (Pettit et al., 2001, Redlich et al., 2002, Li et al., 2004a).

There is no cure for RA but it is managed with a combination of surgery, physiotherapy, painkillers, and drugs such as non-steroidal anti-inflammatory drugs (NSAIDs), disease-modifying anti-rheumatic drugs (DMARDs), biological response modifiers (BRMs), anti-cytokines, such as TNF inhibitors, and steroids, depending on the severity of RA and patient responses (Goldring, 2003, Geiler et al., 2011, McInnes and Schett, 2011). Denosumab (Prolia®) (page 18) has been in clinical trials for the treatment of RA, where it has been shown that it attenuates the development and progression of bone erosions in RA patients (Cohen et al., 2008, Deodhar et al., 2010).

1.4 Mechanical loading in bone

1.4.1 The mechanostat theory

Bones must tolerate voluntary physical activities without breaking. There are physical and biological factors which act together to strengthen bones enough to sustain load-bearing (Frost, 1987b, Frost, 1998). Physical factors include the cross-sectional area, bone size and shape; tissue distribution and presence of microdamage (Martin and Burr, 1989, Martin, 1991). Bone modelling and remodelling, and microfracture repair are the biological determinants (Parfitt, 1983).

The mechanostat theory originates with Frost's proposal (1964) of a minimum effective strain (MES), strain being a measure of how much bone deforms in response to force application (Skerry, 2008a). There are a range of strain values that will not induce an adaptive response to mechanical load (Figure 1.6A). A single strain above this range (MES) leads to an increase in bone mass (Figure 1.6B), whereas, a strain below this range leads to loss of bone mass (Figure 1.6C). The mechanostat theory also states that strains above 1500 microstrain (με) stimulate modelling-induced bone formation (Figure 1.6D); and remodelling-induced bone loss occurs at strains below 100 με (Figure 1.6E). It is because of the difference in strain values that modelling and remodelling are not stimulated at the same time on the same bone surface (Frost, 1987a, Ferretti et al., 1995, Frost, 1996, Frost, 1998). Even though the forces suffered in limb bones of animals decrease as a function of body size, for example 6.9 G in a 7 kg turkey and 0.8 G in a 2500 kg elephant; the peak strains in vertebrates ranging from horses and humans to turkeys and dogs, are very similar ranging from 2000-3500 με (Rubin and Lanyon, 1984a, Rubin and Lanyon, 1984b, Rubin et al., 1990).

The mechanostat theory inspired Frost to generate the 'Utah paradigm of skeletal physiology' which proposed the following (Frost, 1996):

1) Skeletal health and disease is determined by biological mechanisms requiring effector cells and non-mechanical stimuli.
2) Biological mechanisms are guided by biomechanics.
3) Biological mechanisms are dominated by neuromotor anatomy and physiology after birth.
4) Non-mechanical factors can facilitate or hinder mechanical control but cannot replace or duplicate it.

This paradigm was the first to account for the significant effects of mechanical loading on bone structure, changing the dogma in bone physiology.

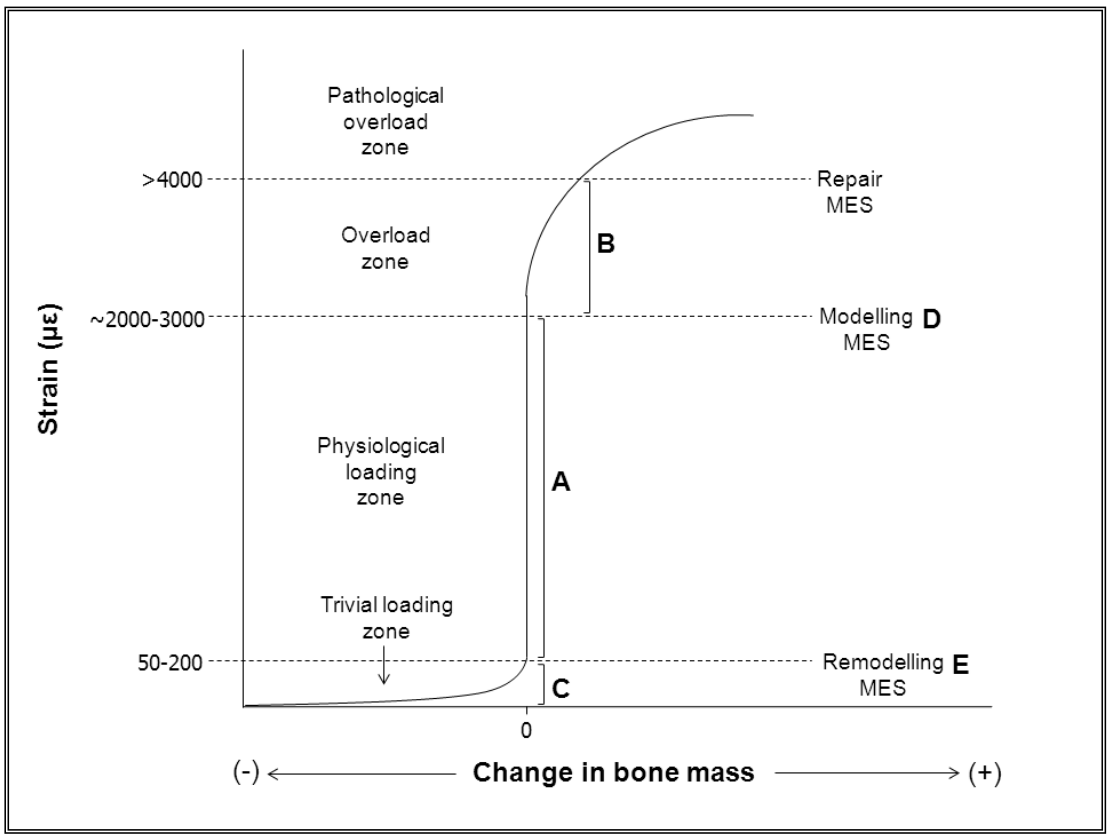

Figure 1.6 *The effect of mechanical strain on bone mass.* The graph shows bone mass is maintained with moderate strain (A), increased with strains higher than 2000-3000 με (B), and lost with trivial strains (C). The graph also shows mechanical strains at which modelling (D) and remodelling (E) occur. MES: minimum effective strain. Figure adapted from (Bailey et al., 1996).

Bone adapts to its environment by regulating its own mass (Lanyon and Smith, 1970, Lanyon, 1973, Lanyon et al., 1975, Jones et al., 1977, Goodship et al., 1979, Woo et al., 1981, Rubin and Lanyon, 1984b). This dynamic link between bone structure and its mechanical environment (Lanyon and Smith, 1970, Lanyon, 1973, Lanyon et al., 1975) is seen in tennis players whose humeri in their 'racquet arm' tends to have 35 % higher bone mass than in their other arm (Lanyon et al., 1975, Jones et al., 1977, Haapasalo et al., 2000, Kontulainen et al., 2003), and in astronauts who experience long periods of weightlessness (Baldwin et al., 1996, Goodship et al., 1998, Carmeliet et al., 2001), or patients subject to paralysis or prolonged bed rest (Gross and Rubin, 1995) resulting in reduced bone mass.

Early bone loading experiments in avian ulnae (Rubin and Lanyon, 1984b) showed that adaptive (re)modelling is largely responsive to short periods of high strain suggesting that it is a process controlled by signals to which bone is not accustomed (Skerry, 2008a). Short periods of high strain (Rubin and Lanyon, 1984b), high strain rates (Mosley and Lanyon, 1998) and periods of rest interrupting strain cycles (Robling et al., 2000) all increase osteogenic potential (Skerry, 2008a).

1.4.2 Mechanical loading models

1.4.2.1 *In vivo* models

The starting point for developing mechanical loading models requires assessment of strains experienced *in vivo*. This has been done by attaching strain gauges directly onto the bone surfaces of sheep (Lanyon, 1973), horses (Rubin and Lanyon, 1982, Gross et al., 1992), turkeys (Rubin and Lanyon, 1985, Adams et al., 1997), goats (Roszek et al., 1993), dogs (Rubin and Lanyon, 1982) and even humans (Lanyon et al., 1975, Hillam et al., 1996), in order to measure the strains engendered during daily activities. Although the attachment of strain gauges to bone *in vivo* has proven to be very useful for the study of load, bone growth and adaptation, this method is invasive and only measures strains. Non-invasive loading models, such as the rat ulna, mouse tibia, rodent vertebrae and tail suspension models, have been developed to study bone mechanotransduction and are briefly described below.

1.4.2.1.1 Ulna loading

The loading of a rodent ulna was first described by Torrance et al. in 1994. They developed a cyclic, axial loading model where the rat forearm is placed between two cups, holding the wrist and the elbow, and compressed in a cyclic manner, which elicits osteogenesis when peak physiological strains are exceeded (Torrance et al., 1994) (Figure 1.7A). Since then, this model has been used in many mechanotransduction studies. For example, it was used to show that bone resorption is inhibited whilst formation is stimulated by loading (Hillam and Skerry, 1995), that oestrogen and loading produce a greater osteogenic response together than separately (Cheng et al., 1994) and that the glutamate signalling pathway may be involved in mechanotransduction, as glutamate/aspartate transporter 1 (GLAST1) is mechanically regulated (Mason et al., 1997). The use of the ulna as a loading model has also been applied to birds (Lanyon and Rubin, 1984, Rubin and Lanyon, 1984b, Lanyon et al., 1986, Pead et al., 1988, Rubin et al., 1996), mice (Hsieh et al., 2001, Robling et al., 2008) and sheep (O'Connor et al., 1982).

1.4.2.1.2 Tibial loading

The loading of a rodent tibia was first described by Seireg and Kempke in 1969 as a technique for the investigation of degenerative and regenerative influence of cyclic loads on living bone (Seireg and Kempke, 1969). Rats were exposed to long periods of low and short periods of high cyclic loading. This model was then updated to the four point bending of the rat tibia, causing compression and tension on different areas of the bone by applying large rods directly on the skin and the underlying periosteum (Figure 1.7B). This method causes dense bone to form in low strain regions, and woven bone to form in high strain regions (Turner et al., 1991). Other interesting results have been found using the four point bending rat tibia model, such as the increase in osteocyte insulin growth factor 1 (IGF-1) mRNA expression (Reijnders et al., 2007b) and OPN expression (Miles et al., 1998) after load; and load induced cyclooxygenase 2 (COX-2) expression mediation of bone formation induction (Forwood, 1996).

1.4.2.1.3 Vertebrae loading

The loading of rodent vertebrae was first described by Chambers et al. in 1993. In this loading model pins are inserted into the seventh and ninth caudal vertebrae of rats which are used to load the eighth caudal vertebra through cyclic compression (Chambers et al., 1993, Chow et al., 1993) (Figure 1.7C). Woven and lamellar bone formation could be induced with short loading regimes (Chambers et al., 1993), with a single 10 minute loading episode inducing 24-fold increases in bone formation (Chow et al., 1993). Although the vertebrae loading model is more invasive than ulna or tibial loading models, interesting results have been obtained including that oestrogen enhances osteogenic responses after load (Jagger et al., 1996); that nitric oxide (NO) is necessary but not sufficient to induce bone formation (Chow et al., 1998a), and that mechanical loading induces bone formation by reactivating bone lining cells (Chow et al., 1998b). Mice vertebrae have also been used as loading models (Webster et al., 2008, Webster et al., Lambers et al., Wasserman et al.).

1.4.2.1.4 Tail suspension

The tail suspension model was first developed in the 1970s with the aim to provide a gravity-based model that could mimic the effects of weightlessness (Morey-Holton and Globus, 1998). In this model rodents are held by a harness in a head-down position, so that they have the use of the front limbs for movement, eating, and grooming, with the hind limbs being unloaded (Morey-Holton and Globus, 1998) (Figure 1.7D). Studies using this model have shown that after a short period of unloading, there was a higher incidence of osteocyte apoptosis which correlated with sites of resorption suggesting that osteocyte death precedes bone loss (Aguirre et al., 2006), that OPN is required for bone resorption as a result of unloading (Ishijima et al., 2001) and that OPN is associated with NFκB during this process (Ishijima et al., 2006). This model was also used to show the effects of bisphosphonates on bone changes (Apseloff et al., 1993) (page 18).

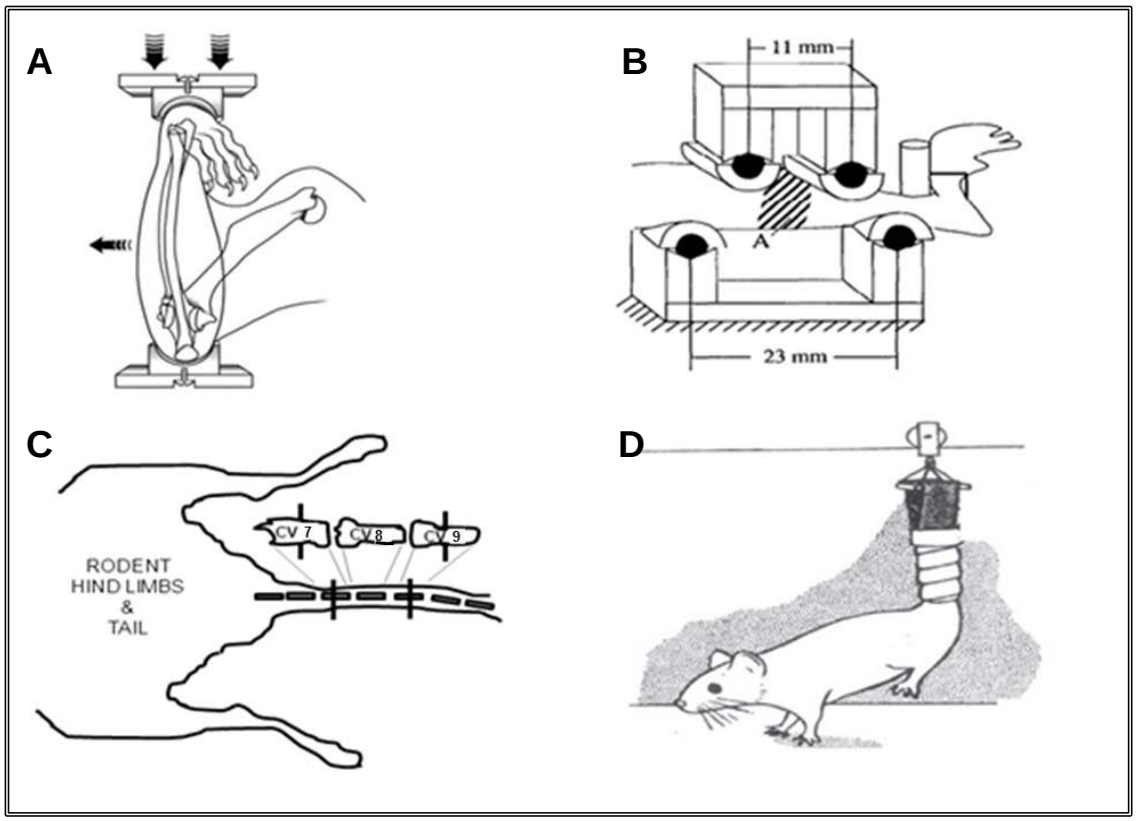

Figure 1.7 *In vivo bone loading models.* Diagrams of the ulna (A), tibia (B), vertebrae (C) and tail (D) loading models, adapted from (Turner et al., 1991, Robling et al., 2001, Barbosa et al., 2011, Lambers et al., 2011). CV: caudal vertebra.

1.4.2.2 *In vitro* models

Although cell specific knockout (KO) animal models are a powerful tool in unravelling specific cellular responses to mechanical loading, the *in vivo* bone environment is highly complex. Bone organ cultures, involving bone explants, have also been used to investigate mechanical loading responses (Davies et al., 2006, Rawlinson et al., 1995, Chan et al., 2009). Although organ cultures have the advantage of simplifying the complexity of the *in vivo* environment whilst maintaining bone cells within their native ECM, they contain a heterogeneous cell population, are awkward to maintain and have a limited life-span (Arnett et al., 1998, Pitsillides and Rawlinson, 2012). Therefore the investigation of direct cell-cell interactions has depended on *in vitro* loading models. The loading method used, the cell type and the cell environment all need to be considered when designing an *in vitro* bone loading model. It is the combination of these factors that will lead to a model which resembles a physiological situation and can therefore be used to answer a range of scientific questions.

1.4.2.2.1 Loading methods

In vitro loading models generally involve cell culture systems, which are subjected to mechanical stimuli such as hydrostatic pressure, fluid shear stress, or substrate strain in a precise manner. For this reason, many mechanical loading devices have been designed which range in complexity, accuracy and consistency of loading (Brown, 2000). Pioneering work on *in vitro* mechanical loading devices started in 1939 (Glücksmann, 1939) and quantitative devices started to be used in the mid-1970s. Since then a range of compression, stretch, substrate bending, distension and fluid shear devices, involving either contact or contactless-loading, have been developed (Brown, 2000). Early devices limited to low loading frequencies have been superseded by those that can mimic osteogenic *in vivo* frequencies of 10-100 Hz (Brown, 2000, Rubin et al., 2001a). Commercially available bone loading systems include BOSE, FlexCell® and ZETOS. For instance, BOSE ElectroForce® devices allow the application of tension, compression, bending, stress, torsion or fluid shear to *in vivo* (Macione et al., 2011), *ex vivo* (Price et al., 2011, Xiao et al., 2011) and three-dimensional (3D) *in vitro* cultures (Sittichockechaiwut et al., 2009),

but not to two-dimensional (2D) cell cultures. FlexCell® has a smaller range of devices which are only applicable to *ex vivo* and 2D or 3D *in vitro* cultures, and has been previously used to load 2D osteocyte cultures *in vitro* (Plotkin et al., 2005, Zhang et al., 2006). Finally, ZETOS systems have been mainly used for long term *ex vivo* loading (Davies et al., 2006, Endres et al., 2009, Aw et al., 2012). The main disadvantage of these industrial designs is the number of specimens or cultures that can be loaded at the same time. The majority of BOSE® systems can only load one sample at a time, with a maximum of 6 for FlexCell®.

1.4.2.2.2 Cell type

The majority of *in vitro* bone loading investigations focus on osteoblasts (page 32). Although osteocytes are the principal load sensors *in vivo*, much less loading research has been done on these cells (pages 9 and 34). This is possibly due to the limited availability of osteocytes. Primary osteocytes are difficult to isolate and culture due to their position within bone. To date, only chick (Nijweide et al., 2003, van der Plas and Nijweide, 2005), mouse (Nakashima et al., 2011, Halleux et al., 2012, Stern et al., 2012) and rat (Gu et al., 2006) primary osteocytes have successfully been isolated using sequential bone digestion. Nevertheless, the yield of live osteocytes after digestion is low and they do not proliferate in culture, limiting their use for experimental procedures. Two mouse osteocyte cell lines, MLO-A5 (osteoid pre-osteocyte) (Kato et al., 2001) and MLO-Y4 (osteocyte-like) (Kato et al., 1997) have been developed to facilitate the study of these cells. Although MLO-Y4 cells are ‘osteocyte-like’ (Kato et al., 1997), they do not express late-osteocyte markers and therefore are not a true representation of mature osteocytes. A recently developed osteoblast-to-late-osteocyte cell line (IDG-SW3) that expresses all mature osteocyte genes when differentiated, provides new potential for investigating osteocyte biology (Woo et al., 2011).

1.4.2.2.3 Cell environment

Over the last three decades, the mechanisms involved in mechanically-induced bone formation have been largely revealed by applying forces to primary osteoblasts or osteoblast-like cell-lines cultured in 2D monolayers. These showed that loading regulates osteoblast survival (Carvalho et al., 1995, Cillo et al., 2000, Cheng et al., 2002, Ogata, 2003, Bucaro et al., 2004), differentiation (Chen et al., 2003, Jagodzinski et al., 2004, Li et al., 2004b, Henriksen et al., 2006) and function (You et al., 2000, Di Palma et al., 2003, Kapur et al., 2003, Li et al., 2004b, Liegibel et al., 2004, Mullender et al., 2004).

The few studies investigating loading of osteocytes in 2D have revealed some of the mechanisms involved in mechanotransduction. For example, the secretion of prostaglandins and NO, mediators of adaptive bone formation, in response to fluid shear (Klein-Nulend et al., 1995a, Klein-Nulend et al., 1995b, Ajubi et al., 1999, Burger and Klein-Nulen, 1999); and also the involvement of the cytoskeleton in mechanotransduction (Ajubi et al., 1996). These investigations supported the idea of osteocytes being the most mechanosensitive cells in bone, as when exposed to fluid shear, osteocytes were more responsive than osteoblasts (Klein-Nulend et al., 1995a).

Studying either osteoblasts or osteocytes in 2D loading models has undoubtedly shed light into the signalling underlying mechanotransduction. However, the more physiological model of 2D co-culture started to reveal how loaded osteocytes control the activities of other bone cells. For example, loaded MLO-Y4 cells regulate osteoclasts by inhibiting osteoclastogenesis of pre-osteoclasts and bone marrow stromal cells (BMSCs) through direct cell-cell contact (You et al., 2008) and by expressing RANKL and OPG, and releasing M-CSF (Zhao et al., 2002). Furthermore, loaded osteocytes rapidly increase ALP activity of osteoblasts through direct communication via gap junctions (Taylor et al., 2007). In addition, osteoblasts also regulate osteoclasts when in 2D co-cultures by reducing osteoclastogenesis when mineralising (Deyama et al., 2000) by increasing secretion of OPG (Schroder et al., 2012) in the absence of load. However, these *in vitro* investigations do not reflect the complex 3D dynamics that control the structure and function of the living bone organ and the interactions of the cells within it (Parfitt,

1994, Collin-Osdoby, 1994, Parfitt, 2000, Pogoda et al., 2005, Matsuo and Irie, 2008, Tortelli and Cancedda, 2009).

In recent years, 3D *in vitro* bone models have become increasingly popular. Some of these models use type I collagen gels as the matrix within which bone cells are embedded (Kurata et al., 2006, Murshid et al., 2007, Qi et al., 2007, Atkins et al., 2009), in an attempt to mimic the bone matrix, however, most of these (Murshid et al., 2007, Qi et al., 2007, Atkins et al., 2009) have not been exposed to loading. Instead these 3D bone models revealed differences in cytoskeleton composition between osteoblast-like cells and primary osteocytes when in 3D collagen gels (Murshid et al., 2007); that adenosine tri-phosphate (ATP) decreases osteoblast-like cells integrins expression (Qi et al., 2007); and that MLO-Y4s increase expression of RANKL and M-CSF but decrease OPG expression when in 3D collagen gels with polyethylene particles, involved in orthopaedic implant bone destruction (Atkins et al., 2009). Interestingly, Kurata et al. applied an undefined load to mimic microdamage by scratching embedded MLO-Y4 cells co-cultured with BMSCs, and as a result MLO-Y4 cells secreted M-CSF and RANKL and induced TRAP positive cells (Kurata et al., 2006).

3D cultures made out of other materials such as other hydrogels (Chatterjee et al., 2010), polybicarbonate membranes (Boukhechba et al., 2009), and scaffolds (Santos et al., 2009, Tortelli et al., 2009, Barron et al., 2010), have also been used. Here cells are not embedded within a matrix, but instead are attached to the scaffold surface and therefore do not accurately capture the environment of an osteocyte within bone. Nevertheless, these systems have proven the feasibility of reproducing the synthesis of an organised matrix (Tortelli et al., 2009) and cell-mediated matrix degradation (Nakagawa et al., 2004, Domaschke et al., 2006, Tortelli and Cancedda, 2009). Still, there are no models that co-culture osteoblasts and osteocytes in 3D and at the same time are mechanically stimulated. This highlights a major gap in the understanding of the interactions that lead to mechanically-induced bone formation.

1.5 Mechanical signalling in bone

Mechanotransduction has been suggested to use similar intracellular signalling cascades to those generated by ligand-receptor binding, resulting in changes in gene expression (Rubin et al., 2006). This has been well demonstrated in endothelial cell responses to shear stress where mechanical stimuli activates signal transduction cascades, including increases in intracellular cyclic adenosine monophosphate (cAMP) (Lavandero et al., 1993), inositol triphosphate (IP_3) and intracellular calcium (Dassouli et al., 1993, Li et al., 2004b), guanine regulatory proteins (Gudi et al., 2003) and MAPK (Rubin et al., 2002).

Application of mechanical load to bone cells such as osteoblasts, marrow stromal cells, periosteal fibroblasts and osteocytes, leads to modulation of cell proliferation (Kaspar et al., 2002, Boutahar et al., 2004, Li et al., 2004b), differentiation (Li et al., 2004b), secretion of inflammatory modulators (Klein-Nulend et al., 1995a, Smalt et al., 1997, Klein-Nulend et al., 1998, McAllister and Frangos, 1999, Zaman et al., 1999, Sanchez et al., 2009) and extracellular matrix protein synthesis (Dumas et al., 2009, Sittichokechaiwut et al., 2010). Therefore, there has been a lot of speculation around the identification of the mechanosensor in bone tissue. Osteoblasts and osteoclasts respond to strain signals (Rubin et al., 2006). Endothelial and smooth muscle cells of the bone blood vessels (Davis et al., 2001, Boo and Jo, 2003), together with stromal cells in the bone marrow (Li et al., 2004b), may also contribute to mechanoresponses (Skerry et al., 1989). However, the osteocyte intercommunicating network within bone, which is connected to bone surface cells, that integrates hormonal, growth factor and prostaglandin signals, is thought to be the main regulator of bone remodelling (Skerry et al., 1989, Lanyon, 1993, Duncan and Turner, 1995, Klein-Nulend et al., 1995a, Klein-Nulend et al., 1995b, Mullender and Huiskes, 1997, Burger and Klein-Nulen, 1999, Han et al., 2004).

Osteocytes contain the necessary cellular machinery to sense mechanical loading (page 13) and they have been shown to respond to loading *in vivo* and *in vitro*. *In vivo*, osteocytes increase transcriptional and metabolic activities in response to short loading periods (Pead et al., 1988, Skerry et al., 1989); increase their DMP1 and MEPE expression, controlling bone matrix mineral quality (Gluhak-Heinrich et al., 2003, Harris et al., 2007); increase IGF-1 and related proteins involved in mechanically-induced bone formation (Reijnders et al., 2007a, Reijnders et al., 2007b), and stimulate NO production (Zaman et al., 1999), an early mediator of mechanically-induced bone formation (Fox et al., 1996). Furthermore, recent *in vivo* studies have shown that load-regulated gene expression in trabecular osteocytes is different to that of compact osteocytes and the genes involved are related to osteoblast and osteoclast life cycles (Zaman et al., 2010, Wasserman et al., 2013). *In vitro*, ultrasound loaded MLO-Y4 cells in 2D increase COX-2 expression, necessary for prostaglandin E_2 (PGE_2) synthesis, and decrease RANKL:OPG ratios (Li et al., 2012a). Primary osteocytes under fluid flow secrete prostaglandins (Klein-Nulend et al., 1995b, Ajubi et al., 1996, Ajubi et al., 1999) and produce NO (Klein-Nulend et al., 1995b). MLO-Y4 cells under cyclic hydraulic pressure decrease apoptosis (Liu et al., 2010); and under fluid flow activate CX43 (Cheng et al., 2001b) resulting in adenosine tri-phosphate (ATP) release (Genetos et al., 2007).

Interestingly, mechanically loaded osteocytes have been shown to directly regulate osteoblast activity through various mechanisms including the downregulation of SOST expression (Robling et al., 2008, Tu et al., 2012) and release of NO, which has an anabolic effect on osteoblast activity (Fox et al., 1996) *in vivo*, and the communication with neighbouring osteoblasts through gap junctions (Taylor et al., 2007), and release of PGE_2, which regulates osteoblast proliferation and differentiation (Li et al., 2012b) *in vitro*. Furthermore, loaded osteocytes also regulate osteoclast activity by regulating RANKL expression (Nakashima et al., 2011), inducing *in vivo* bone resorption in unloading situations (Xiong et al., 2011) increasing SOST expression promoting osteoclast formation (Wijenayaka et al., 2011) and releasing NO after loading inhibiting osteoclast bone resorption (Tan et al., 2007) *in vitro*.

1.5.1 Adenosine, CaSR and glutamate signalling in bone

The adenosine, calcium-sensing and glutamate signalling pathways have been implicated in bone biology, with several *in vivo* studies showing that KO animals of some of these receptors display a bone phenotype (Morimoto et al., 2006, Chang et al., 2008a, Skerry, 2008b, Kara et al., 2010b, Carroll et al., 2012, Mediero et al., 2012). *In vitro* studies have also associated these pathways to bone cell biology, with glutamate (Mason et al., 1997, Spencer and Genever, 2003, Mason, 2004) and ATP (Genetos et al., 2005, Li et al., 2005b, Genetos et al., 2007, Riddle et al., 2007, Liu et al., 2008) being implicated in mechanotransduction. GLAST1, a glutamate transporter, has been shown to be mechanically-regulated in osteocytes (Mason et al., 1997), as well as N-methyl-D-aspartate (NMDA), 2-amino-3-(3-hydroxy-5-methyl-isoxazol-4-yl) propanoic acid (AMPA) and kainate (KA) glutamate receptors in osteoclasts and bone lining cells (Szczesniak et al., 2005). These findings are highly indicative of a role for glutamate in mechanotransduction. Furthermore, a hypothetical model on mechanically-induced glutamate signalling in bone has been proposed (Mason, 2004). On the other hand, ATP has been shown to be released as a result of mechanical stimuli in osteoblasts (Pavlin et al., 2000, Romanello et al., 2001, Genetos et al., 2005, Li et al., 2005b) and osteocytes (Genetos et al., 2007); and consequently, to mediate prostaglandin release (Genetos et al., 2005) and activate ERK 1/2 intracellular signalling (Liu et al., 2008), indicative of a role in mechanotransduction.

1.5.1.1 Adenosine signalling

Adenosine is an endogenous, ubiquitous nucleoside and a metabolite of ATP that acts as an extracellular signalling molecule (Drury and Szent-Gyögyi, 1929). It is usually present at low concentrations (less than 1 μM) in the extracellular space and accumulates in response to metabolic stress and cell damage eliciting physiological responses by binding to and activating one or more of the four G-protein coupled adenosine receptors (A_1, A_{2A}, A_{2B} and A_3) (Jacobson and Gao, 2006, Evans and Ham, 2012). Adenosine receptor signalling occurs through the inhibition or stimulation of adenylyl cyclase, leading to a decrease or an increase in intracellular cAMP concentration ($[cAMP]_i$) respectively. Therefore, adenosine

receptors are classified according to the effect they have on cAMP concentration: A_1 and A_3 decrease $[cAMP]_i$ (Jin et al., 1997), whereas A_{2A} and A_{2B} increase $[cAMP]_i$ (Bruns et al., 1986).

Adenosine research in bone has been recently reviewed (Evans and Ham, 2012). All adenosine receptor messenger ribonucleic acids (mRNAs) are expressed in MG63 osteoblasts (Russell et al., 2007), and all adenosine receptor proteins are expressed in human primary osteoblasts (Costa et al., 2011). A_{2A} and A_{2B} receptors are expressed in human osteoclasts (Pellegatti et al., 2011, Mediero et al., 2012). No data have yet been published on the expression or functionality of adenosine receptors in osteocytes, or as a result of mechanical stimuli *in vivo* or *in vitro* (Evans and Ham, 2012). Although there is a lack of publications on the expression of these receptors in bone, they have an effect on bone biology as a result of activation or inhibition in osteoblasts and osteoclasts (Evans and Ham, 2012).

1.5.1.1.1 Adenosine receptor A_1 in bone

The role of A_1 receptors in osteoblasts is unclear, with some studies not detecting expression in osteoblast-like cells (Lerner et al., 1987). No effects on osteoblast morphology or function were observed in A_1 KO mice (Kara et al., 2010b), although the higher bone volume, smaller osteoclasts with no ruffled border and an absence of osteoclast bone resorption (Kara et al., 2010b) revealed A_1 to be essential for osteoclast differentiation and function (Kara et al., 2010a). A_1 receptors play a role in adipocyte differentiation (Gharibi et al., 2011, Gharibi et al., 2012).

1.5.1.1.2 Adenosine receptor A_{2A} in bone

In osteoblasts, A_{2A} is upregulated during final stages of osteoblast differentiation, during which activation of the receptor stimulates ALP activity (Gharibi et al., 2011). In osteoclasts, deletion of A_{2A} increased bone resorption and osteoclast activity as seen in A_{2A} KO mice (Mediero et al., 2012). In a mouse model of RA, adenosine was shown to decrease bone resorption through the A_{2A} receptor (Mazzon et al., 2011) (page 23).

1.5.1.1.3 Adenosine receptor A_{2B} in bone

In osteoblasts, deletion of A_{2B} decreases osteoblast differentiation and expression of osteoblast-related transcription factors by mesenchymal stem cells (MSCs) (Evans and Ham, 2012, Mediero and Cronstein, 2013). The A_{2B} KO mouse showed a lower bone density, delayed fracture physiology and lower expression of osteoblast differentiation related genes (Carroll et al., 2012). Consistent with this, when overexpressed or activated, A_{2B} stimulates mineralisation, ALP activity and ALP and Runx2 gene expression (Gharibi et al., 2012). In osteoclasts, very little is known about the expression and function of A_{2B}. Although adenosine produced during inflammation inhibits differentiation of mouse bone marrow macrophages through A_{2B} receptor (Xaus et al., 1999), and A_{2B} is expressed in human osteoclast precursors, inhibition of A_{2B} does not affect osteoclast formation (Pellegatti et al., 2011).

1.5.1.1.4 Adenosine receptor A_3 in bone

A_3 is expressed in osteoblasts (Russell et al., 2007, Costa et al., 2011), but there are no published studies on its expression in osteoclasts. Activation of A_3 receptors increases human primary osteoblast proliferation (Costa et al., 2011) and decreases osteoclast number and expression of RANKL in a RA mouse model (Rath-Wolfson et al., 2006).

1.5.1.2 Calcium-sensing signalling

Bone is a calcium (Ca^{2+}) reservoir. Hormonal systems are coupled to bone tissue in order to transport Ca^{2+} in and out of bone according to the body's needs. Parathyroid gland cells ensure extracellular Ca^{2+} homeostasis, secreting PTH when extracellular free ionised calcium concentration ($[Ca^{2+}]_o$) decreases below a threshold. This increases bone resorption, as well as acting on the kidney, to increase $[Ca^{2+}]_o$ into the circulation. Ca^{2+} is sensed by cells through the CaSR, a G-protein coupled receptor (Brown et al., 1993). CaSR can be activated not only by extracellular calcium, but by other compounds including polyamines, Mg^{2+} and L-

amino acids (Riccardi and Brown, 2010) such as glutamate, which acts as a positive allosteric modulator of the CaSR (Conigrave et al., 2000).

In bone, CaSR is expressed in rat and bovine osteoblasts, osteocytes and bone marrow cells *in vivo*, but not in mature osteoclasts (Chang et al., 1999), as well as in osteoblasts, osteocytes and osteoclasts in rat femur and human undecalcified bone (Dvorak et al., 2004). *In vitro*, CaSR is present in rat calvarial osteoblasts (Chattopadhyay et al., 2004) and in several osteoblast-like cell lines (Yamaguchi et al., 1998b, Yamaguchi et al., 2001) including MC3T3-E1 cells (Yamaguchi et al., 1998a, Ye et al., 2000), in addition to pre- and mature osteoclasts (Kameda et al., 1998, Mentaverri et al., 2006). However, no studies have been published yet on the expression of CaSR mRNA in osteocytes *in vitro*.

1.5.1.2.1 CaSR in bone

CaSR tissue-specific KOs in parathyroid gland cells and osteoblasts both display severe growth retardation, small undermineralised skeletons and reduced body weights (Chang et al., 2008a, Dvorak-Ewell et al.). In addition, the parathyroid specific KO also suffers fractures in the ribs and tibiae (Chang et al., 2008a) whereas the osteoblast specific KO has impaired osteoblast bone forming activity (Dvorak-Ewell et al., 2011).

Cultured osteoblasts lacking the CaSR showed decreased type I collagen (COL1A1), OCN, ALP and DMP1 gene expression and reduced mineralisation (Yamauchi et al., 2005, Dvorak-Ewell et al., 2011), suggesting a role of CaSR in osteoblast differentiation. The CaSR is also involved in the proliferation and chemotaxis of osteoblasts (Yamaguchi et al., 1998a, Chattopadhyay et al., 2004, Dvorak et al., 2004). In cultured osteoclast precursors, high $[Ca^{2+}]_o$ activates the CaSR and reduces osteoclast formation (Kanatani et al., 1999), and deletion of CaSR in these cells leads to a decrease in differentiation to mature osteoclasts (Mentaverri et al., 2006). In mature osteoclasts, high $[Ca^{2+}]_o$ induces apoptosis (Mentaverri et al., 2006) and inhibits resorptive activity (Zaidi et al., 1991, Kameda et al., 1998). Deletion of CaSR in osteoblasts increased expression of RANKL and induced osteoclastogenesis in co-cultured pre-osteoclasts (Dvorak-Ewell et al., 2011).

1.5.1.3 Glutamate signalling

Glutamate is a ubiquitous amino acid and the main excitatory neurotransmitter in the vertebrate central nervous system (CNS), where it is involved in cognitive functions, e.g. memory and learning (McEntee and Crook, 1993). Glutamate signals through receptors which are classified into two groups according to signalling mechanism; ionotropic receptors (iGluRs) which act as glutamate gated ion channels, and metabotropic receptors (mGluRs) which are G-protein coupled receptors (Reynolds and Miller, 1988, Hollmann et al., 1989, Nakanishi, 1998, Mason, 2004). iGluRs are categorised into three groups according to homology and selective agonists; NMDA, AMPA and KA (Wisden and Seeburg, 1993, Hollmann and Heinemann, 1994). mGluRs are categorised in to three groups (I, II and III) according to functional groups, agonist sensitivity and signalling (Masu et al., 1991, Tanabe et al., 1992, Wisden and Seeburg, 1993). Glutamate concentrations across cell membranes are maintained by transporters driven by ion-exchange pumps (Schousboe and Divac, 1979, Danbolt, 2001). There are three types of glutamate transporters; excitatory amino acid transporters (EAATs), vesicular glutamate transporters (VGLUTs) and the cysteine/glutamate antiporters. EAATs (5 members), are high-affinity, sodium-dependent glutamate transporters that transport extracellular glutamate into the cell (Kanai and Hediger, 1992, Pines et al., 1992, Storck et al., 1992, Arriza et al., 1994, Fairman et al., 1995, Arriza et al., 1997). VGLUTs have lower affinity to glutamate than EAATs, comprise three transporters and release glutamate from vesicles (Shigeri et al., 2004). Finally, the cysteine/glutamate antiporters are sodium and chloride-dependent, high-affinity transporters which pack glutamate into vesicles ready for release (Bannai and Kitamura, 1980, Bannai and Kitamura, 1981, Waniewski and Martin, 1984, Cho and Bannai, 1990).

Glutamate signalling was first associated with bone when GLAST1, also known as EAAT1 in humans, was identified in a gene screening investigation to reveal mechanically regulated genes in rodent osteocytes (Mason et al., 1997). Since then, other studies reported the expression of glutamate signalling components in bone cells. NMDA and AMPA receptors, together with EAATs are expressed by osteoblasts, osteoclasts and osteocytes, whereas mGluR and KA receptors have only

been detected in osteoblasts and osteoclasts (Brakspear and Mason, 2012). Although receptor function has been reported in both osteoblasts and osteoclasts, no studies to date have been performed in osteocytes. Furthermore, NMDA, AMPA and KA receptors were also shown to be mechanically-regulated in osteoclasts and bone lining cells (Szczesniak et al., 2005). Glutamate concentrations were also found to vary in arthritic joints increasing from 6 µM in healthy joints (Plaitakis et al., 1982, McNearney et al., 2000) to 332.3 ±29.3 and 240 ±38 µM in RA and OA joints respectively (McNearney et al., 2004) (pages 22-23).

1.5.1.3.1 NMDA receptors in bone

In vivo, NMDAR2A and NMDAR2B expression has been reported to be mechanically-regulated in osteoclasts and bone lining cells (Szczesniak et al., 2005). Furthermore, the development of an osteoblast/osteocyte specific NMDAR1 KO mouse, which displayed delayed development, thin bone structure and poor mineralisation of the axial and appendicular bones (Skerry, 2008b), indicates NMDA receptors play a role in bone biology. Inhibition of NMDA receptors delayed onset of RA and reduced bone resorption, swelling and pain symptoms in animal models of RA (Sluka et al., 1994, Lam and Ng, 2010) (page 23).

In osteoblasts *in vivo*, NMDA receptor expression decreased in rats with disuse-induced bone loss (Ho et al., 2005) and mice treated with an NMDA antagonist display reduced cortical thickness (Burford et al., 2004). In rat primary osteoblasts, NMDA receptor antagonists downregulate Runx2 expression, reduce mineralisation, and inhibit ALP activity and OCN expression (Hinoi et al., 2003, Ho et al., 2005, Lin et al., 2008). Consistent with this, NMDA receptor agonists increase OCN expression and mineralisation in osteoblasts (Lin et al., 2008). In osteoclasts *in vitro*, NMDA receptor activation reduces osteoclast differentiation and activity, and promotes apoptosis through a decrease in NO production (Chenu et al., 1998, Peet et al., 1999, Itzstein et al., 2000, Mentaverri et al., 2003).

1.5.1.3.2 AMPA/KA receptors in bone

In vivo, AMPA and KA receptors were shown to be mechanically-regulated (Szczesniak et al., 2005). Rats injected with AMPA showed increased bone volume in their tibia (Lin et al., 2008), whereas mice treated with AMPA/KA receptor antagonist 2,3-dihydroxy-6-nitro-7-sulfamoyl-benzo[f]quinoxaline-2,3-dione (NBQX), displayed decreased trabecular thickness (Burford et al., 2004). Furthermore, NBQX also reduces bone remodelling in rat antigen-induced arthritis (Bonnet, Williams and Mason unpublished data). Consistent with this, in cultured osteoblasts, AMPA receptor agonists increased OCN expression and mineralisation (Lin et al., 2008), whereas the AMPA/KA receptor antagonist NBQX inhibits mineralisation and reduces cell number (Bonnet, Williams and Mason unpublished data). Interestingly, *in vitro*, AMPA treatment of osteoclasts had no effect on osteoclastogenesis (Lin et al., 2008), however, NBQX treatment inhibited osteoclast resorptive activity (Szczesniak et al., 2005).

1.5.1.3.3 mGluRs in bone

To date, there are no studies on the function of mGluRs in osteoblasts. However, agonists for mGluR8 inhibit glutamate release and bone resorption, whilst antagonists activate bone resorption (Morimoto et al., 2006).

1.5.1.3.4 Glutamate transporters in bone

In vivo, GLAST1 expression has been reported to be mechanically regulated, and therefore is a candidate in bone biology (Mason et al., 1997). However, a GLAST1 KO did not affect bone length (Gray et al., 2001). In contrast, a VGLUT1 KO mouse showed low bone mass and large reductions of trabecular bone as a result of an increase in osteoclastic resorption (Morimoto et al., 2006).

In vitro, inhibition of EAATs has been shown to prevent bone formation by calvarial osteoblasts and change their osteoblastic phenotype to a more adipogenic one (Taylor, 2002) and to affect the bone forming phenotype and cell number of osteoblast cell lines by influencing OCN, ALP and OPG mRNA expression, ALP

activity and mineralisation (Brakspear, 2010). On the other hand, there are currently no studies on the direct role of VGLUTs in osteoblasts. Nevertheless, the cysteine/glutamate antiporter has been shown to be functionally required for pre-osteoblast differentiation. The antiporter was also shown to suppress pre-osteoblast proliferation (Uno et al., 2007, Takarada-Iemata et al., 2011) and downregulate Runx2 expression and ALP activity in differentiating osteoblasts (Uno et al., 2011). Osteoclast differentiation requires activation of the cysteine/glutamate antiporter (Hinoi et al., 2007) and VLGUT1 accumulates glutamate with bone degradation products in vesicles for release (Morimoto et al., 2006). There are no studies to date on the role of EAATs in osteoclast biology.

1.5.1.4 Heterodimerisation of receptors in the CNS

In the CNS, glutamate receptors can be controlled by other neuromodulators (Conn and Pin, 1997). Adenosine is a key neuromodulator in the CNS (Phillis and Wu, 1981) and inhibits glutamate signalling in various regions of the brain (Peris and Dunwiddie, 1985). Group I mGluR responses are enhanced by the action of A_1 adenosine receptors (Ogata et al., 1994, Toms and Roberts, 1999). In the CNS, *in vivo* and *in vitro,* mGluR1α and A_1 receptors co-localise and have direct molecular interactions, specific to the mGluR1α splice variant (Ciruela et al., 2001). The CaSR heterodimerises with mGluR1α *in vivo* and *in vitro* (Gama et al., 2001) after CaSR and mGluR1α expression patterns were shown to overlap in the brain (Testa et al., 1995, Chattopadhyay et al., 1997, Rogers et al., 1997, Ferraguti et al., 1998, Tallaksen-Greene et al., 1998, Ferry et al., 2000, Stinehelfer et al., 2000, Tanaka et al., 2000). mGluR5 also co-localises, heterodimerises and has synergistic interactions with both CaSR and adenosine receptor A_{2A} (Pintor et al., 2000, Gama et al., 2001, Popoli et al., 2001, Diaz-Cabiale et al., 2002). Interestingly, A_{2A}/mGluR5 heterodimerisation regulates c-fos expression in the brain (Ferre et al., 2002), a proto-oncogene found to be key in osteoclast formation and bone remodelling (Grigoriadis et al., 1994) and in osteoblast differentiation (Hipskind and Bilbe, 1998). The fact that these G-protein coupled receptors, which have been found to have a role in bone remodelling, heterodimerise to enhance their activity in the CNS, suggests similar events may also take place in bone (Mason et al., 2006, Mattinzoli et al., 2009).

1.6 Hypothesis and aims

Currently, *in vitro* mechanical loading models do not reflect the interactions of the cells within bone. The majority focus on mechanical loading of osteoblasts in monolayers (Wang et al., 2011, Xiao et al., 2011, Li et al., 2012c) (page 30) and the available 3D *in vitro* bone models (page 32), do not elucidate the osteocyte-osteoblast interactions (page 13) that regulate mechanically-induced bone formation (Kurata et al., 2006, Tortelli and Cancedda, 2009, Tortelli et al., 2009, Papadimitropoulos et al., 2011a, Papadimitropoulos et al., 2011b, Barthelemi et al., 2012). Therefore the following hypothesis was generated:

"A 3D osteocyte-osteoblast co-culture model, where osteocytes embedded within type I collagen gels are overlaid with osteoblasts, represents a useful in vitro model for the investigation of the regulation of mechanically-induced bone formation markers."

Furthermore, the adenosine, calcium-sensing, and glutamate signalling pathways have been shown to be involved in bone biology (page 36), as seen in KO animals involving signalling components of these pathways. Additionally, all adenosine receptors have been found to be expressed in osteoblasts (Evans and Ham, 2012) (page 37), and CaSR (page 38) and a variety of glutamate receptors and transporters (Brakspear and Mason, 2012) (page 40) have been found to be expressed in both osteoblasts and osteocytes. Interestingly, two adenosine receptors (A_1, A_{2A}) and CaSR have been shown to heterodimerise with glutamate receptors mGluR1 and/or 5 in the CNS (page 43), and both glutamate and the adenosine precursor ATP have been implicated in mechanotransduction (page 36). However the role of the adenosine, CaSR and glutamate signalling pathways in mechanically-induced bone formation is not fully understood. Therefore the following hypothesis was formulated:

"Adenosine, calcium-sensing and glutamate signalling components are expressed in the 3D osteocyte-osteoblast co-culture model and contribute, individually or in combination, to the regulation of mechanically-induced bone formation markers."

To investigate these hypotheses, the aims of the project were:

1. To establish and characterise a novel *in vitro* mouse 3D osteocyte-osteoblast co-culture model.
2. To determine the expression of osteocyte and osteoblast phenotypic markers.
3. To determine the expression of adenosine receptors, CaSR and glutamate receptors and transporters within the 3D co-culture model.
4. To determine whether embedded osteocytes respond to mechanical load in the 3D model by assessing PGE_2 and IL-6 release, and expression of signalling and phenotypic markers.
5. To determine the responses of 3D co-cultures to mechanical load by assessing PGE_2 release, pro-collagen type I (PINP) synthesis and expression of bone formation markers.
6. To determine the effects of receptor antagonists on the response of 3D co-cultures to mechanical stimuli (as in aim 5).

CHAPTER 2

MATERIALS

AND

METHODS

2. Materials and Methods

2.1 Materials

All reagents were purchased from Sigma-Aldrich® (Poole, UK) unless otherwise stated below.

2.1.1 Tissue culture

Alpha Minimum Essential Medium with L-glutamine and without ribo- and deoxynucleosides (αMEM), Dulbecco's Modified Eagle's Medium with high glucose, GlutaMAX™ and pyruvate (DMEM), 10X Minimum Essential Medium (MEM); foetal bovine serum (FBS), newborn calf serum (NCS), penicillin-streptomycin (PenStrep), and trypsin-EDTA with phenol red were purchased from GIBCO (Life Technologies™, Paisley, UK). Dialysed FBS (DFBS), dialysed by ultra-filtration with a 10,000 molecular weight cut-off membrane was obtained from Sera Laboratories International Ltd. (Bolney, UK). Rat tail tendon type I collagen for coating flasks was from Becton Dickinson Bioscience (BD) (VWR®, Leicestershire, UK). Tissue culture treated plasticware was from BD Falcon (VWR®). CellTiter 96® AQueous One Solution Cell Proliferation Assay (MTS) was from Promega (Southampton, UK). NBQX and 2-(2-Furanyl)-7-[3-(4-methoxyphenyl)propyl]-7H-pyrazolo[4,3-e][1,2,4]triazolo[1,5-c]pyrimidin-5-amine (SCH 442416) were from Tocris Bioscience (Bristol, UK).

2.1.2 Molecular biology

TRIzol® reagent, Quant-iT™ dsDNA High-Sensitivity Assay Kit and SuperScript® III Reverse Transcriptase were purchased from Life Technologies™. DNA-free™ and sodium acetate were obtained from Ambion® (Huntington, UK). All primers were synthesised and purified by MWG (Milton Keynes, UK). QIAquick Gel Extraction Kit was obtained from Qiagen (Crawley, UK). Ampicillin was purchased from Bioline (London, UK). Random primers, deoxynucleotide triphosphates (dNTPs), Recombinant RNasin® Ribonuclease Inhibitor, agarose, tris-borate-EDTA (TBE), pGEM®-T plasmid vector, *Escherichia coli* (*E. coli*) JM109

competent cells, isopropyl β-D-1-thiogalactopyranoside (IPTG), X-Galactosidase (X-Gal) and Wizard® Plus SV Miniprep deoxyribonucleic acid (DNA) Purification kit were purchased from Promega. Safeview was obtained from NBS Biologicals (Huntingdon, UK) and low molecular weight DNA ladder from New England Biolabs Inc.® (Herts, UK). Polypropylene Reverse Transcriptase-quantitative Polymerase Chain Reaction (RT-qPCR) plates and optical strip caps were purchased from Agilent Technologies (Berkshire, UK). All plasticware and consumables were certified ribonuclease (RNase)/deoxyribonuclease (DNase) free.

2.1.3 Immunolocalisation and histochemistry

Ethidium homodimer, anti-CX43 mouse monoclonal antibody (clone: CX-1B1), and goat anti-rabbit secondary antibody conjugated with Alexa 594 were from Life Technologies™. Anti-ColI mouse monoclonal antibody was obtained from Developmental Studies Hybridoma Bank (Iowa, USA). Anti-E11 (podoplanin) goat polyclonal antibody was obtained from R&D Systems® (Abingdon, UK). Anti-A_1, anti-A_{2A}, anti-AMPAR2, anti-mGluR1 and anti-KA1 rabbit polyclonal antibodies were obtained from Abcam® (Cambridge, UK). Anti-A_{2B}, anti-A_3, anti-GLAST1, and anti-excitatory amino acid carrier 1 (EAAC1) rabbit polyclonal antibodies were purchased from Alpha Diagnostics Int. (San Antonio, USA). Anti-CaSR rabbit polyclonal antibody was purchased from AnaSpec (Fremont, USA). Rabbit anti-goat peroxidase conjugated secondary antibody, goat anti-rabbit peroxidase conjugated secondary antibody. Dylight594 streptavidin; Vectamount Universal Elite ABC rabbit kit; rabbit immunoglobulins control (IgG), goat IgG, normal rabbit serum; normal horse serum, mouse IgG, and 3,3'-diaminobenzidine (DAB) were obtained from Vector Laboratories (Peterborough, UK). Optimal cutting temperature (OCT) compound mounting medium for cryotomy, coverslips, and poly-lysine coated slides were purchased from VWR®. Dibutyl phthalate xylene (DPX) was from Raymond A. Lamb Laboratory Supplies (VWR®).

2.1.4 Protein assays

CytoTox 96® Non-Radioactive Cytotoxicity Assay was from Promega. PGE_2 Enzyme-linked Immunosorbent Assay (ELISA) kit was purchased from Enzo Life Sciences® (Exeter, UK). DuoSet mouse Interleukin-6 (IL-6) ELISA Development kit was obtained from R&D Systems®. Rat/Mouse N-terminal pro-peptide of type I pro-collagen (PINP) Enzymeimmuno assay (EIA) was from Immunodiagnostic systems (Tyne & Wear, UK).

2.1.5 Loading device

TECH-SIL 25 Silicone Elastomer for the loading device was purchased from Technovent Ltd. (Newport, South Wales, UK). Face paint for strain measurements was from Snazaroo™ (Minehead, UK).

2.2 Equipment and software

2.2.1 Molecular biology

RNA quantitation was carried out using a Thermo Scientific NanoDrop 2000 with Thermo Scientific NanoDrop 2000/2000c Software. Thermocycling was carried out on a Techne TC-312 Thermal Cycler (Cambridge, UK), or using a Stratagene Mx3000P cycler for quantitative reactions. Quantitative amplifications were monitored using MxPro RT-qPCR software (Agilent Technologies). Agarose DNA gels were viewed using a GelDoc system from BioRad (Hempstead, UK) and photographed using BioRad GelDoc Software.

2.2.2 Microscopy

Light microscope images of live cultures were obtained with a Nikon Coolpix 4500 camera attached to a Nikon eclipse TS100 inverse-light microscope (Surrey, UK). Cryosectioning was carried out using a Bright OTF 5000 cryostat (Huntingdon, UK). Light-microscope images of stained cryosections were obtained with a Motic Moticam 2000 digital camera (Barcelona, Spain) attached to a Leica DMRB light

microscope (Milton Keynes, UK) and using the Motic Images Plus 2.0ML basic image acquisition software. Fluorescence microscope images were obtained with an Olympus Soft Imaging Systems F-view black and white digital camera (Tokyo, Japan) attached to an Olympus BX61 epi-fluorescence microscope and using the Olympus AnalySIS software. Confocal images were obtained with a Leica TCS SP2 AOBS confocal scanning laser microscope and using the Leica Confocal Software.

2.2.3 Microplate assays

All assays requiring a microplate reader were performed using a BMG Labtech FLUOstar Optima plate reader (Bucks, UK) and readings were recorded with the Optima Software for FLUOstar V2.00 R3 (BMG Labtech).

2.2.4 Mechanical loading

A Richmond aerovac vacuum chamber (Fareham, UK) attached to a DVP vacuum pump (San Pietro in Casale, Italy) was used for the manufacturing of the silicone loading plate. Strain measurements of the loading device were performed using a Losenhausen Servo Hydraulic Testing Machine (Delhi, India) with MTS FlexTest® Controller Software and using DANTEC Correlated Solutions cameras with DANTEC Dynamics Q-400 System Software (Columbia, USA). Mechanical loading of cultures in the silicone plate was performed using a BOSE ElectroForce® 3200 instrument (Kent, UK) and controlled with WinTest® Software 4.1 with TuneIQ control optimisation (BOSE).

2.2.5 Statistics

Statistical analysis was performed using Minitab 16 statistical software (Coventry, UK).

2.3 Methods

2.3.1 Cell lines and cell culture

2.3.1.1 MC3T3-E1(14)

MC3T3-E1 is an osteoblast-like cell line initially derived from newborn mouse calvaria by *in vitro* differentiation. This is a spontaneously immortalised cell line (Sudo et al., 1983) which has been characterised into pre-osteoblast subclones (Wang et al., 1999). MC3T3-E1 subclones were defined by their ability to mineralise extracellular matrix and expression of osteoblast-related genes. MC3T3-E1 subclone 14 (MC3T3-E1(14)), a kind gift of Dr Bronwen Evans (School of Medicine, Cardiff University, UK), is a mineralising subclone which expresses high levels of BSP, ColI and OCN mRNA (Wang et al., 1999).

MC3T3-E1(14) cells were cultured in 75 cm^2 flasks with αMEM supplemented with 100 U/ml penicillin, 100 µg/ml streptomycin, 10 % FBS at 37°C in 5 % carbon dioxide (CO_2) /95 % air atmosphere (Wang et al., 1999). Medium was replaced every 2-3 days. After reaching 80 % confluency, cells were treated with 0.25 % (w/v) trypsin-EDTA and re-seeded into new flasks. Passages 15-30 were used for experiments.

2.3.1.2 MLO-Y4

MLO-Y4 osteocyte-like cells were kindly donated by Prof Lynda Bonewald (University of Missouri, USA). The cells were isolated by sequential collagenase digestion from the long bones of transgenic mice expressing the simian virus 40 (SV40) large T-antigen oncogene under the control of the OCN promoter. These cells have been shown to behave like primary osteocytes as they express high amounts of OCN, low amounts of ALP and ColI, and they have complex cytoplasmic processes expressing CD44, CX43 and OPN (Kato et al., 1997).

MLO-Y4 osteocyte-like cells (Kato et al., 1997) were cultured on collagen coated 75 cm^2 or 225 cm^2 flasks (0.15 mg/ml rat tail tendon type I collagen in 0.02 N glacial acetic acid) (Kato et al., 1997) in αMEM supplemented with 100 U/ml penicillin, 100 µg/ml streptomycin, 2.5 % heat-inactivated FBS (HIFBS) and 2.5 % heat-inactivated NCS (HINCS) at 37°C in 5 % CO_2/95 % air atmosphere ((Kitase et al., 2010), personal communication with Prof Lynda Bonewald). Media was replaced every 2-3 days. At 70-80 % confluency, cells were treated with 0.25 % (w/v) trypsin-EDTA and re-seeded into new flasks. Passages 29-50 were used for experiments.

2.3.2 Serum heat inactivation

Both FBS and NCS were heat-inactivated following the instructions provided by Cambrex (Wiesbaden, Germany). The frozen sera bottles were placed at room temperature (rt) for 3-4 hr before thawing completely in a 37ºC water bath. The bottles were then agitated to mix the contents and placed for 30 min in a 56ºC water bath where the water level is above the serum level, and mixed occasionally. Temperature was controlled by placing a thermometer in a bottle with water of equal volume to the sera.

2.3.3 Sera batch test

To maintain optimum culture conditions for MC3T3-E1(14) and MLO-Y4 cells in monolayer, new batches of FBS and NCS were tested using CellTiter 96® AQueous One Solution Cell Proliferation Assay (MTS). In a 96-well plate, 1,500 cells/well were seeded and incubated overnight (o/n) at 37°C in 5 % CO_2/95 % air atmosphere in 100 µl of their corresponding culture medium (page 50). Medium was removed and replaced with medium containing either old (control) or new (test) FBS and/or NCS and cells were incubated o/n at 37°C in 5 % CO_2/95 % air atmosphere. The CellTiter 96® AQueous One Solution Cell Proliferation Assay (MTS) was performed at day 2 and 3 following manufacturer's instructions. Briefly, 20 µl of CellTiter 96® AQueous One Solution reagent was added to each well. The plate was then incubated for 2 hr at 37°C in 5 % CO_2/95 % air atmosphere wrapped in foil to avoid exposure to light. Finally the plate was read at 490 nm using a BMG Labtech

FLUOstar Optima plate reader and absorbance was recorded using Optima Software for FLUOstar V2.00 R3. For results see page 266.

2.3.4 3D collagen co-cultures

Rat tail tendon type I collagen (2.5 mg/ml in 7 mM glacial acetic acid) was mixed on ice in a 4:1 ratio with 5X MEM containing 11 g/L sodium bicarbonate ($NaHCO_3$), and neutralised to pH 7.4 with 1 M tris (hydroxymethyl)aminomethane (Tris) base (pH 11.5) to give a 2 mg/ml collagen solution. MLO-Y4 ($1.5x10^6$ cells/ml gel, page 50) cells were diluted in their corresponding medium (less than 10 % of total gel volume) and then mixed thoroughly into the collagen solution on ice. The collagen-cell mix was dispensed into 48-well plates (250 µl/well) and incubated at 37°C in 5 % CO_2/95 % air atmosphere for 1 hr for polymerisation. 1 ml of MLO-Y4 medium was added on top before gels were incubated o/n at 37°C in 5 % CO_2/95 % air atmosphere. MLO-Y4 medium was then removed and MC3T3-E1(14) cells ($1.5x10^5$ cells/well, page 50) were then layered on top of the collagen gels in DMEM GlutaMAX™ supplemented with 100 U/ml penicillin, 100 µg/ml streptomycin and 5 % DFBS. Co-cultures were kept for up to 7 days and medium was changed every 2-3 days.

2.3.5 Molecular biology

2.3.5.1 RNA extraction from 3D co-cultures

Total RNA was extracted from 3D co-cultures using TRIzol® reagent according to the manufacturer's protocol except with a 2-propanol incubation of 1 hr at -80 ºC. Surface zone cells were treated with 0.5 ml TRIzol® for exactly 10 sec, and deep zone cells with 1 ml TRIzol®, until the collagen gel was completely dissolved, by re-suspending with a pipette. Briefly, 0.2 ml of chlorophorm was added per 1 ml of TRIzol®, samples shaken, centrifuged (12,000 rpm, 15 min, 4ºC), and aqueous phase precipitated with 0.5 ml 2-propanol per 1 ml of TRIzol® (1 hr, -80 ºC) before centrifugation (12,000 rpm, 10 min, 4ºC). RNA pellets were washed with 1 ml 75 % ethanol, centrifuged (7,500 rpm, 5 min, 4ºC), and pellets dried and redissolved in 50 µl DEPC-treated water. Isolated total RNA was DNase-treated using DNA-free™

according to the manufacturer's instructions to remove DNA contamination. Total RNA was then re-precipitated to ensure the removal of all organic contaminants. Briefly, 0.1 volume of 3M sodium acetate (CH_3COONa, pH 5.5) and 3 volumes of ice-cold 100 % ethanol were added to each sample and incubated for 1 hr at -80ºC or o/n at -20ºC. Samples were resuspended by vortexing and centrifuged (7,500 rpm, 4ºC, 5 min). Supernatant was decanted and pellets dried at rt. Finally, pellets were dissolved in DEPC-treated water (25 µl for surface zone; 50 µl for deep zone) and incubated for 10 min at 55ºC. All RNA samples were then used immediately or stored at -80ºC until needed.

2.3.5.1.1 Estimation of RNA concentration and purity

Total RNA was quantified after precipitation using a NanoDrop (page 48). All measurements were done against a blank of DEPC-treated water. RNA purity was indicated by the 260 nm/280 nm (A_{260}/A_{280}) absorbance ratio for the presence of protein contaminants; and the 260 nm/230 nm (A_{260}/A_{230}) absorbance ratio for the presence of carbohydrates, salts and phenol. Pure RNA has an A_{260}/A_{280} ratio of 2.0 and an A_{260}/A_{230} ratio of 1.8-2.2. Samples with A_{260}/A_{280} and A_{260}/A_{230} ratios of $\geq$1.8 were deemed of good quality.

2.3.5.2 DNA extraction from 3D co-cultures

Total DNA was extracted from 3D co-cultures using TRIzol® reagent according to the manufacturer's protocol. Surface and deep zone cells were treated with TRIzol® as described in page 52. Briefly, 0.2 ml of chlorophorm was added per 1 ml of TRIzol®, samples shaken and centrifuged (12,000 rpm, 15 min, 4ºC). The aqueous phase was removed for RNA extraction (page 52) and the DNA in the interphase and organic phase precipitated with 0.3 ml 100 % ethanol (4°C) per 1 ml TRIzol® (2-3 min, rt) before centrifugation (2,000 rpm, 5 min, 4ºC). DNA pellets were washed with 1 ml 0.1 M sodium citrate in 10 % ethanol per 1 ml TRIzol® (30 min, rt, with periodic mixing) and centrifuged (2,000 rpm, 5 min, 4ºC). The DNA pellets were washed twice and then resuspended with 1.5 ml 75 % ethanol per 1 ml TRIzol® (20 min, rt, with periodic mixing) before centrifugation (2,000 rpm, 5 min,

4ºC). DNA pellets were dried and redissolved in 50 µl diethylpyrocarbonate (DEPC) treated water by incubating at 37°C o/n.

2.3.5.2.1 Estimation of DNA concentration

Total DNA was quantified after precipitation using a Quant-iT™ dsDNA High-Sensitivity Assay Kit following the manufacturer's instructions. Briefly Quant-iT™ dsDNA HS reagent (contents are trade secret, CTS) was diluted (1:200) in Quant-iT™ dsDNA HS buffer (CTS) in a plastic container, and 200 µl of the working solution added to the appropriate wells of a microplate. 10 µl of λ DNA standards (0-100 ng/µl) (CTS) and experimental samples were added to the corresponding wells and mixed well. The plate was read immediately using a plate reader (page 49) at 510/527 nm fluorescein wavelength. Fluorescence was recorded using the provided software (page 49). The standard curve was used to determine DNA concentration of the experimental samples. An example of a DNA standard curve can be found in page 270. The sensitivity of the assay was 0.5 ng/µl and was calculated by adding two standard deviations to the mean absorbance value of 0 ng/µl standard replicates and then determining the concentration from the standard curve.

2.3.5.3 Reverse Transcriptase-Polymerase Chain Reaction (RT-PCR)

2.3.5.3.1 Reverse transcription

Total RNA was reverse transcribed to make complementary DNA (cDNA) using SuperScript® III Reverse Transcriptase according to manufacturer's protocol. Quantities of RNA reverse transcribed varied between 0.2-29.8 ng/µl for the surface zone of the model and 12.8-219.4 ng/µl for the deep zone of the model. Briefly, total RNA (8.5 µl) was mixed with 2.5 mM dNTPs and 250 ng of random primers and incubated for 5 min at 65°C and then placed on ice for 2 min. 5X first strand synthesis buffer, 0.1M dithiothreitol (DTT), 40 units Recombinant RNasin® Ribonuclease Inhibitor and 200 units SuperScript® III Reverse Transcriptase were added in a total reaction volume of 20 µl. The reverse transcription reaction was carried out (25°C for 5 min, 50°C for 50 min and 70°C for 15 min), and held at 4ºC

on a thermal cycler (page 48). Samples were used immediately or stored at -20ºC until needed.

2.3.5.3.2 Standard PCR

After reverse transcription, PCR was carried out for non-quantitative amplifications in 25 µl reactions containing 1.5-3.5 mM magnesium chloride ($MgCl_2$), 0.2 µM of each forward and reverse primer, GoTaq® Flexi buffer (pH 8.5), 200 nM dNTPs and 1 unit GoTaq® Flexi DNA polymerase. Using a thermal cycler (page 48), after an initial denaturation step of 3 min at 95°C, samples were amplified for 30-40 cycles at 95°C for 30 sec, 55-66°C for 30 sec (annealing) and 72°C for 30 sec (extension) followed by a final extension step for 10 min at 72°C. Samples were held at 4ºC before the products were separated by agarose gel electrophoresis. Each gene assay was optimised by varying cycle number (30-40), $MgCl_2$ concentration (1.5-3.5 mM), primer concentration (0.02 µM, 0.1 µM and 0.2 µM), and annealing temperature (55-66°C). No template (water blank) and positive controls were included in all reactions.
As a result, these conditions varied between optimised primer pairs (Tables 2.1 and 2.2). PCR was also carried out for 18S ribosomal RNA (18S rRNA) to check the integrity of cDNA.

2.3.5.3.3 Agarose gel electrophoresis

PCR products were separated in 2 % agarose gels containing SafeView nucleic acid stain at 10 µl/100 ml. Gel electrophoresis was carried out in 1X TBE (appendix 9.2) buffer together with a low molecular weight DNA ladder spanning 25-766 base pairs (bp) (page 268). Gels were visualised and photographed under ultraviolet (UV) light (page 48).

2.3.5.3.4 Quantitative PCR (qPCR)

qPCR reactions were carried out using SYBR® Green I fluorescent dye which binds to all double stranded DNA. The fluorescence signal of the dye increases proportionally as more double stranded DNA accumulates during amplification. The

threshold of this increase was automatically set to the centre of the logarithmic phase of the amplification curve for each gene (qPCR software, page 48). As a result, a cycle threshold value (Ct), i.e. the cycle number at which the fluorescence crosses the threshold, was generated. Following amplification, the PCR products are melted during a dissociation cycle. The decrease in fluorescence with increasing temperature gives a dissociation curve of the specificity of the reaction, as the dissociation temperature depends on the length and sequence of the product.

Using a Real-Time PCR System (page 48), polypropylene RT-qPCR plates and optical strip caps, amplifications were carried out for each cDNA sample in 25 µl reactions. Each reaction contained 0.1 or 0.2 µM forward and reverse primers (Tables 2.1 and 2.2), 12.5µl of 2X JumpStart™ Taq ReadyMix™ with SYBR® Green I dye, 2.5 or 3.5 mM $MgCl_2$ (Tables 2.1 and 2.2), 1 µl of cDNA and DEPC-treated water to make up the reaction volume to 25 µl. Thermocycling consisted of 10 min denaturation cycle at 95°C, followed by 40 cycles of 95°C for 30 sec, 60°C for 30 sec (annealing), 72°C for 30 sec (extension) and one dissociation cycle at 95°C for 1 min, 55°C for 1 min and 95°C for 30 sec. Results were analysed using the qPCR Software (page 48).

2.3.5.3.4.1 cDNA standard curves

Standard curves were performed to assess the efficiency and linear range of detection for all primers and optimise their reaction conditions. Stock MLO-Y4 or MC3T3-E1(14) cDNA (1-5 µg RNA reverse transcribed) was serially diluted 1:10 in DEPC-treated water giving a range of cDNA concentrations from 10^1 (stock) to 10^{-6} or 1:5 to give a range of cDNA concentrations from 10^1 (stock) to $6.4x10^{-5}$. Each gene assay was optimised by varying $MgCl_2$ concentrations (2.5 and 3.5 mM) and primer concentrations (0.1 and 0.2 µM). Standard curves of 90-110 % efficiency and with an R^2 value of ≥0.99 were accepted as valid. An example of a standard curve can be found in page 268.

2.3.5.3.4.2 Reference genes (RG)

RGs act as internal controls when performing RT-qPCR. Ideally, a RG would be universally recognised and should have constant expression levels regardless of sample, treatment and experimental design. However, several studies have shown that no such gene has been found (Thellin et al., 1999, Bustin, 2000, Schmittgen and Zakrajsek, 2000, Suzuki et al., 2000, Warrington et al., 2000, Bustin, 2002, Tricarico et al., 2002) and reported expression variation of RGs (Thellin et al., 1999, Bustin, 2000, Suzuki et al., 2000, Tricarico et al., 2002, Bemeur et al., 2004, Sugden et al., 2010). Therefore, identification and validation of a stable RG for each experimental design is important.

In all cases, RT-qPCR was carried out using three RGs, 18S rRNA, glyceraldehyde 3-phosphate dehydrogenase (GAPDH) and hypoxanthine-guanine phosphoribosyltransferase (HPRT1). The most stable RG was determined via NormFinder. Expression data for each gene in an experiment were transformed from $\log_{10}$ to linear scale using a standard curve and then loaded into the NormFinder Microsoft Excel Add-In (http://www.mdl.dk/publicationsnormfinder.htm) (Andersen et al., 2004). NormFinder, is a mathematical algorithm which finds the best RG or combination of two genes from a set of candidates by ranking them according to expression stability in a given sample set and experimental design (Andersen et al., 2004). This algorithm works by calculating the intragroup variation, e.g. differences in expression within all surface zone and all deep zone samples, and the intergroup variation, e.g. differences in expression between surface zone and deep zone samples (Andersen et al., 2004). The intra- and intergroup variation values are then combined to give a stability value which represents the systematic error that will occur when using a particular RG. This approach then ranks the top three genes and combination of two genes with minimum intra- and intergroup variation and provides a stability value for the best gene (Andersen et al., 2004). The top ranked gene or combination of two genes, combined by calculating the geometric mean, was used for normalisation and is clearly stated in the methods section of the appropriate experimental chapter and relevant figure legends of this thesis.

2.3.5.3.4.3 Relative RT-qPCR

Relative quantification involves normalising the expression of the gene of interest to that of a stable RG in a particular sample, e.g. treated sample, and then calibrating this expression to a reference sample, e.g. an untreated control. The experimental sample group used as calibrators is clearly stated in the methods section of the corresponding chapters. This method requires that both primer sets for the RG and the gene of interest have similar efficiencies (90-110 %) for all samples. Relative quantitation of RT-qPCR products was calculated using the $2^{(-\Delta\Delta Ct)}$ method as described by (Livak and Schmittgen, 2001). Briefly, the appropriate RG was determined as in page 57, then for each experimental sample the Ct value of the RG was subtracted from the Ct value of the gene of interest (GOI) ($Ct_{GOI} - Ct_{RG}$). This gives normalised values called delta Ct (ΔCt). Then, the ΔCt for each experimental sample was subtracted from the ΔCt of the chosen calibrator, giving a delta-delta Ct value (ΔΔCt) resulting in values expressed relative to the calibrator. Finally, all ΔΔCt values were converted to Relative Expression Units (REU) by $2^{(-\Delta\Delta Ct)}$. Means, Standard Deviation (STDEV) and Standard Error of the Mean (SEM) were obtained from the REU values.

2.3.5.4 Primer design

Primers were designed for known gene sequences (http://www.ncbi.nlm.nih.gov/gene) using the Primer-BLAST option from the National Center for Biotechnology Information (NCBI) website (http://www.ncbi.nlm.nih.gov), unless otherwise stated. Primer-BLAST uses the Primer 3 web-based program (http://primer3.sourceforge.net/) to design PCR primers and then uses BLAST (Basic Alignment Search Tool) and a global alignment algorithm to avoid primer pairs that may cause non-specific amplifications. Primer-BLAST also ensures similar melting temperatures and GC % content, minimum primer-dimer formation and excludes 3' end complementation. For each gene, except OCN, primers spanned an intron in order to discriminate genomic DNA products and amplicon sizes were between 100-150 bp. Accession number, nucleotide sequences, amplicon size and source for each primer used can be found in Tables 2.1 and 2.2.

Table 2.1 *Primer details for RGs and bone markers with their optimum conditions for RT-PCR and RT-qPCR*

Gene	Primers (5'-3')	Amplicon size (bp)	PCR conditions			qPCR conditions		Source
			[Primers] & [$MgCl_2$]	Cycle Nº	Tm (ºC)	[Primers] & [$MgCl_2$]	Tm (ºC)	
GAPDH NM_008084.2	Fwd - GACGGCCGCATCTTCTTGTGCA Rev - TGCAAATGGCAGCCCTGGTGAC	114	0.2 µM Primers 2.5 mM $MgCl_2$	32	60	0.1 µM Primers 3.5 mM $MgCl_2$	60	Primer-BLAST
18S rRNA NR_003278.3	Fwd - GCAATTATTCCCCATGAACG Rev - GGCCTCACTAAACCATCCAA	125	0.2 µM Primers 2.5 mM $MgCl_2$	30	60	0.2 µM Primers 3.5 mM $MgCl_2$	60	Dr Sophie Gilbert
HPRT1 NM_013556.2	Fwd - CGTGATTAGCGATGATGAACCAGGT Rev - CCATCTCCTTCATGACATCTCGAGC	149	0.2 µM Primers 2.5 mM $MgCl_2$	35	55	0.1 µM Primers 2.5 mM $MgCl_2$	60	Primer-BLAST
COL1A1 NM_007742.3	Fwd - ACTGCCCTCCTGACGCATGG Rev - TCGCACACAGCCGTGCCATT	140	0.2 µM Primers 2.5 mM $MgCl_2$	35	60	0.1 µM Primers 3.5 mM $MgCl_2$	60	Primer-BLAST
ALP NM_007431.2	Fwd - GCTGGCCCTTGACCCCTCCA Rev - ATCCGGAGGGCCACCTCCAC	132	0.2 µM Primers 2.5 mM $MgCl_2$	35	64	0.1 µM Primers 2.5 mM $MgCl_2$	60	Primer-BLAST
SOST* NM_024449.5	Fwd - CCAAAGACGTGTCCGAGTACAG Rev - CACTGGCCGGAGCACAC	112	0.2 µM Primers 2.5 mM $MgCl_2$	40	66	NI	NI	Dr Karen Brakspear
E11 NM_010329.2	Fwd - AAGATGGCTTGCCAGTAGTCA Rev - GGCGAGAACCTTCCAGAAAT	118	0.2 µM Primers 2.5 mM $MgCl_2$	35	60	0.2 µM Primers 3.5 mM $MgCl_2$	60	Dr Deborah Mason
OCN NM_007541.2	Fwd - CCGCCTACAAACGCATCTAT Rev - TTTTGGAGCTGCTGTGACAT	153	0.2 µM Primers 2.5 mM $MgCl_2$	35	60	0.1 µM Primers 3.5 mM $MgCl_2$	60	Primer-BLAST
Runx2 NM_001145920.2	Fwd - GACGAGGCAAGAGTTTCACC Rev - GTCTGTGCCTTCTTGGTTCC	120	0.2 µM Primers 2.5 mM $MgCl_2$	35	58	0.1 µM Primers 2.5 mM $MgCl_2$	60	Dr Deborah Mason
RANKL NM_011613.3	Fwd - CGCTCTGTTCCTGTACTTTCGAGC Rev - TCGAGTCCTGCAAATCTGCGTTTT	116	0.2 µM Primers 2.5 mM $MgCl_2$	35	55	0.2 µM Primers 2.5 mM $MgCl_2$	60	Primer-BLAST
OPG NM_008764.3	Fwd - GAGTGTGAGGAAGGGCGTTAC Rev - GCAAACTGTGTTTCGCTCTG	111	0.2 µM Primers 2.5 mM $MgCl_2$	40	55	0.2 µM Primers 2.5 mM $MgCl_2$	60	Dr Deborah Mason
SV40 large T-antigen YP_003708382.1	Fwd - AGGGGGAGGTGTGGGAGGTTTT Rev - TCAGGCCCCTCAGTCCTCAC	100	0.2 µM Primers 2.5 mM $MgCl_2$	35	64	0.1 µM Primers 2.5 mM $MgCl_2$	60	Primer-BLAST

*Optimised conditions for femur cDNA (positive control) only; NI: not investigated.

Table 2.2 *Primer details for adenosine, calcium-sensing and glutamate receptors and transporters with their optimum conditions for RT-PCR and RT-qPCR*

Gene	Primers (5'-3')	Amplicon size (bp)	PCR conditions			qPCR conditions		Source
			[Primers] & [$MgCl_2$]	Cycle Nº	Tm (ºC)	[Primers] & [$MgCl_2$]	Tm (ºC)	
A_1* NM_001008533.2	Fwd - GATCGGTACCTCCGAGTCAA Rev - TTGGCTATCCAGGCTTGTTC	160	0.2 µM Primers 2.5 mM $MgCl_2$	35	60	NI	NI	Dr Bronwen Evans
A_{2A} NM_009630.2	Fwd - GGCTATTGCCATCGACAGAT Rev - ATGGGTACCACGTCCTCAAA	228	0.2 µM Primers 2.5 mM $MgCl_2$	35	62	0.2 µM Primers 2.5 mM $MgCl_2$	60	Dr Bronwen Evans
A_{2B} NM_007413.4	Fwd - TGCTCACACAGAGCTCCATC Rev - AGTCAATCCAATGCCAAAGG	158	0.2 µM Primers 2.5 mM $MgCl_2$	35	60	0.1 µM Primers 3.5 mM $MgCl_2$	60	Dr Bronwen Evans
A_3* NM_001174169.1	Fwd - TCCCTGATTACCACGGACTC Rev - TCCTTCTGTTCCCCACATTC	151	0.2 µM Primers 2.5 mM $MgCl_2$	40	60	NI	NI	Dr Bronwen Evans
CaSR (exons 6-7)* NM_013803.2	Fwd - GTGGTGAGACAGATGCGAGT Rev - GCCAGGAACTCAATCTCCTT	100	0.2 µM Primers 2.5 mM $MgCl_2$	35	55	NI	NI	(Chang et al., 2008a)
AMPAR2 NM_001083806.1	Fwd - GGAAGTAAGGAAAAGACCAGTGCCCTC Rev - TTGCCAAACCAAGGCCCCCG	85	0.2 µM Primers 2.5 mM $MgCl_2$	40	60	0.2 µM Primers 2.5 mM $MgCl_2$	NI	Dr Cleo Bonnet
KA1 NM_146072.4	Fwd - GAACTTGGGATGGTGTCAGC Rev - AGAAAGCATGGGATTGGTTG	135	0.2 µM Primers 2.5 mM $MgCl_2$	40	60	0.1 µM Primers 3.5 mM $MgCl_2$	NI	Dr Cleo Bonnet
mGluR1* NM_016976.3	Fwd - TGGGCGAGTTCTCACTCATT Rev - TTCCTTGTGTTGGTGTCCAG	169	0.2 µM Primers 2.5 mM $MgCl_2$	40	60	NI	NI	Dr Cleo Bonnet
GLAST1 NM_148938.3	Fwd - GGTCACTGCTGTCATTGTGG Rev - AGCATCTGCAGCATCCTCAT	123	0.2 µM Primers 2.5 mM $MgCl_2$	40	60	0.1 µM Primers 2.5 mM $MgCl_2$	60	Dr Karen Brakspear
EAAC1 NM_009199.2	Fwd - ATCCAGCATGATCACAGGTG Rev - TTACAGCAATGACGGTGGTG	104	0.2 µM Primers 2.5 mM $MgCl_2$	40	60	NI	NI	Dr Karen Brakspear

*Optimised conditions for femur cDNA (positive control) only; NI: not investigated.

2.3.5.5 Plasmid preparations for cloning

RT-PCR products from each of the primer pairs used (Tables 2.1 and 2.2) were cloned and sequenced to confirm primer and target specificity.

2.3.5.5.1 Purification of DNA from gel

PCR products from each gene amplification reaction were excised from an agarose gel using sterile scalpels under UV light and weighed in 1.5 ml microcentrifuge tubes. DNA was extracted and purified using a QIAquick Gel Extraction Kit according to manufacturer's instructions. Briefly, PCR products were incubated at 50ºC for 10 min in Buffer QG (CTS) to dissolve the gel. DNA was mixed with 2-propanol (1 volume) and bound using QIAquick columns with collection tubes by centrifugation (1 min). 0.5 ml of Buffer QG was added and columns centrifuged (1 min). DNA was washed with Buffer PE (0.75 ml, CTS), centrifuged (1 min) and any remaining Buffer PE was removed by a further centrifugation step (1 min). Finally, DNA was eluted into 1.5 ml microcentrifuge tubes with 30 µl DEPC-treated water by centrifugation (1 min). All centrifugation steps were carried out at 13,000 rpm and rt.

2.3.5.5.2 Cloning into pGEM ®-T vector

DNA (5-11.4 ng, according to primer pair amplicon size) was ligated into 50 ng pGEM®-T plasmid vector (page 269), o/n at 4ºC, in the presence of 3 units of T4 DNA ligase and Rapid Ligation Buffer (containing 30 mM Tris-HCl pH 7.8, 10 mM $MgCl_2$, 10 mM DTT, 1 mM ATP, 5 % polyethylene glycol) in a 10 µl reaction volume.

2.3.5.5.3 Transformation into E. coli competent cells

Ligation reactions were transformed into 25 µl *E. coli* JM109 competent cells according to manufacturer's protocol by incubating on ice for 20 min and then heat-shocking for 50 sec at 42ºC. Reactions were then incubated on ice (2 min) before

adding super optimal broth with catabolite repression (SOC) medium (475 µl) and incubating for 1.5 hr at 37°C with shaking (150 rpm). 100 µl of each transformation was then plated onto lysogeny broth (LB) agar plates (containing 100 µg/ml ampicillin, 500 µg/ml IPTG and 100 µg/ml X-gal) (page 267) and incubated o/n at 37°C. Recombinant (white) colonies were picked at random and directly screened for inserts by PCR (page 55, primers as in Table 2.1 and 2.2) using a 10 min 95°C denaturation step to lyse all cells. Positive colonies were grown in LB broth (containing 100 µg/ml ampicillin) (page 267) o/n at 37°C with shaking (150 rpm).

2.3.5.5.4 Plasmid DNA purification

Plasmid DNA was purified from recombinant colony broth cultures using a Wizard® Plus SV Miniprep Kit following the manufacturer's instructions. Briefly, 5 ml broth cultures were pelleted by centrifugation (5 min), supernatant discarded and pellets thoroughly resuspended with Cell Resuspension Solution (250 µl, CTS). Cell Lysis Solution (250 µl, CTS) was then added and mixed. Alkaline Protease Solution (10 µl, CTS) was mixed and samples were then incubated (5 min). Neutralisation Solution (350 µl, CTS) was mixed with samples before centrifugation (10 min). Plasmid DNA was bound by using Spin Columns with collection tubes and by centrifugation (1 min). Samples were washed with Wash Solution (750 µl, CTS) and centrifuged (1 min). Samples were washed for a second time with Wash Solution (250 µl, CTS) and centrifuged (2 min). DNA was eluted into a clean 1.5 ml microcentrifuge tube with 100 µl DEPC-treated water by centrifugation (1 min). All mixing steps were done by inverting 4 times. All centrifugation steps were done at 13,000 rpm and at rt.

2.3.5.5.5 DNA sequencing

pGEM®-T cloned inserts were sequenced by the Cardiff University Molecular Biology Unit DNA sequencing core facility using T7 forward and SP6 reverse primers. nBLAST (nucleotide collection BLAST) was then used to check the identity of the insert sequence with the target sequence.

2.3.6 Microscopy

2.3.6.1 Light microscopy

Monolayer cultures were observed using an inverse-light microscope and images taken with a Coolpix 4500 camera prior to incorporation into gels (page 48). For the duration of each experiment, 3D collagen co-cultures were observed every day, as above, at random fields of view across gel depth and imaged as above at various time points.

2.3.6.2 Specimen preparation for cryosection imaging

3D collagen co-cultures were washed with phosphate buffered saline (PBS) (page 267), fixed with 1 % paraformaldehyde (PFA) (page 267) for 30 min at 4°C and then washed 3-4 times with PBS over 2 days at 4°C. They were then infiltrated with a 1:1 dilution of OCT mounting media compound for cryotomy in PBS o/n at 4°C in order to reduce ice crystal formation. Specimens were removed from wells and cut into quarters (Figure 2.1A) which were then orientated into square plastic moulds; embedded in OCT compound and frozen in 2-methyl butane, previously cooled in dry ice. Specimens were then transferred to a cryostat, removed from the mould and mounted on a cryostat chuck by freezing with OCT compound. 20 µm transverse sections (Figure 2.1B), showing the surface zone down to the bottom of the collagen gel (Figure 2.1C), were cut using a cryostat (page 48) and placed on poly-lysine coated slides (Figure 2.1D). Sections were stored at -20°C until needed.

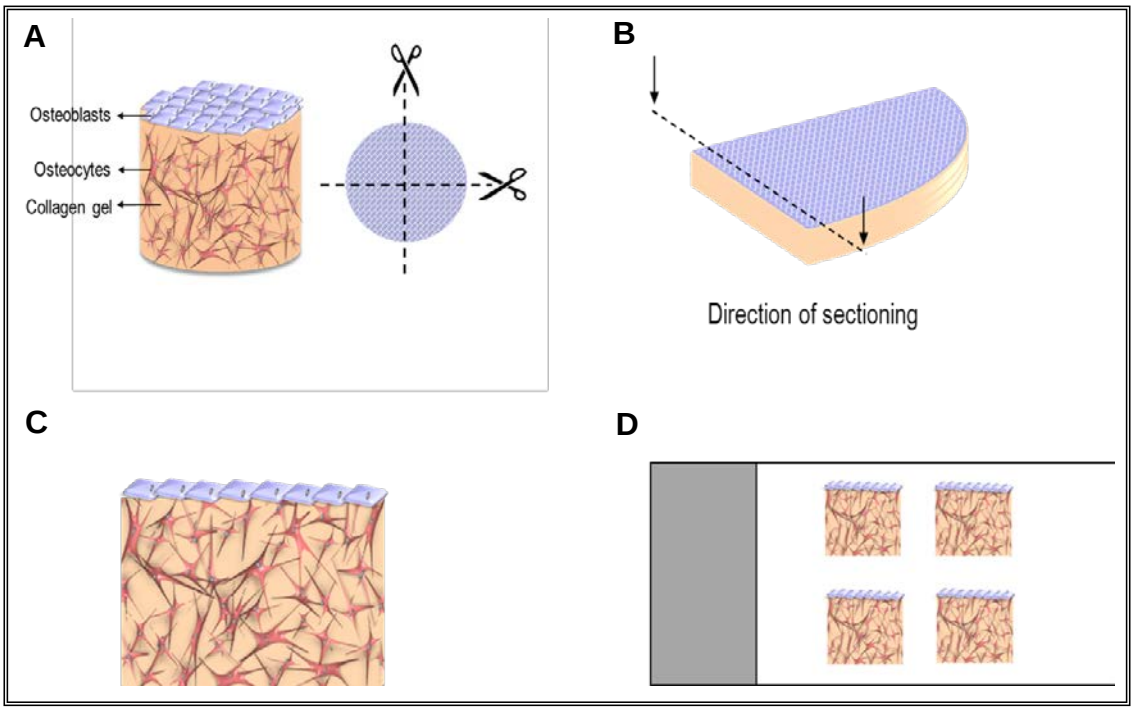

Figure 2.1 *Processing of 3D co-cultures for cryosectioning.* A) Diagram showing a 3D co-culture cut into quarters looking down on the surface zone (osteoblasts). B) Position of a 3D co-culture quarter indicating the direction of cryosectioning to give transverse sections which also show cells from the outside into the middle of the 3D co-culture. C) Transverse section of a 3D co-culture showing the full depth of the gel. D) Position of cryosections in a poly-lysine coated slide.

2.3.6.3 Immunolocalisation and histochemistry

Details on blocking sera, primary and secondary antibodies and nonimmune immunoglobulins used, including concentrations and incubation times, can be found in Tables 2.3 and 2.4. For all immunolocalisation 4-6 sections of each replicate co-culture were observed.

2.3.6.3.1 Immunocytochemistry

2.3.6.3.1.1 Quenching of endogenous peroxidases

Hydrophobic rings were drawn around each cryosection on poly-lysine coated slides using an ImmEdge pen. Cryosections were then rehydrated in PBS 0.1 % TWEEN® 20 (PBST), incubated in 0.3 % hydrogen peroxide (H_2O_2) in PBST for 30 min to block endogenous peroxidase activity and washed in PBST (3 times in 5 min).

2.3.6.3.1.2 Primary and secondary antibody application

For immunostaining with a secondary antibody conjugated to horseradish peroxidase (HRP), sections were blocked for non-specific binding with serum and incubated with primary antibody (Table 2.3). The primary antibody was replaced in control sections with PBST alone as a control for general non-specific binding of the procedure, or with nonimmune immunoglobulins (Table 2.3), to show non-specific binding that may result from the primary antibody. All sections were then washed (page 65) and incubated with the corresponding secondary antibody. Washing in PBST was then repeated (page 65).

For immunostaining using a Vectamount Universal Elite ABC kit, sections were treated with primary antibody or controls as above. After washing in PBST (3 times in 5 min), following manufacturer's instructions, sections were incubated with biotinylated secondary antibody (CTS) for 30 min (Table 2.3), washed (PBST, 3 times in 5 min), and incubated with ABC reagent (100 µl Reagent A, avidin DH

solution) and 100 µl Reagent B (biotinylated enzyme, usually HRP or alkaline phosphatase) mixed together in 5 ml PBST) for 30 min. Washing was repeated as previously described.

2.3.6.3.1.3 Disclosure

All immunostaining was detected by incubating 2-5 min at rt with nickel-enhanced DAB, which acts as a substrate to the HRP or biotinylated enzyme by binding to the secondary antibody. DAB is then oxidised giving a visible brown colour or a grey-black colour if the reaction is nickel-enhanced. Briefly, 2 drops of Buffer Stock Solution (CTS), 4 drops of DAB Stock Solution (CTS), 2 drops of Hydrogen Peroxide Solution (CTS) and 2 drops of Nickel Solution were added to 5 ml of distilled water and mixed well. The reaction was stopped by washing the slides in tap water (3 times in 5 min). All slides were dehydrated in alcohols and cleared in xylene before mounting with DPX. Slides were left to dry o/n before imaging with a digital camera attached to a light microscope, and analysed with the software provided (page 49). All controls, where primary antibodies were omitted or substituted with nonimmune immunoglobulins, showed no labelling.

2.3.6.3.2 Immunofluorescence

For immunostaining with a secondary antibody conjugated to a fluorescent dye, hydrophobic rings were drawn around cryosections (page 65), rehydrated (page 65) and blocked (page 65). Cryosections were either incubated with primary antibody or with PBST or non-immune immunoglobulins as negative controls (Table 2.4), washed (PBST, 3 times in 5 min) and incubated with a secondary antibody conjugated to a fluorescent dye (Table 2.4). Cryosections were washed (PBST, 3 times in 5 min), and mounted with Fluoroshield™ with DAPI as a nuclear counterstain. For immunofluorescence of CaSR, cryosections were incubated with 50 mM ammonium chloride (NH_4Cl) in PBS for 10 min prior to blocking and all washing steps consisted of 4 washes in PBS for 5 min each (personal communication with Mr Martin Schepelmann). Results were analysed with an epi-fluorescence microscope with the provided software (page 48), except for CX43 results which were analysed by confocal microscopy (page 72).

Table 2.3 *Immunocytochemistry conditions.*

Protein	Primary antibody	Secondary antibody	Immunoglobulins control	Block
E11 (#)	2.5 µg/ml anti-mouse E11 (podoplanin) antibody (goat polyclonal) *o/n at 4°C*	1:800 rabbit anti-goat (HRP conjugated) *30 min at rt*	2.5 µg/ml goat IgG *o/n at 4°C*	5 % normal rabbit serum *20 min*
EAAC1 (^)	5 µg/ml anti-rat EAAC1 IgG (rabbit polyclonal) *o/n at 4°C*	1:100 goat anti-rabbit (HRP conjugated) *30 min at rt*	5 µg/ml rabbit IgG *o/n at 4°C*	5 % normal goat serum *20 min*
GLAST1 (^)	5 µg/ml anti-rat glutamate transporter (GLAST1) antiserum 1 (rabbit polyclonal) *o/n at 4°C*	1:100 goat anti-rabbit (HRP conjugated) *30 min at rt*	5 µg/ml rabbit IgG *o/n at 4°C*	5 % normal goat serum *20 min*
KA1* (^)	0.156 µg/ml anti-KA1 antibody (rabbit polyclonal) *o/n at 4°C*	7.5 µg/ml anti-rabbit biotinylated antibody in PBST with 1.5 % serum *30 min at rt*	0.156 µg/ml rabbit IgG *o/n at 4°C*	1.5 % normal goat serum *20 min*
mGluR1 (~)	5 µg/ml anti-mGluR1 antibody (rabbit polyclonal) *o/n at 4°C*	1:100 goat anti-rabbit (HRP conjugated) *30 min at rt*	5 µg/ml rabbit IgG *o/n at 4°C*	5 % normal goat serum *20 min*
Adenosine receptor A_1 (+)	2.5 µg/ml anti-adenosine A_1 receptor antibody (rabbit polyclonal) in 5 % mouse serum *o/n at 4°C*	1:100 goat anti-rabbit (HRP conjugated) *30 min at rt*	2.5 µg/ml rabbit IgG in 5 % mouse serum *o/n at 4°C*	5 % normal goat serum *20 min*
Adenosine receptor A_{2A} (+)	2.5 µg/ml anti-adenosine receptor A_{2A} antibody (rabbit polyclonal) in 5 % mouse serum *o/n at 4°C*	1:100 goat anti-rabbit (HRP conjugated) *30 min at rt*	2.5 µg/ml rabbit IgG in 5 % mouse serum *o/n at 4°C*	5 % normal goat serum *20 min*
Adenosine receptor A_{2B} (+)	5 µg/ml anti-human A_{2B}R IgG (rabbit polyclonal) in 5 % mouse serum *o/n at 4°C*	1:100 goat anti-rabbit (HRP conjugated) *30 min at rt*	5 µg/ml rabbit IgG in 5 % mouse serum *o/n at 4°C*	5 % normal goat serum *20 min*
Adenosine receptor A_3 (+)	5 µg/ml anti-rat A_3R IgG (rabbit polyclonal) in 5 % mouse serum *o/n at 4°C*	1:100 goat anti-rabbit (HRP conjugated) *30 min at rt*	5 µg/ml rabbit IgG in 5 % mouse serum *o/n at 4°C*	5 % normal goat serum *20 min*

*Avidin-biotin complex was added after secondary antibody (30 min at rt). Primary antibodies were kind gifts from (#) Dr Bronwen Evans, (^) Dr Cleo Bonnet (School of Bioscience, Cardiff University, UK), (~) Prof Daniela Riccardi (School of Bioscience, Cardiff University, UK) and (+) Dr Jack Ham (School of Medicine, Cardiff University, UK). All dilutions were in PBST unless otherwise stated.

Table 2.4 *Immunofluorescence conditions.*

Protein	Primary antibody	Secondary antibody	Immunoglobulins control	Block
Type I collagen (-)	5 µg/ml anti-type I collagen (mouse monoclonal) *1 hr at rt*	5 µg/ml goat anti-mouse (Alexa Fluor 594) *1 hr at rt*	5 µg/ml mouse IgG *1 hr at rt*	5 % normal goat serum *20 min*
CX43 (-)	5 µg/ml anti-connexin 43 (mouse monoclonal) *o/n at 4°C*	2.5 µg/ml horse anti-mouse (Dylight 594) *1 hr at rt*	0.25 µg/ml mouse IgG *o/n at 4°C*	5 % normal horse serum *20 min*
SV40 large T-antigen	5 µg/ml anti-SV40 T-antigen antibody (mouse monoclonal) *1 hr at rt*	5 µg/ml horse anti-mouse (Dylight 594) *1 hr at rt*	5 µg/ml mouse IgG *1 hr at rt*	5 % normal horse serum *20 min*
CaSR (~)	2 µg/ml anti-CaSR (rabbit polyclonal) diluted in 0.1 % (v/v) Triton X100 with 1 % (w/v) BSA in PBS *o/n at 4°C*	4 µg/ml goat anti-rabbit (Alexa Fluor 594) diluted in 0.1 % (v/v) Triton X100 with 1 % (w/v) BSA in PBS *1 hr at rt*	2 µg/ml rabbit IgG diluted in 0.1 % (v/v) Triton X100 with 1 % (w/v) BSA in PBS *o/n at 4°C*	0.1 % (v/v) Triton X100 with 1 % (w/v) BSA in PBS *1 hr at rt*

Primary antibodies were a kind gift from (-) Dr Jim Ralphs (School of Bioscience, Cardiff University, UK) and (~) Prof Daniela Riccardi. BSA: bovine serum albumin. All dilutions were in PBST unless otherwise stated.

2.3.6.4 Actin filament staining

Actin filament staining was performed in order to assess morphology of the surface and deep zones of the model by delineating the cytoskeleton of the cells. In all cases results were analysed by confocal microscopy (section 2.3.6.6).

2.3.6.4.1 Surface zone

The 3D co-cultures contain a layer of osteoblasts which could be easily lost whilst cryosectioning, therefore analysis of the surface zone was performed on whole gel quarters, as opposed to cryosections, as for the deep zone. Day 7 3D collagen co-cultures were fixed and washed (page 63), cut into quarters and directly placed in the middle of a 2 mm thick nylon washer (which served as a well) attached onto a poly-lysine coated slide. The gel quarters were stained o/n at 4°C with 5 µM phalloidin conjugated with Atto488 (Phalloidin-Atto488). They were then washed in PBST (3 times in 5 min) and mounted with Fluoroshield™ with DAPI as a nuclear counterstain and observed by looking directly down on to the gel surface (page 72). For analysis, 5 arbitrary regions of the surface zone of each replicate co-culture were observed.

2.3.6.4.2 Deep zone

Hydrophobic rings were drawn around day 7 3D co-culture cryosections (page 65), rehydrated (page 65), incubated with 5 µM Phalloidin-Atto488 (1 hr at rt), washed and mounted (page 67). For analysis, 4-6 sections of each replicate co-culture were observed (page 72).

2.3.6.5 Cell death

Ethidium homodimer is a membrane-impermeable fluorescent dye that is weakly fluorescent unless bound to DNA when it emits red fluorescence (Gaugain et al., 1978a, Gaugain et al., 1978b). The dye is generally used for viability assays as dead or dying cells have disrupted cell and nuclear membranes and therefore ethidium homodimer is able to penetrate and bind to DNA. The dye is not able to do this in live cells as their membranes are intact (Glazer et al., 1990).

DAPI is a fluorescent dye that binds strongly to A-T rich regions of double-stranded DNA and so emitting blue fluorescence. The dye can also bind to A-U rich regions in RNA but it is not as strongly fluorescent as when it binds DNA. DAPI is a membrane-permeable dye and therefore it can bind to DNA in both dead and live cells (Kapuscinski, 1995).

At day 1 and day 7, culture medium was removed and 3D collagen co-cultures were washed with PBS and then incubated with 1 µM ethidium homodimer in serum-free medium for 2 hr at 4°C with gentle agitation. This procedure was done to ensure the dye penetrates the depth of the gel whilst slowing down cell metabolism of the dye. Co-cultures were then incubated for a further 2.5 hr at 37°C in 5 % CO_2/95 % air atmosphere and washed o/n at 37°C in 5 % CO_2/95 % air atmosphere with culture medium containing serum. Positive control co-cultures were frozen for 1 hr at -20°C and thawed for 10 min, three times to ensure 100 % death, before treating with ethidium homodimer as above.

2.3.6.5.1 Surface zone

For cell death analysis of the surface zone, all 3D collagen co-cultures were fixed, washed, cut into quarters (page 63), placed directly into a 2 mm thick nylon washer attached onto a poly-lysine coated slide, and mounted (page 67). For analysis, 5 arbitrary regions of the surface zone of each replicate co-culture were observed using confocal microscopy (page 72).

2.3.6.5.2 Deep zone

For cell death analysis of the deep zone, 3D collagen co-cultures were washed with PBS, fixed, infiltrated with diluted OCT compound and cryosectioned (page 63). For analysis, 5 random slides of each replicate co-culture were rehydrated (page 65) and mounted (page 67). One random section from each slide was observed with a fluorescence microscope (page 48). DAPI (blue) labelled nuclei (total number of cells) and ethidium homodimer and DAPI (purple) labelled nuclei (number of dead cells) were counted across 10 fields of view per section at x20 magnification.

2.3.6.6 Confocal microscopy

Confocal microscopy was performed by Dr Anthony Hayes and Mr Marc Isaacs (School of Bioscience, Cardiff University) using a confocal scanning laser microscope (page 48). Specimens were observed either directly down onto the surface zone (actin filament stain, page 70, and cell death of surface zone, page 71) or by observing transverse cryosections (Figure 2.1) (deep zone actin filament stain, page 70 and CX43 immunofluorescence, page 67). Samples were scanned using appropriate excitation and emission settings for simultaneous recording of DAPI (358 $\text{Excitation}_{(max)}$, $\text{Ex}_{(max)}$, 461 $\text{Emission}_{(max)}$, $\text{Em}_{(max)}$) and Phalloidin-Atto488 (495 $\text{Ex}_{(max)}$, 519 $\text{Em}_{(max)}$) for actin filament staining; DAPI and ethidium homodimer (590 $\text{Ex}_{(max)}$, 617 $\text{Em}_{(max)}$) for cell death, or DAPI and Alexa 594 (590 $\text{Ex}_{(max)}$, 617 $\text{Em}_{(max)}$) for CX43 immunostaining. Specimens were optically sectioned using a x63 objective with an arbitrary zoom (surface and deep zone actin filament stain, and CX43 immunofluorescence) or x10 objective with a 2.32 zoom (surface zone cell death). 5 µm (surface zone) or 0.5 µm (deep zone) step size z-stack optical sections through the specimen were reconstructed using confocal software (page 48). Maximum intensity models were prepared showing detail of the surface zone or deep zone.

2.3.7 Protein assays

2.3.7.1 Lactate dehydrogenase assay (LDH)

LDH is an enzyme released naturally by cells into cell culture medium upon lysis as a result of cell death. LDH release can also be used to quantify cell number by purposely lysing the cultures in question. In this case LDH release is directly proportional to cell number. Culture supernatants from 3D MLO-Y4 mono-cultures were collected for analysis of LDH release as a result of cell death. For analysis of cell number, 3D MLO-Y4 mono-cultures were lysed by adding 200 µl of cell lysis buffer (9 % Triton™ X-100 in distilled water), frozen at -80°C for 1 hr, thawed and then incubated at 37°C for 45 min. The supernatant of the lysed cultures was then collected into a 1.5 ml microfuge and centrifuged (1000 rpm, rt, 5 min) to pellet cell debris, the clear lysate kept for analysis. LDH assay was carried out using a CytoTox 96® Non-Radioactive Cytotoxicity Assay following the manufacturer's instructions. Briefly, 50 µl of experimental samples were added to a 96-well plate followed by 50 µl of Substrate Mix (CTS). The plate was covered with foil and incubated in the dark at rt for 10-30 min according to the reaction. 50 µl of Stop Solution (CTS) was added and the plate read at 492 nm wavelength using a plate reader (page 49). If necessary, samples were diluted in order to avoid saturation of the assay. Dilutions of samples are clearly stated in the relevant experimental chapters.

2.3.7.2 ELISAs

2.3.7.2.1 PGE_2

PGE_2 ELISA was carried out using an Enzo Life Sciences PGE_2 kit following manufacturer's instructions. A dilution series of experimental samples defined the required dilutions for samples to fit within the standard curve of the assay, dilutions are clearly stated in the relevant experimental chapters. All experimental samples were within the standard curve. An example of a PGE_2 ELISA standard curve can be found in page 270. The sensitivity of the assay is 8.26 µl as stated by the manufacturer.

Briefly, 100 µl of experimental samples and standards (7.81-1000 pg/ml PGE_2 in standard diluent) were pipetted into the appropriate wells of the provided 96-well plate. Blue conjugate (50 µl, blue solution of alkaline phosphatase conjugated with PGE_2) was added to all wells except the Total Activity (TA) and Blank wells. Yellow antibody (50 µl yellow solution of monoclonal antibody to PGE_2) was added to all wells except the Blank, TA and non-specific binding (NSB) wells. The plate was covered and incubated (o/n, 4ºC). The plate was then emptied, and washed 3 times with Wash Solution (400 µl, 5 % Tris buffered saline with detergents in distilled water). Blue conjugate (5 µl) was added to the TA wells, pNpp Substrate Solution (200 µl, p-nitrophenyl phosphate (pNpp) in buffer) was added to all wells, the plate covered and incubated (1 h, 37ºC). Stop Solution (50 µl, trisodium phosphate in water) was added to all wells and the plate was read immediately using a plate reader (page 49) at 405 nm wavelength with correction between 570 and 590 nm to correct for optical imperfections in the plate. Absorbance was recorded using the provided software (page 49). The standard curve was used to determine PGE_2 concentration of the experimental samples. Data normalisation is clearly stated in the relevant experimental chapters.

2.3.7.2.2 IL-6

IL-6 ELISA was carried out using an R&D Systems DuoSet IL-6 ELISA kit, a kind gift from Dr Bronwen Evans, following the manufacturer's instructions. A dilution series of experimental samples defined the required dilutions for samples to fit within the standard curve of the assay, dilutions are clearly stated in the relevant experimental chapters. All experimental samples were within the standard curve range. An example of an IL-6 ELISA standard curve can be found in page 270.

Briefly, Capture Antibody (2 µg/ml in PBS of rat anti-mouse IL-6) was used to coat a 96-well microplate (100 µl/well, o/n, rt). Wells were aspirated and thoroughly washed 3 times with Wash Buffer (400 µl, 0.05 % TWEEN® 20 in PBS, pH 7.2-7.4), blocked with Reagent Diluent (300 µl, 1 % BSA in PBS, pH 7.2-7.4, 0.2 µm filtered), incubated (1 hr, rt) and washed. 100 µl of experimental samples and standards (15.62-1000 pg/ml, recombinant mouse IL-6 diluted in Reagent Diluent) was added in the appropriate wells, incubated (2 hr, rt), and washed before adding Detection Antibody (100 µl, 400 ng/ml biotinylated goat anti-mouse IL-6 diluted in Reagent Diluent). The plate was incubated (2 hr, rt) and washed. Streptavidin-HRP (100 µl, 1:200 streptavidin conjugated to HRP in Reagent Diluent) was added to each well, and the plate incubated in the dark (20 min, rt), and washed. Substrate Solution (100 µl, 1:1 mix of Colour Reagent A, H_2O_2 and Colour Reagent B, Tetramethylbenzidine, TMB) was added, and the plate incubated in the dark (20 min, rt), before adding Stop Solution (50 µl, 2 N sulphuric acid, H_2SO_4). The plate was read using a plate reader (page 49) at 450 nm wavelength with wavelength correction at 540 nm and 570 nm to correct for optical imperfections of the plate. The absorbance was recorded using the provided software (page 49). The standard curve was used to determine IL-6 concentration of the experimental samples. Data normalisation is clearly stated in the relevant experimental chapters.

2.3.7.2.3 PINP

PINP ELISA was carried out using an Immunodiagnostic systems Rat/Mouse PINP EIA kit, a kind gift from Dr Cleo Bonnet, following the manufacturer's instruction. A dilution series of experimental samples defined the required dilutions for samples to fit within the standard curve of the assay, dilutions are clearly stated in the relevant experimental chapters. All experimental samples were within the standard curve range. An example of a PINP ELISA standard curve can be found in page 270. The sensitivity of the assay was 0.7 ng/ml as stated by the manufacturer.

Briefly, 50 µl of experimental samples, controls (mouse serum in PBS with BSA and 0.025 % sodium azide) and standards (0-77 ng/ml, mouse PINP in PBS with mouse and goat serum, BSA and 0.025 % sodium azide) were added to the appropriate wells of the 96-well plate provided. 50 µl of PINP Biotin (PINP labelled with biotin in PBS with BSA) was added to each well; the plate was covered and incubated (1 hr, rt) with shaking (500-700 rpm). The plate was emptied and washed 3 times with Wash Solution (PBS with Tween). 150 µl of Enzyme Conjugate (avidin-linked HRP in PBS with protein, enzyme stabilisers and preservative) was added to all wells. The plate was then covered, incubated (30 min, rt) and washed. 150 µl of TMB Substrate (aqueous formulation of TMB and H_2O_2) was added to all wells, the plate covered and incubated (30 min, rt). 50 µl of Stop Solution (0.5 M hydrochloric acid, HCl) was then added and the plate immediately read using a plate reader (page 49) at 450 nm wavelength with correction at 650 nm wavelength to correct for optical imperfections of the plate. The absorbance was recorded using the provided software (page 49). The standard curve was used to determine PINP concentration of the experimental samples. Data normalisation is clearly stated in the relevant experimental chapters.

2.3.8 Mechanical loading

2.3.8.1 Manufacturing of loading device

In order to be able to apply strain to the 3D cultures, a 16-well loading plate was generated from TECH-SIL 25 Silicone Elastomer (Technovent, Newport, South Wales, UK). TECH-SIL 25 (S-25) is a medical-grade silicone with low viscosity. 200 g of silicone was mixed thoroughly for 2-3 min in a plastic container at a 9:1 ratio by weight with the platinum catalyst provided. The mixed silicone in the container was then placed inside a vacuum chamber (page 49) attached to a vacuum pump (page 49) for 10-20 min until all bubbles in the mix disappeared. During this process, air was gently let out of the vacuum once or twice by opening the vacuum valve and then closing it again in order to help remove bubbles from the mix. The silicone mix was then gently poured into the middle of a clean custom-made metal mould with its borders previously coated with polyvinyl chloride (PVC) tape. The mould was made based upon the dimensions of a standard 48-well tissue culture plate in order to fit a 48-well plate lid, and also give 16 wells of 10 mm diameter with 150 µm well base thickness. However, the spaces between the wells were filled with silicone, and the mould allowed for a series of holes to be made on each side of the plate to accommodate hooks for the attachment of the plate to the BOSE loading instrument. The mould was overfilled by 10 %, and at this point any remaining bubbles were removed with a scalpel. The base of the mould was then pressed down and clamped with a G-clamp so that excess silicone seeped out. The clamped mould was then placed into a dry oven at 80°C for a minimum of 1 h to cure the silicone. After this, the plate was removed from the mould and immediately wrapped in tin foil or lint free tissue paper to avoid dust or dirt sticking to it. The silicone plate was then further cured by boiling it at 100°C in distilled water for 3-4 hr. The silicone plate was then washed thoroughly with water and detergent and then soaked in 2-3 changes of tap water per day for 2-3 weeks in order to remove any remaining dirt or detergent. The last 2-3 days of soaking were done in distilled water (dH_2O). Once clean, the plate was autoclaved and was then ready to use. After each use, the plate was washed thoroughly with tap water and dH_2O but without detergent and

autoclaved for re-use. The silicone plate was designed by and manufactured with help from Prof Sam Evans (School of Engineering, Cardiff University, UK).

2.3.8.2 Strain measurements

Digital Image Correlation (DIC), based on the use of contrast produced by arbitrary speckle patterns, can be used to measure strain (Barranger et al., 2012) in the loading plate. DIC compares two digital images of two different mechanical states of a particular object: a reference state and a deformed state. A previously applied speckle pattern follows the strain of the object, and so the displacement that occurs between both reference and deformed state can be measured by matching the speckle pattern in small regions of the image (Peters and Ranson, 1982, Chu et al., 1985). By using two cameras and matching speckle patterns in each image, the position and displacement in three dimensions can be obtained, after calibrating the system using a grid of known dimensions to determine the position of the cameras.

The bottom of the plate was covered in a light layer of white Snazaroo face paint with a sponge and then a speckle pattern was applied using a sponge and black face paint. The patterned was formed by carefully covering the whole bottom of the plate in random white and black speckles. The plate was attached using hooks to the testing machine vertically (Figure 2.2B) and stretched using a 5 N load cell (Figure 2.2A) attached to a Servo Hydraulic Testing Machine, which was controlled by an MTS FlexTest® GT controller and software (page 49). Images were captured at 2.5 N using DIC cameras (page 49) (Figure 2.2C), and the strain was measured with the provided software. This method was performed by Prof Sam Evans, Mr John McCrory and Miss Hayley Wyatt (School of Engineering, Cardiff University, UK).

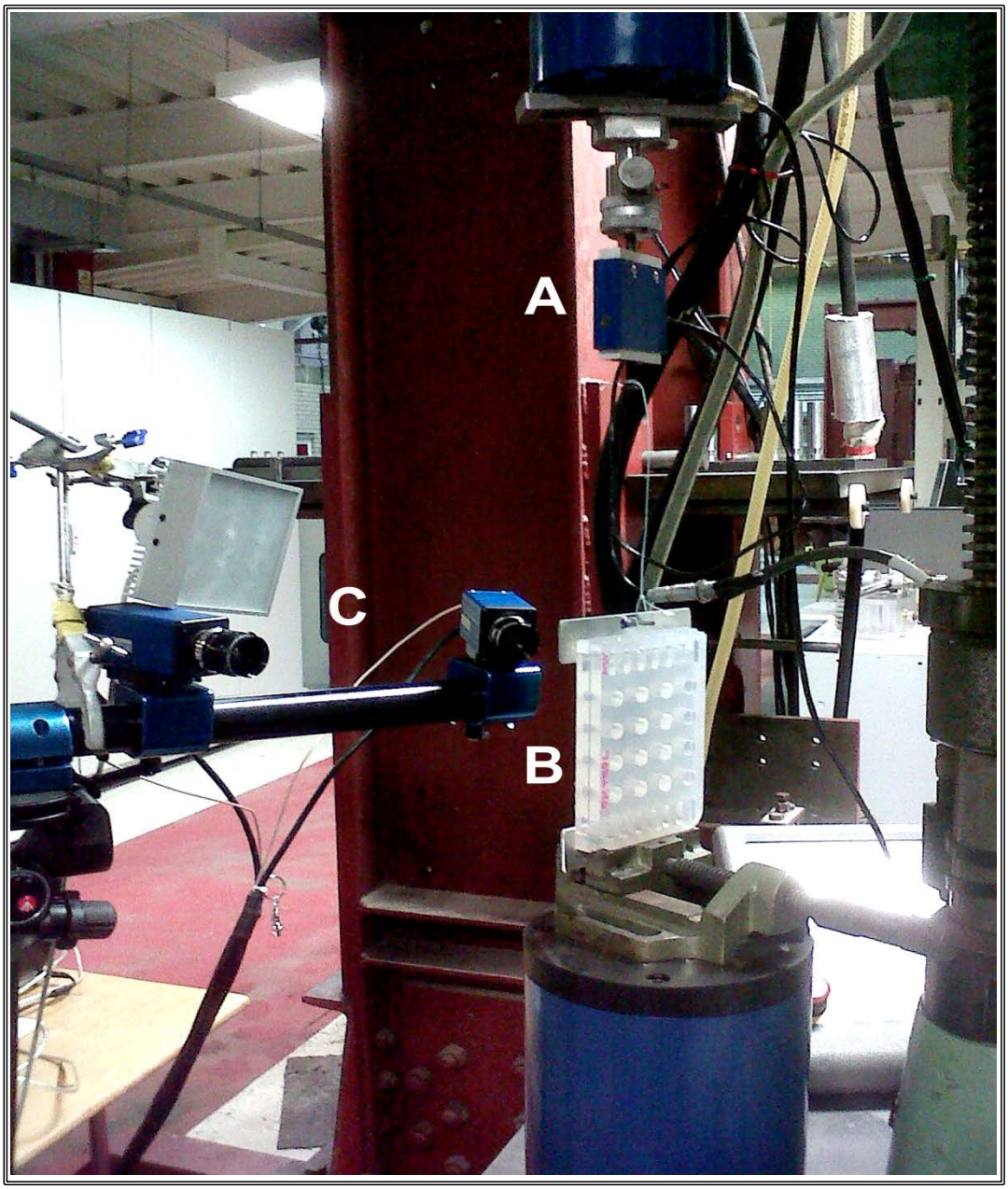

Figure 2.2 *Set-up for strain testing of loading device.* A 5N load cell (A) pulls on a string attached to the 16-well silicone plate (B) causing strain in each individual well. The strain is detected by the cameras (C) filming the speckle pattern on the bottom of the plate.

2.3.8.3 Mechanical loading of 3D collagen mono- and co-cultures

Mechanical loading using the developed silicone loading device (page 77) was performed on 3D collagen osteocyte mono-cultures, or on 3D collagen osteocyte-osteoblast co-cultures.

3D osteocyte mono-cultures were prepared and cultured in the silicone plate (page 77) by embedding MLO-Y4 cells in type I collagen gels (page 52). 800 µl of DMEM GlutaMAX™ supplemented with 100 U/ml penicillin, 100 µg/ml streptomycin and 5 % DFBS was added on top of the 3D collagen MLO-Y4 mono-cultures and they were then incubated o/n at 37°C in 5 % CO_2/95 % air atmosphere for 24, 48 or 72hr without changing culture medium prior to load, or 7 days where culture medium was changed every 2-3 days and prior to loading.

3D collagen co-cultures were prepared and cultured in the silicone loading device (page 77) for 7 days (page 52). At day 7, cultures were treated for 1 h with either AMPA/KA antagonist NBQX (200 µM in DMEM 5% DFBS), A_{2A} antagonist SCH 442416 (1 µM in DMEM 5% DFBS), or with standard culture medium (DMEM 5% DFBS) for untreated cultures. Antagonist carriers, PBS for NBQX or dimethyl sulfoxide (DMSO) for SCH 442416, were present in all cultures. 3D collagen co-cultures were mechanically loaded in the presence of antagonists.

In both cases, the silicone plate was attached to a BOSE ElectroForce® loading instrument (page 49) by a custom-made device in order to stretch the plate on one side only causing cyclic compression and tension forces at the same time but in perpendicular directions in all wells. A 250 N load cell was used to apply a loading regime of 5 min, 10 Hz, 2.5 N to the 3D collagen cultures. Loading was controlled using the provided software (page 49). The time points at which cultures were terminated post-load are clearly stated in the appropriate experimental chapters of this thesis.

2.4 Statistics

Statistical tests were performed using Minitab (page 49). Data points >2 standard deviations away from the mean were considered outliers and not included in analyses. All data were tested for normality (Anderson-Darling test) and equal variances (Barlett's test) in order to fulfil the assumptions of the statistical tests used. If these assumptions were violated, data were transformed or non-parametric tests were used. Transformations are clearly stated in the relevant results sections. Differences were deemed significant if $P<0.05$.

Some results are presented graphically using boxplots showing the smallest sample and the largest sample as whiskers (Figure 2.3A and B), the lower quartile and the upper quartile (25 % of the data presented is lower or higher than interquartile range respectively) (Figure 2.3 C and D), the interquartile range (range of data between the lower and upper quartiles, represented by a box) (Figure 2.3E) and the median (line across middle of data set) (Figure 2.3 F). If the median line is not central and/or the whiskers are of different lengths, the data may not be normally distributed. Boxplots can also detect outliers, usually shown by an asterisk (Figure 2.3G) (Rubin, 2010, Peck et al., 2012).

The number of independent experiments, and replicates per experiment (n), for each method is clearly stated in the relevant materials and methods and figure legends of this thesis. Independent experiments were set up so that each 3D culture replicate was derived from the same pool of cells. However, because each culture replicate was plated in different wells within a plate and all subsequent manipulations (e.g. surface osteoblasts, antagonist treatments and loading) were performed independently in each culture, it cannot be assumed that all cells behaved in the same manner, even if derived from the same pool. Therefore, when performing all statistical analyses in this thesis, raw data was used from each culture replicate within each independent experiment. An example of an experimental design can be found in Figure 2.4.

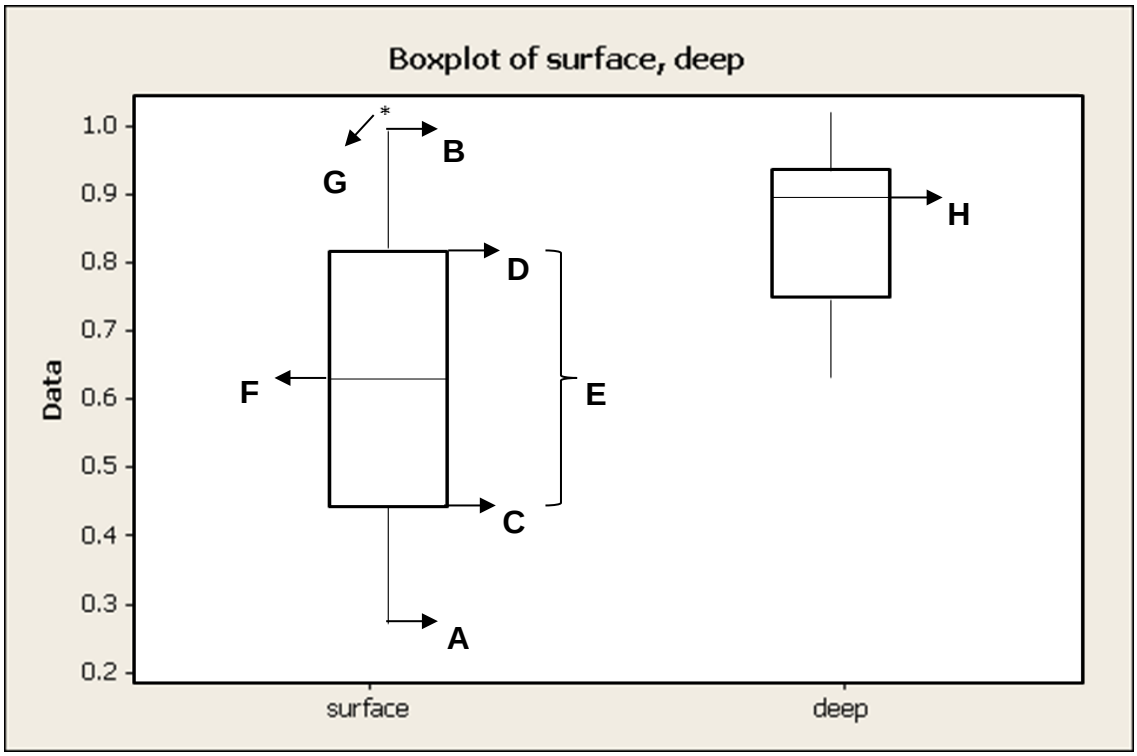

Figure 2.4 *Example of a boxplot.* A) Smallest sample whisker. B) Largest sample whisker. C) Lower quartile showing 25 % of data is lower than 0.45. D) Upper quartile showing 25 % of data is higher than 0.8. E) Interquartile range. F) Median indicating the middle of the data set. G) An outlier from the dataset. H) A non-central median line indicating data are not normally distributed.

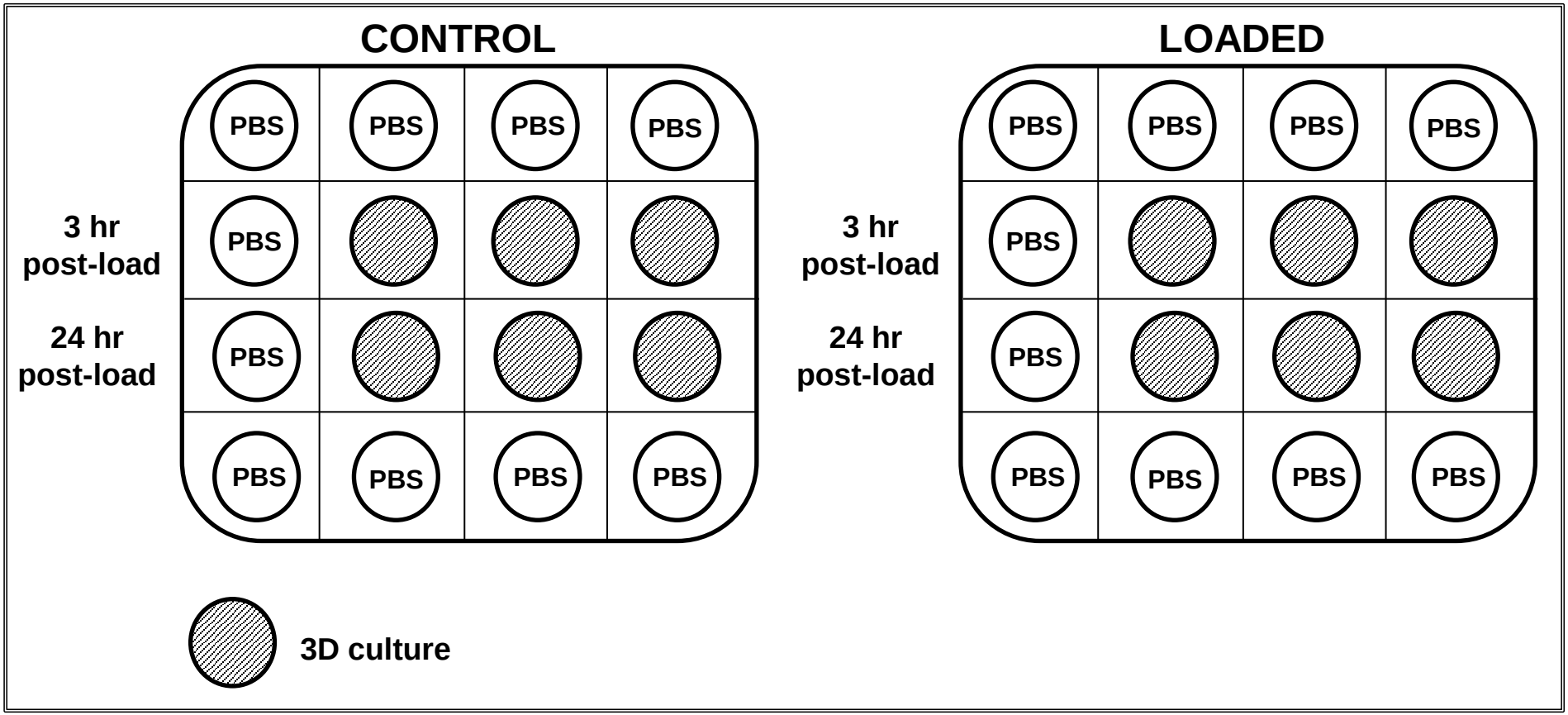

Figure 2.5 *Example of experimental design.* Diagram showing a single independent experiment of 3 replicates per condition for both control and loaded plates. For repetition of independent experiments the same design as the initial experiment was used.

CHAPTER 3

CHARACTERISATION OF A NOVEL *IN VITRO* 3D OSTEOCYTE-OSTEOBLAST CO-CULTURE MODEL

3. Characterisation of a novel 3D *in vitro* osteocyte-osteoblast co-culture model

3.1 Background

Normal mechanical loading potently induces bone formation via effects of loading on osteocytes, which transmit the signal to osteoblasts, increasing their activity and so leading to bone formation (Heino et al., 2004, Taylor et al., 2007, Rhee et al., 2011, Zarrinkalam et al., 2012). Current *in vitro* mechanical loading models do not reflect the interactions of the cells within bone, with most focusing on mechanical loading of osteoblasts in monolayers (Wang et al., 2011, Xiao et al., 2011, Li et al., 2012c) (page 30). Furthermore, although interesting findings have been obtained from the available 3D *in vitro* bone models (section 1.4.2.3.2), none elucidate the osteocyte-osteoblast interactions that regulate mechanically-induced bone formation (Kurata et al., 2006, Tortelli and Cancedda, 2009, Tortelli et al., 2009, Papadimitropoulos et al., 2011a, Papadimitropoulos et al., 2011b, Barthelemi et al., 2012). This highlights a major gap in the understanding of bone mechanotransduction. In order to address this issue, a 3D osteocyte-osteoblast co-culture model was developed by Mason et al. using the mouse osteocyte-like cell line MLO-Y4 and a human osteoblast cell line (MG63 and SaOS-2) (Mason D., 2009, Mason et al., 2009). However, this model has the disadvantage that it uses cell lines from different species, which could affect the interactions between osteocytes and osteoblasts.

3.1.1 Aims

The experiments in this chapter aimed to develop and characterise a novel mouse 3D *in vitro* osteocyte-osteoblast co-culture model suitable for investigating osteocyte-osteoblast interactions and mechanotransduction. Viability, morphology and phenotype of the cells within the model, and the ability of the osteocytes to form a network within the 3D model, were assessed.

3.2 Materials and Methods

The 3D co-culture model was adapted from Mason et al. (Mason D., 2009, Mason et al., 2009), to incorporate cell lines representing osteocytes and osteoblasts from the same species, in this case, mouse. For all experiments in this chapter, 3D collagen co-cultures from 3 independent experiments of n=3 per experiment, unless otherwise stated, were prepared and cultured for 1 or 7 days as outlined in page 52.

3.2.1 3D osteocyte-osteoblast co-culture model

At day 7, 3D co-cultures were fixed, infiltrated and cryosectioned (page 63), immunostaining for type I collagen was performed to reveal the 3D collagen gel and counterstaining with DAPI revealed the presence of cell nuclei (page 67 and Table 2.4).

3.2.2 Cell death

In situ cell death assays for both surface and deep zones of the model were carried out as described in section page 70 at day 1 and day 7. Percentage death was quantified as a proportion of total cell number and statistically analysed using General Linear Model (GLM) for crossed factors (page 81). Pairwise comparisons where $P \leq 0.05$ were recorded. GLM is used to test hypotheses by taking into account all of its contributing factors in a linear combination, whilst also accounting for error contribution. The hypotheses tested may be univariate (involving one variable) or multivariate (involving two or more variables).

3.2.3 Morphology

Monolayer cultures of MC3T3-E1(14) (page 50) and MLO-Y4 (page 50) cells and 3D co-cultures (page 52) were observed and imaged daily over 7 days using an inverse light microscope (page 63). At day 7, 3D co-cultures were fixed, infiltrated and cryosectioned (page 63). Cryosections of all replicates were stained with Phalloidin-Atto488 for actin filament labelling (page 70).

3.2.4 mRNA expression

Total RNA from the surface and deep zones of day 7 3D co-cultures was extracted, reverse transcribed and cDNA integrity checked by RT-PCR of 18S rRNA or amplified for SOST (pages 52-55). mRNA levels were quantified by relative RT-qPCRs for E11, COL1A1, ALP, OCN, Runx2 and SV40 large T-antigen; 18S rRNA, GAPDH and HPRT1 were amplified as RGs. For all templates, amplifications were carried out on cDNA diluted 1:10, in DEPC water, for all genes except SV40 large T-antigen and HPRT1 (page 55). Primer details are outlined in pages 56, 58 and Table 2.1). RT-qPCR data were normalised to the optimal RF using NormFinder as in page 57. Data for each GOI were calibrated to the highest expresser, expressed as REU (page 58) and statistically analysed using GLM for crossed factors (page 81). Pairwise comparisons where $P \leq 0.05$ were recorded. RT-qPCR products were resolved by agarose gel electrophoresis (page 55). Data are from 3 independent experiments of n=4 per experiment for both the surface and deep zones.

3.2.5 Protein expression

At day 7, 3D co-cultures were fixed, infiltrated and cryosectioned (page 63). 4-6 cryosections per culture were immunostained for E11 (page 65 and Table 2.3), SV40 large T-antigen or CX43 (page 67 and Table 2.4).

3.3 Results

3.3.1 3D osteocyte-osteoblast co-culture model

MLO-Y4 osteocyte-like cells embedded within a 3D type I collagen gel overlaid with MC3T3-E1(14) osteoblasts (Figure 3.1A) and maintained for 7 days revealed a single osteoblast surface cell layer and osteocytes embedded throughout the depth of the type I collagen gel (Figure 3.1B). This confirmed the original organisation of the 3D co-culture is maintained for up to 7 days in culture.

3.3.2 Cell death

3.3.2.1 Surface zone

Confocal images of the surface zone across 5 arbitrary fields of view were taken at x10 magnification with a 2.32 zoom for all 9 replicates. At both day 1 (Figure 3.2A) and day 7 (Figure 3.2B), viability of MC3T3-E1(14) mouse osteoblast-like cells was 100 %. Freeze-thaw controls showed 100 % death of the surface zone of the model (Figure 3.2C).

3.3.2.2 Deep zone

10 arbitrary fields of view from 5 random transverse cryosections from all 9 replicates were used for quantification of cell death as a proportion of total cell number (Figure 3.3E) at x20 magnification. At day 1 (Figure 3.3A) and day 7 (Figure 3.3B) a mixture of live and dead MLO-Y4 cells was observed. Live osteocytes had a blue nucleus and dendritic morphology, whereas a purple nucleus and rounded morphology was observed for dead cells. Some live MLO-Y4 cells also had red staining in their cytoplasm but not their nucleus (Figures 3.3A and B). Freeze-thaw controls showed 100 % osteocyte death (Figure 3.3C). Across the 3 independent experiments, an average of 16.13 ±3.16 % osteocyte cell death was observed at day 1 and 13.85 ±2.35 % at day 7 (Figure 3.3D) as a proportion of total number of osteocytes at day 1 and day 7, respectively. MLO-Y4 cell death within 3D co-

cultures was not significantly different between day 1 and day 7, however a significant difference was observed between replicate experiments (GLM, *P=0.002*) (pairwise comparisons: day 1 experiment 1 vs. 3, *P=0.0069* and experiment 2 vs. 3, *P=0.004*; day 7 experiment 1 vs. 2, *P=0.0414*) with means ± standard errors ranging from; 20.62 ±2.28 % (experiment 1), 17.32 ±1.43 % (experiment 2) and 10.04 ±1.14 % (experiment 3) at day 1; and 18.08 ±1.86 % (experiment 1), 9.35 ±1.39 % (experiment 2) and 13.48 ±1.41 % (experiment 3) at day 7, and an interaction between both factors (day and experiment) was observed (GLM, *P=0.018*). A significant difference was seen in total cell number between day 1 and day 7 (GLM, *P=0.003* of $\log_{10}$ data) and between replicate experiments (GLM, *P=0.00001* of $\log_{10}$ data). At day 1, total cell number was 2-fold higher in experiment 3 when compared to experiment 1 (GLM, *P=0.0089* of $\log_{10}$ data), and 1.5-fold higher when compared to experiment 2 (GLM, *P=0.0187* of $\log_{10}$ data). At day 7, total cell number was 1.7-fold higher in experiment 3 when compared to experiment 1 (GLM, *P=0.0494* of $\log_{10}$ data) (Figure 3.3E).

3.3.3 Morphology

3.3.3.1 Surface zone

MC3T3-E1(14) cells in a 3D co-culture (Figure 3.4C) had a similar ovoid or pyriform morphology to those in monolayer cultures (Figure 3.4A). The osteoblasts formed a thin pavement-like single cell layer on top of the 3D co-cultures which were difficult to image under the inverse light microscope (Figure 3.4C). However, when labelled for actin filaments (Figure 3.4E), the osteoblast layer and cell morphology were clearer. The osteoblasts were seen projecting stress fibres throughout their cell bodies. Actin filament labelling also showed similar osteoblast morphology after a 7 day culture period (Figure 3.4E).

3.3.3.2 Deep zone

MLO-Y4 cells in 3D co-cultures (Figure 3.4D) had a similar dendritic morphology to those in monolayer cultures (Figure 3.4B) across the collagen gel. At day 7, osteocytes showed their typical dendritic morphology and connections between neighbouring osteocytes as revealed by actin filament staining (Figure 3.4F).

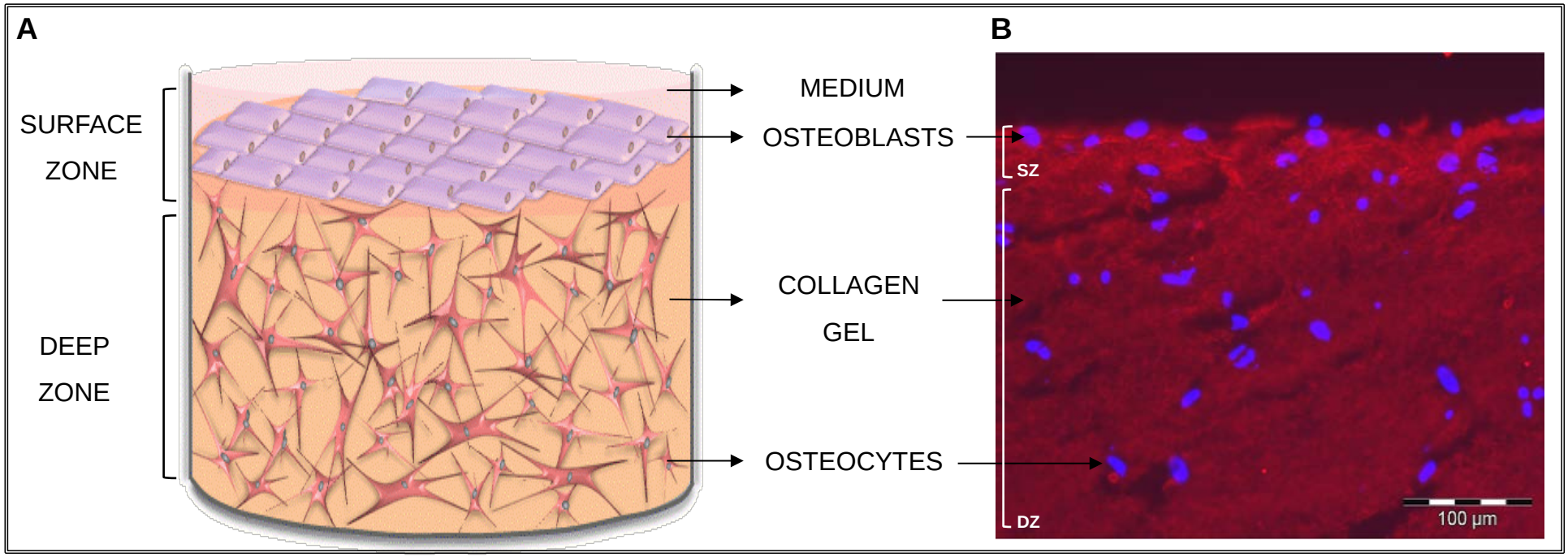

Figure 3.1 *Novel 3D osteocyte-osteoblast co-culture model.* A) Diagram of the 3D *in vitro* model indicating the surface and deep zone, and positions of the osteoblasts and osteocytes. B) Fluorescence microscope image of a 3D co-culture transverse cryosection immunostained to reveal the 3D type I collagen gel (Alexa594) and cell nuclei (DAPI). The image shows a single cell layer of cells on top of the collagen gel and cells embedded within the gel (SZ: surface zone; DZ: deep zone). Scale bar: 100 µm (B). Image was taken at an arbitrary field of view and is representative of 3 independent experiments of n=3 per experiment. Controls performed by omitting (PBST) or substituting (IgG) the primary antibody, showed no labelling (page 271).

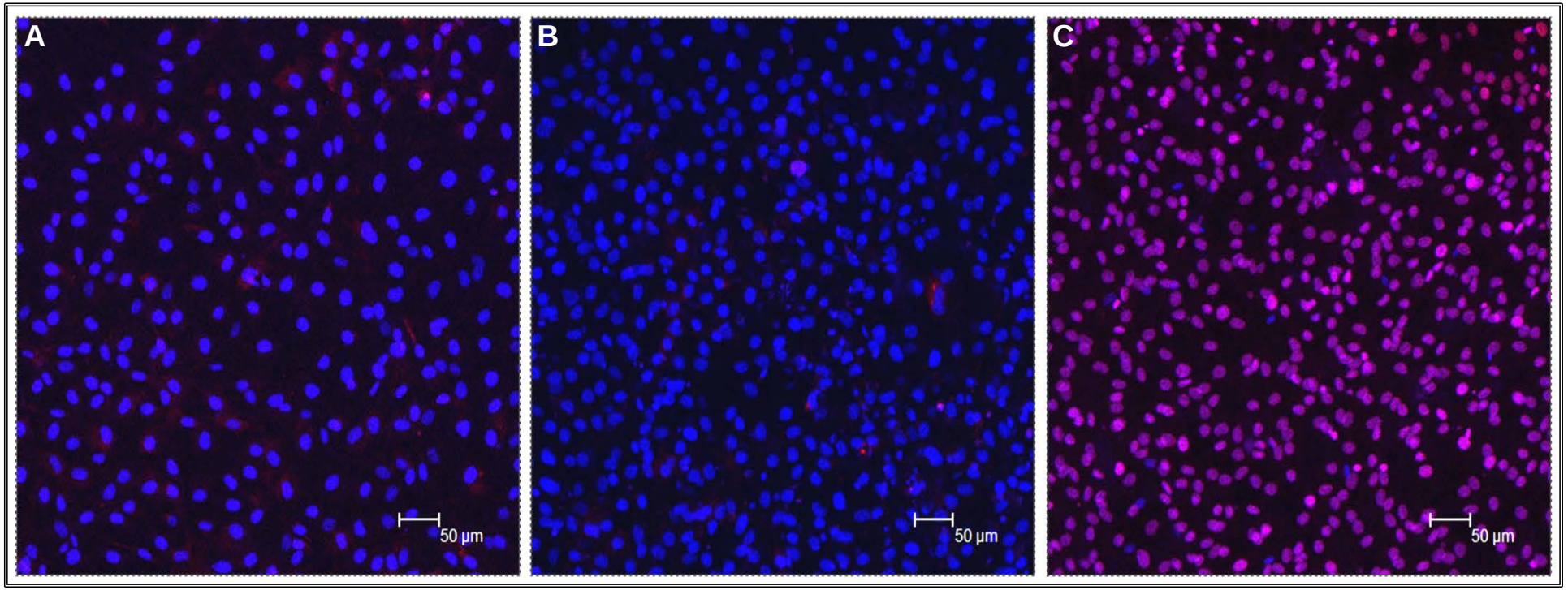

Figure 3.2 *Osteoblast viability on the surface of the 3D co-culture (red: ethidium homodimer, blue: DAPI, purple: combination of both dyes).* A) Confocal microscope image of an arbitraty field of view showing only live (blue nuclei) osteoblasts at day 1 and at day 7 (B). Some live osteoblasts show red staining in their cytoplasm but not their nucleus at both time points. C) Confocal microscope image of an arbitrary field of view from a freeze-thaw control where all osteoblasts are dead. Images are taken at the level of the surface zone and are representative of 3 independent experiments, n=3 per experiment, 5 arbitrary fields of view per replicate. Scale bars: 50 µm (A, B and C). (x10 magnification with a 2.32 zoom).

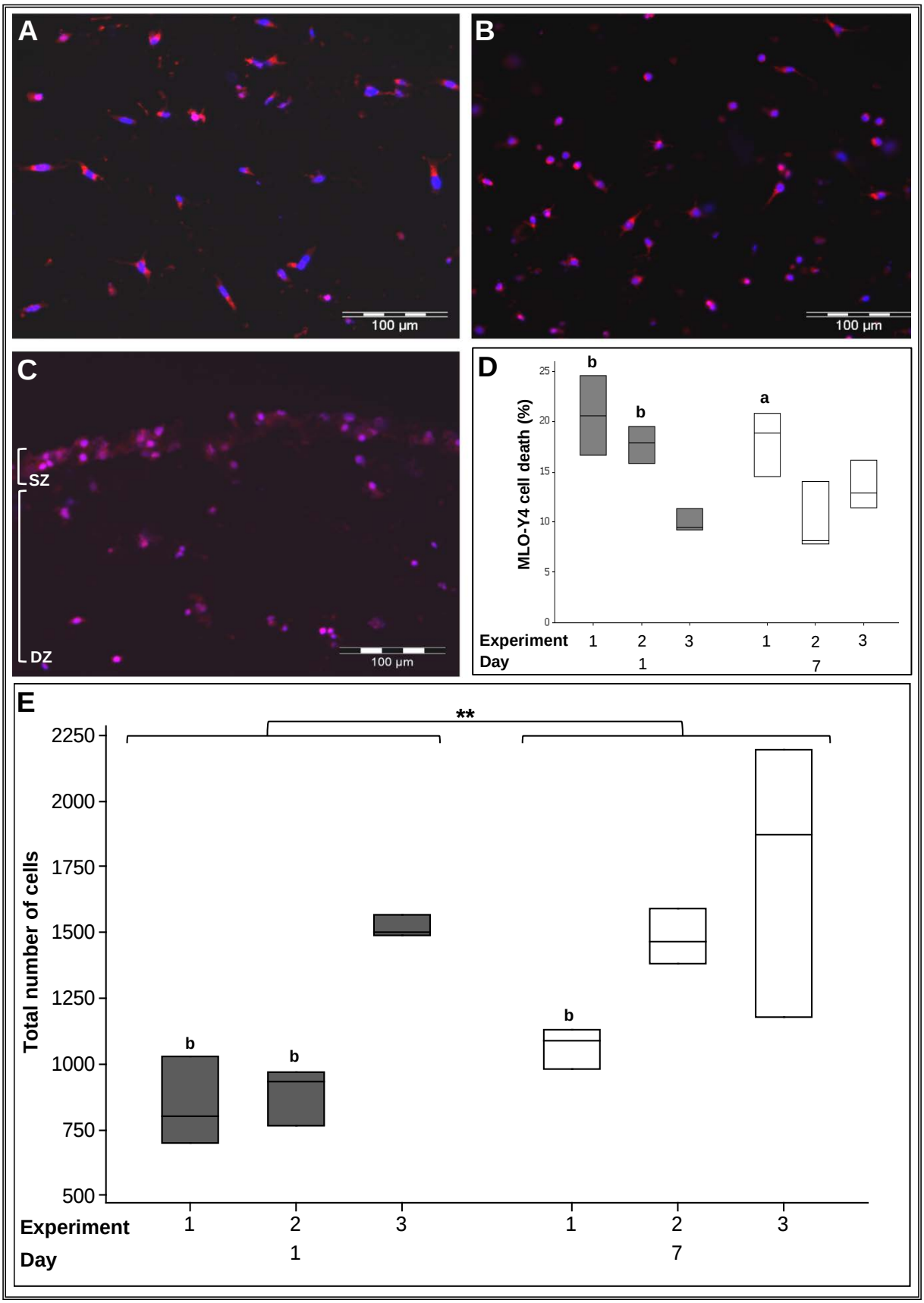
A
100 µm
B
100 µm
C
SZ
DZ
100 µm
D
MLO-Y4 cell death (%)
0
5
10
15
20
25
b
b
a
Experiment 1 2 3 1 2 3
Day 1 7
E
**
Total number of cells
500
750
1000
1250
1500
1750
2000
2250
b
b
b
Experiment 1 2 3 1 2 3
Day 1 7

Figure 3.3 *Osteocyte viability in 3D co-cultures (red: ethidium homodimer; blue: DAPI, purple: combination of both dyes).* A) Fluorescence microscope image of an arbitrary field of view showing a mixture of live (blue nuclei) and dead (purple nuclei) osteocytes at day 1 and at day 7 (B). Some live osteocytes also show red staining in the cytoplasm but not their nucleus. C) Fluorescence microscope image of an arbitrary field of view from a freeze-thaw control where all osteoblasts and osteocytes are dead (SZ: surface zone, DZ: deep zone). D) Boxplot of percentage cell death as a proportion of total number of cells at day 1 and day 7. E) Boxplot showing total cell number counted for each replicate experiment at day 1 and day 7 in each independent experiment. For total cell number, signifcant differences obtained by GLM of $\log_{10}$ data between day 1 and day 7 denoted by $^{**}P<0.01$. Significant differences from pairwise comparisons, within each day, between independent experiments are shown by 'a', with respect to experiment 2, and 'b', with respect to experiment 3. Images are taken from 3D co-culture transverse cryosections and are representative of 3 independent experiments, n=3 per experiment, 5 sections per replicate, 10 arbitrary fields of view per section. (x20 magnification, Scale bars: 100 µm A, B and C).

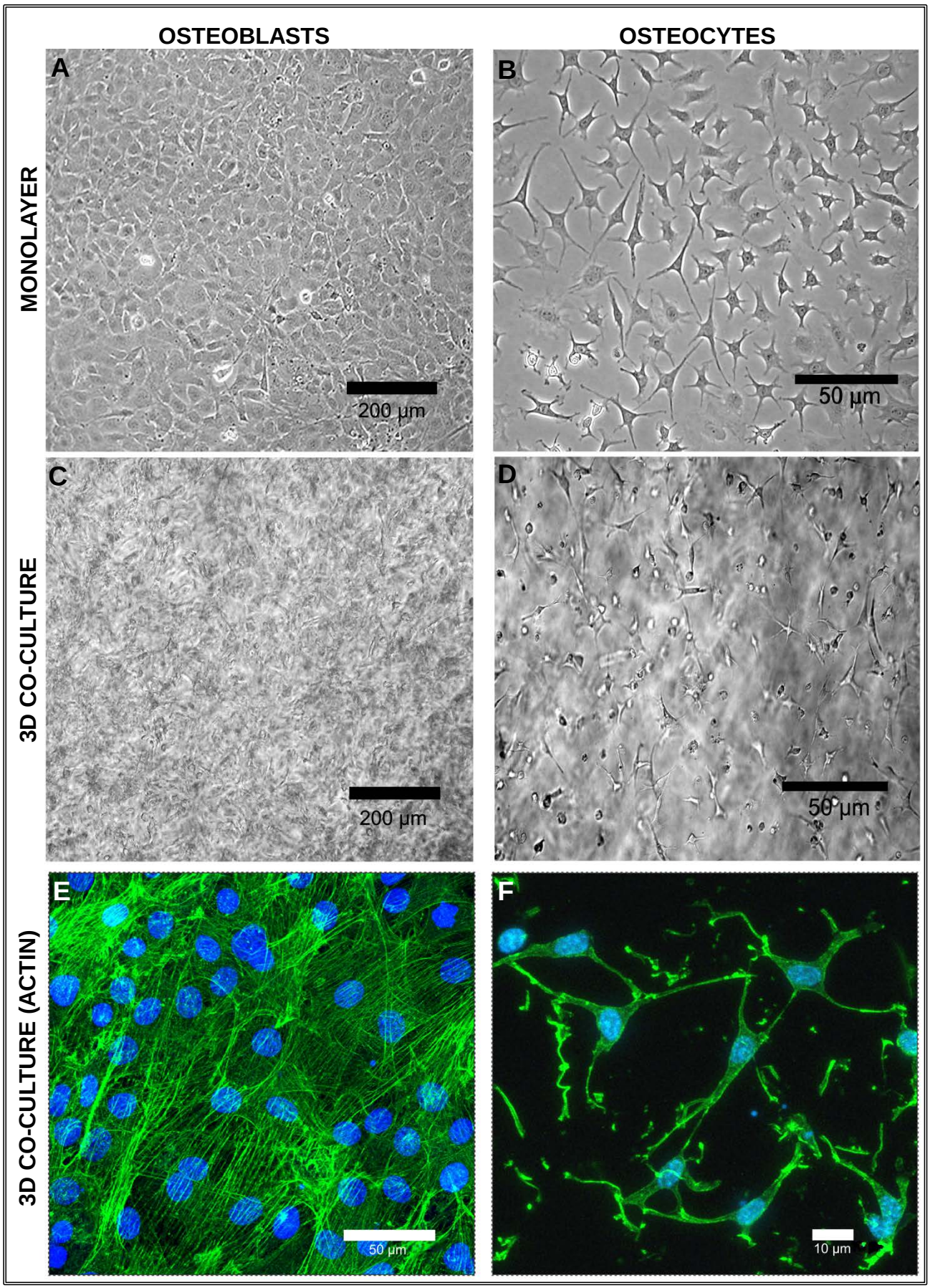
OSTEOBLASTS
OSTEOCYTES
MONOLAYER
3D CO-CULTURE
3D CO-CULTURE (ACTIN)
A
B
C
D
E
F
200 µm
50 µm
200 µm
50 µm
50 µm
10 µm

Figure 3.4 *Osteoblast and osteocyte morphology in the 3D co-cultures.* A) Inverse light microscope image of MC3T3-E1(14) cells in monolayer with a typical array of osteoblastic morphologies, mainly ovoid or pyriform. B) Inverse light microscope image of MLO-Y4 cells in monolayer with a typical dendritic morphology. C) Inverse light microscope image taken from the surface zone of the 3D model. A confluent monolayer of osteoblasts is observed. D) Inverse light microscope image of MLO-Y4 cells halfway through the depth of a 3D co-culture showing a similar dendritic morphology to that seen in monolayer cultures. E) Confocal microscope image looking down onto the surface zone of a 3D co-culture at day 7. Osteoblasts were stained to reveal actin filaments (Phalloidin-Atto488) and cell nuclei (DAPI). Image shows a pavement-like osteoblast monolayer, with individual osteoblasts containing well-developed stress fibres, and therefore maintenance of MC3T3-E1(14) morphology. F) Confocal microscope image of a 3D co-culture transverse cryosection at day 7. Osteocytes were stained to reveal actin filaments (Phalloidin-Atto488) and cell nuclei (DAPI). Image shows connections between neighbouring osteocytes and with dendritic morphology, therefore maintenance of MLO-Y4 morphology. Images are arbitrary fields of view representative of 3 independent experiments, n=3 per experiment. (Scale bars: 200 µm (A), 50 µm (B), 200 µm (C), 50 µm (D), 50 µm (E) and 10 µm (F) respectively).

3.3.4 mRNA expression

Low quantities of total RNA were obtained from the surface zone of the model, and therefore, the A_{260}/A_{230} (0.06-6.69) and the A_{260}/A_{280} (1.09-3.19) surface zone ratios were generally suboptimal (page 54) indicating presence of contaminants. However, concentration absorbances close to the NanoDrop detection limit (2 ng/µl) are less accurate. Therefore, cDNA for the surface zone was generated by reverse transcribing the maximum volume of RNA permitted in the reaction. This approach was also taken with deep zone RNA for consistency (page 54). The range of total RNA reverse transcribed varied between 17-1655.80 ng for the surface zone and 108.80-1817.30 ng for the deep zone.

mRNA expression was assessed in both surface and deep zones of day 7 3D collagen co-cultures by relative RT-qPCR using primers against osteoblast and osteocyte phenotypic markers. Data were expressed in REU and normalised to GAPDH, which was ranked as the most stable RG through NormFinder as it had the lowest stability value and inter- and intragroup variation (page 57, Table 3.1 and Figure 3.5). SOST expression was determined by RT-PCR. Data were from 3 independent experiments of n=4 for both surface and deep zones. However, an outlier was detected in the surface zone samples for all genes except COL1A1 where 3 outliers were detected in the surface zone samples. Therefore, data analysed were from 3 independent experiments where n=3 for the surface zone and n=4 for the deep zone, except COL1A1 (2 independent experiments).

All mRNAs were detected in both zones of the co-culture (Figure 3.6A) except for SOST (Figure 3.6B). No significant difference in expression was detected between zones of the model for E11 (surface zone, 0.264 ±0.072 REU; deep zone, 0.361 ±0.087 REU) (Figure 3.7A), OCN (surface zone, 0.212 ±0.076 REU; deep zone, 0.269 ±0.080 REU) (Figure 3.7D) and Runx2 (surface zone, 0.275 ±0.083 REU; deep zone, 0.157 ±0.025) (Figure 3.7E). However, the surface zone of the model showed a significantly higher expression of COL1A1 (0.168 ±0.085 REU) compared to the deep zone (0.028 ±0.007 REU) (GLM, $P=0.0001$ of $\log_{10}$ data) (Figure 3.7B). In contrast, the deep zone (0.366 ±0.075 REU) of the 3D co-culture

showed a significantly higher ALP expression than the surface zone (0.185 ±0.047 REU) (GLM, *P=0.001* of ranked data) (Figure 3.7C). Quantification of the SV40 large T-antigen, only expressed by MLO-Y4 cells (deep zone), was performed to indicate levels of MLO-Y4 RNA cross-contamination in the surface zone (MC3T3-E1(14)) of the model. SV40 large T-antigen expression was significantly lower in the surface zone (0.102 ±0.018 REU) of the model compared to the deep zone (0.315 ±0.079 REU) (GLM, *P=0.005* of $\log_{10}$ data) (Figure 3.7F). This indicates a 3-fold decrease in SV40 large T-antigen mRNA expression in the surface zone.

Whilst all genes showed a significant difference in expression between replicate experiments (GLM, E11 *P=0.0001* of $\log_{10}$ data, OCN *P=0.0001* of $\log_{10}$ data, Runx2 *P=0.013* of ranked data, COL1A1 *P=0.0001* of $\log_{10}$ data, ALP *P=0.0001* of ranked data, SV40 large T-antigen *P=0.002* of $\log_{10}$ data) (pairwise comparisons: surface zone E11 experiment 1 vs. 3, *P=0.0099* and experiment 2 vs. 3, *P=0.0097*, OCN experiment 1 vs. 2, *P=0.0011*, Runx2 experiment 2 vs. 3, *P=0.044*, ALP experiment 1 vs. 3, *P=0.0009*; deep zone E11 experiment 1 vs. 3, *P=0.0094* and experiment 2 vs. 3, *P=0.047*, OCN experiment 1 vs. 2, *P=0.0057* and experiment 1 vs. 3, *P=0.0046*, COL1A1 experiment 1 vs. 2, *P=0.001*, ALP experiment 1 vs. 2, *P=0.0281* and experiment 1 vs. 3, *P=0.0009*, SV40 large T-antigen deep zone experiment 1 vs. 3, *P=0.0030*) the trend within each experiment was generally consistent, except for Runx2 experiment 3.

Table 3.1 *NormFinder outputs.* Stability values, inter- and intragroup variation outputs for all 3 candidate reference genes.

Gene	Stability value	Intergroup variation		Intragroup variation	
		Surface zone	Deep zone	Surface zone	Deep zone
18S rRNA	0.603	0.477	-0.477	0.000	0.435
GAPDH	0.398	0.376	-0.376	0.000	0.012
HPRT1	1.192	-0.853	0.853	0.015	5.851

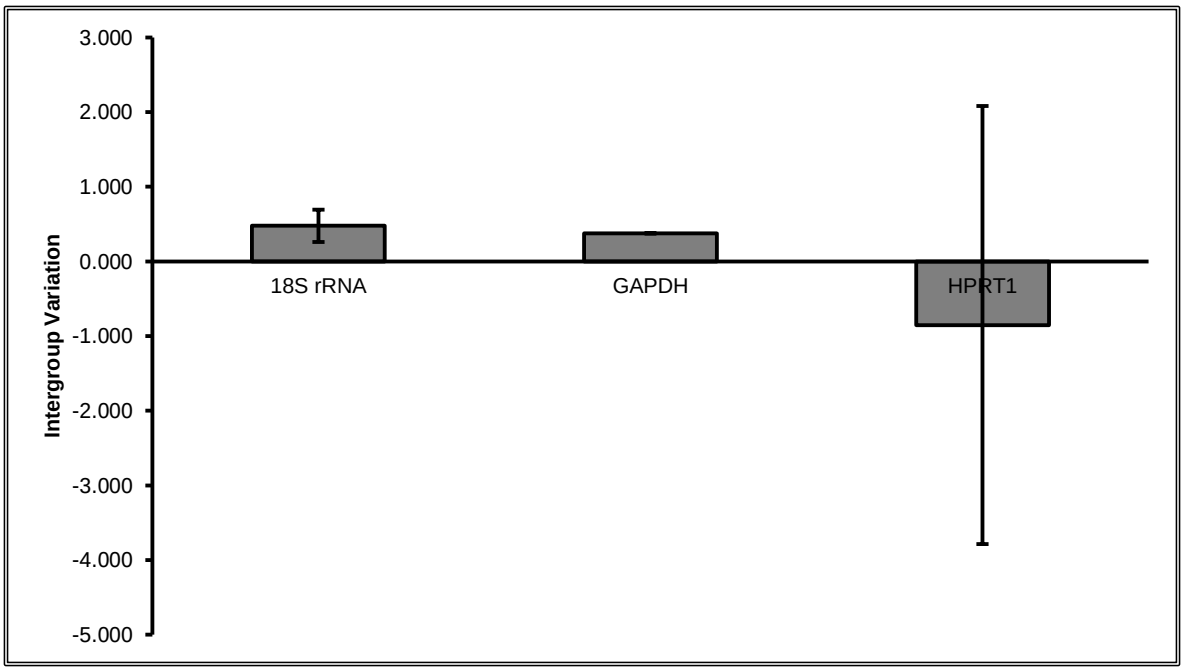

Figure 3.5 *Determination of the most stable reference gene through NormFinder.* Graph shows the intergroup variation for all candidate reference genes in all replicates. Standard error of the mean was calculated from the average intragroup variation in all replicates. (3 independent experiments, n=3 for surface and 4 for deep zones).

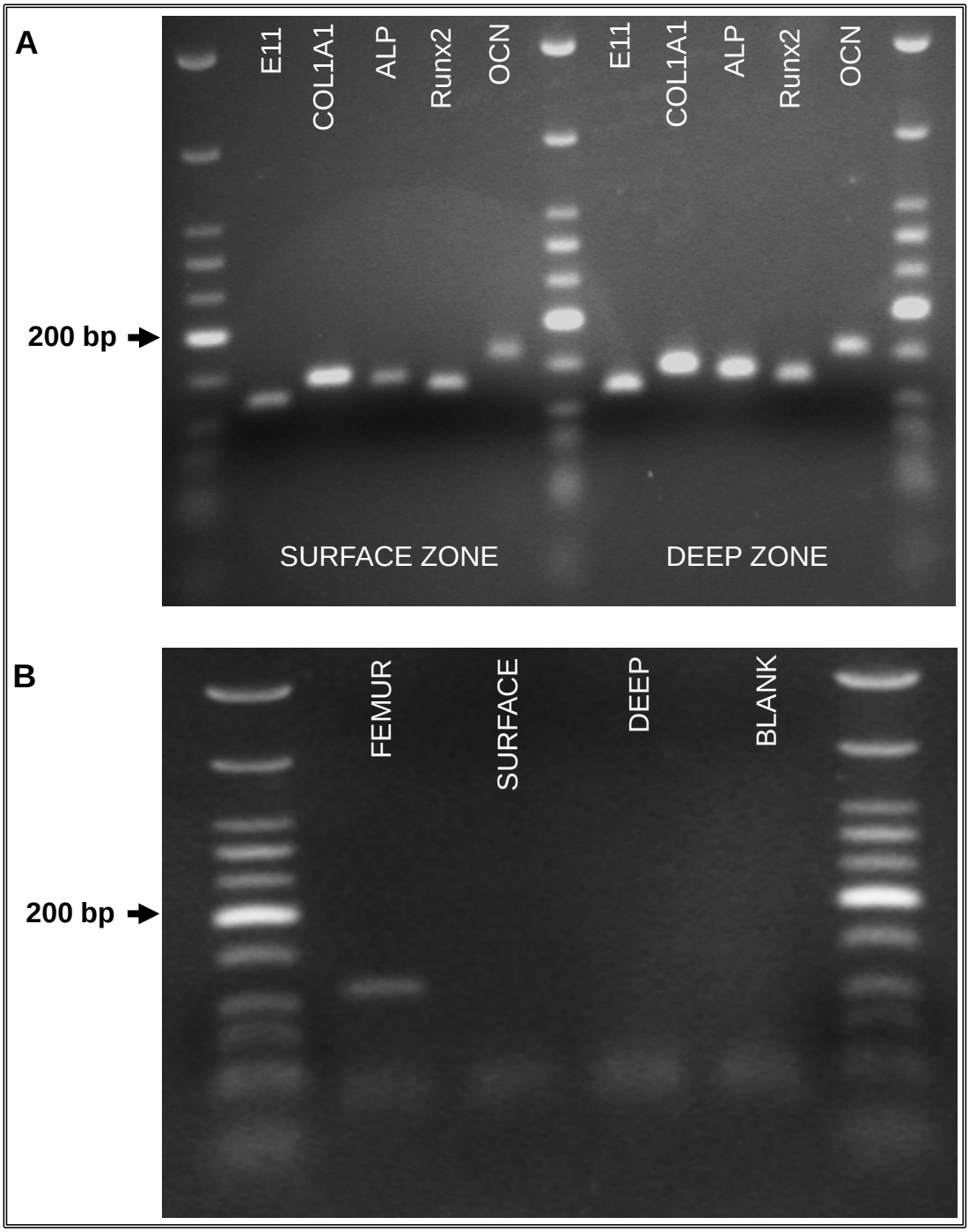

Figure 3.6 *Gene expression in 3D co-cultures after 7 days.* A) Gel electrophoresis of RT-qPCR products shows expression of E11 (118 bp), COL1A1 (140 bp), ALP (132 bp), Runx2 (120 bp) and OCN (153 bp) in both surface and deep zones of the model. B) Gel electrophoresis showing expression of SOST (112 bp) by RT-PCR in mouse femur (positive control), but absence of expression in the surface and deep zones of the model. Negative controls (blank) were clean for all reactions. Gels are representative of 2 (COL1A1) or 3 (others) independent experiments, n=3 for surface and 4 for deep zones.

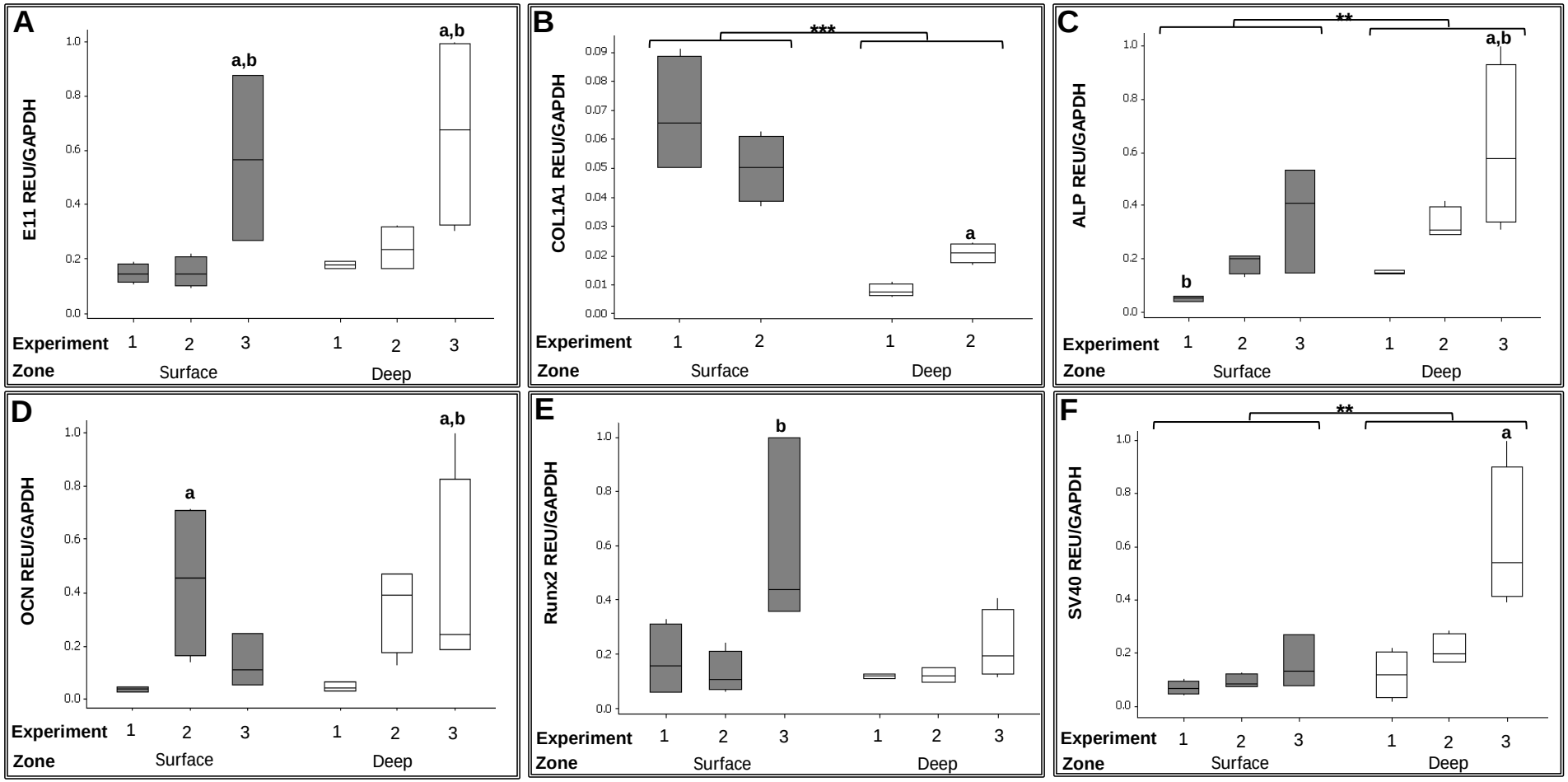

Figure 3.7 *Quantification of gene expression in the 3D co-culture after 7 days by relative RT-qPCR.* Boxplots of E11 (A), COL1A1 (B), ALP (C), OCN (D), Runx2 (E) and SV40 large T antigen (F) expressed as REU and normalised to GAPDH expression. Significant differences obtained by GLM of $\log_{10}$ data (E11, COL1A1, OCN and SV40) or ranked data (ALP and Runx2) between surface and deep zones denoted by ***P<0.01*, ****P<0.0001*. Significant differences from pairwise comparisons, within each zone, between independent experiments denoted by 'a' with respect to experiment 1, and 'b' with respect to experiment 2. (2 (COL1A1) or 3 (others) independent experiments, n=3 for surface and 4 for deep zones).

3.3.5 Protein expression

In all cases, presented data are representative of day 7, 3D co-cultures from 3 independent experiments where n=3. 4-6 cryosections of all 9 replicates were observed. IgG controls showed no immunoreaction (Figure 3.8G-L).

3.3.5.1 Surface zone

Osteoblasts in 3D co-cultures showed strong uniform immunolabelling for the dendricity marker E11 (Figure 3.8A), in agreement with gene expression results. Abundant CX43 immunostaining was also observed in these cells in the cell membrane and cytoplasm when cultured in 3D co-cultures (Figure 3.8C). As expected, no immunostaining of SV40 large T-antigen was detected in the surface zone of the 3D model (Figure 3.8E).

3.3.5.2 Deep zone

Osteocytes in 3D co-cultures showed E11 (Figure 3.8B) and connexin 43 (Figure 3.8D) immunostaining. CX43 was detected, in high abundance, along the processes, as well as within the cytoplasm, around the nucleus of the osteocytes (Figure 3.8D) and also in junctions between cells (Figure 3.8D inset). Connections between MLO-Y4 cells in 3D co-cultures were also observed in images where actin filaments were labelled (Figure 3.4F). Nuclear SV40 large T-antigen immunolabelling was also detected in the deep zone of the model, however osteocytes showed varying strengths of SV40 large T-antigen staining (Figure 3.8F).

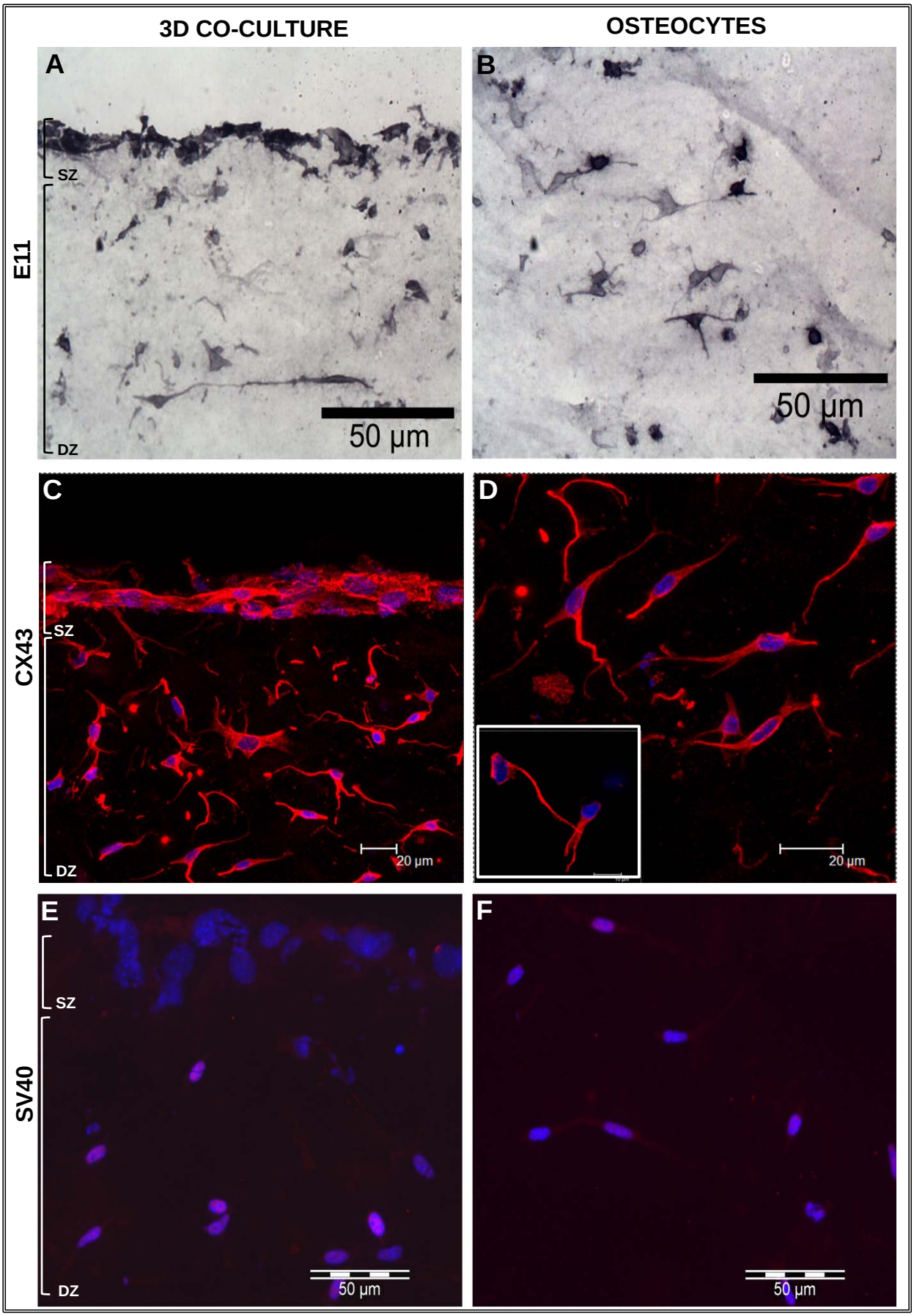
3D CO-CULTURE
OSTEOCYTES
A
B
E11
SZ
DZ
50 µm
50 µm
C
D
CX43
SZ
DZ
20 µm
20 µm
E
F
SV40
SZ
DZ
50 µm
50 µm

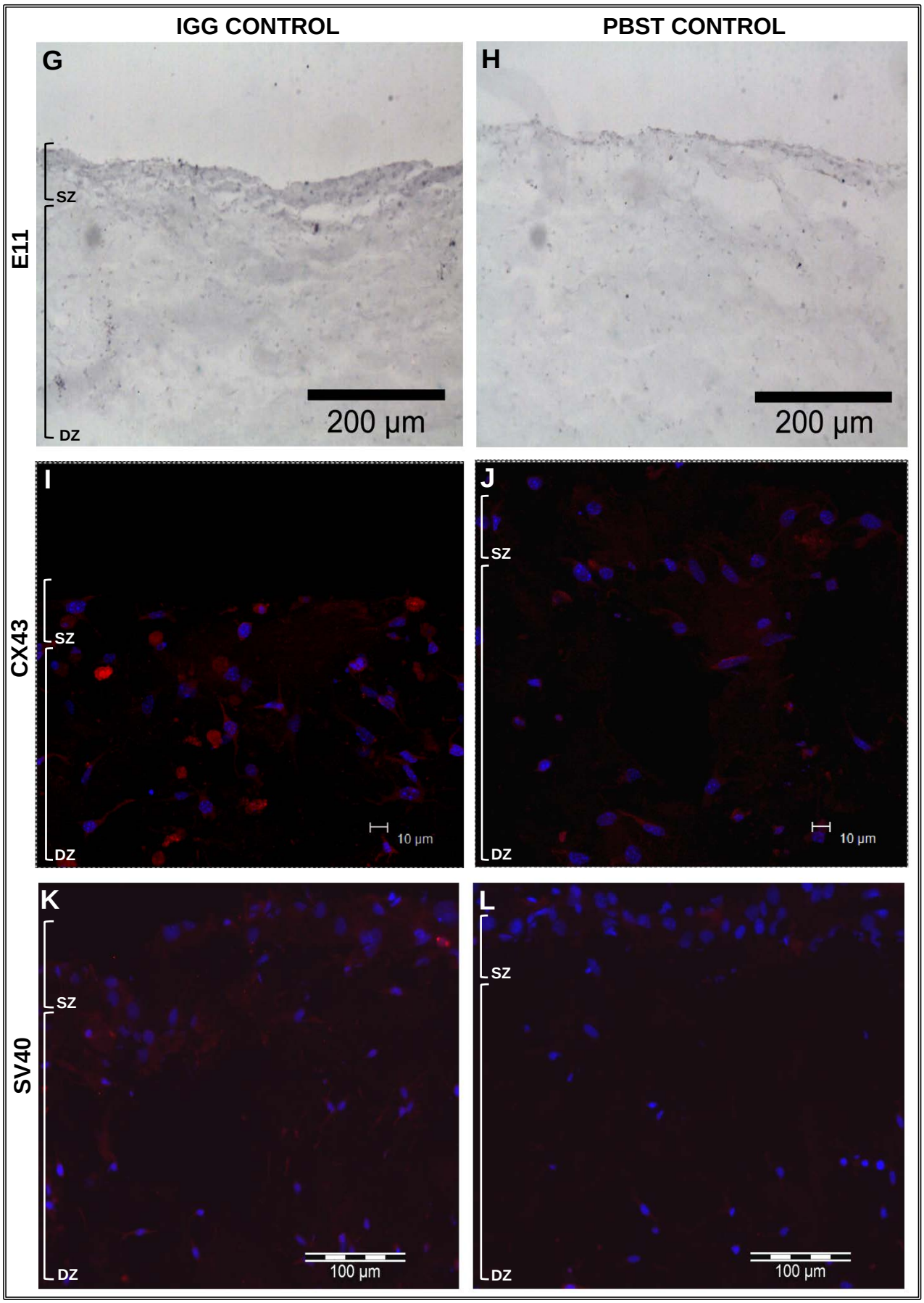
IGG CONTROL
PBST CONTROL
E11
CX43
SV40
G
H
I
J
K
L
SZ
DZ
200 µm
10 µm
100 µm

Figure 3.8 *Protein expression in 3D co-cultures after 7 days by immunostaining (SZ: surface zone, DZ: deep zone).* A) Light microscope image revealing immunostaining for the dendricity marker E11 in both osteoblasts (SZ) and osteocytes (DZ). B) Light microscope image showing E11 immunostaining in the osteocytes highlighting their morphology. C) Confocal microscope image showing CX43 (Dylight594) immunolabelling and cell nuclei stain (DAPI) in the osteoblasts and osteocytes (D). Image reveals abundant quantities of CX43 present in the cytoplasm and cell membranes of both cell types, around the nucleus of the osteocytes, and connections between embedded osteocytes (D, inset). E) Fluorescence microscope image shows immunolabelling for SV40 large T-antigen (Dylight594) and cell nuclei stain (DAPI) in osteocytes only, represented by the purple colour (combination of both dyes). However, the image reveals no SV40 large T-antigen immunostaining in the osteoblasts. F) Fluorescence microscope image showing varying degrees of SV40 large T-antigen immunostaining in the osteocytes. In all cases, controls performed by omitting (PBST: E11 (H), CX43 (J), SV40 large T-antigen (L)) or substituting (IgG: E11 (G), CX43 (I), SV40 large T-antigen (K)) the primary antibody, showed no labelling. Images are arbitrary fields of view taken from 3D co-culture transverse cryosections representative of 3 independent experiments, n=3 per experiment. Scale bars: 50 µm (A), 50 µm (B), 20 µm (C), 20 µm (D), 10 µm (inset), 50 µm (E), 50 µm (F), 200 µm (G), 200 µm (H), 10 µm (I), 10 µm (J), 100 µm (K), 100 µm (L).

3.4 Discussion

A novel *in vitro* 3D mouse osteocyte-osteoblast co-culture model has been morphologically and phenotypically characterised. The model is a two-phase culture system where osteocytes were first embedded within collagen gels and left in culture overnight before osteoblasts were added the following day (Figure 3.1). In this model, cells were viable, expressed appropriate phenotypic markers and connected to neighbouring cells (Figure 3.9). For all quantitative data presented, there appeared to be a significant difference between independent experiments. The reasons for this are discussed at the end of the discussion

The model was developed as an all mouse adaptation of a previously published 3D human osteoblast-mouse osteocyte co-culture model (Mason D., 2009, Mason et al., 2009). The model developed by Mason et al. (Mason D., 2009, Mason et al., 2009), has been fully characterised (article awaiting re-submission). However, the main disadvantage of this model is the use of two different species of cells: human osteoblasts (MG63) and mouse osteocytes (MLO-Y4) which does not represent an *in vivo* situation. Likewise, the osteocyte-osteoblast interactions observed may be influenced by the difference in species between cell types. A further disadvantage of using MG63 cells is that they are a heterogeneous osteosarcoma-derived cell line which is arrested at the pre-osteoblast state. Whereas, MC3T3-E1 cells are a non-cancer cell line which can be differentiated from immature to mature osteoblast. Furthermore, MC3T3-E1 subclones, such as MC3T3-E1(14), provide homogeneous cell populations (Czekanska et al., 2012).

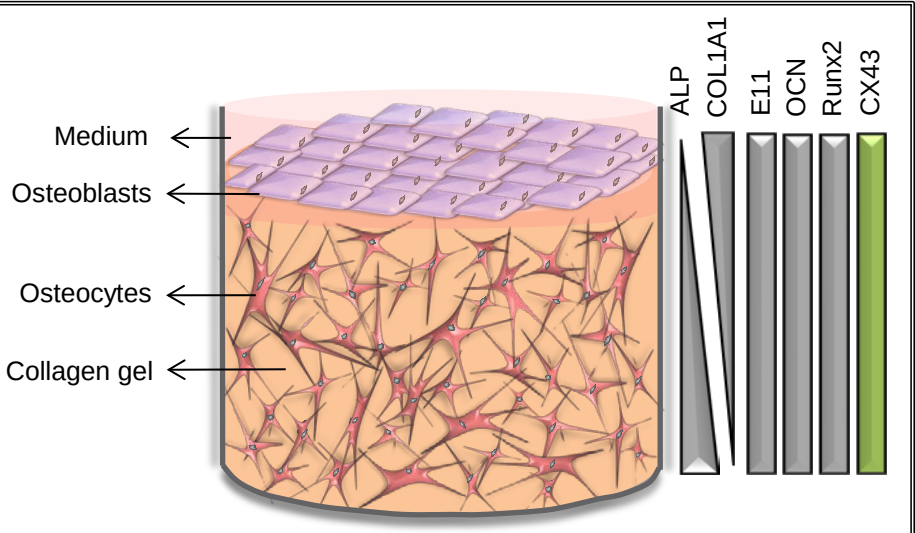

Cell death	Osteoblasts	Osteocytes
Day 1	0 %	16.13 ±3.16 %
Day 7	0 %	13.85 ±2.35 %

Signalling components	Osteoblasts	Osteocytes
A_{2A}	✓	✓
A_{2B}	✓	✓
CaSR	✓	✓
GLAST1	✓	✓
CaSR	✓	✓
AMPAR2	X	✓

Figure 3.9 *Summary of results.* Osteoblasts and osteocytes were shown to have minimal cell death at both day 1 and 7 of culture, as well as maintain their phenotype through the expression of bone markers (grey bars), and their connectivity through the expression of CX43 (green bar), and express signalling components.

3.4.1 Cell viability

3.4.1.1 Surface zone

In the 3D co-cultures, MC3T3-E1(14) mouse osteoblasts were 100 % viable (Figure 3.2). The most likely explanation is that osteoblasts behave like a monolayer of cells with dead osteoblasts detaching from the top of the collagen gel and being replaced by new osteoblasts to maintain the single cell layer on the co-culture (personal observation).

3.4.1.2 Deep zone

In the 3D co-culture, MLO-Y4 mouse osteocyte-like cells displayed an average of 16.13 ±3.16 % death after 1 day of culture and an average of 13.85 ±2.35 % death after 7 days of culture (Figure 3.3A-D). It has previously been reported that osteocytic death, common in normal human bone (Noble et al., 1997), increases with age from less than 1 % at birth up to 75 % by 80 years old (Frost, 1960, Mullender et al., 1996, Tomkinson et al., 1997). Assuming there is a linear relationship between age and osteocyte death, 20 % death would occur by 21 years of age. Thus the 16.13 ±3.16 % osteocyte viability observed in the 3D model appears consistent with *in vivo* viabilities.

Furthermore, osteocyte cell death rates at day 1 were not significantly different from those at day 7 (Figure 3.3D). Although this could suggest that cell death was caused by the experimental set up, the method used to quantify cell death does not take into account cell proliferation, which could mask any further cell death.

In vivo, most cells undergoing cell death are destroyed by neighbouring or phagocytic cells (Gregory and Pound, 2011). However, this is only subject to the accessibility of the cells in question. In bone, osteocytes are embedded within a mineralised matrix and so are inaccessible, unless during osteoclastic resorption. Consistent with this hypothesis, *in vivo*, dead osteocytes can be detected within their lacunae (Tomkinson et al., 1998, Weinstein et al., 2000). In *in vitro* 3D cultures it is

difficult to determine whether all dead cells remain embedded within the 3D matrix. However, in the 3D co-culture a similar percentage osteocyte cell death was observed at day 1 and day 7. This observation suggests that the dead osteocytes present at day 1 did not disintegrate, but like *in vivo*, remained encased within the matrix. Osteocyte death has been shown to be common in both healthy and unhealthy bone and to trigger bone resorption (page 13), suggesting that the 3D co-culture model could also be modified to study bone resorption and remodelling in physiological and pathophysiological conditions, by adding osteoclasts.

3.4.2 Morphology

3.4.2.1 Surface zone

In the 3D co-culture model, MC3T3-E1(14) cells displayed a range of osteoblastic morphologies, mainly ovoid and pyriform with stress fibres, which were maintained for 7 days (Figure 3.4A, C and E). They also formed a pavement-like monolayer on top of the 3D culture (Figure 3.4E). *In vivo*, osteoblasts range in shape, they can be ovoid, rectangular, columnar, cuboidal or pyriform (Bourne, 1972). Osteoblasts have been shown to be situated on top of the bone matrix containing osteocytes (Gegenbaur, 1864 as cited in (Bourne, 1972)) forming a pavement-like or 'overlapping roof tiles' monolayer on top of the bone surface (Bidder, 1906 as cited in (Bourne, 1972), (Sudo et al., 1983)) and their position is essential for osteocyte-osteoblast interactions which ultimately lead to the regulation of bone matrix formation (Heino et al., 2004, Taylor et al., 2007, Rhee et al., 2011, Zarrinkalam et al., 2012). *In vitro*, monolayer cultures of MC3T3-E1(14) cells show a fibroblastic morphology during their logarithmic growth phase. However, when confluent they assume a pyriform shape with prominent stress-fibres across their cell bodies (Sudo et al., 1983, Murshid et al., 2007). Therefore, osteoblasts morphology in the 3D co-culture is consistent with *in vivo* and *in vitro* observations.

3.4.2.2 Deep zone

In the 3D co-culture model, MLO-Y4 cells maintain their osteocytic morphology throughout all gel depths for 7 days and appear to connect to each other (Figure 3.4B, D and F). *In vivo*, osteocytes present a dendritic morphology, which allows communication with neighbouring osteocytes. This forms an extensive network known as LCS (Doty, 1981, Menton et al., 1984, Palumbo et al., 1990, Bonewald, 1999, Plotkin et al., 2002), which permits metabolic traffic and exchange in the mineralised environment of the bone matrix. *In vitro*, monolayer cultures of MLO-Y4 cells display a two-dimensional dendritic morphology, which becomes three-dimensional in 3D collagen cultures (Kato et al., 1997, Murshid et al., 2007). Thus, the osteocyte morphology in the 3D co-cultures is consistent with *in vivo* and *in vitro* observations, indicating that these cells have the morphological characteristics necessary for network formation throughout the 3D co-culture.

3.4.3 mRNA expression

In the 3D co-culture model, surface zone cells showed a significantly higher expression of COL1A1 compared to the deep zone of the model (Figure 3.7B). This correlates with *in vivo* and *in vitro* data which showed both osteoblasts (Collin et al., 1992, Zhou et al., 1994, Shi et al., 1996, Wang et al., 1999), and osteocytes express COL1A1 however, osteocytes express COL1A1 at lower levels (Sun et al., 1995, Kato et al., 1997). Interestingly, deep zone cells within the 3D co-cultures were found to express significantly higher levels of ALP compared to the surface zone of the model (Figure 3.7C). Osteoblasts have been shown to express ALP both *in vivo* and *in vitro* (Takuwa et al., 1991, Collin et al., 1992, Whyte, 1994, Zhou et al., 1994, Wang et al., 1999). However, previous *in vivo* and *in vitro* data has shown that osteocytes express low levels of ALP (Dodds et al., 1993, Mikuni-Takagaki et al., 1995, Kato et al., 1997). This suggests that under appropriate conditions the MLO-Y4 cells within the 3D model may be able to mineralise the collagen matrix within which they are embedded.

OCN and Runx2 are also expressed in both the surface and deep zones of the model (Figure 3.7D and E respectively). This correlates with both *in vivo* and *in vitro* studies which showed both osteoblasts and osteocytes express OCN (osteoblasts: (Collin et al., 1992, Zhou et al., 1994); osteocytes: (Mason et al., 1996, Kato et al., 1997)) and Runx2 in osteoblasts *in vivo* and *in vitro* (Ducy et al., 1997, Komori et al., 1997, Otto et al., 1997, Gilbert et al., 2002, Choi et al., 2005) and in osteocytes *in vitro* (Fujita et al., 2001). Both surface osteoblasts and embedded osteocytes were also shown to express E11 when cultured in 3D co-cultures (Figure 3.7A). E11 is an early osteocyte marker (Wetterwald et al., 1996, Schulze et al., 1999, Hadjiargyrou et al., 2001, Zhang et al., 2006) which has also been detected in mature osteoblasts and osteoblasts undergoing bone matrix synthesis (Nose et al., 1990, Wetterwald et al., 1996, Hadjiargyrou et al., 2001, Zhang et al., 2006, Jahn et al., 2010). The fact that there is E11 expression in the surface zone of the model suggests that the osteoblasts may be not only sending out projections to connect with neighbouring osteoblasts and/or embedded osteocytes, but also be attempting to differentiate into osteocytes.

SOST was not detected in either zones of the model (Figure 3.6B). In bone *in vivo*, SOST is exclusively expressed by mature osteocytes (van Bezooijen et al., 2004, Poole et al., 2005, van Bezooijen et al., 2005, Li et al., 2008). Whilst some studies have reported the expression of SOST in osteocytes (Bellido et al., 2005, Papanicolaou et al., 2009, Woo et al., 2011) and osteoblasts (Galea et al., 2011, Yu et al., 2011) *in vitro*, the MLO-Y4 (Papanicolaou et al., 2009, Yang et al., 2009) and MC3T3-E1 (Papanicolaou et al., 2009) cell lines do not express SOST. This finding is consistent with the idea that MLO-Y4 cells are not mature osteocytes and lack a mineralised environment in culture (Yang et al., 2009).

There are several matters to take into account when analysing gene expression in this 3D co-culture. According to the minimum information for publication of quantitative real-time PCR experiments (MIQE) guidelines, in order to perform RT-qPCR, ideally, the mass of RNA reverse transcribed should be equal for all samples in order to reduce variance when comparing, in this case, between surface and deep zone mRNA expression (Gu and Publicover, 2000, Kalariti et al.,

2004). However, due to the low and variable amounts of total RNA extracted from the surface zone samples, this is not possible as there would be a high risk of not detecting low expression genes. Nevertheless, normalisation to the most stable RG accounts for differences in quality and quantity of the reverse transcribed RNA used in the reaction.

Another matter to take into account is the possibility of RNA cross-contamination between zones due to the extraction protocol. The fact that there is expression of SV40 large T-antigen in the surface zone (Figure 3.7F), albeit at lower levels, suggests that there are small levels of RNA cross-contamination from the osteocytes. MLO-Y4 cells express SV40 large T-antigen as they were initially isolated from transgenic mice expressing the SV40 large T-antigen oncogene under the control of the OCN promoter (Kato et al., 1997) (page 50). However, MC3T3-E1(14) are a spontaneously immortalised cell line and therefore do not express SV40 large T-antigen (Wang et al., 1999) (page 50). There is not a gene that is only expressed by the osteoblasts in the model, therefore RNA cross-contamination from the surface zone into the deep zone of the model could not be quantified. However, light microscope images of toluidine blue stained transverse cryosections where MC3T3-E1(14) cells were cultured on top of empty 3D collagen gels for 7 days, showed no invasion of the osteoblasts (page 272). This contradicts previous data which showed the human osteoblast cell line MG63 invading empty 3D collagen gels and the invasion being controlled by embedding MLO-Y4 cells in the 3D gel (Mason D., 2009, Mason et al., 2009). However, the invasion of empty collagen gels by MG63 cells may be due to their cancer phenotype, as they are osteosarcoma-derived, and the lack of contact-inhibition, which leads to uncontrolled proliferation (Czekanska et al., 2012). Therefore, the fact that MC3T3-E1(14) cells do not invade empty 3D collagen gels, and that there are low levels of MLO-Y4 RNA present in the surface zone preparation, suggests limited cross-contamination between zones.

Significant differences in gene expression observed between replicate experiments should also be taken into consideration. Relative RT-qPCR was used as the quantification method by normalising to GAPDH, selected as the most stable RG. Therefore, any intra- and/or intergroup variation in individual replicates should be

accounted for and so there should no difference between independent experiments. However, this is not the case and this is addressed at the end of the discussion.

Finally, even though there are significant differences in expression of COL1A1, ALP and SV40 large T-antigen between surface and deep zones, the actual amount of expression of each gene, in terms of mRNA copy number, is not known. Thus the changes seen could be between relatively low levels. This is because relative RT-qPCR was performed. To be able to quantify copy numbers of each gene absolute RT-qPCR should be carried out. This method would particularly be useful to assess the extent of osteocyte RNA cross-contamination by determining the exact amount SV40 large T-antigen mRNA present in the two zones.

3.4.4 Protein expression

3.4.4.1 Surface zone

In the 3D co-culture, osteoblasts showed immunolabelling for E11, supporting gene expression data (page 109), and CX43 protein throughout osteoblast cytoplasm and cell membrane (Figure 3.8A and C), suggesting that the surface osteoblasts are indeed connecting to neighbouring cells through projections that have the potential to be functional. Osteoblasts have been previously shown to express E11 and the gap junction CX43 protein, *in vivo* and *in vitro* (Wetterwald et al., 1996, Lecanda et al., 2000, Hadjiargyrou et al., 2001, Yamaguchi and Ma, 2003, Zhang et al., 2006, Taylor et al., 2007). The fact that osteoblasts synthesise E11 protein is not surprising. Previous studies have shown that osteoblasts have cytoplasmic processes connecting them to neighbouring cells (Spuler, 1899 as cited in (Bourne, 1972), (Wetterwald et al., 1996, Schulze et al., 1999)). Additionally, MC3T3-E1 cells have been shown to have prominent stress fibres that stretch across their cell bodies into small cytoplasmic processes (Murshid et al., 2007). Furthermore, these connections between osteoblasts and neighbouring cells are mainly through CX43. This gap junction is not only the most abundant in bone, but also has an important role in skeletal development and function (Stains and Civitelli, 2005, Rhee et al.). No SV40 large T-antigen immunostaining was observed in the surface zone of the model even

after 7 days of co-culture (Figure 3.8E); as it is only MLO-Y4 cells that express this protein within the 3D model (Kato et al., 1997). This shows that no osteocytes have migrated to the surface zone of the 3D co-culture and that this zone is solely composed of osteoblasts.

3.4.4.2 Deep zone

In the 3D co-culture, MLO-Y4 cells showed expression of E11, in agreement with gene expression data (page 112), and CX43 protein (Figure 3.8A-D). Confocal images of osteocytes in 3D co-cultures showed presence of CX43 throughout the cytoplasm, osteocytic processes and around the nucleus (Figure 3.8C and D). Osteocytes, like osteoblasts, have been shown to express proteins for E11 (Wetterwald et al., 1996, Hadjiargyrou et al., 2001, Zhang et al., 2006) and CX43 both *in vivo* and *in vitro* (Kato et al., 1997, Cheng et al., 2001b, Taylor et al., 2007). Both of these proteins are key in osteocyte morphology and function. E11 helps maintain osteocyte dendricity (Zhang et al., 2006) whereas CX43 not only allows the formation of the LCS within the bone matrix, but also permits connection of osteocytes to surface osteoblasts, as shown *in vitro* by Yellowley et al. and Taylor et al. (Shalhoub et al., 2006, Taylor et al., 2007). Most importantly, CX43 has been shown to contribute to bone remodelling and formation (Bivi et al., 2012). This is further evidence that osteocytes within the 3D co-culture are potentially able to form a network similar to the LCS, as well as connect to the osteoblasts on the surface.

In the 3D co-culture, osteocytes showed nuclear expression of SV40 large T-antigen as they were immortalised by the overexpression of the SV40 large T-antigen (Figure 3.8E and F) (page 50) (Kato et al., 1997). Although the nuclear localisation of SV40 large T-antigen in MLO-Y4 cells has not previously been shown, it has been demonstrated in other cells (Haddaway et al., 2007, Ralston and Layfield, 2012). SV40 large T-antigen is considered an oncogene, due to its ability to arrest cell cycle and apoptosis, leading to uncontrolled proliferation (reviewed in (Barker and Gardner, 1974, Siris, 1994, Langston et al., 2007). Thus, the proliferation of the MLO-Y4 cell line is driven by the expression of the SV40 large T-antigen. In day 7 3D co-cultures, osteocytes showed varying strengths of SV40 large T-antigen

immunostaining suggesting not all embedded osteocytes may be undergoing proliferation (Figure 3.8F), and those which are may have a low proliferation rate. Cells staining for SV40 large T-antigen, regardless of strength of staining, were only observed embedded within the 3D collagen gel. This observation supports evidence of no osteoblast invasion into the deep zone of 3D gel or of osteocytes into the surface zone (pages 109 and 272).

3.4.5 Differences between replicate experiments

As previously mentioned, for all quantitative data presented, a significant difference was observed between independent experiments. This difference could be due to variability in setting up the 3D co-cultures. Total cell number was significantly different between replicate experiments (Figure 3.3E) and also some differences were observed between individual replicates within each experiment (page 273). The total cell number fold differences seen when comparing experiment 3 with either experiment 1 or 2 at day 1 or 7, suggests that when cells were mixed well within the collagen solution before polymerising the gels, some gels had more cells than others. Another possible explanation is that because of the variance in cell density, there would be a change in behaviour of the cells in the 3D co-culture and as a consequence osteocyte-osteoblast interactions would have differed between replicate co-cultures and between independent experiments. Thus, differences in cell densities and, consequently, differences in osteocyte-osteoblast interactions, could have affected the overall percentage death and gene expression across replicate experiments.

3.5 Conclusion

The mouse osteocyte-osteoblast 3D co-culture model characterised in this chapter provides a 3D platform to study the osteocyte control of osteoblast activity as a result of mechanical loading, something other current 3D models do not provide (Kurata et al., 2006, Murshid et al., 2007, Atkins et al., 2009). The next challenge is to determine whether this model is functional and can be used to investigate physiological mechanical stimuli and the resulting signalling that regulates osteocyte control of osteoblast activity.

CHAPTER 4

EXPRESSION OF ADENOSINE, CALCIUM-SENSING AND GLUTAMATE SIGNALLING COMPONENTS IN THE 3D CO-CULTURE MODEL

4. Expression of adenosine, calcium-sensing and glutamate signalling components in the 3D co-culture model

4.1 Background

The adenosine, calcium-sensing, and glutamate signalling pathways have been shown to influence bone biology (page 36), as seen in KO animals involving signalling components of these pathways. Briefly, for the adenosine signalling pathway, the A_1 KO model had increased bone volume and small osteoclasts (Kara et al., 2010b), the A_{2A} KO mouse displayed increased bone resorption and osteoclast activity (Mediero et al., 2012), and the A_{2B} KO model exhibited decreased bone density (Carroll et al., 2012) (pages 37-38). Furthermore, CaSR KO mice displayed growth retardation, small skeletons and several fractures (Chang et al., 2008a) (page 38). In addition, for the glutamate signalling pathway, the NMDAR1 KO model exhibited a thin bone structure and poor mineralisation (Skerry, 2008b), and the VGLUT1 KO model displayed a decrease in bone mass and an increase in osteoclast resorption (Morimoto et al., 2006) (pages 41-42)

All adenosine receptors have been found to be expressed in primary osteoblasts and osteoblast cell lines. However, currently there are no studies on the expression of these receptors in osteocytes (Evans and Ham, 2012) (page 36). CaSR has been found to be expressed in osteoblasts and osteocytes (page 38). Glutamate receptors NMDARs and AMPARs together with transporters EAATs are expressed in both osteoblasts and osteocytes, however, receptors KAs and mGluRs have only been shown to be expressed in osteoblasts (Brakspear and Mason, 2012) (page 40). Interestingly, receptors A_1, A_{2A} and CaSR have been shown to heterodimerise with mGluR1 and/or 5 in the CNS (page 43). Furthermore, both glutamate and ATP have been implicated in mechanotransduction (page 36). ATP has a short half-life and is quickly broken down to smaller products such as adenosine, suggesting that adenosine may also be a mechanical signal. However the role of the adenosine, CaSR and glutamate signalling pathways in mechanically-induced bone formation is not fully understood.

4.1.1 Aims

The experiments in this chapter aimed to determine the expression of signalling components of the adenosine, calcium-sensing and glutamate signalling pathways within the novel 3D osteocyte-osteoblast co-culture model. This study provided a platform for the investigation of the roles of these pathways in bone biology. The mRNA and protein expression of the all of the adenosine receptors, CaSR and a range of the glutamate receptors and transporters was selected according to previous data linking them to bone remodelling, mechanical loading or to the adenosine or CaSR pathways (pages 40 and 43).

4.2 Materials and Methods

For all experiments in this chapter, 3D collagen co-cultures were prepared and cultured for 7 days as described in page 52.

4.2.1 mRNA expression

Total RNA from the surface and deep zones of day 7 3D co-cultures was extracted, reverse transcribed, cDNA integrity checked by RT-PCR of 18S rRNA and then amplified for A_1, A_{2A}, A_{2B} and A_3 adenosine receptors, CaSR, or AMPAR2, KA1, mGluR1, mGluR5 glutamate receptors and GLAST1 and EAAC1 glutamate transporters (pages 52-55). Primer details are outlined in page 58 and Table 2.2. Data presented are representative from 3 independent experiments of n=4 for both surface and deep zones.

4.2.2 Protein expression

At day 7, 3D co-cultures were fixed, infiltrated and cryosectioned (page 63). Cryosections were immunostained for adenosine receptors (A_1, A_{2A}, A_{2B}, A_3), glutamate receptors (AMPAR2, KA1, mGluR1), and glutamate transporters (GLAST1, EAAC1) (page 65 and Table 2.3), or CaSR (page 67 and Table 2.4). Data presented are representative of 3 independent experiments of n=1 per experiment and 4-6 cryosections per gel.

4.3 Results

4.3.1 mRNA expression

Adenosine receptors A_{2A} and A_{2B} (Figure 4.1A) and glutamate transporter GLAST1 (Figure 4.1C) mRNAs were detected in both surface and deep zones, whereas, glutamate receptors AMPAR2 and KA1 were only detected in the deep zone of the model (Figure 4.1C). However, mRNAs for adenosine receptors A_1 and A_3 (Figure 4.1A), CaSR (Figure 4.1B), glutamate receptor mGluR1 and 5 (page 273) and transporter EAAC1 (Figure 4.1C) could not be detected in either zone of the model. In all experiments and primer combinations RT-PCR negative controls did not amplify any products.

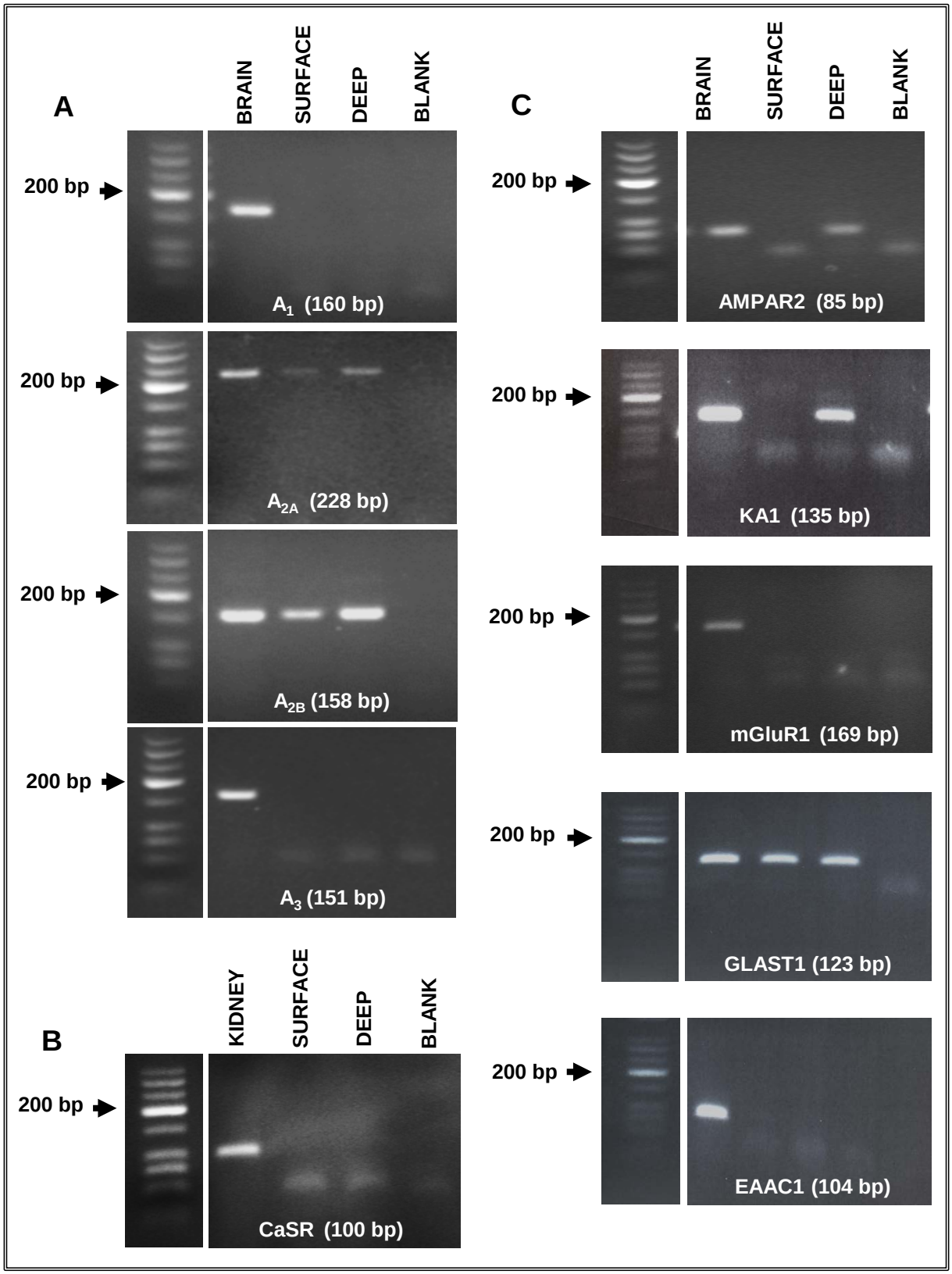
A
BRAIN
SURFACE
DEEP
BLANK
200 bp
A1 (160 bp)
200 bp
A2A (228 bp)
200 bp
A2B (158 bp)
200 bp
A3 (151 bp)
B
KIDNEY
SURFACE
DEEP
BLANK
200 bp
CaSR (100 bp)
C
BRAIN
SURFACE
DEEP
BLANK
200 bp
AMPAR2 (85 bp)
200 bp
KA1 (135 bp)
200 bp
mGluR1 (169 bp)
200 bp
GLAST1 (123 bp)
200 bp
EAAC1 (104 bp)

Figure 4.1. *RT-PCR expression of adenosine, calcium-sensing and glutamate signalling components in day 7 3D co-cultures.* Gel electrophoresis shows RT-PCR products for all adenosine receptors (A), CaSR (B) and glutamate receptors (AMPA2, KA1 and mGluR1) and transporters (GLAST1 and EAAC1) (C) in osteoblasts (surface) and osteocytes (deep). Mouse brain cDNA was the positive control for all RT-PCRs except CaSR, where mouse kidney cDNA was used. Negative controls did not yield any products. Gels are representative of 3 independent experiments, n=4 for both surface and deep zones.

4.3.2 Protein expression

Both osteoblasts and osteocytes in 3D co-cultures showed strong uniform immunolabelling for the adenosine receptor A_{2A} (Figures 4.2C and D) and for CaSR (Figures 4.3A and B). Immunolabelling for the glutamate receptor KA1 (Figures 4.4C and D) and transporter GLAST1 (Figures 4.4G and H) was also observed in both osteoblasts and osteocytes. However, adenosine receptors A_1 (Figures 4.2A and B), A_{2B} (Figures 4.2E and F) and A_3 (Figures 4.2G and H); and glutamate receptors AMPAR2 (Figures 4.4A and B) and mGluR1 (Figures 4.4E and F); and glutamate transporter EAAC1 (Figures 4.4I and J) were not detected in either zone of the model with the antibodies used. Negative controls where primary antibodies were omitted (PBST) or substituted with non-immune immunoglobulins (IgG) did not reveal immunolabelling (Figures 4.3C and D, and 4.4K-T), except for adenosine receptor controls where non-specific background staining is observed (Figures 4.2I and J).

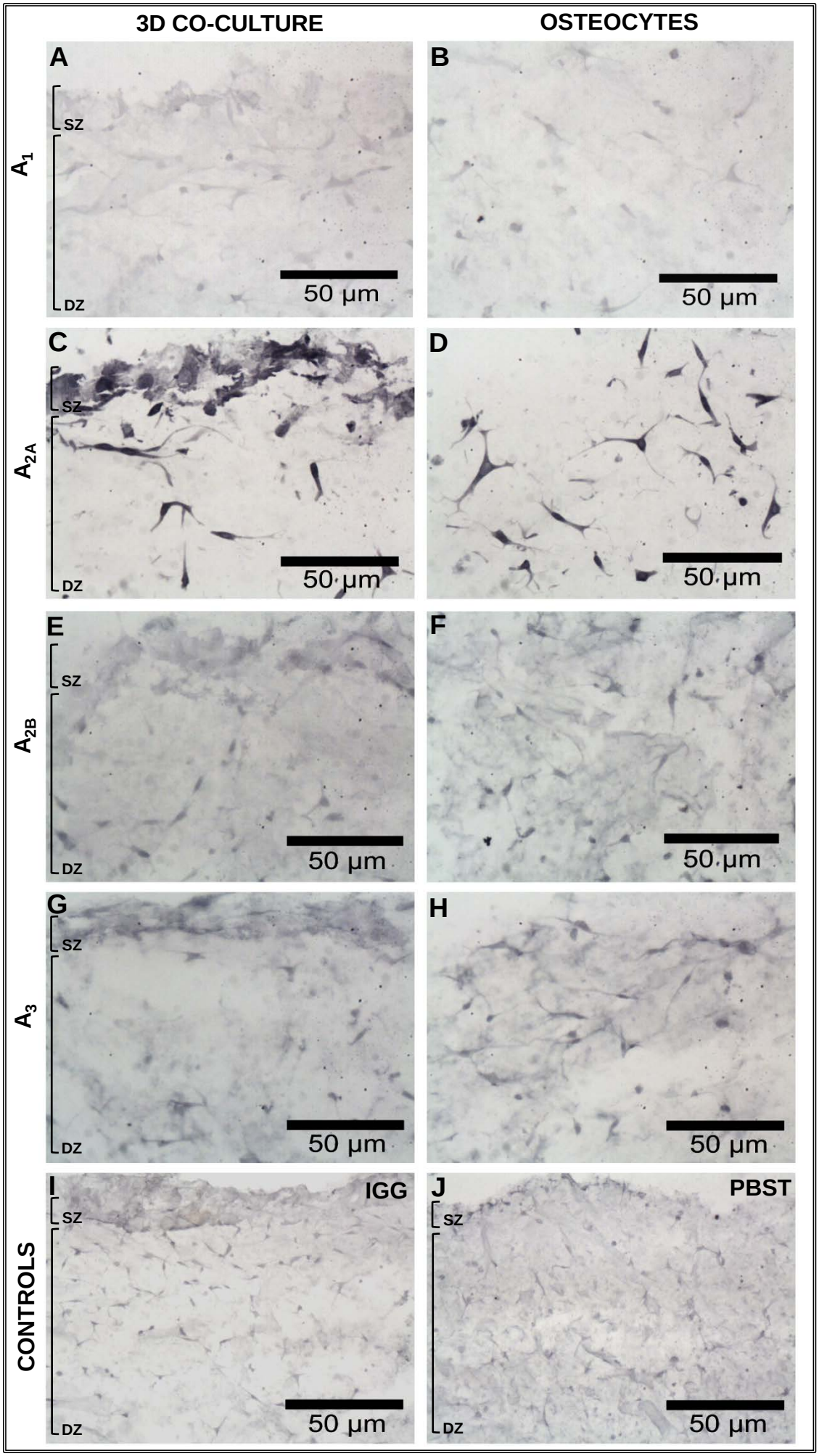
3D CO-CULTURE
OSTEOCYTES
A
B
C
D
E
F
G
H
I
J
A1
A2A
A2B
A3
CONTROLS
SZ
DZ
50 µm
IGG
PBST

Figure 4.2 *Adenosine receptors protein expression in day 7 3D co-cultures detected by immunostaining.* Light microscope images from transverse cryosections of 3D co-cultures immunolabelled for adenosine receptor A_1 (A and B), A_{2A} (C and D), A_{2B} (E and F), and A_3 (G and H) in osteoblasts (SZ) and osteocytes (DZ). Controls where primary antibodies were omitted (PBST) or substituted with non-immune immunoglobulins (IgG) showed non-specific background staining (I and J). Scale bars: 50 µm. Images are arbitrary fields of view representative of 3 independent experiments, n=1 per experiment.

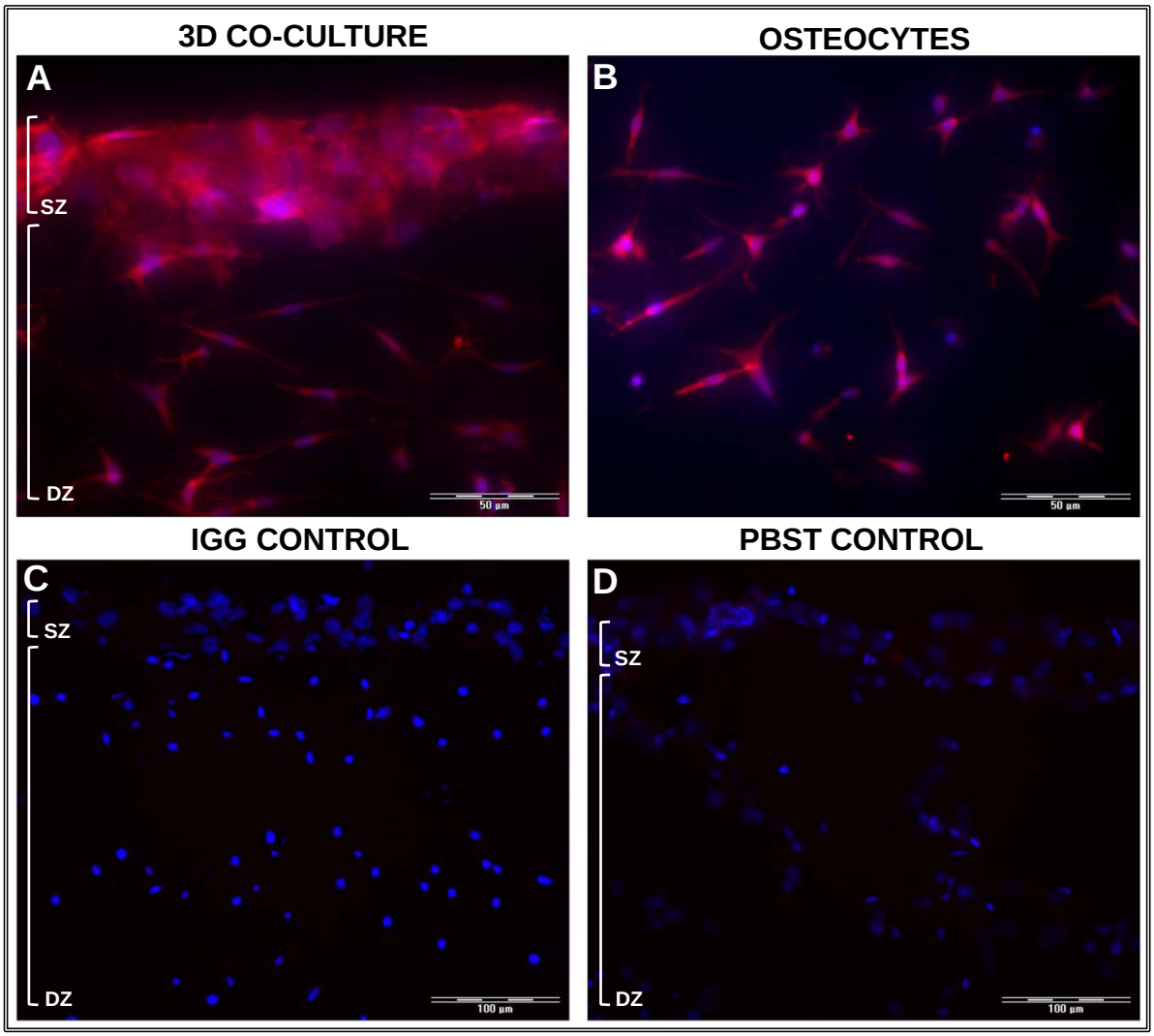

Figure 4.3 *CaSR protein expression in day 7 3D co-cultures detected by immunostaining (red: CaSR, blue: DAPI).* Fluorescence microscope images of transverse cryosections of 3D co-cultures immunolabelled for CaSR (A and B) in osteoblasts (SZ) and osteocytes (DZ). Controls where primary antibodies were omitted (PBST) or substituted with non-immune immunoglobulins (IgG) showed no labelling (C and D). Scale bars: 50 µm, 50 µm, 100 µm, 100 µm. Images are arbitrary fields of view representative of 3 independent experiments, n=1 per experiment.

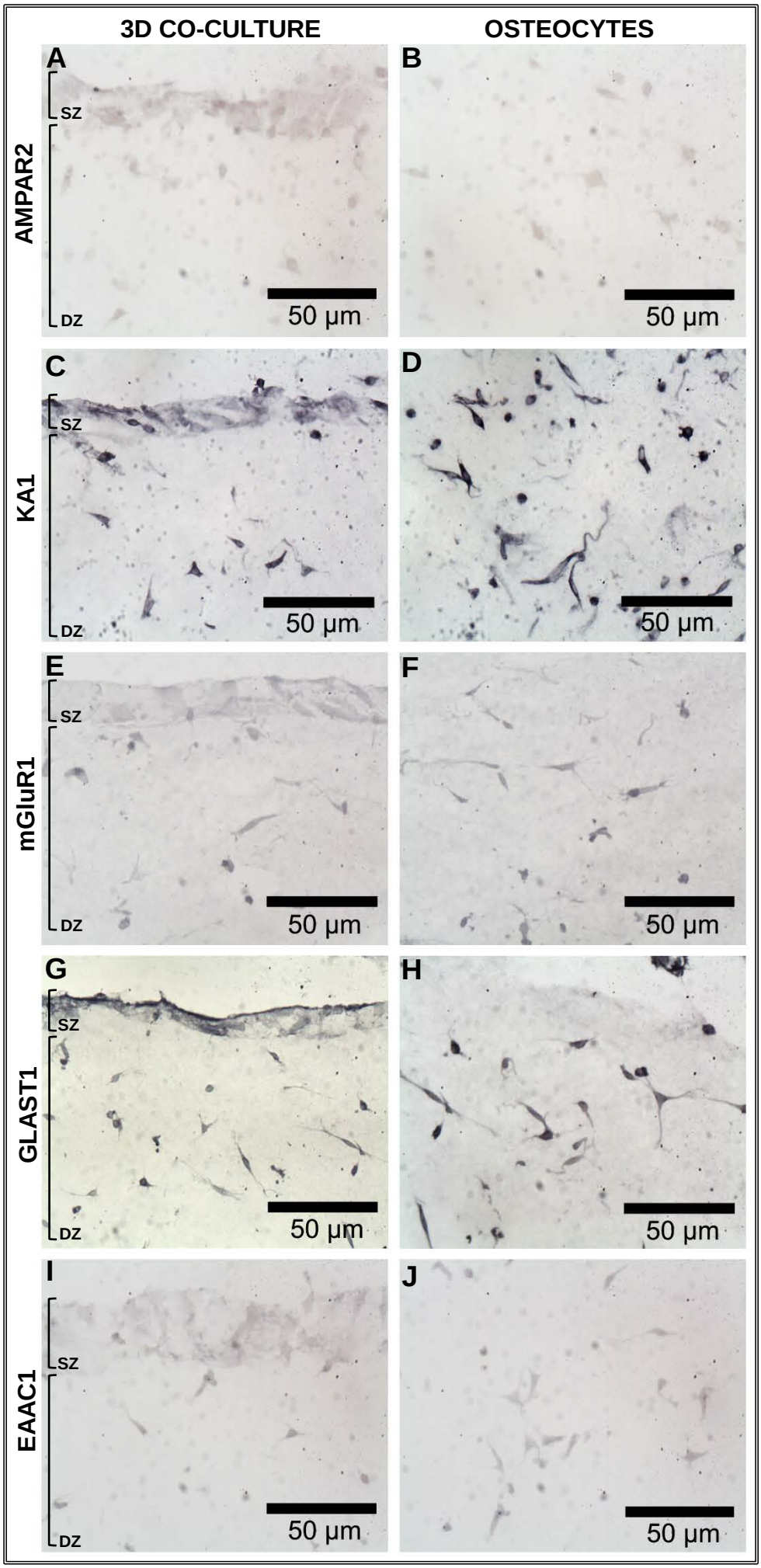
3D CO-CULTURE
OSTEOCYTES
AMPAR2
KA1
mGluR1
GLAST1
EAAC1
A
B
C
D
E
F
G
H
I
J
SZ
DZ
50 µm

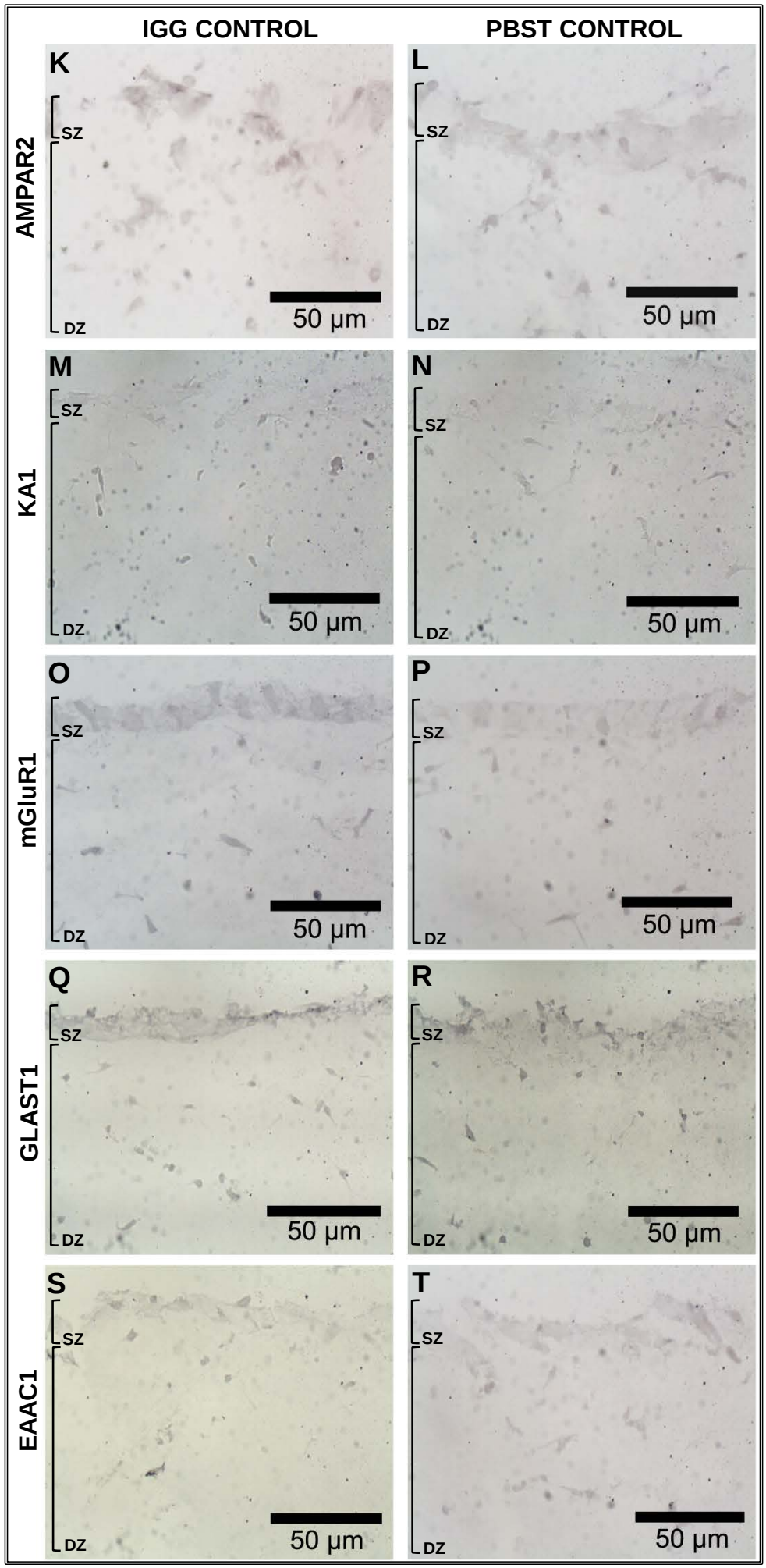
IGG CONTROL
PBST CONTROL
AMPAR2
KA1
mGluR1
GLAST1
EAAC1
K
L
M
N
O
P
Q
R
S
T
SZ
DZ
50 µm

Figure 4.4 *Glutamate receptors and transporters protein expression in day 7 3D co-cultures detected by immunostaining.* Light microscope images of transverse cryosections of 3D co-cultures immunolabelled for AMPAR2 (A and B), KA1 (C and D), mGluR1 (E and F), GLAST1 (G and H), and EAAC1 (I and J), in osteoblasts (SZ) and osteocytes (DZ). Controls where primary antibodies were omitted (PBST: AMPA2 (L), KA1 (N), mGluR1 (P), GLAST1 (R), EAAC1 (T)) or substituted with non-immune immunoglobulins (IgG: AMPA2 (K), KA1 (M), mGluR1 (O), GLAST1 (Q), EAAC1 (S)) showed no labelling. Scale bars: 50 µm. Images are arbitrary fields of view representative of 3 independent experiments, n=1 per experiment.

4.4 Discussion

Various adenosine, calcium-sensing and glutamate signalling component mRNAs and proteins were detected by RT-PCR and immunolabelling respectively (Table 4.1).

Table 4.1 *3D co-culture mRNA and protein expression of signalling components.*

Signalling Pathway	Receptor/Transporter	mRNA		Protein	
		Surface Zone	Deep Zone	Surface Zone	Deep Zone
Adenosine	A_1	-	-	-	-
	A_{2A}	+	+	+	+
	A_{2B}	+	+	-	-
	A_3	-	-	-	-
Calcium-sensing	CaSR	-	-	+	+
Glutamate	AMPAR2	-	+	-	-
	KA1	-	+	+	+
	mGluR1	-	-	-	-
	mGluR5	-	-	NI	NI
	GLAST1	+	+	+	+
	EAAC1	-	-	-	-

+ present; - absent; NI not investigated.

It is important to note that to confirm the absence of protein expression of some of these receptors, immunostaining must be repeated with different antibodies to those used in this thesis and with a positive control alongside. Furthermore, quantification of these proteins in the 3D model by western blotting in surface osteoblasts and deep osteocytes should also be carried out. Nevertheless, these results provide an expression prolife of adenosine, calcium-sensing and glutamate signalling components within the 3D co-culture model.

4.4.1 mRNA expression

In the 3D co-culture model, surface osteoblasts and deep osteocytes expressed mRNAs for adenosine receptors A_{2A} and A_{2B}, and glutamate transporter GLAST1, after 7 days of culture (Figure 4.1A and C). Glutamate receptors AMPAR2 and KA1 were only expressed in the deep zone osteocytes (Figure 4.1C). Adenosine receptors A_1 and A_3, CaSR, glutamate receptors mGluR1 and 5, and glutamate transporter EAAC1 were not expressed in the 3D model (Figure 4.1A-C) (Table 4.1).

To date, studies on the mRNA expression of adenosine receptors are scarce and *in vitro* (page 36). Osteoblasts have been previously shown to express mRNA for adenosine receptors A_1, A_{2A} and A_{2B}, but not for A_3, in MG63 human osteoblast-like cells (Russell et al., 2007). In the 3D co-culture, surface osteoblasts express A_{2A} and A_{2B} receptors, but no A_3; consistent with MG63 data. However, the lack of A_1 mRNA expression in 3D co-culture surface osteoblasts contradicts previous findings. This difference in expression could be due a difference in species as MG63 cells are a human osteoblast cell line. Other explanations include low gene expression, and the fact that previous studies were done on cells in monolayer, and not in a 3D co-culture, both of which are discussed later in this section.

No data have been published yet on the mRNA expression of adenosine receptors in osteocytes *in vivo* or *in vitro* (Evans and Ham, 2012). Therefore, this thesis reports, for the first time, the expression of adenosine receptors A_{2A} and A_{2B}, and absence of A_1 and A_3 mRNA in MLO-Y4 osteocyte-like cells when cultured in 3D co-cultures.

CaSR mRNA has previously been found to be expressed in osteoblasts *in vivo* in rat and bovine bone (Chang et al., 1999) and in rat and human undecalcified bone (Dvorak et al., 2004), and *in vitro* in rat calvarial osteoblasts (Chattopadhyay et al., 2004) and in several osteogenic cell lines (Yamaguchi et al., 1998b, Yamaguchi et al., 2001) including MC3T3-E1 cells (Yamaguchi et al., 1998a). In osteocytes, expression of CaSR mRNA has been previously shown *in vivo* (Chang et al., 1999, Dvorak et al., 2004), however, the absence of CaSR mRNA in MLO-Y4 osteocyte-

like cells reported here is the first investigation of CaSR mRNA expression in osteocytes *in vitro*. The fact that no CaSR mRNA could be detected in the 3D co-culture surface MC3T3-E1(14) cells contradicts previous findings. CaSR is a G-protein coupled receptor and many of this type of receptors are highly difficult to detect at the mRNA level as they are scarce (Yang et al., 1999, Sarramegna et al., 2003, Hansen et al., 2007). Indeed, expression of CaSR mRNA has been shown to be controversial in vascular smooth muscle cells (VSMCs) with some studies showing expression (Smajilovic et al., 2006, Molostvov et al., 2007) and others failing to detect CaSR mRNA (Farzaneh-Far et al., 2000, Shalhoub et al., 2006). This issue could also be the case in osteoblasts and osteocytes, accounting for the inability to detect it in the surface and deep zones of the 3D model. Further reasons for the inability to detect CaSR mRNA in the 3D co-culture are discussed at the end of this section.

As reviewed in (Kalariti et al., 2004, Brakspear and Mason, 2012), of the selected receptors and transporters, osteoblasts have been shown to express *in vivo* mRNA for glutamate transporter GLAST1 (Mason et al., 1997). *In vitro,* studies have demonstrated that osteoblasts also express mRNAs for GLAST1 in rat primary osteoblasts (Takarada et al., 2004), human osteoblast-like cell lines MG63 (Kalariti et al., 2004) and SaOS-2 (Huggett et al., 2002), EAAC1 in rat primary osteoblasts (Takarada et al., 2004); glutamate receptors KA1 in rat calvarial osteoblasts (Hinoi et al., 2002), and mGluR1 in rat femoral osteoblasts and MG63 cells (Gu and Publicover, 2000, Kalariti et al., 2004) and 5 in MG63 cells (Kalariti et al., 2004). However, to date, there are no reports on the expression of AMPAR2 mRNA in osteoblasts *in vivo*, whereas *in vitro* Hinoi et al reported absence of AMPAR2 in rat calvarial osteoblasts (Hinoi et al., 2002). Surface osteoblasts in 3D co-cultures express GLAST1 mRNA but no AMPAR2 mRNA was detected, consistent with published data. However, surface osteoblasts showed no expression of mRNAs for EAAC1, KA1 or mGluR1 or 5, contradicting previous studies. Whilst this may reflect rare transcripts for the receptors, this is unlikely for EAAC1 which is relatively abundant (Brakspear, 2010).

Osteocytes have previously been found to express GLAST1 mRNA *in vivo* in rat bone (Mason et al., 1997) and *in vitro* in MLO-Y4 cells (Huggett et al., 2002), consistent with 3D co-culture data for osteocytes, which also express GLAST1. This thesis reports for the first time expression of AMPAR2 and KA1, and absence of expression of EAAC1, and mGluR1 and 5 mRNA in osteocytes *in vitro*.

The differences in mRNA expression of some genes between previous studies and the 3D co-culture surface osteoblasts could be due low amounts of RNA and low abundance mRNA expression genes by RT-PCR. Alternatively, expression of some of these genes in the surface osteoblasts may be inhibited by the presence of embedded osteocytes, which would suggest a direct effect of osteocytes on osteoblast behaviour. This hypothesis could be tested by culturing M3CT3-E1(14) osteoblasts on empty gels and in 3D co-cultures with a different cell type embedded in the collagen gel, then assessing mRNA expression. Indeed, regulation of osteoblast phenotype, through the expression of COL1A1, in 3D co-cultures with osteocytes has already been shown in the human-mouse 3D co-culture model by Mason et al. (Mason et al., 2009, Mason D., 2009), suggesting this could also be the case in the all mouse 3D model.

An explanation for the differences in gene expression, for the embedded osteocytes, is the fact that all previous *in vitro* studies have been performed in monolayer cultures of cells. Embedding cells within a 3D matrix has been shown to alter gene expression (Boukhechba et al., 2009, Kozlowski et al., 2009).

4.4.2 Protein expression

In the 3D co-culture model, both osteoblasts and osteocytes expressed A_{2A} (Figure 4.2C and D), CaSR (Figure 4.3A and B), KA1 and GLAST1 proteins (Figure 4.4C-D and G-H respectively), but A_1 (Figure 4.2A and B), A_{2B} (Figure 4.2E and F), A_3 (Figure 4.2G and H), AMPAR2 (Figure 4.4A and B), mGluR1 (Figure 4.4E and F) or EAAC1 (Figure 4.4I and J) were not detected (Table 4.1).

Osteoblasts have been shown to express protein for all adenosine receptors in human primary osteoblasts (Costa et al., 2011), A_1, A_{2A} and A_{2B}, but not for A_3, in MG63 human osteoblast-like cells (Russell et al., 2007). In the 3D co-culture, surface osteoblasts stained for A_{2A} receptor, consistent with previous studies and mRNA data (page 130). However, none of the other receptors were detected contradicting previous data. The difference in expression with previous studies could be due a difference in species as MG63 cells are a human osteoblast cell line. The lack of A_{2B} protein in the 3D co-culture contradicts previous studies and mRNA expression data (page 130). This finding could be due to the degradation of A_{2B} protein and therefore not being detected by immunostaining, or because the mRNA produced is not being translated to protein. However, even though the absence of A_1 and A_3 protein in surface osteoblasts contradicts previous findings, it is consistent with mRNA data (page 130), suggesting that A_1 and A_3 receptors are not present in MC3T3-E1(14) cells when cultured in 3D co-cultures.

Since protein expression of adenosine receptors has not previously been reported for osteocytes *in vitro* or *in vivo* (Evans and Ham, 2012), this is the first observation of A_{2A} protein expression, and absence of A_1, A_{2B} and A_3 protein in MLO-Y4 osteocyte-like cells in 3D co-cultures.

CaSR protein is expressed in osteoblasts *in vivo* in rat and bovine bone (Chang et al., 1999), and *in vitro* in rat calvarial osteoblasts (Chattopadhyay et al., 2004) and in various osteoblast-like cell lines (Yamaguchi et al., 1998b, Yamaguchi et al., 2001) including MC3T3-E1 cells (Yamaguchi et al., 1998a). This is consistent with 3D co-culture surface osteoblasts data. CaSR protein expression has only been shown *in vivo* in rat, human and bovine osteocytes (Chang et al., 1999, Dvorak et al., 2004) with no *in vitro* studies in osteocytes or osteocyte-like cell lines. Thus, this thesis reports, for the first time, immunolabelling of CaSR protein in embedded MLO-Y4 cells, consistent with *in vivo* data. Interestingly, the presence of CaSR protein in the 3D model contradicts CaSR mRNA expression data obtained from surface osteoblasts and deep osteocytes, possibly reflecting rare and/or unstable CaSR mRNA (Smajilovic et al., 2006, Molostvov et al., 2007).

As reviewed in (Brakspear and Mason, 2012, Cowan et al., 2012), of the selected receptors and transporters, osteoblasts and osteocytes have been shown to express, *in vivo*, protein for glutamate transporters GLAST1 (Mason et al., 1997) and EAAC1 in rat bone (Bonnet, Williams and Mason, unpublished data). *In vitro*, GLAST1 and EAAC1 proteins are expressed in human osteoblast-like cell lines (Brakspear, 2010) with EAAC1 protein also being present in human primary osteoblasts (Brakspear, 2010), but there are no reports of expression in mouse osteoblasts *in vitro*. GLAST1 protein is abundant in MLO-Y4 osteocyte-like cells (Huggett et al., 2002), but there are no reports of EAAC1 protein in these cells. 3D co-culture surface osteoblasts and embedded osteocytes stained for GLAST1 protein, consistent with mRNA data (page 130), *in vivo* data for osteoblasts and both *in vivo* and *in vitro* data for osteocytes. Furthermore, it is reported for the first time the presence of GLAST1 protein in MC3T3-E1 mouse osteoblasts *in vitro*. Absence of EAAC1 protein in the 3D co-culture, although consistent with mRNA data (page 130), contradicts previous *in vivo* and *in vitro* studies.

AMPAR2 protein is expressed by osteoblasts *in vivo* in human and rat bone (Bonnet, Williams and Mason unpublished data, (Szczesniak et al., 2005)). However, there is contradicting evidence in osteocytes *in vivo*, where Bonnet et al. reported AMPAR2 protein in osteocytes (Bonnet, Williams and Mason unpublished data), whereas, Szczesniak et al. showed absence of AMPAR2 in these cells (Szczesniak et al., 2005). Both studies used rat bone, but there were differences in terms of rat strains, age and sex, which could account for the contradicting results. *In vitro*, AMPAR2 protein was not expressed in rat primary osteoblasts (Szczesniak et al., 2005), but studies on *in vitro* osteocyte expression of AMPAR2 protein have not yet been carried out. The absence of AMPAR2 protein in 3D co-culture osteoblasts is consistent with mRNA data (page 130) and *in vitro* studies, but not with *in vivo* data. Absence of AMPAR2 protein in 3D co-culture osteocytes contradicts mRNA expression data (page 130), but is consistent with the *in vivo* studies, and also is a novel *in vitro* finding. These differences in expression could be ascribed to the low amount of protein being produced, or because the mRNA produced is not being translated to protein.

Finally, no studies have reported the presence of KA1 or mGluR1 protein in osteoblasts or osteocytes *in vivo* or *in vitro*. Therefore, this thesis shows, for the first time, presence of KA1 and absence of mGluR1 protein in mouse osteoblasts and osteocytes *in vitro*. Immunostaining for KA1 in surface osteoblasts contradicts the absence of KA1 mRNA in the surface zone of the model (page 130).

4.5 Conclusion

In conclusion, a concise profile of expression of adenosine, calcium-sensing and glutamate receptors and transporters was developed. Components of each of the three signalling pathways are expressed in one or both zones of the 3D co-culture (Table 4.1). The lack of expression of mGluR1 and 5 means that the heterodimerisation between A_1 and mGluR1, A_{2A} and mGluR5, or CaSR and mGluR1 or 5 (section 4.1) cannot be investigated. However, it is probable that there is functional adenosine signalling, involving receptor A_{2A} and possibly receptor A_{2B}, glutamate signalling involving transporter GLAST1 and receptor KA1, and possibly receptor AMPAR2, and also CaSR signalling within the 3D model. This sets a platform for further investigation of the roles of adenosine, calcium and glutamate in mechanically-induced bone formation.

CHAPTER 5

DEVELOPMENT OF A NOVEL LOADING DEVICE FOR MECHANICAL LOADING OF 3D OSTEOCYTE CULTURES

5. Development of a novel loading device for mechanical loading of 3D osteocyte cultures

5.1 Background

Currently, many mechanical loading devices exist which allow the application of osteogenic loads *in vitro* (Brown, 2000) . However, most of these are custom-made devices which range in complexity, accuracy and consistency of loading and are not commercially available (page 30). Commercially available bone loading instruments include BOSE ElectroForce®, FlexCell® and ZETOS. These devices can be used to load *in vivo*, *ex vivo* or 2D and 3D *in vitro* cultures. For instance, BOSE ElectroForce® can be used to apply tension, compression, bending, and shear loads of up to 450 N and frequencies between 0.00001-300 Hz *in vivo* (Macione et al., 2011), *ex vivo* (Price et al., 2011, Xiao et al., 2011) and 3D *in vitro* cultures (Sittichockechaiwut et al., 2009), but not to 2D cell cultures. Although BOSE ElectroForce® systems have the right specifications to mechanically load the 3D model, they can only load one specimen at a time and its set-up would disrupt the surface osteoblast layer of the 3D model (page 30).

FlexCell® is only applicable to *ex vivo* and 2D or 3D *in vitro* cultures, and can be used to apply tension, compression or fluid flow with forces of up to 62 N and frequencies between 0.01-5 Hz. FlexCell® has the advantage of being able to load 6 specimens at a time for compression and up to 24 for tension loads. However, the frequency range of FlexCell® is not suitable for physiological osteogenic loads which require a minimum frequency of 10 Hz (Rubin et al., 2001a, Fritton et al., 2000) (page 30). Furthermore, the FlexCell® compression system cannot be used to apply a defined force or strain as it does not have a load cell and functions by using a piston and compressed air to apply forces, which could be affected by, for example, changes in temperature or atmospheric pressure.

Finally, ZETOS systems have only been validated for *ex vivo* specimens and the set-up would disrupt the surface osteoblast layer. Therefore this system would not be appropriate for the loading of the 3D co-culture model (Davies et al., 2006, Endres et al., 2009, Aw et al., 2012) (page 30).

For the mechanical loading of the 3D co-culture model, a device that applies physiological osteogenic mechanical stimuli without disrupting the osteoblast layer or the 3D collagen gel itself, as this is not very stiff, is essential. Also, it must have the ability to load numerous 3D co-cultures at the same time, maintaining equal strains across cultures. Currently there are no loading devices which are suitable for the 3D co-culture model developed in this thesis.

5.1.1 Aims

The experiments in this chapter aimed to develop a novel mechanical loading device suitable for the application of forces to the 3D co-culture model. The performance of the device was assessed by validating strain measurements using DIC and assessing responses of embedded osteocytes to physiological loads in 3D mono-cultures. The effect of culture time prior to load (time pre-load) on the osteocyte responses, and the effect of load on specific signalling pathways (Chapter 4) were also investigated.

5.2 Materials and methods

For all experiments in this chapter, 3D collagen osteocyte mono-cultures were prepared, cultured in a flexible multi-well plate (page 77) and mechanically loaded (5 min, 10 Hz, 2.5 N) using a BOSE ElectroForce® loading instrument (page 77). For all experiments, medium was not changed before mechanical stimulation, except in the 7 days pre-load culture time experiment where medium was changed immediately before load. Data presented are from 3D osteocyte mono-cultures and as in Table 5.1, unless otherwise stated. Control (non-loaded) cultures underwent all manipulations, such as movements in and out of incubators and to and from loading instrument, except mechanical loading.

Table 5.1 *Source of data presented*

Time pre-load	N° of experiments	N° of culture replicates (control and loaded)
24 hr (pilot)	1	2
24 hr	2	3
48 hr	1	3
72 hr	1	3
7 days	1	3

5.2.1 Mechanical loading device

A 16-well loading plate was manufactured from solid silicone so that the wells of the plate were of the same dimensions (10 mm diameter) as a standard 48-well tissue culture plate but with a 150 μm thick base to allow microscopic observation of the cells. The plate was also manufactured to fit a 48-well plate lid (page 77). The spaces between the wells were filled with silicone and a series of holes were made on each side of the plate to accommodate hooks, which enabled the BOSE loading instrument to stretch the plate causing cyclic compression and tension forces at the same time, but in perpendicular directions in all wells (pages 77 and 80).

Strain measurements were carried out by applying a speckle pattern to the base of the plate, which was then stretched at 2.5 N using a 5 N load cell attached to a Servo Hydraulic Testing Machine. Images were captured using DIC cameras and strains measured with the software provided (page 78).

For loading 3D cultures, the silicone plate was attached to a BOSE ElectroForce® loading instrument by a custom-made device. A 250 N load cell was used to apply a cyclic loading regime of 5 min, 10 Hz, 2.5 N to the 3D cultures (page 80).

5.2.2 Cell death/number

LDH assays were carried out at all time-points post-load with medium or culture lysates from 3D osteocyte mono-cultures (control and loaded) cultured for 24, 48 or 72 hr or 7 days pre-load to assess cell death and cell number respectively (page 73). For all experimental samples, the assay was carried out on media/lysates diluted in culture medium or lysis buffer (respectively) as indicated in Table 5.2. LDH absorbance values obtained from culture lysates (cell number) were expressed as a percentage of the average of 0 hr control cultures except the 7 days experiment where the average of 0.5 hr control cultures was used. LDH absorbance values from culture lysates were also used to normalise PGE_2 and IL-6 ELISA data.

5.2.3 PGE_2 release

PGE_2 ELISAs were carried out (page 74) on media from control and loaded 3D osteocyte mono-cultures cultured for 24 hr pre-load at 0 (immediately after load), 0.5, 1, 3, 6, 12 and 24 hr post-load (1 pilot experiment, n=2) and then at 0.5 hr post-load in a further 2 independent experiments (n=3). Control and loaded 3D osteocyte mono-cultures cultured for 48 hr, 72 hr and 7 days pre-load were also analysed 0.5 hr post-load (1 independent experiment, n=3). For all experimental samples, the assay was carried out on media diluted in standard diluent as indicated in Table 5.2. Data from all experiments were normalised to cell number (page 139) except the pilot experiment, which was not normalised. The average release of 0.5 hr

control samples was subtracted from all values as medium was not changed before mechanical stimulation, except in the 7 days pre-load culture time experiment where medium was changed before mechanical stimulation. Raw data for all assays can be found in page 275.

5.2.4 mRNA expression

Total RNA was harvested at 3 and 24 hr post-load from control and loaded osteocytes cultured in 3D collagen gels for 24, 48, 72 hr or 7 days pre-load. RNA was extracted, reverse transcribed and cDNA integrity checked by RT-PCR of 18S rRNA (pages 52-55). Relative RT-qPCR for A_{2A}, A_{2B}, AMPAR2, GLAST1, KA1, E11 and RANKL, and 18S rRNA, GAPDH and HPRT1 as RGs, was carried out (pages 55-56, 58, Tables 2.1 and 2.2). For all templates, amplifications were carried out on cDNA diluted in DEPC water as indicated in Table 5.2. RT-qPCR data were normalised to the correct RG using NormFinder (page 57). Data for each GOI were calibrated to the average ΔC_T of the unloaded samples at each time point and expressed as REU (page 58).

5.2.5 IL-6 release

IL-6 ELISAs were carried out (page 75) on medium from control and loaded 3D osteocyte mono-cultures cultured for 24 hr pre-load at 0.5, 1, 3, 6, 12 and 24 hr post-load (1 pilot experiment, n=2) and then at 0 (immediately after load), 0.5, 6 and 24 hr post-load in a further 2 experiments (n=3). Control and loaded 3D osteocyte mono-cultures cultured for 48 hr and 72 hr pre-load were also analysed at 0 (immediately after load), 0.5, 6 and 24 hr post-load (1 independent experiment, n=3). For all experimental samples, the assay was carried out on media diluted in reagent diluent as indicated in Table 5.2. Data from all experiments were normalised to cell number (page 139), except the pilot experiment which was not normalised, and the average release of 0 hr control samples was subtracted from all values as medium was not changed before mechanical stimulation. Raw data for all assays can be found in page 279.

Table 5.2 *Experimental sample dilutions used.*

Time pre-load	N° of experiments	LDH Media	LDH Lysates	RT-qPCR	PGE_2	IL-6
24 hr (pilot)	1	-	NI	-	1:64	-
24 hr	2	-	1:4	-	1:64	-
48 hr	1	-	-	-	1:16	1:10
72 hr	1	-	-	-	1:16	1;10
7 days	1	-	1:4	-	1:40	NI

-: not diluted (neat); NI: not investigated.

5.2.6 Statistics

Data were statistically analysed using GLM for crossed factors or one-way Analysis of Variance (ANOVA) with Tukey-Kramer post-hoc test for parametric data. When transformation did not make data parametric Kruskal-Wallis with Mann-Whitney post hoc tests were used (page 81). Pairwise comparisons where $P \leq 0.05$ were recorded.

5.3 Results

5.3.1 Novel loading plate

A 16-well loading plate was generated from solid silicone (Figure 5.1B) so that it was deformable and optically transparent to allow microscopic observation of the cells, and was manufactured to the dimensions of a 48-well tissue culture plate (Figure 5.1A). Before loading 3D cultures, the strain that occurs within each empty well when 2.5 N of force is applied to the silicone plate, was measured using DIC. Strain testing showed that there is a large variability in strains across wells (from approximately 3000 με to 6000 με), with some wells demonstrating inward welling (Figure 5.1C). Furthermore, strain variability was also observed in between wells ranging from approximately 500 to 3500 με (Figure 5.1C). However, 9 out of the 16 wells had strains of 4000-4500 με (Figure 5.1C).

When applying a cyclic loading regime of 5 min, 10 Hz, 2.5 N to the 3D cultures, the provided software showed that the force was maintained at a 2.5 N peak and a smooth sine-wave was produced during each loading cycle applied, indicating negligible loading variance and a reproducible loading regime (Figure 5.3).

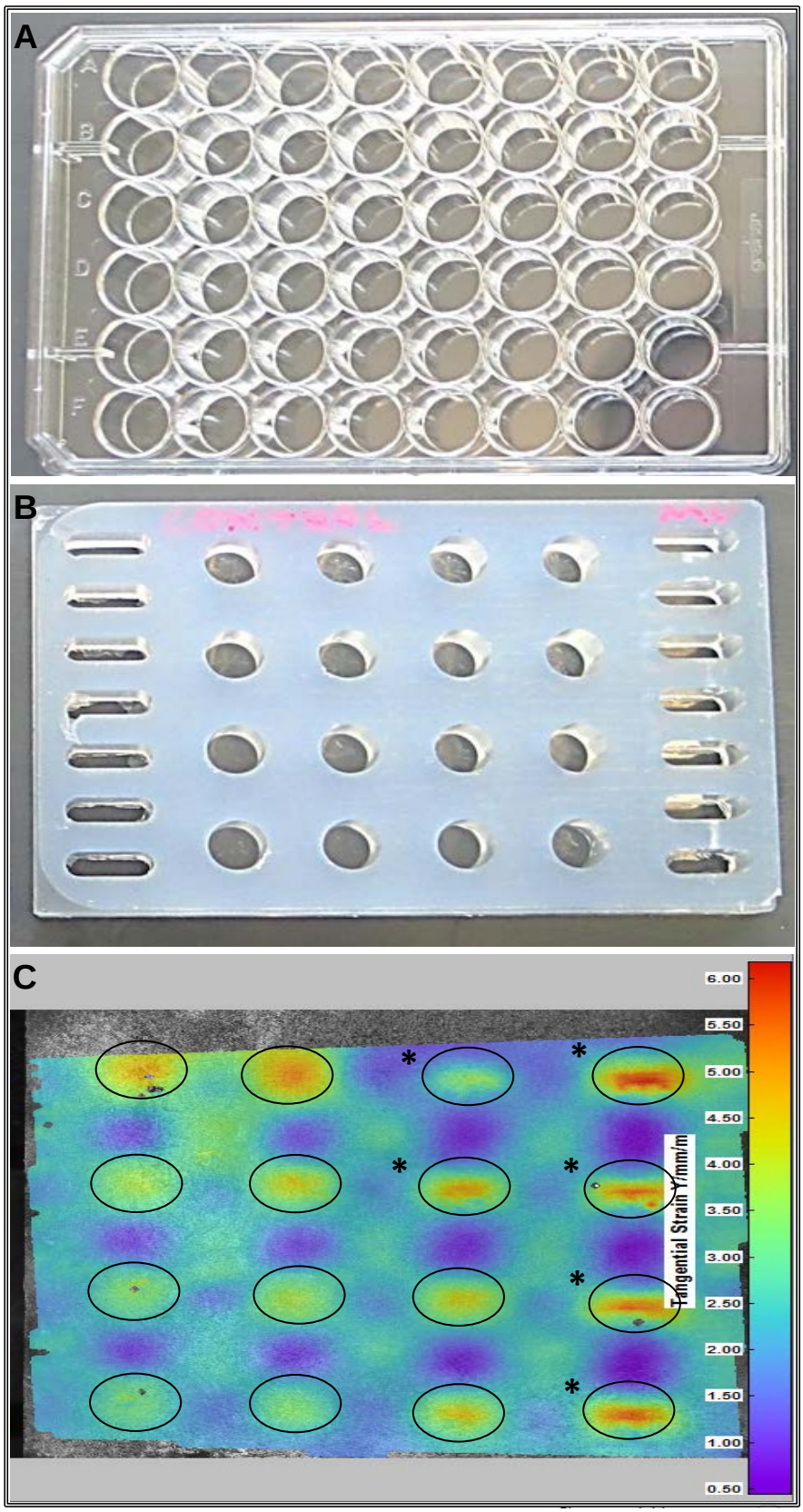

Figure 5.1 *A novel mechanical loading device.* A) A standard 48-well tissue culture plate. B) 16-well silicone loading plate with holes for its attachment to a BOSE loading instrument. C) Heat map generated by DIC showing strains occurring in each well of the loading device when 2.5 N of force is applied. Inward welling (*) is also observed in some wells.

Figure 5.2 *Mechanical loading of 3D cultures.* The silicone loading plate (C) is attached to a BOSE ElectroForce® loading instrument with a custom-made device (A) which contains pins holding the plate in place and small rollers to allow the plate to move during loading (B). *: load cell; arrows: direction of stretching of the plate.

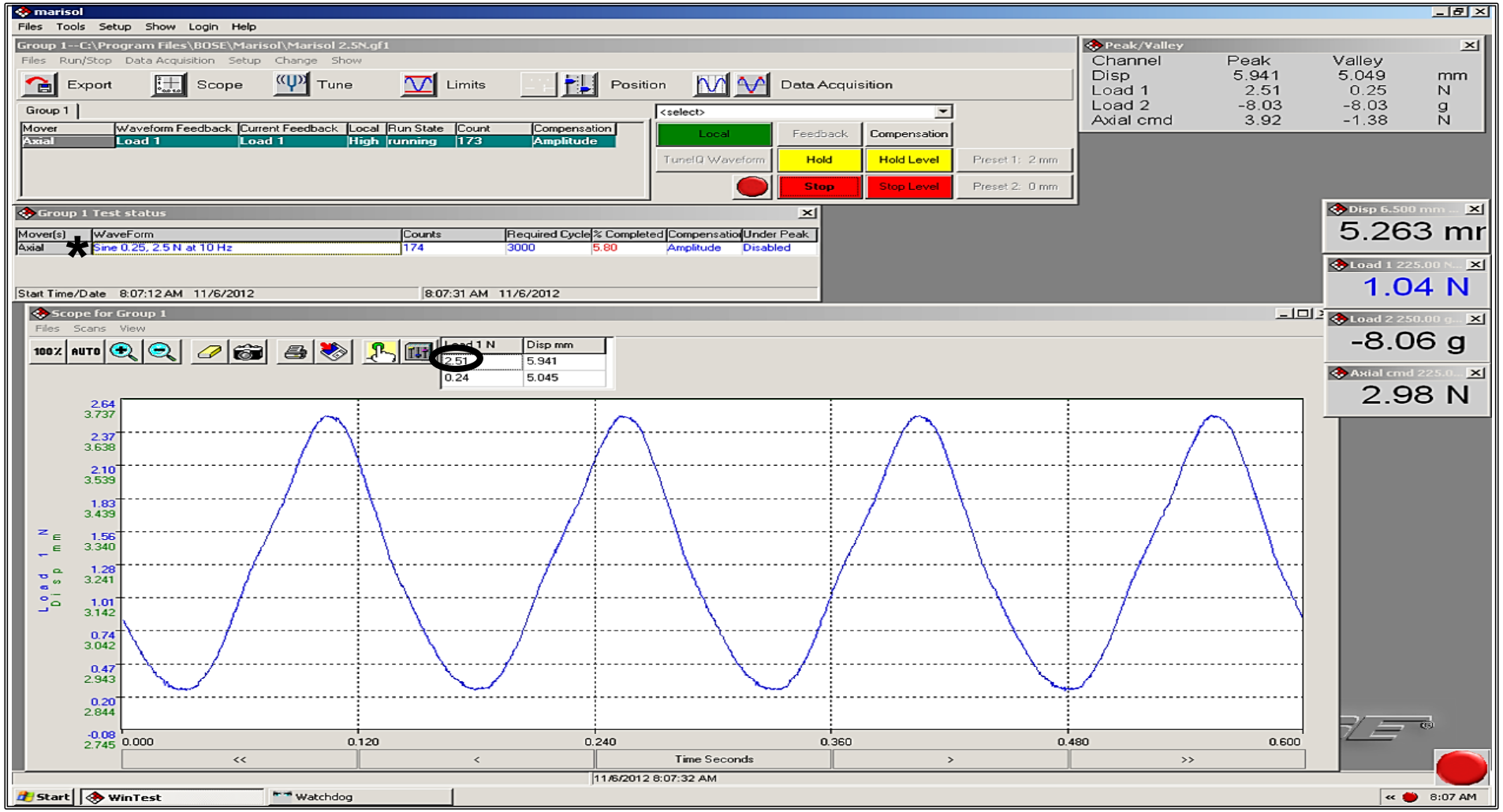

Figure 5.3 *Example of mechanical loading control performed with WinTest® Software 4.1 with TuneIQ control optimisation (BOSE).* Image is a screen-shot of the output observed whilst performing a 5 min, 10 Hz, 2.5 N cyclic loading regime (*) using the silicone plate and custom-made adaptor on a BOSE ElectroForce® loading instrument. A 2.5 N force peak (circle) and a smooth sine-wave were observed during each loading regime.

5.3.2 Cell death/number

LDH release into the medium as a result of cell death was measured at all time-points post-load in all experiments. LDH was not detected indicating no measurable cell death as a result of mechanical loading (raw data can be found in page 284).

To assess cell number, LDH release from culture lysates was measured at all time-points in all experiments, except for the 24 hr pre-load pilot experiment. Data were expressed as a percentage of the average of 0 hr control cultures for all values in all experiments except the 7 days pre-load experiment where the average of 0.5 hr control cultures was used. The effect of load and time pre-load on cell number was assessed at 0.5, 6 and 24 hr post-load. At 0.5 hr post-load there was a significant effect of load (GLM, *P=0.027* of $\log_{10}$ data) but no effect of time pre-load, and pairwise comparisons at each pre-load time were not significant (Figure 5.4A). At 6 hr post-load there was a significant effect of time pre-load (GLM, *P=0.0015* of ranked data) but no effect of load (Figure 5.4B). Cell number was significantly higher in loaded osteocytes cultured for 72 hr pre-load compared to loaded osteocytes cultured for 24 hr pre-load (24 hr loaded 93.02 ±2.53 %, 72 hr loaded 152.60 ±12.03 %; *P=0.0266*) (Figure 5.4B). At 24 hr post-load there was a significant effect of time pre-load (GLM, *P=0.0001*) but no effect of load (Figure 5.4C). Cell number was significantly higher in loaded osteocytes cultured for 72 hr pre-load compared to those cultured for 24 hr or 48 hr pre-load (24 hr loaded 102.53 ±4.05 %, 48 hr 104.32 ±8.93 %, 72 hr 182.08 ±5.51 %; 24 hr vs. 72 hr *P=0.0011*, 48 hr vs. 72 hr *P=0.0055*) (Figure 5.4C).

Data from osteocytes cultured for 48 and 72 hr pre-load were combined and re-analysed at 0.5, 6 and 24 hr post-load, and showed no significant effect of load or time post-load on cell number (control; 0.5 hr 128.80 ±17.87 %, 6 hr 105.78 ±9.51 %, 72 hr 122.18 ±15.06 %; loaded: 0.5 hr 91.17 ±4.61 %, 6 hr 125.21 ±13.46 %, 24 hr 143.20 ±18.01 %) (Figure 5.4D). When osteocytes were cultured for 7 days prior to mechanical stimuli, there was also no significant effect of load on 3D osteocyte mono-cultures (control 100 ±2.41 %, loaded 99.65 ±1.48 %) (Figure 5.4E).

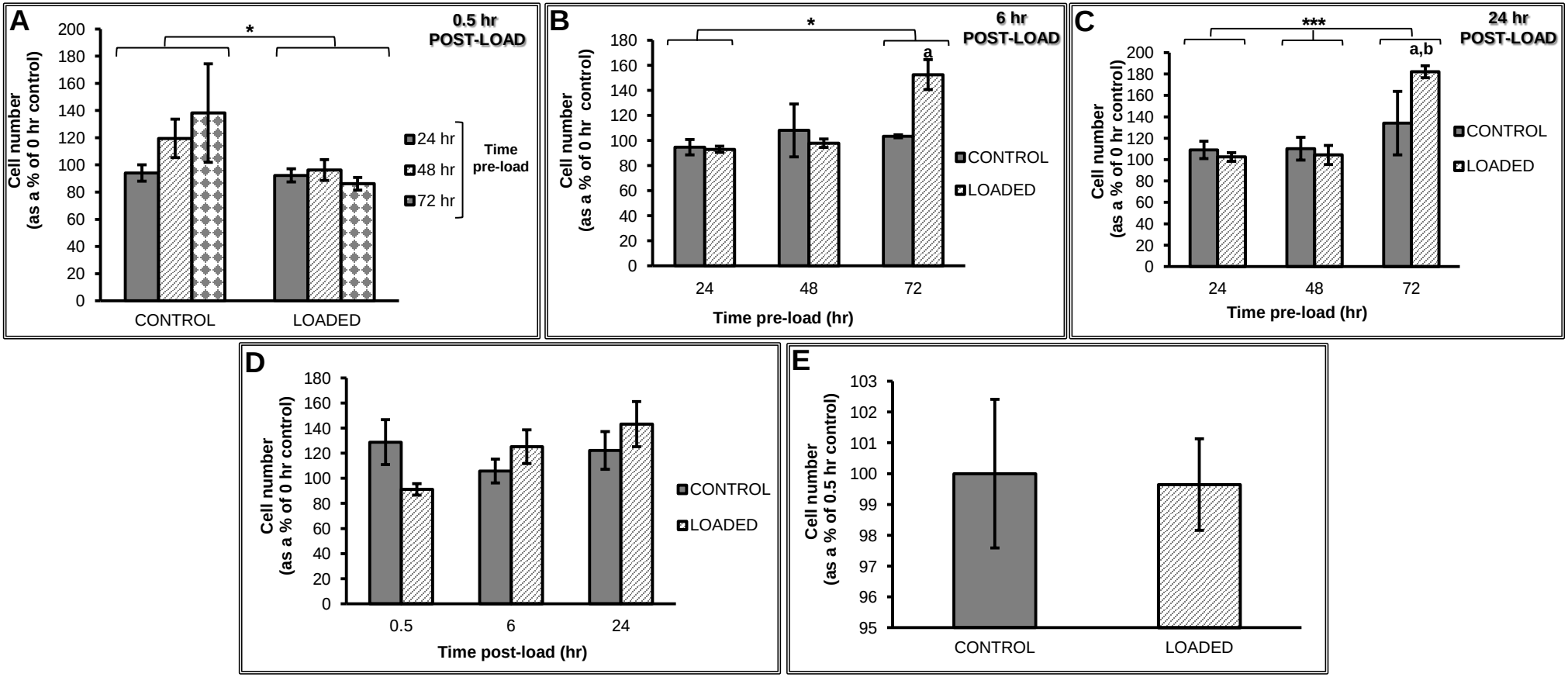

Figure 5.4 *Cell number in mechanically-loaded 3D osteocyte mono-cultures by LDH assay*. Graphs showing cell number categorised by time of culture (A-C), combined 48-72 hr cultures (D) and 7 day cultures (E) at 0.5, 6 and 24 hr post-load unless other time-points are indicated. Data were expressed as a percentage of the average of 0 hr control cultures (A-D) or the average of 0.5 hr control cultures (E). **P<0.05, ***P<0.001* as obtained by GLM (C), GLM of $\log_{10}$ data (A) or ranked data (B). Significant differences as obtained by GLM pairwise comparisons denoted by 'a' with respect to 24 hr loaded cultures (B-C) and 'b' with respect to 48 hr loaded cultures (C). Data presented are from (A-C) 1 (48-72 hr cultures) or 2 (24 hr cultures) independent experiments, n=3; (D) 2 independent experiments, n=3 and (E) 1 independent experiment, n=3.

5.3.3 PGE_2 release

A pilot experiment (1 independent experiment, n=2) was carried out in order to determine when and whether PGE_2 is released from 3D osteocyte mono-cultures after being mechanically stimulated using the loading device. In this experiment, where 3D osteocyte mono-cultures were cultured for 24 hr prior to loading, there was a significant effect of load (GLM, *P=0.040*) but not time post-load (Figure 5.5A), and pairwise comparisons of control vs. loaded at each time-point were not significant (Figure 5.5B). Although not significantly different in this pilot experiment, mean PGE_2 release increased approximately 4-fold at 0.5 hr post-load (control 1206.55 ± 37.32 pg/ml/$OD_{492\ nm}$; loaded 4632.91 ±1773.78 pg/ml/$OD_{492\ nm}$) in loaded cultures (Figure 5.5B).

This experiment was then repeated twice measuring PGE_2 release at 0.5 hr post-load only and normalising data to cell number (page 139). At 0.5 hr post-load, there was a significant effect of load (GLM, *P=0.002* of ranked data), time pre-load (GLM, *P=0.0275* of ranked data) and an interaction between both factors (GLM, *P=0.033* of ranked data). PGE_2 was barely detectable in 3D osteocyte mono-cultures cultured for 24 hr pre-load and so mean PGE_2 was significantly higher in loaded osteocytes cultured for 48 hr prior to loading (24 hr: loaded -246.47 ±216.99 pg/ml/$OD_{492\ nm}$; 48 hr: loaded 36120.75 ±13357.06 pg/ml/$OD_{492\ nm}$, *P=0.0249*) (Figure 5.5C), and although not significant, those cultured for 72 hr pre-load also revealed a load-induced increase in mean PGE_2 (control 0 ±4661.30 pg/ml/$OD_{492\ nm}$; loaded 15896.88 ±2361.87 pg/ml/$OD_{492\ nm}$) (Figure 5.5C). Since osteocytes cultured for 48 and 72 hr pre-load increased PGE_2 release in response to loading, these data were combined and re-analysed.

Following loading, PGE_2 release significantly increased at 0.5 hr post-load in 3D mono-cultures cultured for 48-72 hr prior to loading (control 0 ±2505.57 pg/ml/$OD_{492\ nm}$; loaded 26008.81 ±7566.25 pg/ml/$OD_{492\ nm}$) (one-way ANOVA, *P=0.0001* of ranked data) (Figure 5.5D). When cultured for 7 days prior to mechanical stimuli, 3D osteocyte mono-cultures also showed a significant increase in PGE_2 release 0.5 hr post-load in loaded cultures compared to control cultures (control 1195.40 ±109.72 pg/ml/$OD_{492\ nm}$; loaded 3152.26 ±435.20 pg/ml/$OD_{492\ nm}$) (one-way ANOVA, *P=0.041*) (Figure 5.5E).

.

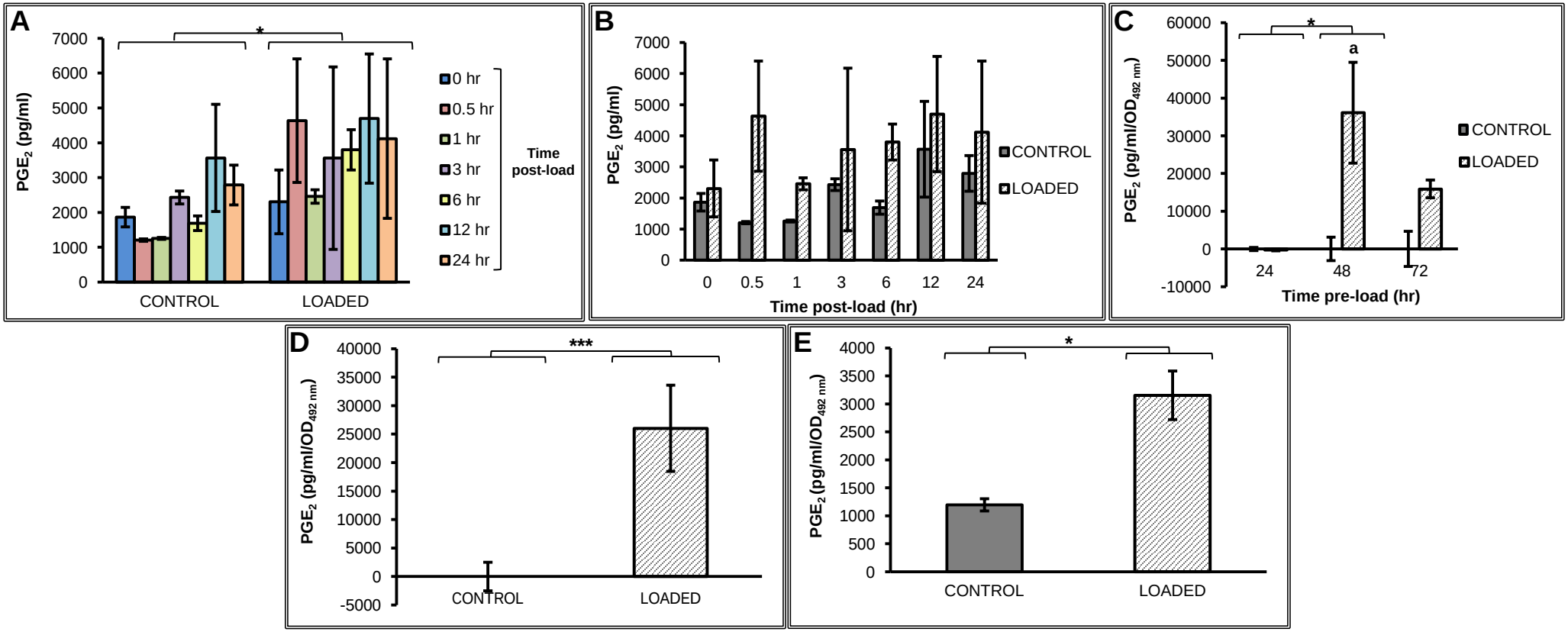

Figure 5.5 *PGE_2 release in mechanically-loaded 3D osteocyte mono-cultures by ELISA.* Graphs showing PGE_2 release in a pilot experiment of 24 hr cultures (A-B), categorised by time of culture (C), combined 48-72 hr cultures (D) and 7 day cultures (E) at 0.5 hr post-load unless other time-points are indicated. Data was normalised to the absorbance ($OD_{492\ nm}$) of LDH lysates (cell number) (C-E). *$P<0.05$* as obtained by GLM (A), GLM of ranked data (C) or one-way ANOVA (E). ***$P<0.001$* as obtained by one-way ANOVA of ranked data (D). Significant differences as obtained by GLM pairwise comparisons denoted by 'a' with respect to 24 hr loaded cultures (C). Data presented are from (A) 1 independent experiment, n=2 or 3; (B) 1 (48-72 hr cultures) or 2 (24 hr cultures) independent experiments, n=3; (C) 2 independent experiments, n=3 and (D) 1 independent experiment, n=2 or 3.

5.3.4 mRNA expression

A pilot experiment (1 independent experiment, n=2) was carried out in order to determine A_{2A}, A_{2B}, AMPAR2, GLAST1, KA1, E11 and RANKL mRNA expression by relative RT-qPCR at 3 and 24 hr post-load in control and loaded 3D osteocyte mono-cultures after being mechanically stimulated using the loading device. Data were expressed in REU and normalised to the geometric mean of GAPDH and HPRT1 as selected by NormFinder (page 57). In this experiment, mRNAs for A_{2A}, A_{2B}, E11 and RANKL were detected in 3D osteocyte control and loaded mono-cultures (Figure 5.6A-D) but GLAST1, AMPAR2 and KA1 mRNAs were not detected. Although not significantly different, loading increased A_{2A} mRNA expression 1.5-fold after 3 hr (control 1.000 ± 0.0364 REU; loaded 1.512 ± 0.162 REU) (Figure 5.6A). A_{2B} mRNA expression was significantly increased in loaded cultures (3 hr: control 1.000 ± 0.039 REU, loaded 1.302 ± 0.068 REU; 24 hr: control 1.000 ± 0.007 REU, loaded 1.368 ± 0.163 REU) (effect of load GLM, *P=0.021*) (Figure 5.6B). E11 mRNA expression was also significantly increased by load (GLM, *P=0.002*) at both 3 and 24 hr (3 hr: control 1.000 ± 0.033 REU, loaded 1.248 ± 0.048 REU, *P=0.460*; 24 hr: control 1.000 ± 0.004 REU, loaded 1.383 ± 0.060 REU, *P=0.0101*) (Figure 5.6.C). RANKL mRNA expression decreased by half 24 hr post-load (control 1.026 ± 0.230 REU; loaded 0.615 ± 0.161 REU) (Figure 5.6D) in loaded cultures as a result of loading.

This experiment was then repeated twice and data was compared to that observed in 3D osteocyte mono-cultures cultured for 48 or 72 hr prior to load (Figure 5.7). No significant differences were observed between osteocytes cultured for 24, 48 or 72 hr pre-load in A_{2A} mRNA expression 3 hr post-load (Figure 5.7A), A_{2B} (Figures 5.7C and D) and E11 (Figure 5.7E and F) 3 or 24 hr post-load, or in RANKL mRNA expression 24 hr post-load (Figure 5.7H). However, there was a significant effect of time pre-load (GLM, *P=0.013*) and load (GLM, *P=0.035*) in A_{2A} mRNA expression 24 hr post-load; and an interaction was observed between both factors (GLM, *P=0.016*). In loaded cultures, A_{2A} mRNA expression was significantly higher in osteocytes cultured for 72 hr pre-load when compared to those cultured for 24 and 48 hr pre-load (24 hr loaded 1.11 ±0.062 REU; 48 hr loaded

0.895 ±0.146 REU; 72 hr loaded 1.651 ±0.175 REU) (pairwise comparisons: 24 hr loaded vs. 72 hr loaded *P=0.0186*; 48 hr loaded vs. 72 hr loaded *P=0.0037*) (Figure 5.7B). There was also a significant effect of time pre-load in RANKL mRNA expression at 3 hr post-load as a result of culture time (GLM, *P=0.018* of ranked data). However, no significant effects of load were observed. RANKL mRNA expression was significantly higher in osteocytes cultured for 48 hr pre-load compared to those cultured for 24 hr pre-load (24 hr loaded 0.908 ±0.125 REU; 48 hr loaded 2.072 ±0.095 REU, *P=0.0353*) (Figure 5.7G). Since loading-induced increases in PGE_2 release only appeared to occur when osteocytes were cultured for 48 hr or greater pre-load, mRNA data was re-analysed, combining experiments where 3D osteocyte mono-cultures were cultured for a minimum of 48 hr prior to mechanical loading.

No significant effect of load or time was observed in A_{2A} or A_{2B} mRNA expression at 3 or 24 hr post-load in 3D mono-cultures cultured for 48-72 hr prior to loading (Figures 5.8A and B). However, there was a trend of load increasing mean A_{2A} expression at both 3 and 24 hr post-load (3 hr: control 1.007 ±0.056 REU, loaded 1.190 ±0.125 REU; 24 hr: control 1.014 ±0.077 REU, loaded 1.273 ±0.197 REU), although this was a small increase. Load significantly decreased E11 mRNA expression (3 hr: control 1.001 ±0.015 REU, loaded 0.937 ±0.030 REU; 24 hr: control 1.022 ±0.096 REU, loaded 0.819 ±0.050 REU) (GLM, *P=0.018* of ranked data), however pairwise comparisons were not significant (Figure 5.8C). Furthermore, there was a significant effect of time on RANKL mRNA expression in loaded cultures (GLM, *P=0.022*). RANKL mRNA expression increased at 3 hr post-load but decreased to control levels at 24 hr post-load (3 hr loaded 1.688 ±0.181 REU; 24 hr loaded 1.027 ±0.220 REU, *P=0.0486*) (Figure 5.8D).

In osteocytes cultured for 7 day pre-load, mRNA expression was analysed at 3 hr post-load only. Data were expressed in REU and normalised to GAPDH as selected by NormFinder (page 57). A_{2A} mRNA expression was doubled in loaded cultures (control 1.019 ±0.144 REU; loaded 2.128 ±0.379 REU) (one-way ANOVA, *P=0.052*) (Figure 5.9A) and E11 increased 1.3-fold (control 1.002 ±0.049 REU; loaded 1.336 ±0.101 REU) (one-way ANOVA, *P=0.041*) (Figure 5.9C) when compared to control cultures. There was no significant effect of load in A_{2B} (Figure 5.9B) and RANKL mRNA expression (Figure 5.9D), although a 1.8-fold increase in RANKL expression was observed (control, 1.020 ±0.141 REU; loaded, 2.126 ±0.430 REU).

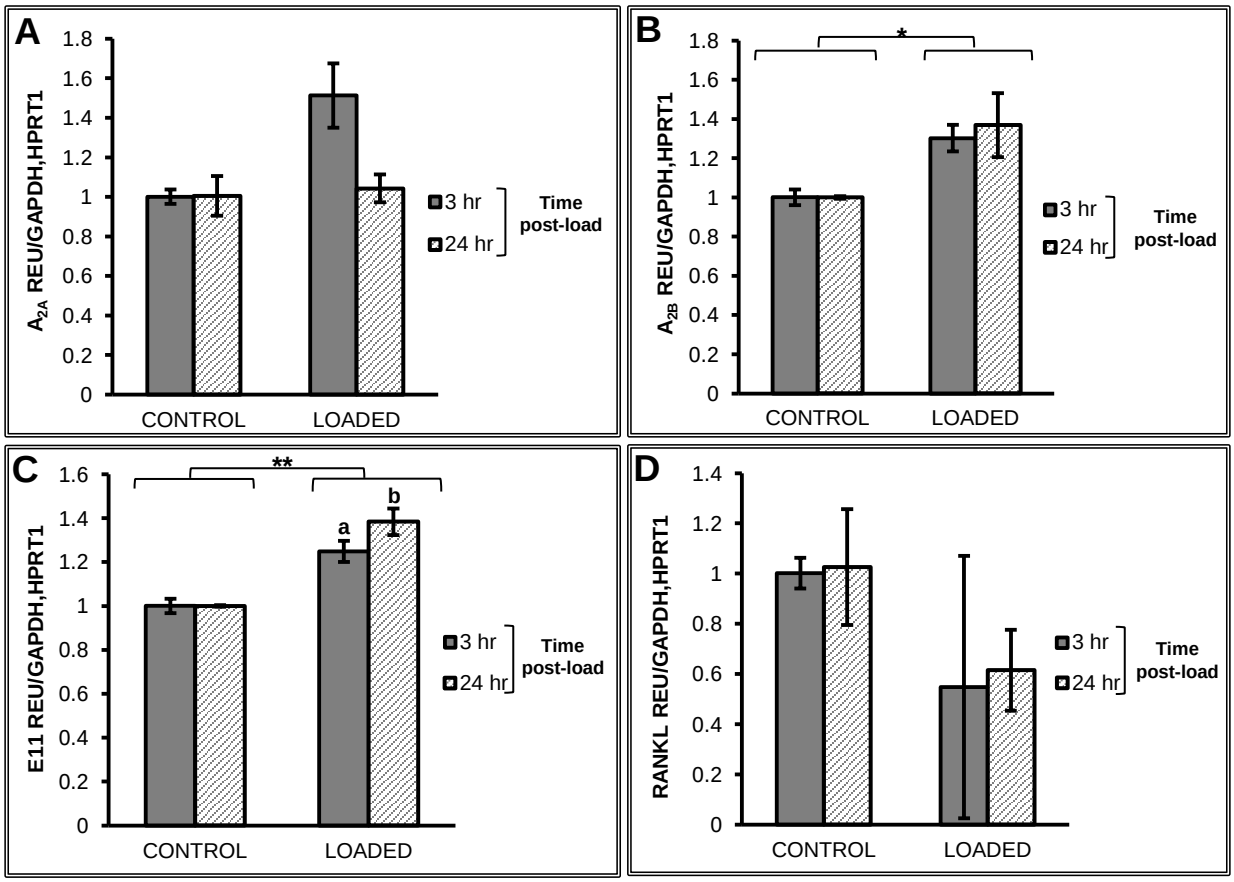

Figure 5.6 *Quantification of mRNA expression in mechanically-loaded 3D osteocyte mono-cultures from a pilot experiment by relative RT-qPCR.* Graphs of A_{2A} (A), A_{2B} (B), E11 (C) and RANKL (D) expression in cultures incubated for 24 hr prior to load. Data expressed as REU and normalised to the geometric mean of GAPDH and HPRT1 expression. Significant differences as obtained by GLM between control and loaded cultures are denoted by *$P<0.05$, **$P<0.01$. Significant differences as obtained by GLM pairwise comparisons denoted by 'a' with respect to 3 hr control, and 'b' with respect to 24 hr control. (1 independent experiment, n=2).

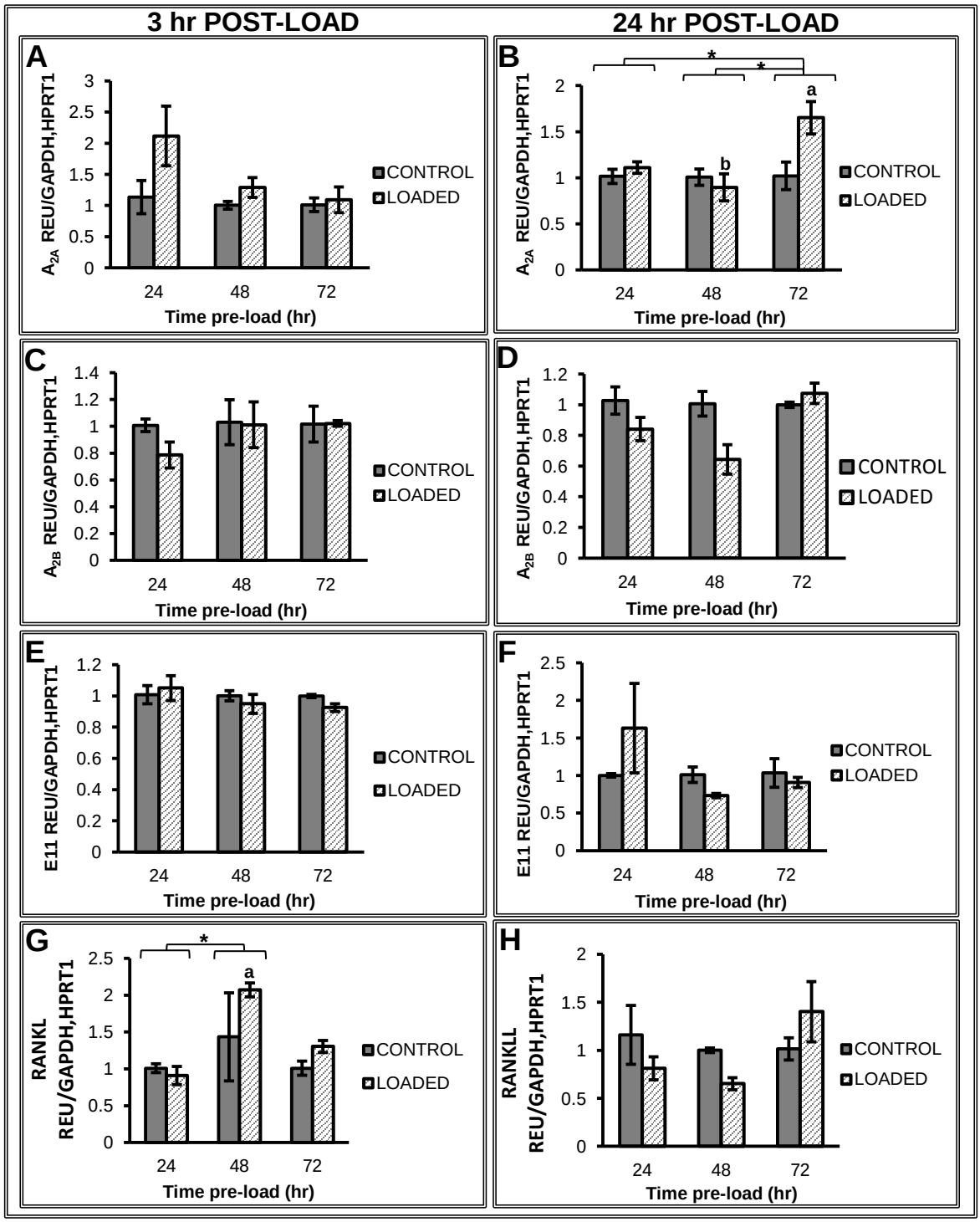

Figure 5.7 *Quantification of mRNA expression in mechanically-loaded 3D osteocyte mono-cultures by relative RT-qPCR categorised by time of culture prior to load.* Graphs of A_{2A} (A-B), A_{2B} (C-D), E11 (E-F) and RANKL (G-H) mRNA expression at 24, 48 and 72 hr culture time pre-load. Data were recorded 3 and 24 hr post-load and are expressed as REU and normalised to the geometric mean of GAPDH and HPRT1. Significant differences as obtained by GLM between culture times are denoted by *$P<0.05$, **$P<0.01$. Significant differences as obtained by GLM pairwise comparisons denoted by 'a' with respect to 24 hr loaded, and 'b' with respect to 72 hr loaded. (1 (48 and 72 hr) or 2 (24 hr) independent experiments, n=3).

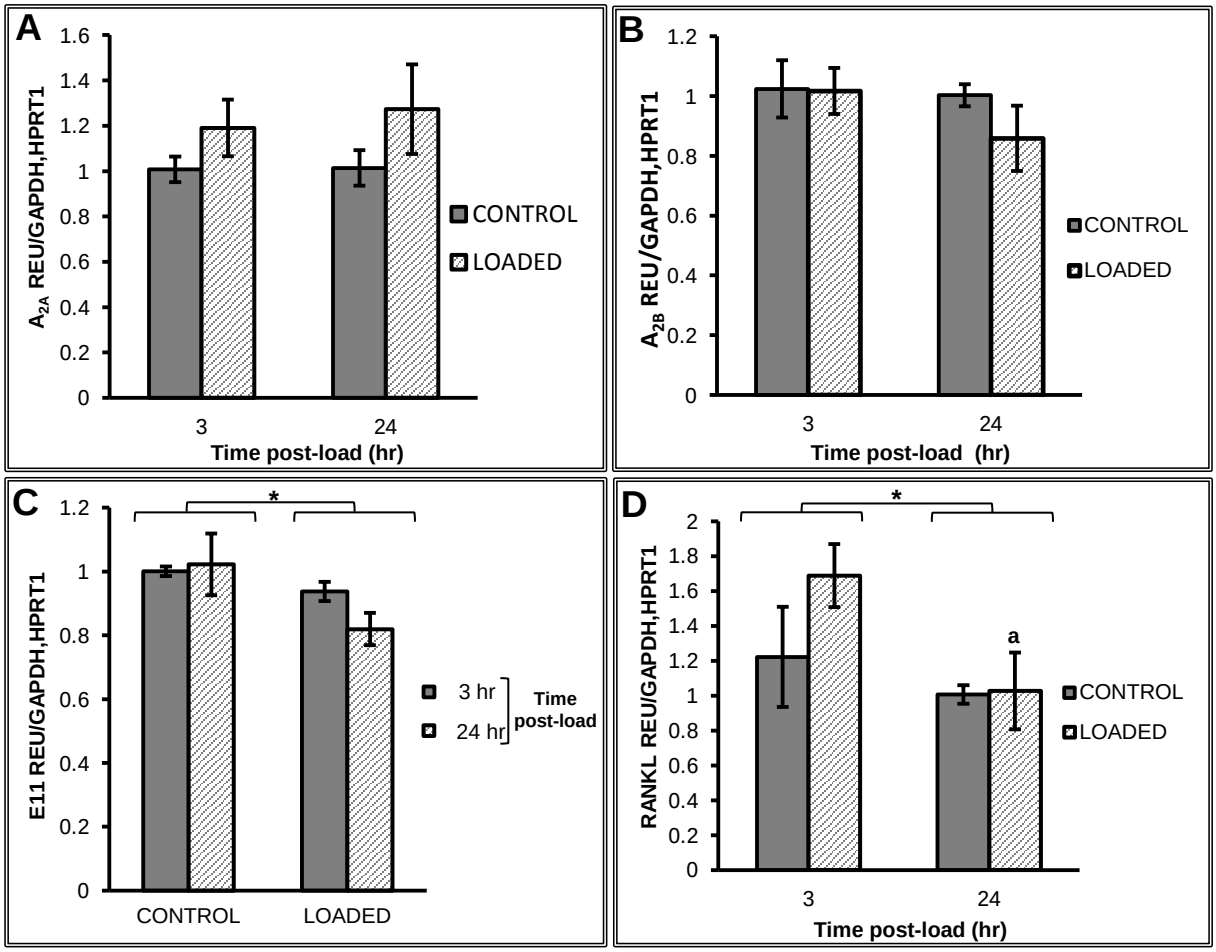

Figure 5.8 *Quantification of mRNA expression in mechanically-loaded 3D osteocyte mono-cultures cultured for 48-72 hr prior to load by relative RT- qPCR.* Graphs of A_{2A} (A), A_{2B} (B), E11 (C) and RANKL (D) mRNA expression. Data were taken at 3 and 24 hr after loading and are expressed as REU and normalised to the geometric mean of GAPDH and HPRT1. Significant differences as obtained by GLM are denoted by *$P<0.05$. Significant differences as obtained by GLM pairwise comparisons denoted by 'a' with respect to 3 hr loaded. (2 independent experiments, n=3).

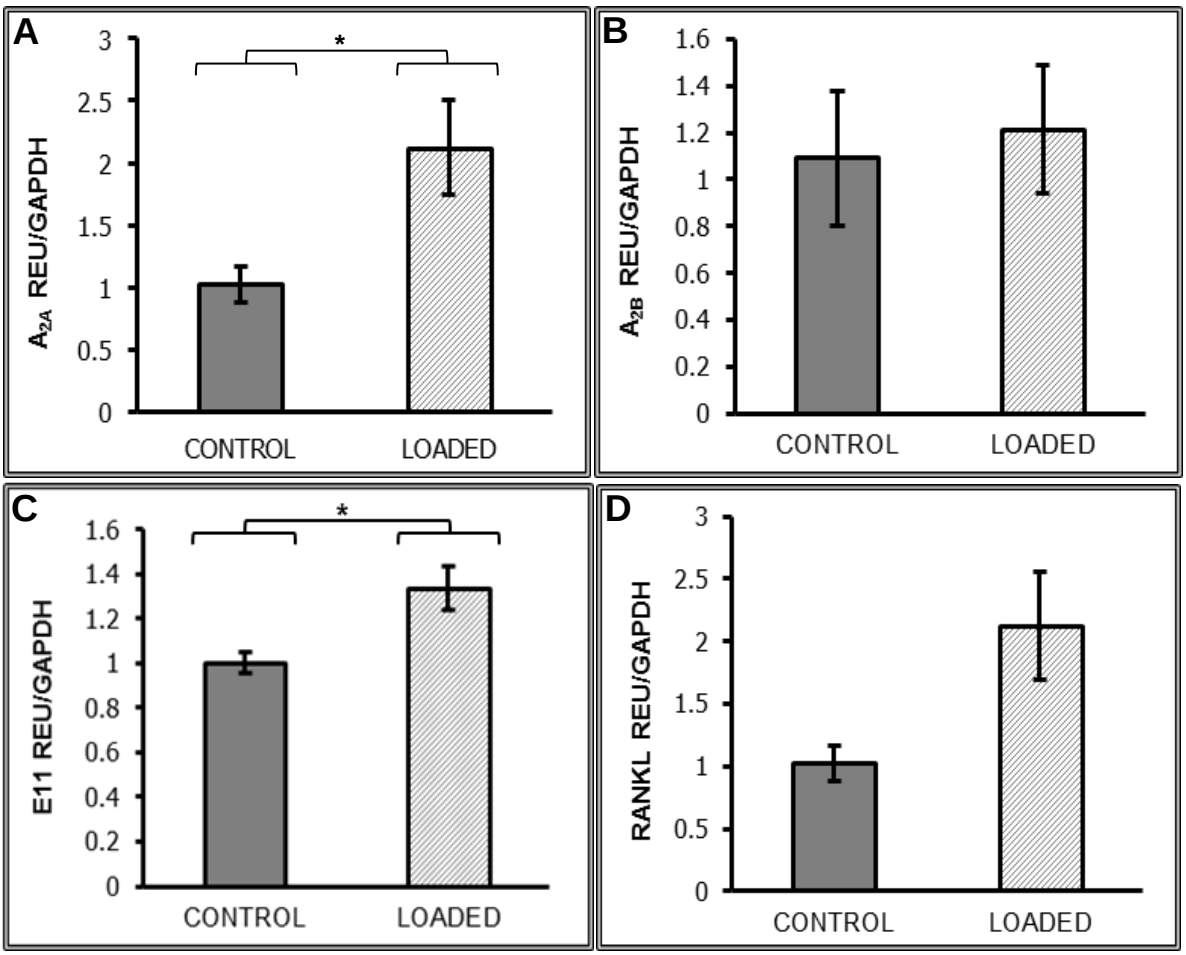

Figure 5.9 *Quantification of mRNA expression in mechanically-loaded 3D osteocyte mono-cultures cultured for 7 days prior to load by relative RT-qPCR.* Graphs of A_{2A} (A), A_{2B} (B), E11 (C) and RANKL (D) mRNA expression. Data were taken at 3 hr post-load and expressed as REU and normalised to GAPDH expression. Significant differences as obtained by one-way ANOVA are denoted by *$P<0.05$. (1 independent experiment, n=3).

5.3.5 IL-6 release

In the pilot experiment of 3D osteocyte mono-cultures cultured for 24 hr prior to loading, there was a significant effect of load (GLM, *P=0.00001*) (Figure 5.10A) but not time, however pairwise comparisons at each time-point were not significant (Figure 5.10B). This experiment was then repeated twice at 0 (immediately after loading), 0.5, 6 and 24 hr post-load, and data was compared to that observed in 3D osteocyte mono-cultures cultured for 48 or 72 hr prior to load (Figure 5.10 C-E) and expressed relative to the average of 0 hr control samples.

At 0.5 hr post-load, there was a significant effect of loading (GLM, *P=0.038* of ranked data) and time pre-load (GLM, *P=0.009* of ranked data) on IL-6 release (Figure 5.10C). Although there was a significant effect of load on the whole data set which appeared to increase mean IL-6 at 48 and 72 hr time pre-load, within individual time-points there were no significant effects of load. IL-6 release was significantly greater at 0.5 hr in osteocytes cultured for 48 hr prior to loading compared to those cultured for 24 hr pre-load (24 hr: control 134.17 ±51.37 pg/ml/$OD_{492\ nm}$, loaded 107.46 ±19.69 pg/ml/$OD_{492\ nm}$; 48 hr: control 3989.93 ±2153.05 pg/ml/$OD_{492\ nm}$, loaded 6524.92 ±1498.27 pg/ml/$OD_{492\ nm}$) (GLM, *P=0.0134* of ranked data) (Figure 5.10C). At 6 hr post-load, there was an effect of time pre-load (GLM, *P=0.00001* of ranked data) but no effect of load on IL-6 release. IL-6 release from osteocytes cultured for 24 hr pre-load was significantly different when compared to those cultured for 48 hr and 72 hr pre-load (GLM, *P=0.00001* of ranked data for both 24 hr vs. 48 hr and 24 hr vs. 72 hr) (Figure 5.10D). IL-6 significantly increased in control osteocytes cultured for 48 and 72 hr pre-load when compared to control osteocytes cultured for 24 hr pre-load (24 hr control 214.10 ±37.12 pg/ml/$OD_{492\ nm}$; 48 hr control 7935.85 ±3110.22 pg/ml/$OD_{492\ nm}$; 72 hr control 8898.65 ±3849.85 pg/ml/$OD_{492\ nm}$, *P=0.0001* for both pairwise comparisons); and in loaded cultures at 48 hr when compared to 24 hr loaded cultures (24 hr loaded 252.51 ±27.09 pg/ml/$OD_{492\ nm}$; 48 hr loaded 7036.81 ±898.95 pg/ml/$OD_{492\ nm}$, *P=0.0004*) (Figure 5.10D). Finally, at 24 hr post-load, there was an effect of time pre-load (GLM, *P=0.00001* of ranked data) but no effect of load on IL-6 release. IL-6 release was significantly increased in control osteocytes cultured for 48 and 72 hr pre-load when compared to control osteocytes cultured 24 hr pre-load

(24 hr control 263.51 ±42.28 pg/ml/$OD_{492\ nm}$; 48 hr control 12351.79 ±3993.19 pg/ml/$OD_{492\ nm}$; 72 hr control 7192.60 ±3387.89 pg/ml/$OD_{492\ nm}$) (pairwise comparisons: 24 hr control vs. 48 hr control *P=0.0094*; 24 hr control vs. 72 hr control *P=0.0326*); and in loaded osteocytes cultured for 48 hr pre-load when compared to those cultured for 24 hr pre-load (24 hr loaded 299.57 ±73.13 pg/ml/$OD_{492\ nm}$; 48 hr loaded 6506.72 ±1864.32 pg/ml/$OD_{492\ nm}$) (pairwise comparisons: 24 hr loaded vs. 48 hr loaded *P=0.0399*) (Figure 5.10E). Since IL-6 release was much lower in osteocytes cultured for 24 hr pre-load and PGE_2 responses to loading were increased in osteocytes cultured for 48 hr or greater pre-load, these data were combined for 3D osteocyte mono-cultures cultured for a minimum of 48 hr prior to mechanical loading.

One-way ANOVAs were used to analyse 48-72 hr time pre-load data as transformation did not make data parametric when using GLM. Therefore the only comparisons made were between control and loaded cultures at the individual time-points. Although there was no significant effect of load on IL-6 release in 3D mono-cultures cultured for 48-72 hr prior to loading (Figure 5.10F), a trend of decreased mean IL-6 release as a result of load was observed at 6 and 24 hr post-load, but not at 0.5 hr post-load.

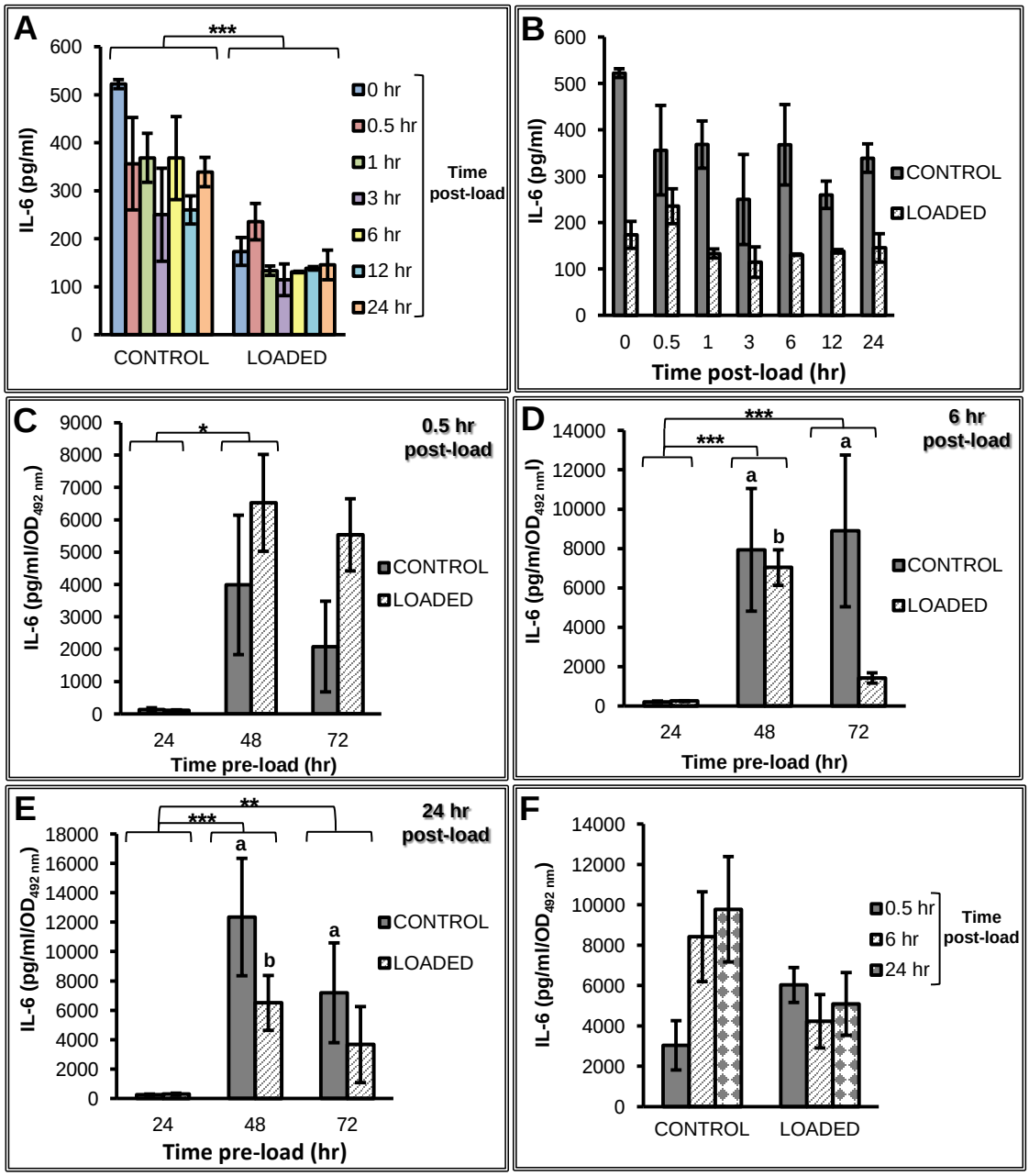

Figure 5.10 *IL-6 release in mechanically-loaded 3D osteocyte mono-cultures by ELISA*. Graphs showing IL-6 release in a pilot experiment of cultures incubated for 24 hr prior to load (A-B), categorised by time of culture pre-load (C-E) and combined 48-72 hr pre-load cultures (F) at time-points indicated post-load. Data were normalised to total cell number (C-F). **P<0.05, ***P<0.001* as obtained by GLM of ranked data. Significant differences as obtained by GLM pairwise comparisons denoted by 'a' with respect to 24 hr control cultures, and 'b' with respect to 24 hr loaded cultures (D-E). Data presented are from (A) 1 independent experiment, n=2 or 3; (B-D) 1 (48-72 hr cultures) or 2 (24 hr cultures) independent experiments, n=2 or 3; (E) 2 independent experiments, n=3.

5.4 Discussion

A novel mechanical loading device was developed in order to facilitate the application of mechanical stimuli to the 3D co-culture model (Figure 5.1A and B). The ability of the device to induce a cellular response was assessed by loading osteocytes, the mechanosensing cell in bone, in 3D type I collagen gels. The work in this chapter aimed to test the loading device and characterise the osteocyte response. A summary of the results shown can be seen in Figure 5.11. It is important to mention that the results presented in this chapter from the 24 hr pilot experiment and 7 day pre-load cultures are each derived from single experiments (n=2 or 3) and therefore all trends observed should be discussed with caution. In order to increase the reliability of the results presented, these experiments should be repeated. Nevertheless, the data presented give an indication of the load responses from 3D collagen embedded osteocytes using a novel loading device.

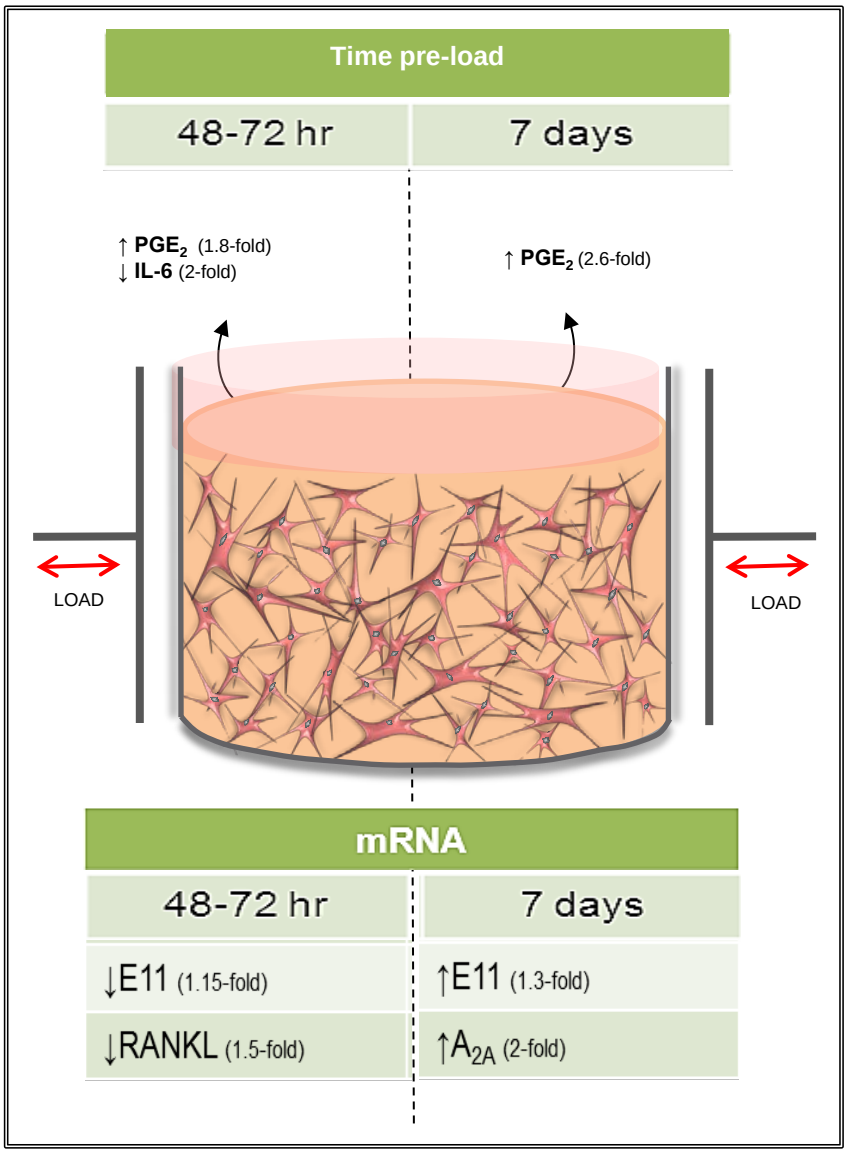

Figure 5.11 *Summary of results*. Embedded osteocytes were shown to respond to physiological loads by releasing PGE_2, and this loading response was maintained if the embedded osteocytes were cultured for a minimum of 48 hr and up to 7 days prior to mechanical stimuli. Culture time pre-load appeared to have an effect on E11 mRNA expression as a result of loading. Furthermore, the adenosine receptor A_{2A} was shown to be mechanically regulated.

5.4.1 Mechanical loading device

A 16-well silicone plate was developed where the wells were of the same dimensions as a standard 48-well tissue culture plate but with thinner bottoms (Figure 5.1A and B). The silicone plate accommodates hooks to stretch the plate, therefore when stretched it causes compression and tension forces at the same time but in perpendicular directions (Figure 5.2). This silicone plate was attached to the BOSE ElectroForce® 3200 loading instrument and the loading regime (5 min, 10 Hz, 2.5 N) was based on previous publications showing that a short period of 10 Hz, 4000-4500 με loading is physiological and osteogenic (Hillam and Skerry, 1995, Mason et al., 1996, Rubin et al., 2001a). The loading device was designed so that when stretched, a uniform strain would be produced in every well causing compression and tension forces at the same time but in perpendicular directions. Furthermore, it was shown that when 2.5 N is applied to the silicone plate, the wells experience strains of approximately 4000-4500 με (Figure 5.1C). However, there was variability in strain across wells. The majority of the wells showed 4000-4500 με when loaded at 2.5 N (Figure 5.1C), which has been shown to be a high osteogenic strain in rats *in vivo* (Mason et al., 1996). Some wells experienced inward welling during strain testing, which resulted in higher strains being recorded, with the highest being approximately 6000 με, but other wells showed lower strains, between 3000-3500 με (Figure 5.1C). In an ideal situation, all wells would experience the same strain, and that strain would be physiological and osteogenic (4000-4500 με), as if wells were to experience different strains it could lead to a variation in load response across repeats within an independent experiment. Furthermore, even though some of the strain values measured are lower than physiological strains (3000-3500 με), they are still within the peak strain values observed in vertebrates which range from 2000-3500 με (Rubin and Lanyon, 1984a, Rubin and Lanyon, 1984b, Rubin et al., 1990). However, wells with strains recorded at 6000 με are exposed to pathophysiological strains.

Inward welling was probably caused by the fact that the base of the wells are thin and without a 3D gel inside the well, the base is flexible and can bend inwards when the plate is stretched. The base of the plate could be made thicker which may help resolve the inward welling, however a previous prototype of this silicone plate was made with a thicker base and it interfered with microscopic observation of the cells as it was not transparent enough. A compromise between thickness and transparency of the base of the plate should be found in order to address the inward welling. However, if this compromise is not possible, a thicker base should be prioritised over transparency, as observation of the cells in culture could be done using other microscopy techniques.

The strain testing performed was carried out on an empty plate. Therefore, testing the silicone plate with 3D cultures may prevent inward welling and variable strains, and thus give a more accurate reading of the strains occurring within each well when 2.5 N of force is applied. This method was previously tested by applying a speckle pattern on the surface of 3D collagen gels within the silicone plate. However, the speckles were too big for the surface area to be analysed by the DIC cameras and the 3D gels were also found to reflect the light of the cameras, interfering with the readings. This method should be optimised by taking into account the 3 main requirements for speckle patters: image contrast, randomness of the pattern and attachment of the pattern to the surface of the specimen (Ning et al., 2011). The incorporation of toner into the 3D gels before polymerisation within the silicone plate may be a possible solution (Sutton et al., 2009). The toner would give a smaller speckle pattern which would be detectable by the DIC cameras. However, the natural pink colour of the 3D gels may not produce enough contrast for the cameras to detect the individual speckles. Furthermore, the light reflective properties of the 3D gels may not be able to be addressed. Application of the speckle pattern to the base of the silicone plate, with 3D collagen gels in the wells, may be a better solution. It is vital to accurately measure strains within the developed loading device and further work should be carried out to improve this methodology, as previously mentioned, if the strains across wells are truly variable, it could lead to a variation in load response across experimental repeats. For example, osteocytes within 3D gels in wells which

experience higher strains may release more PGE_2 than those in wells suffering lower strains.

Currently, there are two devices similar to the one developed in this thesis, based on a silicone plate format (Neidlinger-Wilke et al., 2005, Tata et al., 2011). Tata et al developed a silicone plate in a six-well plate format to mechanically load VSMCs in monolayers, whereas the device developed by Neidlinger-Wilke et al is a single-well silicone plate which was designed to load 3D collagen cultures of intervertebral disc cells. Both devices were used to apply cyclic mechanical stimuli by stretching in a similar fashion to the device developed in this thesis (Neidlinger-Wilke et al., 2005, Tata et al., 2011). The loading regimes applied using these plates (Neidlinger-Wilke et al., 24 hr, 0.1 Hz, 10,000 με; Tata et al., 6-72 hr, 1 Hz, 10-20% strain) (Neidlinger-Wilke et al., 2005, Tata et al., 2011) are indeed very different to the regime used in this thesis and used frequencies below osteogenic values (Mason et al., 1996, Rubin et al., 2001a). Both published devices were not designed to fit a commercially available loading instrument and therefore require their own custom-made loading apparatus (Neidlinger-Wilke et al., 2005). Furthermore, Neidlinger-Wilke et al did not publish strain test data and Tata et al assessed the strain field at the bottom surface of the wells using finite element (FE) modelling, but did not directly measure strains to validate this FE model by using DIC, or any other methods (Neidlinger-Wilke et al., 2005, Tata et al., 2011). Thus the strains applied with the published models are not validated, nor have been shown to be uniform.

Although further work must be done in order to fully characterise the loading device developed in this thesis and ensure the application of uniform strains, the strain measurements obtained by DIC gave an initial indication that 2.5 N of force may result in physiological osteogenic strains. Furthermore, the device can be successfully used with a BOSE ElectroForce® loading instrument and allows the application of mechanical stimuli to 16 3D collagen co-cultures at the same time, a higher number of specimens than the published or commercially available devices.

5.4.2 Cell death/number

In 3D osteocyte mono-cultures, under the stated experimental conditions, there was no detectable cell death as a result of mechanical loading at any time pre-load or post-load time. However, cell number was found to be significantly higher in osteocytes cultured for 72 hr pre-load compared to those cultured for 24 and 48 hr pre-load (Figure 5.4B and C). These data suggest that there may be an increase in proliferation or a decrease in cell death within the first 24 hr of culturing osteocytes in 3D gels. Therefore, 3D osteocyte mono-cultures should be cultured for at least 48 hr prior to loading.

In osteocytes cultured for 48-72 hr and 7 day pre-load, there was no significant effect of loading on cell number (Figure 5.4D and E), correlating with cell death data. Previous *in vivo* (Noble et al., 2003, Plotkin et al., 2005, Kulkarni et al., 2012) and *in vitro* (Bakker et al., 2004, Tan et al., 2006, Tan et al., 2008) studies have shown that loading reduces osteocyte cell death. Furthermore, *in vitro* studies have shown that loading increases osteoblast number (Kaspar et al., 2000, Pavlin et al., 2000, Kaspar et al., 2002, Ignatius et al., 2005, Jackson et al., 2006). These *in vitro* studies contradict 3D osteocyte mono-culture data. However, this could be explained by the fact that osteoblasts were cultured in monolayers and subjected to stretching or fluid flow loading regimes of 0.5 or 1 Hz and approximately 1000 or 10000 με, for a minimum of 0.5 hr each day for the duration of their experiments (Kaspar et al., 2000, Kaspar et al., 2002, Ignatius et al., 2005, Jackson et al., 2006); whereas, the 3D osteocyte mono-cultures in this thesis were exposed to a single loading regime of 5 min, 10 Hz, 2.5 N (4000-4500 με). To date there appear to be no studies on the effect of load on osteocyte cell number *in vitro*.

5.4.3 PGE_2 release

In 3D osteocyte mono-cultures, load induced PGE_2 release at 0.5 hr post-load was found to be significantly higher in osteocytes cultured for 48 hr pre-load when compared to those cultured for 24 hr pre-load (Figure 5.5C). Although not significant, there was also a higher release of PGE_2 in osteocytes cultured for 72 hr pre-load than those cultured for 24 hr pre-load (Figure 5.5C). These data suggest mechanical loading responses from embedded osteocytes using the developed silicone plate, are more reliable after the osteocytes have been cultured in 3D collagen gels for at least 48 hr prior to loading. This could be because the osteocytes may take over 24 hr to form dendrites and develop an osteocytic phenotype within the 3D collagen gels. Of particular importance is the expression of functional CX43 gap junctions, which have been previously shown to be involved in the release of PGE_2 from osteocytes *in vitro* (Jiang and Cherian, 2003, Cherian et al., 2005).

In osteocytes cultured for 24 hr pre-load from a pilot experiment, there was a significant increase in PGE_2 release at all time-points post-load, in particular at 0.5 hr post-load, though not significant (Figure 5.5A and B). In osteocytes cultured for 48-72 hr pre-load there was a significant increase in PGE_2 release 0.5 hr post-load, consistent with the pilot data (Figure 5.5D). This significant increase at 0.5 hr post-load was also observed in loaded osteocytes cultured for 7 days pre-load (Figure 5.5E). Previous *in vitro* studies have shown that mechanically-loaded osteocytes in monolayer increase PGE_2 release (Cheng et al., 2001a, Jiang and Cheng, 2001, Saini et al., 2011, Li et al., 2012b), as early as 0.5 hr post-load (Cheng et al., 2001a), consistent with the data presented here. No previous studies have investigated osteocyte response to load in 3D. Thus the combination of MLO-Y4 cells in 3D collagen gels with the new loading device has shown load-induced PGE_2 release by these cells for the first time. It is important to note that PGE_2 release resulting from load appeared to be 10 times lower in loaded osteocytes cultured for 7 days pre-load (3152.26 ±435.20 pg/ml/$OD_{492\ nm}$) compared to loaded osteocytes cultured 48-72 hr pre-load (26008.81 ±7566.25 pg/ml/$OD_{492\ nm}$). However, without normalisation to cell number, loaded osteocytes cultured for 48-72 hr pre-load released 3087.11 ±727.17 pg/ml whereas loaded osteocytes cultured for 7 day pre-load released

2076.96 ±307.44 pg/ml, suggesting that the difference observed in normalised values is due to a difference in total cell number between 48-72 hr and 7 days time pre-load.

Nevertheless, it can be concluded that in the 3D model, osteocytes are able to respond to mechanical stimuli when embedded in 3D collagen gels, but the extent of the response is affected by time pre-load time.

5.4.4 mRNA expression

Although for most genes analysed there was no significant difference in mRNA expression between 3D osteocytes cultured for 24, 48 and 72 hr pre-load, some differences were observed in A_{2A} expression 24 hr post-load (Figure 5.7B) and in RANKL expression 3 hr post load (Figure 5.7G). This suggests that generally culture time has no effect on the osteocyte response to load at the mRNA level. The differences observed could be due to the phenotype state of the 3D osteocyte mono-culture. A_{2A} mRNA expression was higher 24 hr post-load in osteocytes cultured for 72 hr pre-load than in those cultured for 24 or 48 hr pre-load (Figure 5.7B), and RANKL mRNA expression 3 hr post-load was higher in osteocytes cultured for 48 hr pre-load than in those cultured for 24 hr pre-load (Figure 5.7G). As previously hypothesised (page 166), the embedded osteocytes may take over 24 hr to develop an osteocytic phenotype, and form dendrites with connections to neighbouring cells within the 3D collagen gels.

In osteocytes cultured for 24 hr pre-load from a pilot experiment, there was no significant effect of load on A_{2A} mRNA expression, although an increase in A_{2A} expression was observed at 3 hr post-load (Figure 5.6A). However, mechanical stimuli significantly increased A_{2B} mRNA expression in loaded cultures (Figure 5.6B). In osteocytes cultured for 48-72 hr pre-load there was no significant effect of load in A_{2A} (Figure 5.8A), consistent with preliminary data, or A_{2B} mRNA expression (Figure 5.8B), contradicting preliminary data. However, mean A_{2A} mRNA expression increased by approximately 1.2-fold in loaded cultures at both 3 and 24 hr post-load, consistent with pilot data. There was also a significant 2-fold increase in A_{2A} mRNA expression observed in 3D osteocyte mono-cultures cultured

for 7 days pre-load (Figure 5.9A). Thus A_{2A} mRNA expression appears to increase in response to mechanical load in 3D osteocyte mono-cultures. The lack of load effect on A_{2B} mRNA expression was also observed in osteocytes cultured for 7 days pre-load (Figure 5.9B). There are no *in vivo* or *in vitro* studies on the effect of mechanical stimuli on the expression of adenosine receptors in bone and this is the first report of mechanical regulation of A_{2A} expression in osteocytes *in vitro*.

In osteocytes cultured for 24 hr pre-load from a pilot experiment, mechanical loading significantly increased E11 mRNA expression at both 3 and 24 hr post-load (Figure 5.6C). In 48-72 hr 3D mono-cultures, mechanical loading significantly decreased E11 mRNA expression by 1.15-fold at both 3 and 24 hr post-load (Figure 5.8C), contradicting preliminary data. However, a significant increase in E11 expression of 1.3-fold was observed in 7 day loaded cultures 3 hr post-load (Figure 5.9C). Previous *in vitro* studies have shown that E11 mRNA expression in MLO-Y4 monolayers increased 2 hr after exposure to fluid shear (Yang et al., 2004, Zhang et al., 2006), which contradicts 48-72 hr time pre-load data, but is consistent with observations from osteocytes cultured for 7 days pre-load. However, all previous studies were carried out in monolayer cultures, suggesting that in order for E11 mRNA expression to increase as a result of load, osteocytes embedded in a 3D matrix may require a longer culture time prior to mechanical stimuli. This observation also suggests that embedded osteocytes cultured for 24 hr pre-load may not respond adequately to mechanical stimuli because of a lack of dendritic process extension, which is dependent on E11 expression, and therefore connection to neighbouring cells. Furthermore, this observation supports the previous hypothesis that osteocytes may take over 24 hr to settle down in the 3D gels, potentially affecting the expression of functional CX43 gap junctions (page 166).

In osteocytes cultured for 24 hr pre-load from a pilot experiment, although not significant, mean RANKL mRNA expression decreased by half 24 hr post-load (Figure 5.6D). In 3D mono-cultures cultured for 48-72 hr pre-load, although there was no load effect on RANKL mRNA, time post-load significantly decreased RANKL mRNA expression in both control and loaded cultures (Figure 5.8D). Furthermore, there was no significant effect of load or time post-load in RANKL

mRNA expression in loaded osteocytes cultured for 7 days pre-load (Figure 5.9D). However there was a 1.8-fold increase 3 hr post-load in loaded osteocytes cultured for 7 days pre-load. Previous *in vitro* studies have shown that RANKL mRNA expression increases in MLO-Y4 cells in monolayers soon after mechanical load by fluid flow (You et al., 2008, Kulkarni et al., 2010), contradicting preliminary and 48-72 hr time pre-load data, but consistent with 7 days time pre-load observations. This suggests a pre-load culture time of 7 days is beneficial, consistent with E11 data.

Interestingly, neither 24 hr, 48-72 hr nor 7 day time pre-load control and loaded cultures expressed detectable levels of GLAST1, AMPAR2 or KA1. These data contradicts previous observations that showed expression of all 3 genes in 3D co-culture embedded osteocytes (Chapter 4). Although there are no previous studies on the mechanical regulation of AMPAR2 or KA1 mRNA expression in osteoblasts or osteocytes, GLAST1 was found to be mechanically-regulated in loaded osteocytes *in vivo* (Mason et al., 1997). However, the same regulation has not yet been shown *in vitro*. The data presented suggests that the presence of osteoblasts may be essential for the expression of GLAST1, AMPAR2 and KA1 in osteocytes embedded in a 3D matrix. This could be tested by culturing 3D co-cultures and osteocyte mono-cultures at the same time and quantifying these mRNAs under each condition. If loaded, the mechanical regulation of GLAST1 in embedded osteocytes could also be tested.

It is important to note that although significant differences in the mRNA expression between control and loaded cultures were observed, some of these differences involved small fold changes. Therefore, the sensitivity of the relative RT-qPCR assay used should be considered. It has been previously been shown that, in general, sensitivity of RT-qPCR assays depend on the handling and purity of the RNA, the reverse transcription step, and the qPCR assay itself (Bustin et al., 2009). Even performing absolute qPCR, which could be considered to be a more accurate method than relative qPCR, has been shown to only be sensitive enough to detect a minimum of 3 gene copies (Bustin et al., 2009). Therefore, even though the small differences in mRNA expression as a result of load were found to be statistically significant in this chapter, these should be considered with caution and confirmed by

assays which are known to be highly sensitive to small changes, such as digital PCR (Vogelstein and Kinzler, 1999, Dube et al., 2008, Schmittgen and Livak, 2008).

5.4.5 IL-6 release

In 3D osteocyte mono-cultures, IL-6 release at 0.5, 6 and 24 hr post-load as a result of loading was found to be significantly higher in osteocytes cultured for 48 hr and 72 hr pre-load when compared to those cultured for 24 hr pre-load (Figure 5.10C-E). These data give further evidence that mechanical loading responses from embedded osteocytes using the developed silicone plate are more reliable after at least 48 hr incubation prior to mechanical stimuli.

In 3D osteocyte mono-cultures cultured for 24 hr pre-load from a pilot experiment, there was a decrease in IL-6 release at all time-points post-load (Figure 5.10A and B). Although not significant, mean IL-6 release was reduced to approximately one half of control values at 6 and 24 hr post-load, but not at 0.5 hr post-load, in osteocytes cultured for 48-72 hr pre-load (Figure 5.10F), consistent with preliminary data. To date there are no *in vivo* or *in vitro* studies on the effects of mechanical loading on IL-6 release from osteocytes, however a previous *in vitro* study has shown that osteoblasts in monolayers exposed to compression highly increase their IL-6 synthesis (Sanchez et al., 2009).

5.5 Conclusion

In conclusion, a novel loading device, designed to apply uniform strain in a multi-well plate format, induced release of PGE_2 in 3D osteocyte mono-cultures in response to loads of 5 min, 10 Hz, 2.5 N. The device can be attached to a commercially available loading rig and be used to mechanically stimulate 16 3D co-cultures or mono-cultures at the same time. Validation of strain by DIC revealed that although there is strain variability across wells ranging from 3000 to 6000 με, 9 out of 16 wells were exposed to 4000-4500 με, although further work should be done to validate the loading device. Furthermore, it was shown for the first time that osteocytes within 3D gels exposed to cyclic strains using the developed loading device, increased PGE_2 release, and A_{2A} and E11 mRNA expression, and decreased IL-6 synthesis. These responses were found to be dependent on culturing osteocytes within gels for at least 48 hr prior to load. Although some of these experiments must be repeated in order to confirm the observations reported, it was demonstrated that the silicone plate provides a platform for the study of mechanically-induced bone formation and signalling in the 3D co-culture model.

CHAPTER 6

THE EFFECT OF MECHANICAL LOADING ON OSTEOGENESIS IN THE 3D CO-CULTURE MODEL AND THE ROLE OF GLUTAMATE AND ADENOSINE RECEPTORS IN THIS PROCESS

6. The effect of mechanical loading on osteogenesis in the 3D co-culture model and the role of glutamate and adenosine receptors in this process

6.1 Background

In previous chapters of this thesis it was shown that within the 3D co-culture model, adenosine receptors A_{2A} and A_{2B}, CaSR and the glutamate transporter GLAST1 and receptors KA1 and AMPAR2 are expressed, indicating their potential for functional signalling (Chapter 4). Furthermore, it was also shown that osteocytes embedded in 3D type I collagen gels respond to mechanical stimuli (Chapter 5).

Currently, there is only one published osteocyte-osteoblast co-culture model (Taylor et al., 2007). Although this is a 2D model, it has been used to investigate the effects on osteoblasts of mechanically-induced signals from osteocytes by exposing monolayer osteocytes to fluid flow whilst shielding the osteoblasts (Taylor et al., 2007). Taylor et al showed that functional gap junction connections between osteoblasts and osteocytes, and the MAPK/ERK1/2 intracellular signalling pathway, are essential for the response of osteoblasts (proliferation and ALP activity) to osteocyte mechanical signals (Taylor et al., 2007). Such signals from osteocytes have previously been shown to include IGF-1 and related proteins (Reijnders et al., 2007a, Reijnders et al., 2007b), NO (Fox et al., 1996, Zaman et al., 1999), BMP2 (Rawadi et al., 2003), SOST (Winkler et al., 2003, van Bezooijen et al., 2004, Poole et al., 2005, van Bezooijen et al., 2005, Lowik and van Bezooijen, 2006, van Bezooijen et al., 2007), and PGE_2 (Klein-Nulend et al., 1995b, Ajubi et al., 1996, Ajubi et al., 1999).

Previous studies have implicated adenosine, calcium-sensing and glutamate mediated signalling in osteogenesis. Several *in vivo* studies showed that KO animals of some of the receptors involved display a bone phenotype (Morimoto et al., 2006, Chang et al., 2008b, Skerry, 2008b, Kara et al., 2010b, Carroll et al., 2012, Mediero et al., 2012) (pages 36, 38 and 40). *In vitro* studies have also associated these pathways with bone cell biology (pages 36, 38 and 40). However, to date, only glutamate (Spencer and Genever, 2003, Mason, 2004) and ATP (Genetos et al., 2005, Li et al., 2005b, Genetos et al., 2007, Riddle et al., 2007, Liu et al., 2008) have

been implicated in mechanotransduction, with GLAST1, being mechanically regulated in osteocytes (Mason et al., 1997), and NMDA, AMPA and KA receptors in osteoclasts and bone lining cells (Szczesniak et al., 2005) (page 40) ATP was released as a result of mechanical stimuli from both osteoblasts (Pavlin et al., 2000, Romanello et al., 2001, Li et al., 2005b) and osteocytes (Genetos et al., 2007) (page 36). However, mechanically-induced glutamate signalling has only been hypothesised (Mason, 2004), and although ATP has a short half-life with one of its metabolites being adenosine, the role of adenosine itself in mechanically-induced signalling has not yet been investigated.

6.1.1 Aims

This chapter aimed to determine whether mechanical loading of the 3D co-culture model induced osteogenesis. The roles of glutamate and adenosine in mechanotransduction were also investigated by studying the effects of NBQX, an AMPA/KA receptor antagonist, and SCH 442416, an A_{2A} receptor antagonist, on the 3D co-culture responses to mechanical stimuli.

6.2 Materials and Methods

For all experiments in this chapter, 3D co-cultures were prepared, cultured for 7 days, and pre-treated with AMPA/KA (NBQX, 200 µM in DMEM 5% DFBS) or A_{2A} (SCH 442416, 1µM in DMEM 5% DFBS) antagonists for 1 hr before being mechanically-loaded (5 min, 10 Hz, 2.5 N) in the presence of antagonists (page 80). Antagonist carriers, PBS for NBQX and DMSO for SCH 442416 were present in all cultures (page 80). The antagonist medium was removed 30 min post-load, retained, and replaced with standard culture medium. 3D co-cultures were cultured for a further 1 or 5 days post-load. Indicators of bone formation, COL1A1 and ALP mRNA and PINP release; as well as indicators of load response, A_{2A} mRNA expression and PGE_2 release, were measured. Control (non-loaded) cultures underwent all manipulations, such as medium changes, movements in and out of incubators and to and from loading instrument, except for mechanical loading. Data presented are as in Table 6.1.

Table 6.1 *Source of data presented from control and loaded cultures.*

		Analysed	Treatment	Time post-load	N° of experiments	N° of culture replicates (control and loaded)	Statistical test used
mRNA	**A_{2A}**	DZ	Untreated	Day 1	1	2 Untreated	one-way ANOVA
	COL1A1	SZ	Untreated NBQX SCH 442416	Day 1	1	2 Untreated 3 NBQX 3 SCH 442416	GLM
	ALP	SZ	Untreated NBQX SCH 442416	Day 1	1	2 Untreated 3 NBQX 3 SCH 442416	GLM
Microplate assays	**LDH**	Released from whole co-culture	Untreated NBQX, SCH 442416	Day 1 Day 5	1	2 Untreated 3 NBQX 3 SCH 442416	-
	DNA	SZ and DZ	Untreated NBQX, SCH 442416	0.5 hr Day 1 Day 5	1	3 Untreated 3 NBQX 3 SCH 442416	0.5 hr: one-way ANOVA Day 1 and Day 5: GLM
	PGE_2	Released from whole co-culture	Untreated	0.5 hr	1	3 Untreated	one-way ANOVA
	PINP	Released from whole co-culture	Untreated NBQX SCH 442416	Day 1 Day 5	1	2 Untreated 3 NBQX 3 SCH 442416	GLM

SZ: surface zone (osteoblasts); DZ: deep zone (osteocytes); -: No statistical test performed.

NOTE: one-way ANOVAs were performed with Tukey-Kramer post-hoc test; GLMs were for crossed factors and pairwise comparisons where $P \leq 0.05$ were recorded.

6.2.1 Cell death/number

LDH assays were carried out at day 1 and day 5 post-load with medium from untreated and NBQX or SCH 442416 treated 3D co-cultures (control and loaded) to assess cell death (page 73).

DNA quantification assays were carried out at all time-points post-load with total DNA extracted from both surface and deep zones of untreated and NBQX or SCH 442416 treated 3D co-cultures (control and loaded) (pages 53-54). Total ng of DNA from surface and deep zones from each 3D co-culture were added to give total ng of DNA per 3D co-culture and then used to normalise PGE_2 and PINP ELISA data, and calculate cell number per 3D co-culture assuming there is 5.8 µg of DNA per $1x10^6$ mouse diploid cells. Cell number data were expressed as a percentage of the average of 0.5 hr control cultures for all values. Raw data can be found in page 290.

6.2.2 PGE_2 release

PGE_2 ELISA was carried out (page 74) on medium harvested at 0.5 hr post-load from untreated 3D co-cultures (control and loaded) only. Data were normalised to total DNA content (pages 53-54) and analysed as in Table 6.1. Raw data can be found in page 290.

6.2.3 mRNA expression

Total RNA from the surface and deep zones of day 1 post-load 3D co-cultures was extracted separately, reverse transcribed and cDNA integrity checked by RT-PCR of 18S rRNA (pages 52-55). Relative RT-qPCRs for COL1A1 and ALP in the surface zone of all cultures, A_{2A} in the deep zone of untreated cultures only; and 18S rRNA, GAPDH and HPRT1, as RGs were carried out (page 55). Primer details are outlined in pages 56 and 58 and Tables 2.1 and 2.2. RT-qPCR data were normalised to the optimal RG using NormFinder as in page 57. Data for each GOI

were calibrated to the average ΔCt of the untreated control cultures and expressed as REU (page 58). Data was analysed as in Table 6.1.

6.2.4 PINP release

PINP ELISA was carried out (page 76) on medium harvested at day 1 and 5 post-load from treated and untreated 3D co-cultures (control and loaded). Data was normalised to total DNA content (pages 53-54) and statistically analysed as in Table 6.1

6.3 Results

In all cases, data were as in Table 6.1. However, 2 repeats of day 5 3D co-cultures had to be removed from the experiment due to a suspected infection. Therefore, day 5 data analysed were from 1 independent experiment where n=3 for SCH 442416 control and loaded, and n=2 NBQX and untreated control and loaded.

6.3.1 Cell death/number

LDH release into the medium as a result of cell death was measured in all cultures and at day 1 and day 5 post-load. No LDH was detected indicating no measurable cell death as a result of mechanical loading or antagonist treatment (raw data can be found in page 284).

Total ng of DNA were measured at all time-points and treatments to assess cell number. Data were expressed as a percentage of the average of 0.5 hr control cultures for all values. The effect of load, time post-load and treatment on cell number was assessed in untreated cultures only at 0.5 hr post-load (Figure 6.1A), and in all cultures at day 1 and 5 (Figure 6.1B) post-load. However, no significant effects of any of these factors were observed (0.5 hr: untreated control 100 ±13.89 % and loaded 145.43 ±61.55 %; day 1: untreated control 94.97 ±9.88 % and loaded; 85.85 ±2.81 %, NBQX control 114.45 ±34.98 % and loaded 87.05 ±5.18 %; SCH 442416 control 129.45 ±40.66 % and loaded 81.89 ±2.75 %; day 5: untreated control 84.44 ±4.78 % and loaded 79.67 ±2.12 %; NBQX control 79.96 ±2.26 % and loaded 78.69 ±0.13 %; SCH 442416 control 91.24 ±5.12 % and loaded 82.93 ±5.88 %).

6.3.2 PGE_2 release

Whilst mean PGE_2 release appeared to decrease 0.5 hr after loading (Figure 6.2), a significant difference was not observed between untreated control and loaded cultures (control, 0.031 ±0.005 pg/ml/ng DNA; loaded, 0.023 ±0.006 pg/ml/ng DNA) (one-way ANOVA, *P=0.371*).

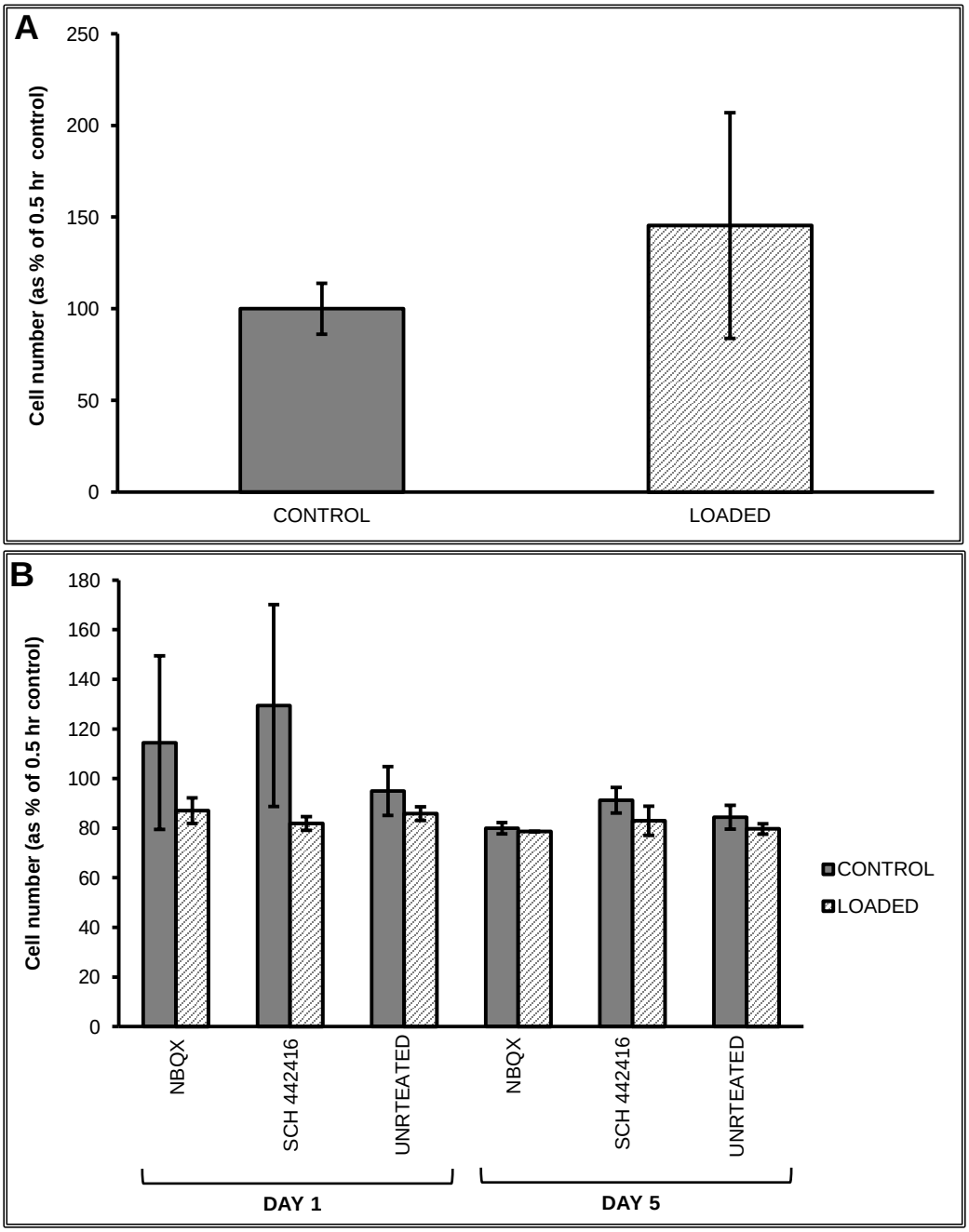

Figure 6.1 *Cell number in mechanically-loaded 3D co-cultures by DNA quantification*. Graphs showing cell number at 0.5 hr post-load (A) and day 1 and 5 post-load (B). Data were expressed as a percentage of the average of 0.5 hr control cultures (A and B). Data presented are from 1 independent experiment, n=3 (A), or 1 independent experiment, n=3 NBQX day 1, SCH 442416 days 1 and 5, and n=2 NBQX and day 5 and untreated control and loaded cultures days 1 and 5 (B).

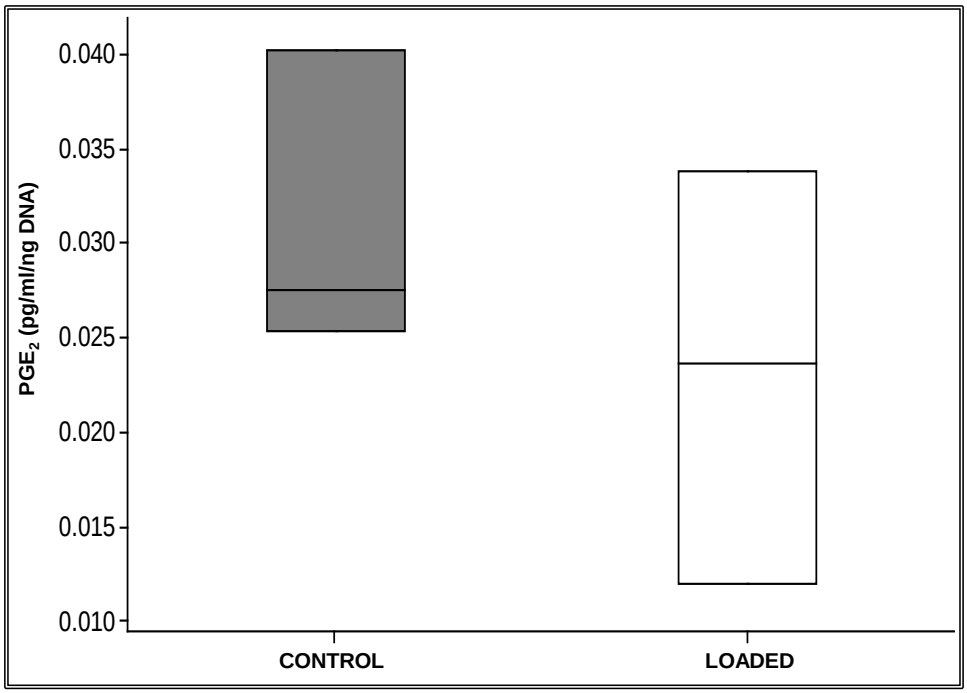

Figure 6.2 *PGE_2 release in untreated mechanically-loaded 3D co-cultures by ELISA.* Boxplot of PGE_2 release from untreated 3D co-cultures 0.5 hr post-load normalised to total ng of DNA. (1 independent experiment, n=3 control and loaded).

6.3.3 mRNA expression

mRNA expression was assessed by relative RT-qPCR in the surface zone of day 1 control and loaded cultures in the presence or absence of NBQX or SCH 442416 using primers against COL1A1 and ALP, and in the deep zone of day 1 untreated control and loaded cultures using primers against A_{2A}. Data were expressed in REU and normalised to either GAPDH for the surface zone, or the geometric mean of GAPDH and HPRT1 for the deep zone (NormFinder used to calculate most stable RG) (page 57).

Mechanical loading did not have a significant effect on embedded osteocyte A_{2A} mRNA expression (control 1.006 ±0.111 REU; loaded 1.047 ±0.227 REU) (Figure 6.3A), or osteoblast COL1A1 (control 1 ±0.003 REU; loaded 0.902 ±0.087 REU) (Figure 6.3B) or ALP (control 1 ±0 REU; loaded 1.566 ±0.607 REU) (Figure 6.3C) mRNA expression in untreated cultures. However, mean ALP mRNA expression appeared to increase by 1.5-fold as a result of loading.

Treatment with NBQX did not have a significant effect on COL1A1 (control 1.186 ±0.236 REU; loaded 1.217 ±0.299 REU) (Figure 6.3B) or ALP (control 0.928 ±0.047 REU; loaded NBQX 3.457 ±1.469 REU) (Figure 6.3C) mRNA expression on loaded surface osteoblasts. However, NBQX treatment seemed to increase mean ALP mRNA expression in loaded cultures by 3.7-fold.

Treatment with SCH 442416 did not have a significant effect on COL1A1 (control 1.252 ±0.270 REU; loaded 0.956 ±0.224 REU) (Figure 6.3B) or ALP (control 0.683 ±0.166 REU; loaded 2.417 ±1.392 REU) (Figure 6.3C) mRNA expression on loaded surface osteoblasts. However, SCH 442416 treatment had a similar effect to that observed with NBQX on mean ALP mRNA expression as it appeared to increase by 3.5-fold in loaded cultures treated with the A_{2A} antagonist.

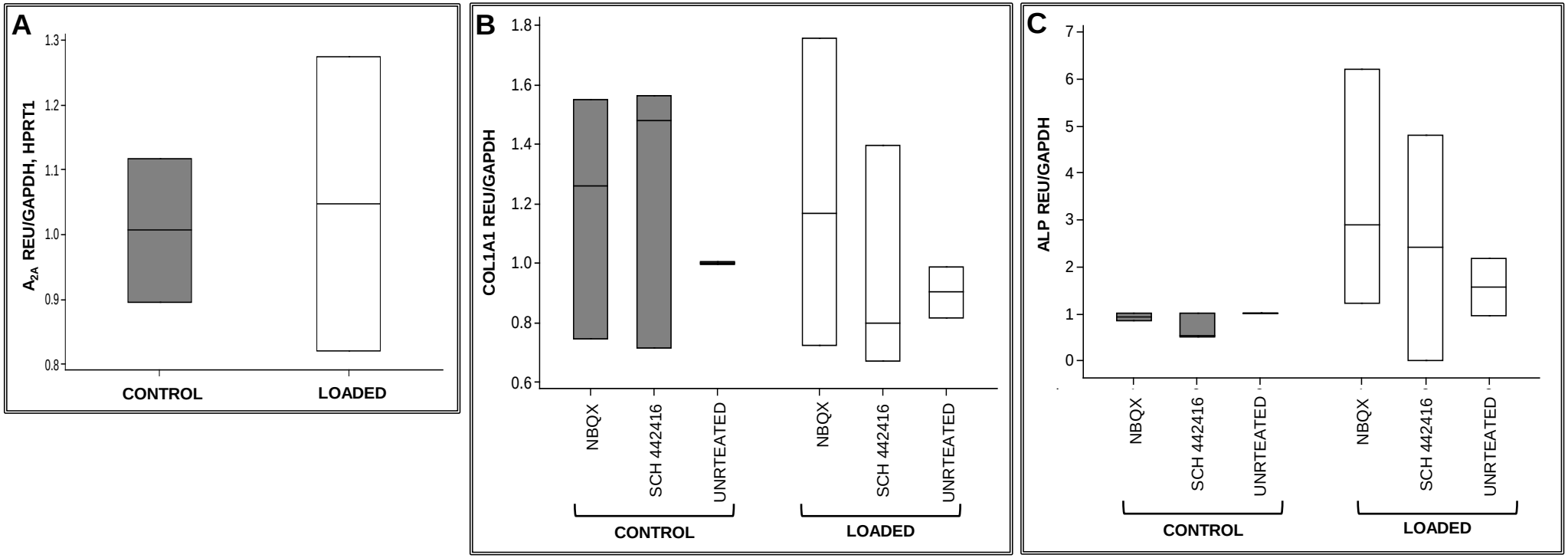

Figure 6.3 *Quantification of gene expression in mechanically-loaded 3D co-cultures at day 1 post-load by relative RT-qPCR.* Boxplots of A_{2A} (A) in the deep zone, and COL1A1 (B) and ALP (C) in the surface zone, expressed as REU and normalised to the geometric mean of GAPDH and HPRT1 expression for $A_{2A,}$ or GAPDH expression for COL1A1 and ALP. Data were from 1 independent experiment, where n=2 deep zone for A_{2A}; and n=3 for NBQX and SCH 442416 treated control and loaded cultures, n=2 untreated control and loaded cultures).

6.3.4 PINP release

Mechanical loading and day had a significant effect on PINP release (GLM, load: *P=0.002*; day: *P=0.005*). Whilst antagonist treatment had no significant effect on PINP synthesis, an interaction between antagonist treatment and load was observed (GLM, *P=0.033*). Although there was a significant effect of day on the whole data set which appeared to increase mean PINP release at day 5, pairwise comparisons were not significant.

PINP release was significantly 1.9-fold higher in untreated loaded 3D co-cultures when compared to control cultures (GLM, *P=0.022*) (Figure 6.4A). However, no significant differences were observed between untreated control and loaded 3D co-cultures at day 1 or 5 (day 1: control 0.0011 ±0.0002 ng/ml/ng DNA loaded 0.0017 ±0, ng/ml/ng DNA; day 5: control 0.0008 ±0.0002 ng/ml/ng DNA; day 5 0.0019 ±0.0003 ng/ml/ng DNA) (Figure 6.4A).

Treatment with NBQX had no significant effect on PINP synthesis from loaded 3D co-cultures at day 1 or 5 (Figure 6.4B). The mean PINP increase at day 1 and 5 in loaded cultures was not as high as that observed in day 1 or 5 loaded untreated cultures (day 1: untreated control 0.0011 ±0.0002 ng/ml/ng DNA, NBQX loaded 0.0013 ±0.0002 ng/ml/ng DNA; day 5: untreated control 0.0008 ±0.002 ng/ml/ng DNA, NBQX loaded 0.0016 ±0 ng/ml/ng DNA), (Figure 6.4B). At day 1, there was no basal effect of NBQX treatment on mean PINP release from control cultures (untreated control 0.0011 ±0.0002 ng/ml/ng DNA; NBQX control 0.00106 ±0.0003 ng/ml/ng DNA), however, at day 5, NBQX treatment increased mean PINP release by 2-fold, approximately the same levels of those observed in untreated mechanically loaded cultures (untreated loaded 0.0019 ±0.0003 ng/ml/ng DNA; NBQX control 0.0019 ±0 ng/ml/ng DNA) (Figure 6.4B).

Treatment with SCH 442416 had no significant effect on PINP synthesis from loaded 3D co-cultures at day 1 or 5 (Figure 6.4C). At day 1, an increase in mean PINP levels in loaded cultures was observed (untreated control 0.0011 ±0.0002 ng/ml/ng DNA; SCH 442416 loaded 0.0014±0.0001 ng/ml/ng DNA); though this increase was not as high as that observed in day 1 loaded cultures without SCH 442416 treatment (Figure 6.4C). Furthermore, at day 1, SCH 442416 treatment decreased mean PINP release from control cultures (untreated control 0.0011 ±0.0002 ng/ml/ng DNA; SCH 442416 control 0.0009±0.0002 ng/ml/ng DNA) (Figure 6.4C). At day 5, SCH 442416 increased mean PINP release to levels slightly higher than those observed in untreated mechanically-loaded cultures, but mean PINP levels were significantly higher than those observed in untreated control cultures (untreated control 0.0011 ±0.0002 ng/ml/ng DNA; untreated loaded 0.0019 ±0.0003 ng/ml/ng DNA; SCH 442416 loaded 0.0021 ±0.0003 ng/ml/ng DNA; $P = 0.0114$) (Figure 6.4C). Furthermore, at day 5, SCH 442416 treatment increased mean PINP release from control cultures (untreated control 0.0011 ±0.0002 ng/ml; SCH 442416 control 0.00154±0.0002 ng/ml) (Figure 6.4C).

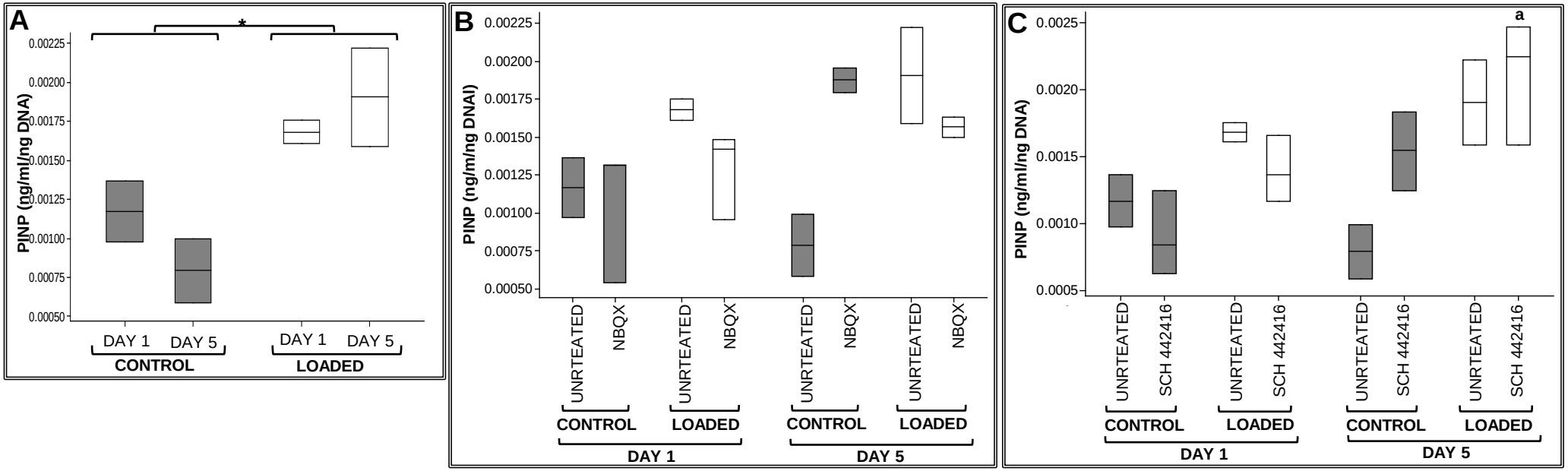

Figure 6.4 *PINP release in mechanically-loaded 3D co-cultures by ELISA.* Boxplots of PINP release from untreated (A), NBQX (B) and SCH 442416 (C) treated 3D co-cultures day 1 and 5 post-load, normalised to total DNA. Significant differences as obtained by GLM denoted by *$P<0.05$ (A). Significant differences from pairwise comparisons denoted by 'a' with respect to day 5 untreated control (C). (1 independent experiment, n=3 NBQX day 1, SCH 442416 days 1 and 5, and n=2 NBQX and day 5 and untreated control and loaded cultures days 1 and 5).

6.4 Discussion

The preliminary experiment in this chapter was used to determine whether the novel 3D osteocyte-osteoblast co-culture model could be used to investigate mechanical loading responses. Furthermore, mechanical signalling was also investigated by exposing the co-cultures to mechanical stimuli and to treatment with AMPA/KA and A_{2A} antagonists. A summary of the results obtained can be found in Figure 6.5. The data presented in this chapter are preliminary as they are obtained from 1 independent experiment with replicate numbers of 2 or 3. Thus the trends observed should be treated with caution. Nevertheless, the data presented helped establish the initial platform for the investigation of mechanically induced bone formation in the novel 3D co-culture model, and mechanotransduction through the adenosine and glutamate signalling pathways.

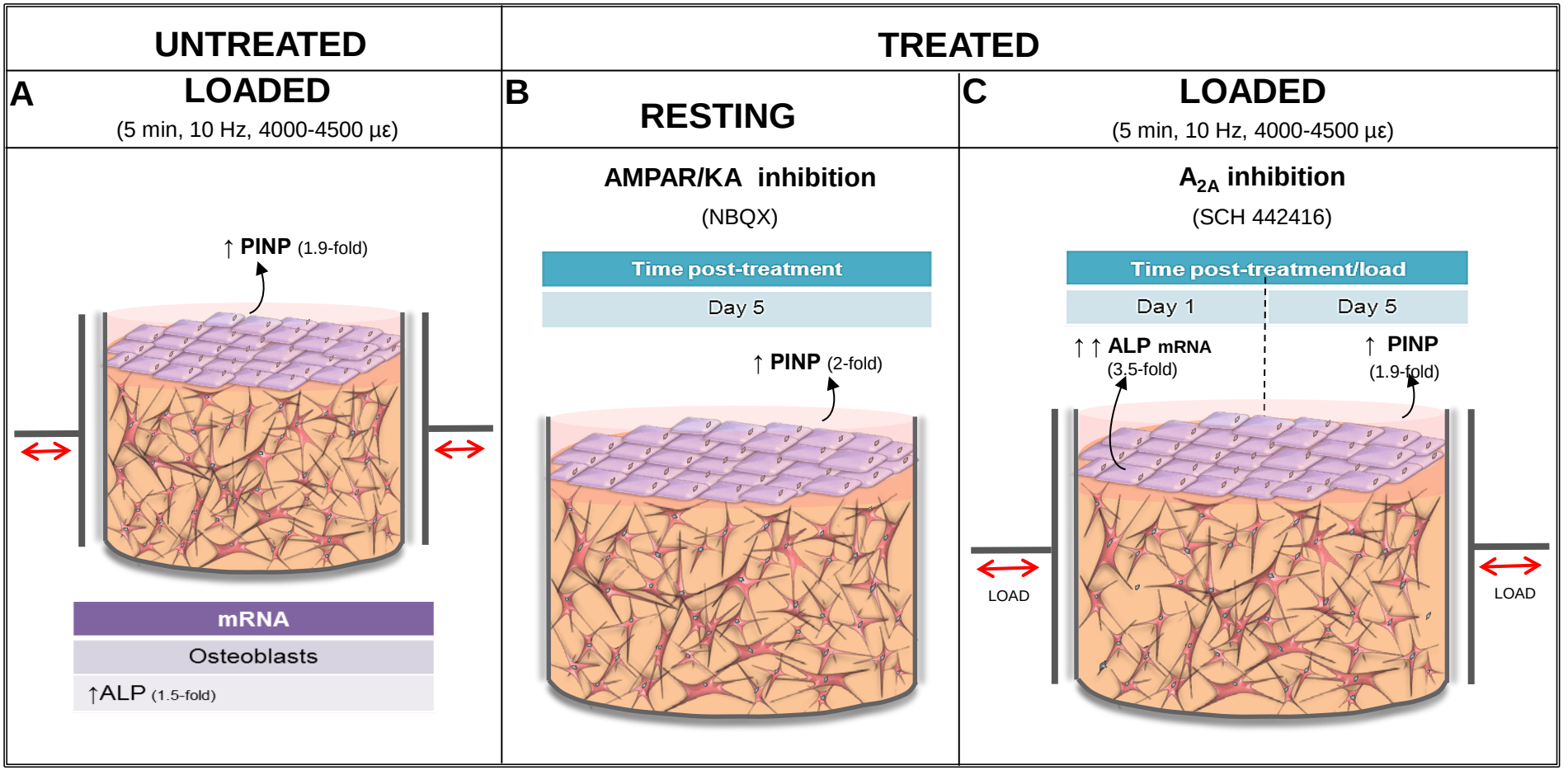

Figure 6.5 *Summary of results.* A) A physiological loading regime applied to the 3D co-culture increases synthesis of PINP and ALP mRNA expression by the osteoblasts. B) In control cultures, at day 5 post-treatment, inhibition of AMPA/KA receptors induced a similar anabolic response to that obtained by mechanical loading (A). C) Mechanical loading and A_{2A} inhibition lead to a doubling of ALP mRNA expression at day 1 and a 1.9-fold increase in PINP release at day 5 when compared to untreated control cultures (A).

6.4.1 Cell death/number

In the 3D co-cultures, under the stated experimental conditions, there was no detectable cell death as a result of mechanical loading or treatment with NBQX or SCH 442416, at any time post-load. There was also no significant difference in cell number observed (Figure 6.1). As previously mentioned (page 166), *in vitro* studies have shown that loading increases osteoblast number (Kaspar et al., 2000, Pavlin et al., 2000, Kaspar et al., 2002, Ignatius et al., 2005, Jackson et al., 2006), which contradict 3D co-culture data. However, this could be because the loading regimes used (0.5 or 1 Hz, 1000 or 10000 με, 0.5 hr minimum per day of culture) (Kaspar et al., 2000, Kaspar et al., 2002, Ignatius et al., 2005, Jackson et al., 2006) do not involve a short single loading bout of mechanical stimulus.

Human primary osteoblasts (HPOBs) cell number has previously been shown to significantly decrease by approximately 19 % and 23 % after 2 and 5 days of treatment with 200 μM NBQX (Bonnet, Mason, Williams and Evans unpublished data), contradicting 3D co-culture data. However, this could be explained by the fact that 3D co-cultures were only incubated with NBQX for 1 hr, whereas Bonnet et al used longer incubation times of 2 and 5 days. Furthermore, the decrease in cell number observed by Bonnet et al was relatively small.

Treatment with 1 μM SCH 442416 has previously been shown to have no effect on the cell number of MSCs differentiating to osteoblasts (Gharibi et al., 2011), correlating with 3D co-culture data.

6.4.2 PGE_2 release

In the 3D co-culture, there was no significant difference in PGE_2 release 0.5 hr after load (Figure 6.2), suggesting no response to mechanical load. This effect contradicts previous data which showed a significant load-induced increase in PGE_2 release in 3D osteocyte mono-cultures (Chapter 5), and previous studies showing that both osteoblasts (Reich and Frangos, 1993, Nauman et al., 2001, Rubin et al., 2001b, Ponik and Pavalko, 2004) and osteocytes (Cheng et al., 2001a, Jiang and

Cheng, 2001, Saini et al., 2011, Li et al., 2012b) in monolayers *in vitro* release PGE_2 in response to mechanical stimuli. Overall, PGE_2 release was considerably lower when osteocytes were in a 3D co-culture (0.023 ±0.006 pg/ml normalised to ng of total DNA) compared to that observed in 3D mono-cultures (78.806 ±10.880 pg/ml normalised to cell number) (Chapter 5). Even without normalisation, PGE_2 release from loaded 3D co-cultures (20.053 ±2.453 pg/ml) was still lower than in loaded 7 day 3D osteocyte mono-cultures (51.924 ±7.686 pg/ml). Furthermore, these values are lower than those previously observed in osteocyte monolayer cultures (Cheng et al., 2001a, Jiang and Cheng, 2001, Saini et al., 2011, Li et al., 2012b). This reduction in PGE_2 release could be due to a failure in inducing a mechanical response or due to a failure in the assay performing correctly, however the standard curve produced indicated the assay worked and that all samples fell within the standard curve (standard curve and raw data can be found in page 284). Another reason for the reduction in PGE_2 release and lack of response to loading could be the presence of osteoblasts. To test this hypothesis, 3D osteocyte mono-cultures and 3D co-cultures should be exposed to load at the same time and PGE_2 release assessed 0.5 hr post-load.

6.4.3 mRNA expression

In the 3D co-culture, there was no significant difference in A_{2A} mRNA expression between day 1 untreated control and loaded embedded osteocytes (Figure 6.3A), which could be due to a failure in inducing a mechanical response, consistent with PGE_2 data. Another explanation could be that the presence of surface osteoblasts regulates osteocyte gene expression, which have not previously been investigated, and thus reflecting the same effect observed with PGE_2 release. In order to confirm this osteoblast regulation of osteocyte gene expression, 3D osteocyte mono-cultures and 3D co-cultures should be exposed to load at the same time and A_{2A} mRNA expression assessed post-load.

In day 1 3D co-cultures, mechanical stimuli had no effect on osteoblast COL1A1 mRNA expression (Figure 6.3B). Previous *in vivo* and *in vitro* studies have shown an increase in osteoblast COL1A1 mRNA expression in response to load. On one hand, *in vivo* studies showed osteoblast COL1A1 mRNA expression is not altered 24 hr after cyclic compression load, but instead begins to increase 2-4 days after loading (Pavlin et al., 2001, Mantila Roosa et al., 2011), consistent with 3D co-culture data. However, *in vitro* osteoblast studies have shown an increase in COL1A1 expression 24 hr after compression or tension loading (Liu et al., 2005, Rath et al., 2008, Lu et al., 2012), contradicting 3D co-culture data. NBQX and SCH 442416 had no effect on day 1 osteoblast COL1A1 mRNA expression regardless of mechanical stimuli (Figure 6.3B). To date there are no studies on the effect of NBQX or SCH 442416 on COL1A1 mRNA expression by osteoblasts.

In day 1 3D co-cultures, mechanical stimuli increased ALP mRNA expression by surface osteoblasts (Figure 6.3C). *In vivo*, osteoblasts increase ALP mRNA expression 24 hr after being mechanically stimulated (Pavlin et al., 2001), which was also observed *in vitro* in MC3T3-E1 cells (Lu et al., 2012) and is consistent with 3D co-culture data. Interestingly, this load-induced increase in ALP mRNA expression was further amplified with NBQX or SCH 442416 treatment (Figure 6.3C). Furthermore, in the absence of mechanical stimuli, SCH 442416 or NBQX treatment had no effect on ALP mRNA expression by surface osteoblasts at day 1 (Figure 6.3C). Consistent with this data, SCH 442416 was previously shown to have no effect on ALP expression during osteoblast differentiation *in vitro* (Gharibi et al., 2011). To date, there are no studies on the effects of NBQX on ALP mRNA expression in osteoblasts or SCH 442416 on ALP mRNA expression by mechanically loaded osteoblasts.

6.4.4 PINP release

In untreated 3D co-cultures, mechanical loading significantly increased PINP release (Figure 6.4A), suggesting that mechanical loading of 3D co-cultures elicits an osteogenic response. These results are consistent with previous studies which demonstrated that osteoblasts *in vitro* increase ColI synthesis after loading (Yang et al., 2012), which contradicts PGE_2 and A_{2A} mRNA data, and therefore the theory that no mechanical response was induced in this experiment. However, these results contradict COL1A1 mRNA expression data from the same cultures, which showed no effect of loading on day 1 COL1A1 expression. This could be explained by fact that mRNA data was obtained only from day 1 surface osteoblasts whereas protein synthesis was measured from the medium of whole 3D co-cultures. Therefore, PINP synthesis may not only be from surface osteoblasts, but also from embedded osteocytes. Primary osteocytes have been previously shown to produce ECM proteins including ColI *in vitro* (Tata et al., 2011). However MLO-Y4 cells produce lower levels of COL1A1 mRNA compared to osteoblasts both in monolayer (Kato et al., 1997) and in 3D co-cultures (Chapter 1), but the production of ColI protein from these cells in the presence or absence of load has not been previously investigated. Therefore, 3D osteocyte mono-cultures and 3D co-cultures should be exposed to load at the same time in order to address the hypothesis that PINP release may be from both cell types within the 3D co-culture. Furthermore, analysis of COL1A1 mRNA expression in loaded embedded osteocytes should also be carried out as it would give an indication of how much collagen these cells may be synthesising. Nevertheless, this PINP release data has shown that mechanically-induced collagen synthesis can be achieved in the 3D co-culture under a physiological and osteogenic loading regime (5 min, 10 Hz, 4000-4500 με) (Hillam and Skerry, 1995, Mason et al., 1996, Rubin et al., 2001a).

Treatment with NBQX in control cultures induced an increase in PINP which was highly similar to that observed in untreated loaded cultures at day 5 post-load (Figure 6.4B). This data contradicts previous *in vivo* studies which have shown that mice injected with NBQX have a decreased trabecular thickness (Lin et al., 2008), whereas rats injected with AMPA have an increased bone volume (Burford et al.,

2004), suggesting that activation of AMPA/KA receptors increases bone formation. To date, the effects of NBQX on bone formation have not been investigated *in vitro* and therefore these are reported for the first time in this thesis. This data suggests that a single dose of NBQX may have the same long-term anabolic effects as mechanical stimuli and, therefore, could be considered a novel anabolic target for bone disease therapies. Furthermore, this data also provides further evidence for the hypothesis that glutamate signalling may have a role in mechanically-induced bone formation (Mason, 2004)

On the other hand, treatment with SCH 442416 caused a significant increase in PINP release in day 5 loaded cultures compared to untreated control cultures (Figure 6.4C). Although not significant, SCH 442416 treatment increased PINP release in control cultures. Furthermore, mechanical loading and a single dose of SCH 442416 treatment appeared to have, although small, an additive effect on PINP release, as PINP levels were higher in loaded SCH 442416 treated cultures than in untreated loaded cultures or treated control cultures. To date, the effects of SCH 442416 on collagen synthesis have not been investigated in osteoblasts. This data suggests that SCH 442416 treatment could be considered as a novel anabolic therapeutic target for bone diseases, similar to NBQX. Furthermore, it could be hypothesised that adenosine signalling may have a role in mechanically-induced bone formation.

6.4.5 Data reliability

As previously mentioned, the results presented in this chapter are preliminary, with low replicate numbers, and therefore all trends and significant P-values observed should be treated with caution. The data were presented in boxplots as a way of performing descriptive statistics and to show the data spread (page 81), to indicate how reliable the trends observed are. One of the main points of discussion is whether a mechanical response was induced in this experiment or not. In this experiment there was no significant effect of load in A_{2A} mRNA expression and PGE_2 release, indicating no mechanical response. According to the data reported in Chapter 5, approximately 2.6-fold and 2-fold increases should be observed for PGE_2

release and A_{2A} mRNA expression, respectively. However, this experiment is based on a small data set with a large range in data points for each of the groups compared and therefore the trends may not be reliable. Although PGE_2 and A_{2A} data may not be reliable enough to indicate load responses, this experiment showed a load-induced osteogenic response. The disparity between COL1A1 mRNA expression and PINP release was also a point of discussion. The boxplot for COL1A1 mRNA expression indicates a large range in the REUs measured within each group indicating the data may not be reliable, whereas the data range of PINP synthesis is much smaller in comparison. The increase in ALP mRNA expression appeared more robust as the ALP data range is large in loaded cultures but not in control cultures. In order to increase the reliability of the data, this experiment should be repeated with a larger replicate number.

6.5 Conclusion

In conclusion, preliminary data show the 3D co-culture model can be used to investigate the osteocyte-osteoblast interactions that lead to mechanically-induced osteogenesis in terms of type I collagen synthesis and alkaline phosphatase activity. This thesis showed that both NBQX and SCH 442416 increased osteoblast ALP mRNA expression in loaded cultures at day 1 and increased PINP release in both control and loaded cultures at day 5. These anabolic effects of AMPA/KA and A_{2A} antagonists support the hypothesis of functional adenosine and glutamate signalling within 3D co-cultures (Chapter 4), and of the potential roles of glutamate and adenosine in mechanotransduction (Mason, 2004) (section 6.1) and osteogenesis. Although the experiments in this chapter must be repeated in order to verify the results obtained, it has tested the platform for the investigation of mechanically-induced bone formation and mechanotransduction through novel signalling pathways.

CHAPTER 7

GENERAL DISCUSSION

7. General discussion

7.1 Validation of the novel 3D co-culture model

This thesis developed a novel 3D osteocyte-osteoblast co-culture mechanical loading model, where osteocytes embedded within type I collagen gels are overlaid with osteoblasts. The cells within the model were shown to be viable, at both day 1 and 7, maintain their morphology and appear to connect to neighbouring cells through CX43 (Figure 7.1A). Both osteoblasts and osteocytes were also shown to maintain their phenotype, through the expression of appropriate phenotypic markers (Figure 7.1A). Osteoblasts expressed higher levels of COL1A1 mRNA than osteocytes, whereas osteocytes expressed higher levels of ALP mRNA than osteoblasts (Figure 7.1A). Both cell types within the model were also shown to express components of the adenosine, calcium-sensing and glutamate signalling pathways (Figure 7.1A), previously shown to be of importance in bone biology as seen in KO animals involving signalling components of these pathways. Briefly, for the adenosine signalling pathway, the A_1 KO model had increased bone volume and small osteoclasts (Kara et al., 2010b), the A_{2A} KO mouse displayed increased bone resorption and osteoclast activity (Mediero et al., 2012), and the A_{2B} KO model exhibited decreased bone density (Carroll et al., 2012) (pages 37-38). For the calcium-sensing signalling pathway, CaSR KO mice displayed growth retardation, small skeletons and several fractures (Chang et al., 2008a) (page 38). Finally, for the glutamate signalling pathway, the NMDAR1 KO model exhibited a thin bone structure and poor mineralisation (Skerry, 2008b); and the VGLUT1 KO model displayed a decrease in bone mass and an increase in osteoclast resorption (Morimoto et al., 2006) (pages 41-42).

Furthermore, the osteocytes within the model were found to respond to physiological mechanical loading and some of these responses depended on the culture time prior to load (Figure 7.1B). Most importantly, this thesis demonstrated that mechanical loading of the 3D co-culture is able to apparently induce an osteogenic response by increasing PINP synthesis (Figure 7.1B) as well as regulate the mRNA expression of adenosine receptor A_{2A} in embedded osteocytes.

There is a great need for a fully characterised *in vitro* 3D matrix based bone model. The majority of the available 3D models involve culturing cells on scaffolds (Tortelli et al., 2009, Barron et al., 2010, Papadimitropoulos et al., 2011b), which does not represent the bone environment *in vivo* where osteocytes, are embedded within a matrix (section 1.4.2.3.2). Published models involving embedding osteoblasts (Maeno et al., 2005, Murshid et al., 2007), MLO-Y4 (Kurata et al., 2006, Murshid et al., 2007) or normal human bone-derived cells (NHBCs) (Atkins et al., 2009) within a matrix showed maintenance of cell viability (Maeno et al., 2005, Kurata et al., 2006), osteocyte cell morphology (Kurata et al., 2006, Murshid et al., 2007, Atkins et al., 2009), connectivity (Kurata et al., 2006), and gene expression (Atkins et al., 2009). However, none of these models have been individually assessed in all key areas of viability, morphology, connectivity and gene expression. Furthermore, none of the available 3D collagen based cultures involve co-culturing osteocytes and osteoblasts, nor they have been exposed to mechanical stimuli. Therefore none investigate the important interactions between these cell types which lead to mechanically-induced bone formation.

A comparison of the 3D co-culture model to previous 3D and 2D *in vitro* models, as well as, to bone *in vivo* can be found in Table 7.1. This table shows that the 3D co-culture model developed in this thesis is better characterised than any other current 3D mono-culture and 2D co-culture models, as the majority of these previous models show gaps in cell viability data, expression of some bone markers, and connectivity of the cells within the model. The 3D co-culture model has osteoblast and osteocyte cell viabilities, morphologies, phenotypes and loading and osteogenic responses similar to those found *in vivo*, some of which also correlate with previous *in vitro* monolayer culture data. However, unlike *in vivo*, there is a lack of expression of SOST, an important mechanically-regulated bone formation regulator, due to the use of MLO-Y4 cells which do not express SOST. The model developed in this thesis has also provided novel information on the expression of adenosine, calcium-sensing and glutamate signalling components in bone cells, and the effect of mechanical load on their expression (Table 7.1).

A RESTING

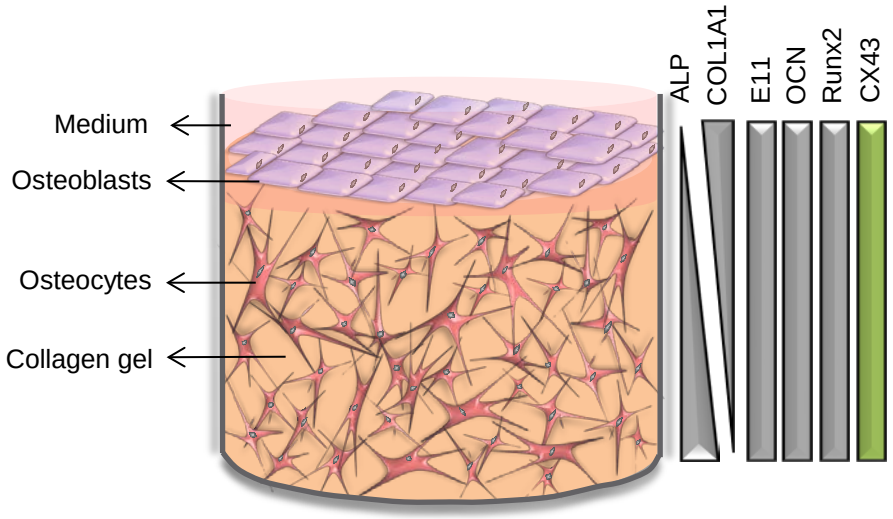

Cell death	Osteoblasts	Osteocytes
Day 1	0 %	16.13 ±3.16 %
Day 7	0 %	13.85 ±2.35 %

Signalling components	Osteoblasts	Osteocytes
A_{2A}	✓	✓
A_{2B}	✓	✓
CaSR	✓	✓
GLAST1	✓	✓
CaSR	✓	✓
AMPAR2	X	✓

B LOADED

(5 min, 10 Hz, 2.5 N)

OSTEOCYTES

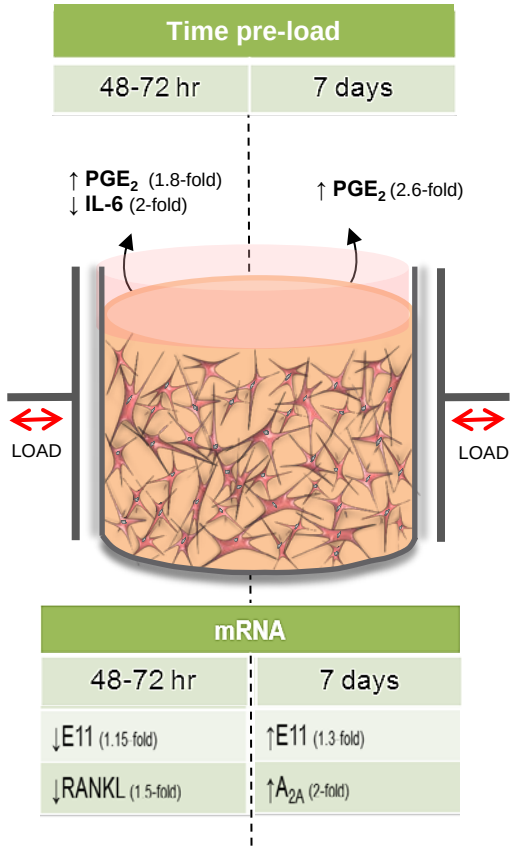

3D CO-CULTURE

(preliminary data)

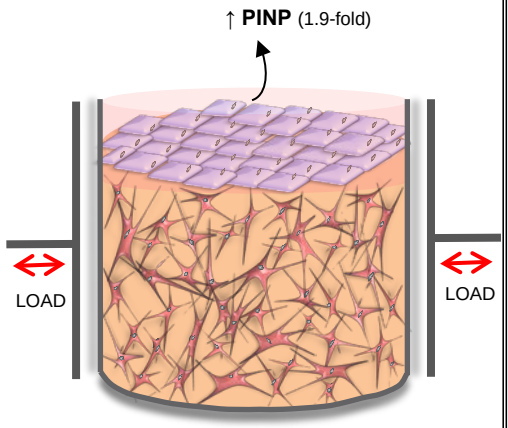

mRNA

Osteoblasts

↑ALP (1.5-fold)

Figure 7.1 *A summary of the results presented in this thesis characterising the novel 3D co-culture model.* A) In a resting state, the osteoblasts and osteocytes were shown to have minimal cell death at both day 1 and 7 of culture, as well as maintain their phenotype through the expression of bone markers (grey bars), and their connectivity through the expression of CX43 (green bar), and express signalling components (Table 7.1). B) Embedded osteocytes were shown to respond to physiological loads through the release of PGE_2, and that this loading response was maintained if the embedded osteocytes were cultured for a minimum of 48 hr and up to 7 days prior to mechanical stimuli. However, time pre-load appeared to have an effect on E11 mRNA expression as a result of loading, highlighting that culture time pre-load of the osteocytes within the 3D model is of great importance. Furthermore, the adenosine receptor A_{2A} was shown to be mechanically regulated and therefore identified as a potential novel indicator of load response. Most importantly, although as preliminary data, it was shown that a physiological mechanical stimulus applied to the 3D co-culture is able to potentially induce an osteogenic response through an increase in the synthesis of PINP and ALP mRNA expression by the osteoblasts.

Table 7.1 *Comparison of the 3D co-culture model to bone in vivo and published in vitro models.* 3D co-culture data is highlighted in red.

		In vivo (human or rodent)		**3D co-culture**		**3D mono-culture**		**2D co-culture** (Taylor et al., 2007)		**Monolayer culture**	
		Osteoblasts	**Osteocytes**	**Osteoblasts**	**Osteocytes**	**Osteoblasts**	**Osteocytes**	**Osteoblasts**	**Osteocytes**	**Osteoblasts**	**Osteoctyes**
CELL DEATH		Transient cells only present as osteoblasts during bone formation. **Humans** **After bone formation:** 50-70 % death The rest become bone lining cells or osteocytes (Parfitt, 1990, Jilka et al., 1998)	**Humans** **Birth:** 1 % **80 years old:** 75 % (Frost, 1960, Mullender et al., 1996, Tomkinson et al., 1997)	**Day 1:** 0 % **Day 7:** 0 %	**Day 1:** 16.13 ±3.16 % **Day 7:** 13.85 ±2.35 %	86 % embedded in type II collagen gels (Maeno et al., 2005)	~ 3 dead cells/field of view (Kurata et al., 2006)	Cells remained viable (quantification of death/viability not shown)	Cells remained viable (quantification of death/viability not shown)	**Primary osteoblasts** **Day 1 to 4:** ~5-8 % (Gohel et al., 1999)	**Primary osteocytes** **Day 6:** ~ 25 % (Bakker et al., 2004)
CELL MORPHOLOGY		Ovoid Pyriform Rectangular Cuboidal Columnar (Bourne, 1972)	Dendritic (Doty et al., 1976, Menton et al., 1984, Palumbo, 1986)	Ovoid/pyriform with stress fibres	Dendritic	Dendritic (within 3D matrix) (Murshid et al., 2007)	Dendritic (Kurata et al., 2006, Murshid et al., 2007, Atkins et al., 2009)	Confluent monolayer Individual cell morphology: **NI**	Dendritic	**MC3T3-E1:** Fibroblastic during logarithmic growth phase, pyriform when confluent with stress fibres (Sudo et al., 1983, Murshid et al., 2007)	**MLO-Y4:** Dendritic (Kato et al., 1997)

NI: not investigated; ↑: increased; ↓: decreased; ✓ : expressed; **X**: not expressed

Table 7.1 continued.

				In vivo (human or rodent)		3D co-culture		3D mono-culture		2D co-culture (Taylor et al., 2007)		Monolayer culture	
				Osteoblasts	**Osteocytes**	**Osteoblasts**	**Osteocytes**	**Osteoblasts**	**Osteocytes**	**Osteoblasts**	**Osteocytes**	**Osteoblasts**	**Osteoctyes**
CELL PHENOTYPE	**mRNA**	**COL1A1**		✓ (Zhou et al., 1994)	✓ (Sun et al., 1995)	✓	✓	✓ (Atkins et al., 2009)	**NI**	**NI**	**NI**	✓ (Collin et al., 1992, Shi et al., 1996, Wang et al., 1999)	✓ (Kato et al., 1997)
		ALP		✓ (Whyte, 1994, Zhou et al., 1994)	✓ (Dodds et al., 1993)	✓	✓	**NI**	**NI**	**NI**	**NI**	✓ (Takuwa et al., 1991, Collin et al., 1992, Wang et al., 1999)	✓ (Mikuni-Takagaki et al., 1995, Kato et al., 1997)
		E11		✓ (Wetterwald et al., 1996)	✓ (Wetterwald et al., 1996, Schwab et al., 1999)	✓	✓	✓ (Atkins et al., 2009)	**NI**	**NI**	**NI**	✓ (Nose et al., 1990, Hadjiargyrou et al., 2001, Zhang et al., 2006, Jahn et al., 2010)	✓ (Hadjiargyrou et al., 2001, Zhang et al., 2006)
		SOST		**X** (Bezooijen et al., 2005, Poole et al., 2005)	✓ (Bezooijen et al., 2005, Poole et al., 2005, Li et al., 2008)	X	X	✓ differentiating osteoblasts (Atkins et al., 2009)	**NI**	**NI**	**NI**	✓ UMR 106.01 SaOS-2 (Papanicolaou et al., 2009, Galea et al., 2011, Yu et al., 2011) **X** MC3T3-E1 (Papanicolaou et al., 2009)	✓ Primary osteocytes MLO-A5 IDG-SW3 (Bellido et al., 2005, Papanicolaou et al., 2009, Woo et al., 2011) **X** MLO-Y4 (Papanicolaou et al., 2009, Yang et al., 2009)
		Runx2		✓ (Ducy et al., 1997, Komori et al., 1997, Otto et al., 1997)	**NI**	✓	✓	✓ (Atkins et al., 2009)	**NI**	**NI**	**NI**	✓ (Gilbert et al., 2002, Choi et al., 2005)	✓ (Fujita et al., 2001)
		OCN		✓ (Zhou et al., 1994)	✓ (Mason et al., 1996)	✓	✓	✓ (Atkins et al., 2009, Maeno et al., 2005)	**NI**	**NI**	**NI**	✓ (Collin et al., 1992)	✓ (Kato et al., 1997)

NI: not investigated; ↑: increased; ↓: decreased; ✓ : expressed; **X**: not expressed

Table 7.1 continued.

				In vivo (human or rodent)		**3D co-culture**		**3D mono-culture**		**2D co-culture** (Taylor et al., 2007)		**Monolayer culture**	
				Osteoblasts	**Osteocytes**	**Osteoblasts**	**Osteocytes**	**Osteoblasts**	**Osteocytes**	**Osteoblasts**	**Osteocytes**	**Osteoblasts**	**Osteoctyes**
PHENOTYPE	**PROTEIN**	**E11**		✓ (Wetterwald et al., 1996, Hadjiargyrou et al., 2001)	✓ (Wetterwald et al., 1996, Hadjiargyrou et al., 2001)	✓	✓	**NI**	**NI**	**NI**	**NI**	✓ (Zhang et al., 2006)	✓ (Zhang et al., 2006)
		CX43		✓ (Lecanda et al., 2000)	✓ (Bivi et al., 2012, Loiselle et al., 2013)	✓	✓	**NI**	**NI**	Functional gap junctions but not specifically CX43	Functional gap junctions but not specifically CX43	✓ (Yamaguchi and Ma, 2003)	✓ (Kato et al., 1997, Cheng et al., 2001b)

NI: not investigated; ↑: increased; ↓: decreased; ✓ : expressed; **X**: not expressed

Table 7.1 continued.

				In vivo (human or rodent)		3D co-culture		3D mono-culture		2D co-culture (Taylor et al., 2007)		Monolayer culture	
				Osteoblasts	Osteocytes	Osteoblasts	Osteocytes	Osteoblasts	Osteocytes	Osteoblasts	Osteocytes	Osteoblasts	Osteoctyes
SIGNALLING COMPONENTS	ADENOSINE	A_1	mRNA	NI	NI	X	X	NI	NI	NI	NI	✓ (Russell et al., 2007)	NI
			Protein	NI	NI	X	X	NI	NI	NI	NI	✓ (Russell et al., 2007, Costa et al., 2011)	NI
		A_{2A}	mRNA	NI	NI	✓	✓	NI	NI	NI	NI	✓ (Russell et al., 2007)	NI
			Protein	NI	NI	✓	✓	NI	NI	NI	NI	✓ (Russell et al., 2007, Costa et al., 2011)	NI
		A_{2B}	mRNA	NI	NI	✓	✓	NI	NI	NI	NI	✓ (Russell et al., 2007)	NI
			Protein	NI	NI	X	X	NI	NI	NI	NI	✓ (Russell et al., 2007, Costa et al., 2011)	NI
		A_3	mRNA	NI	NI	X	X	NI	NI	NI	NI	X (Russell et al., 2007)	NI
			Protein	NI	NI	X	X	NI	NI	NI	NI	✓ HPOBs (Costa et al., 2011) X MG63 (Russell et al., 2007)	NI

NI: not investigated; ↑: increased; ↓: decreased; ✓: expressed; **X**: not expressed

Table 7.1 continued.

				In vivo (human or rodent)		**3D co-culture**		**3D mono-culture**		**2D co-culture** (Taylor et al., 2007)		**Monolayer culture**	
				Osteoblasts	**Osteocytes**	**Osteoblasts**	**Osteocytes**	**Osteoblasts**	**Osteocytes**	**Osteoblasts**	**Osteocytes**	**Osteoblasts**	**Osteoctyes**
SIGNALLING COMPONENTS	**CALCIUM-SENSING**	**CaSR**	**mRNA**	✓ (Chang et al., 1999, Dvorak et al., 2004)	✓ (Chang et al., 1999, Dvorak et al., 2004)	**X**	**X**	**NI**	**NI**	**NI**	**NI**	✓ (Chattopadhyay et al., 2004, Yamaguchi et al., 1998a, Yamaguchi et al., 1998b, Yamaguchi et al., 2001)	**NI**
			Protein	✓ (Chang et al., 1999, Dvorak et al., 2004)	✓ (Chang et al., 1999, Dvorak et al., 2004)	✓	✓	**NI**	**NI**	**NI**	**NI**	✓ (Chattopadhyay et al., 2004, Yamaguchi et al., 1998a, Yamaguchi et al., 1998b, Yamaguchi et al., 2001)	**NI**

NI: not investigated; ↑: increased; ↓: decreased; ✓ : expressed; **X**: not expressed

Table 7.1 continued.

				In vivo (human or rodent)		3D co-culture		3D mono-culture		2D co-culture (Taylor et al., 2007)		Monolayer culture	
				Osteoblasts	**Osteocytes**	**Osteoblasts**	**Osteocytes**	**Osteoblasts**	**Osteocytes**	**Osteoblasts**	**Osteocytes**	**Osteoblasts**	**Osteoctyes**
SIGNALLING COMPONENTS	**GLUTAMATE**	**AMPAR2**	**mRNA**	**NI**	**NI**	**X**	✓	**NI**	**NI**	**NI**	**NI**	**X** (Hinoi et al., 2002)	**NI**
			Protein	✓ (Bonnet, Mason, Williams unpublished data)	✓ (Bonnet, Mason, Williams unpublished data) **X** (Szczesniak et al., 2005)	**X**	**X**	**NI**	**NI**	**NI**	**NI**	**X** (Szczesniak et al., 2005)	**NI**
		KA1	**mRNA**	**NI**	**NI**	**X**	✓	**NI**	**NI**	**NI**	**NI**	✓ (Hinoi et al., 2002)	**NI**
			Protein	**NI**	**NI**	✓	✓	**NI**	**NI**	**NI**	**NI**	**NI**	**NI**
		mGluR1	**mRNA**	**NI**	**NI**	**X**	**X**	**NI**	**NI**	**NI**	**NI**	✓ (Gu and Publicover, 2000, Kalariti et al., 2004)	**NI**
			Protein	**NI**	**NI**	**X**	**X**	**NI**	**NI**	**NI**	**NI**	**NI**	**NI**

NI: not investigated; ↑: increased; ↓: decreased; ✓ : expressed; **X**: not expressed

Table 7.1 continued.

				In vivo (human or rodent)		**3D co-culture**		**3D mono-culture**		**2D co-culture** (Taylor et al., 2007)		**Monolayer culture**	
				Osteoblasts	**Osteocytes**	**Osteoblasts**	**Osteocytes**	**Osteoblasts**	**Osteocytes**	**Osteoblasts**	**Osteocytes**	**Osteoblasts**	**Osteoctyes**
SIGNALLING COMPONENTS	**GLUTAMATE**	**GLAST1**	**mRNA**	✓ (Mason et al., 1997)	✓ (Mason et al., 1997)	✓	✓	**NI**	**NI**	**NI**	**NI**	✓ (Huggett et al., 2002, Kalariti et al., 2004, Takarada et al., 2004)	✓ (Huggett et al., 2002)
			Protein	✓ (Mason et al., 1997)	✓ (Mason et al., 1997)	✓	✓	**NI**	**NI**	**NI**	**NI**	✓ (Brakspear, 2010)	✓ (Huggett et al., 2002)
		EAAC1	**mRNA**	**NI**	**NI**	**X**	**X**	**NI**	**NI**	**NI**	**NI**	✓ (Takarada et al., 2004)	**NI**
			Protein	✓ (Bonnet, Mason, Williams, unpublished data)	**NI**	**X**	**X**	**NI**	**NI**	**NI**	**NI**	✓ (Brakspear, 2010)	**NI**

NI: not investigated; ↑: increased; ↓: decreased; ✓ : expressed; **X**: not expressed

Table 7.1 continued.

			In vivo (rodent unless otherwise stated)		3D co-culture	3D mono-culture		2D co-culture (Taylor et al., 2007)		Monolayer culture	
			Osteoblasts	**Osteocytes**		**Osteoblasts**	**Osteocytes**	**Osteoblasts**	**Osteocytes**	**Osteoblasts**	**Osteocytes**
MECHANICAL LOADING RESPONSES	**PGE_2**	**Released/ Synthesised**	**NI**	**NI**	3D osteocyte mono-culture: **↑ release** 3D co-culture: **No significant change**	**NI**	**NI**	**NI**	**NI**	**↑ release** (Smalt et al., 1997, Nauman et al., 2001, Ponik and Pavalko, 2004, Genetos et al., 2005)	**↑ release** (Cheng et al., 2001a, Jiang and Cheng, 2001, Saini et al., 2011, Li et al., 2012)
	NO	**Released/ Synthesised**	**NI**	**↑ release** (Fox et al., 1996, Zaman et al., 1999)	3D osteocyte mono-culture: **NI** 3D co-culture: **NI**	**NI**	**NI**	**NI**	**NI**	**↑ release** (McAllister and Frangos, 1999, Mehrotra et al., 2006)	**↑ release** (Klein-Nulend et al., 1995b, Tan et al., 2007)
	SOST	**mRNA/ Protein**	**NI**	**↑ expression** (Robling et al., 2008, Tu et al., 2012)	3D osteocyte mono-culture: **NI** 3D co-culture: **NI**	**NI**	**NI**	**NI**	**NI**	**↓ expression** (Galea et al., 2011, Galea et al., 2013)	**↑ expression** (Wijenayaka et al., 2011)

NI: not investigated; ↑: increased; ↓: decreased; ✓: expressed; **X**: not expressed

Table 7.1 continued.

			In vivo (human or rodent)		3D co-culture	3D mono-culture		2D co-culture (Taylor et al., 2007)		Monolayer culture	
			Osteoblasts	**Osteocytes**		**Osteoblasts**	**Osteocytes**	**Osteoblasts**	**Osteocytes**	**Osteoblasts**	**Osteocytes**
MECHANICAL LOADING RESPONSES	**RANKL**	**mRNA**	↑ **expression** with unloading (Xiong et al., 2011)	↑ **expression** (Nakashima et al., 2011, Xiong et al., 2011)	3D osteocyte mono-culture: ↓**expression (48-72 hr pre-culture)** **No significant change (7 days pre-culture)** 3D co-culture: **NI**	**NI**	**NI**	**NI**	**NI**	↑ **expression** (Mehrotra et al., 2006, Rucci et al., 2007, Kreja et al., 2008)	↑ **expression** (You et al., 2008, Kulkarni et al., 2010)
	IL-6	**Released/ Synthesised**	**NI**	**NI**	3D osteocyte mono-culture: ↓ **release** 3D co-culture: **NI**	**NI**	**NI**	**NI**	**NI**	↑ **release** (Sanchez et al., 2009)	**NI**
	A_{2A}	**mRNA**	**NI**	**NI**	3D osteocyte mono-culture: **No significant change (48-72 hr pre-culture)** ↑ **expression (7 days pre-culture)** 3D co-culture: ↑ **expression (osteocytes only)**	**NI**	**NI**	**NI**	**NI**	**NI**	**NI**
	A_{2B}	**mRNA**	**NI**	**NI**	3D osteocyte mono-culture: **No significant change (48-27 hr and 7 days pre-culture)** 3D co-culture: **NI**	**NI**	**NI**	**NI**	**NI**	**NI**	**NI**

NI: not investigated; ↑: increased; ↓: decreased; ✓ : expressed; **X**: not expressed

Table 7.1 continued.

			In vivo (human or rodent)		3D co-culture	3D mono-culture		2D co-culture (Taylor et al., 2007)		Monolayer culture	
			Osteoblasts	**Osteocytes**		**Osteoblasts**	**Osteocytes**	**Osteoblasts**	**Osteocytes**	**Osteoblasts**	**Osteocytes**
MECHANICAL LOADING RESPONSES	**AMPAR2**	**mRNA**	**NI**	**NI**	3D osteocyte mono-culture: **X** 3D co-culture: **NI**	**NI**	**NI**	**NI**	**NI**	**NI**	**NI**
	KA1	**mRNA**	**NI**	**NI**	3D osteocyte mono-culture: **X** 3D co-culture: **NI**	**NI**	**NI**	**NI**	**NI**	**NI**	**NI**
	GLAST1	**mRNA**	**NI**	**↓ expression** (Mason et al., 1997)	3D osteocyte mono-culture: **X** 3D co-culture: **NI**	**NI**	**NI**	**NI**	**NI**	**NI**	**NI**
	E11	**mRNA**	**NI**	**NI**	3D osteocyte mono-culture: **↓expression (48-72 hr pre-culture)** **↑ expression (7 days pre-culture)** 3D co-culture: **NI**	**NI**	**NI**	**NI**	**NI**	**NI**	**↑ expression** (Yang et al., 2004, Zhang et al., 2006)

NI: not investigated; ↑: increased; ↓: decreased; ✓ : expressed; **X**: not expressed

Table 7.1 continued.

			In vivo (human or rodent)		3D co-culture	3D mono-culture		2D co-culture (Taylor et al., 2007)		Monolayer culture	
			Osteoblasts	**Osteocytes**		**Osteoblasts**	**Osteocytes**	**Osteoblasts**	**Osteocytes**	**Osteoblasts**	**Osteocytes**
MECHANICAL LOADING RESPONSES	**ALP**	**mRNA**	↑ **expression** (Pavlin et al., 2001)	**NI**	3D osteocyte mono-culture: **NI** 3D co-culture: ↑ **expression (osteoblasts only)**	**NI**	**NI**	**NI**	**NI**	↑ **expression** (Lu et al., 2012)	**NI**
	COL1A1	**mRNA**	↑ **expression** (Pavlin et al., 2001, Mantila Roosa et al., 2011)	**NI**	3D osteocyte mono-culture: **NI** 3D co-culture: **No significant change (osteoblasts only)**	**NI**	**NI**	**NI**	**NI**	↑ **expression** (Liu et al., 2005, Rath et al., 2008, Lu et al., 2012)	**NI**
	Pro-collagen I	**Released/ Synthesised**	↑ **synthesis** (Yang et al., 2012)	**NI**	3D osteocyte mono-culture: **NI** 3D co-culture: ↑**release**	**NI**	**NI**	**NI**	**NI**	↑ **synthesis** (Yang et al., 2012)	**NI**

NI: not investigated; ↑: increased; ↓: decreased; ✓: expressed; **X**: not expressed

7.1.1 Limitations of the 3D co-culture model

7.1.1.1 Osteoblast morphology

Surface osteoblasts were shown to maintain their ovoid/pyriform morphology (Table 7.1) and form a confluent monolayer in an 'overlapping roof tiles' pattern when cultured in 3D co-cultures. However, this morphology could only be determined by staining the osteoblasts for actin filaments and using confocal microscopy. Observation of individual surface osteoblasts using inverse-light microscopy proved difficult due to the fact that MC3T3-E1 cells are not very thick (personal observation) and the fact that the 3D gel with embedded osteocytes can be seen underneath the osteoblast monolayer. MC3T3-E1 cells could be replaced by mouse primary osteoblasts, which may be easier to observe under the light-microscope as they may be thicker cells.

7.1.1.2 Phenotype

This thesis showed the expression of a selection of osteocyte phenotypic markers, but other markers were not assessed, namely PHEX, MEPE, DMP1 and FGF23. MLO-Y4 cells in monolayer have previously been shown to express mRNAs for PHEX, MEPE, DMP1 and FGF23 (Bonewald, 2010), and therefore these genes should be investigated in the 3D co-culture model in order to further characterise the osteocyte phenotype within the model. Moreover, as previously shown MLO-Y4 cells do not express SOST within the 3D co-culture model, consistent with previous monolayer studies (Papanicolaou et al., 2009, Yang et al., 2009, Woo et al., 2011). The lack of SOST expression within the 3D co-culture model is not physiological as SOST is both mechanically regulated (Robling et al., 2008, Tu et al., 2012) and a key regulator of bone formation (Winkler et al., 2003, van Bezooijen et al., 2004, Poole et al., 2005, Lowik and van Bezooijen, 2006, van Bezooijen et al., 2007). This limitation could be solved by replacing the MLO-Y4 cells with mouse, primary osteocytes (Halleux et al., 2012, Nakashima et al., 2011, Stern et al., 2012). However, the yield of primary osteocytes after isolation tends to be low and they do not proliferate in culture, limiting the number of cells that can be used for

experiments. The IDG-SW3 cell line is likely to be the best option to replace the MLO-Y4 in the 3D model, as these cells have already been cultured within 3D type I collagen gels and are able to differentiate into mature osteocytes which express SOST and mineralise (Woo et al., 2011).

7.1.1.3 Connectivity

Both embedded osteocytes and surface osteoblasts were shown to express CX43 (Chapter 3), and osteocytes were shown to contact neighbouring cells. However, the functionality of these connections was not shown. Such testing is usually carried out by a scrape-loading dye transfer assay. Briefly, using a needle, a monolayer of cells is scratched in the presence of two dyes, lucifer yellow which can penetrate through gap junction channels and rhodamine dextran which cannot and so serves as a tracer dye for the cells originally receiving the dye, the number of cells containing lucifer yellow away from the scratch line is then counted (el-Fouly et al., 1987, Cheng et al., 2001b, Cherian et al., 2003, Xia et al., 2010). Attempts to perform this method in the 3D co-culture failed. Therefore a different method, such as fluorescence replacement after photobleaching (FRAP), which involves turning cells fluorescent using a cell permeable dye and then using a confocal microscope to photochemically bleach cells to a sufficient level so that fluorescence recovery can be observed without damaging the cell (Kamioka et al., 2007, Ishihara et al., 2008, Sugawara et al., 2011, Wang et al., 2013), should be tested to confirm functional connectivity between osteocytes and also between these cells and surface osteoblasts.

7.1.1.4 Mineralisation

Although the 3D model is designed to investigate mechanically-induced osteogenesis in a similar *in vivo* physiological environment, it is not mineralised and so it would only represent interactions that occur in newly formed osteoid rather than mineralised bone. Several previous studies have shown the mineralisation of 3D collagen gels is possible with IDG-SW3 cells (Woo et al., 2011) and MC3T3-E1 cells (Scully et al., 2013a, Scully et al., 2013b) both during differentiation to osteocytes, and therefore the 3D co-culture could be mineralised. Mineralisation of

the 3D collagen gel would affect the properties of the matrix and cell-ECM interactions. For example, it is known from bone *in vivo* that it is the mineral component of bone matrix, which gives bone its load-bearing strength and ability to withstand compression (Currey, 1984, Landis, 1995). This change in the biomechanical properties of the ECM after mineralisation has also been shown *in vitro*, where the ECM of both 3D collagen gels and monolayer cultures became gradually stiffer (Meng et al., 2009, Scully et al., 2013a). Furthermore, ECM composition has been shown to affect gene expression (Bissell et al., 1982) and osteoblast differentiation, cell number and behaviour (Prideaux et al., 2012, Scully et al., 2013a). Therefore, mineralising the 3D co-culture would make the collagen gels stiffer and alter phenotype, further mimicking a physiological environment. However, if mineralisation of the 3D co-culture was to be carried out, further investigations should be done to test the mechanical properties of the mineralised 3D co-cultures as well as the viability and phenotype of the cells within the model and assess whether the medium nutrients can still diffuse to all areas of the 3D gel.

7.1.1.5 Experimental variability

A further limitation is that, even though data trends seemed to be constant in independent experiments, significant cross-experiment variability was observed on several occasions. One explanation for this variability is the way the model is set-up. The mixing of the osteocytes within the collagen solution is a crucial stage of the model set-up as it must be done carefully in order to avoid bubbles, but thoroughly in order to ensure the osteocytes are evenly distributed within the solution. If this method is not performed accurately, some 3D cultures will have more or less osteocytes than others, therefore creating cell number variability between experimental replicates which could lead to, for example, differences in amounts of connections formed between embedded osteocytes and in turn lead to discrepancies in loading responses. Cell phenotype, behaviour and signalling could also be affected. The solution to this experimental variability is to increase the osteocyte cell number being embedded within the gels. This increase in cell number will decrease the chance of inaccurately mixing more cells in some gels than others, which in turn will reduce the chance of observing differences in phenotype, connectivity and

signalling between experimental replicates. However, an experiment should be conducted in order to assess the best osteocyte cell density for the 3D co-culture, as too many cells may lead to, for example, the contraction of the 3D gels.

7.1.1.6 Loading device

The loading plate also has some limitations. Although the device elicited the same trend in cell response to mechanical stimuli every time it was used, the extent of the response was different between independent experiments. This difference could be attributed to the variability between experiments due to cell number or also due to the fact that the strains across the wells of the silicone plate may not be equal during the same loading episode. An attempt was made to measure the strains in 3D cultures within the wells of the silicone plate by applying a speckle pattern on the surface of 3D collagen gels within the silicone plate. However, the speckles were too big for the surface area to be analysed by the DIC cameras and the 3D gels were also found to reflect the light of the cameras, interfering with the readings. Strain testing by applying the speckle pattern to the base of the silicone plate, but with 3D collagen gels within the plate, may be a better solution and would reveal the range of strains being applied and whether they are equal across all wells of the plate. The properties of the silicone used to make the loading plate should also be tested under the same mechanical loading conditions used. This testing would give information on whether the elasticity of the silicone is maintained throughout several uses of the same plate or not. Finally, the adaptor used to attach the silicone plate to the BOSE loading instrument was a prototype and therefore a finalised version must be manufactured. The use of a string to pull on the plate and mini-rollers which are not permanently attached to the adaptor could also cause variability in the applied strains and therefore the cell response produced. The string of the adaptor is the link between the silicone plate and the BOSE loading instrument but the properties of the string need to be measured in order to determine whether its elasticity deteriorates, and thus whether this affects the strains in the wells of the plate. The mini-rollers, which aid movement of the plate, must be a permanent part of the adaptor. At the moment, the rollers are carefully manually positioned avoiding the wells of the plate. However, manual positioning does not guarantee the rollers will be on the same place every

time or that the rollers will not move underneath a well, causing different strains across wells and thus causing variable results.

7.1.1.7 Human 3D co-culture model

Although a human 3D co-culture model would be more meaningful in the study of osteocyte-osteoblast interactions, particularly if screening for novel therapeutic targets, the development of such model poses many obstacles, such as the lack of a human osteocyte cell line and the difficulty in obtaining human primary osteocytes (section 1.4.2.3.2). However, having a 3D mouse co-culture model is an advantage as all findings obtained using the 3D mouse model can be related to *in vivo* mouse models, which in turn are generally used to model human disease.

7.2 Application of the novel 3D co-culture model

This thesis used the 3D co-culture model to investigate the roles of AMPA/KA and A_{2A} receptors on mechanically-induced bone formation by inhibiting these receptors with specific antagonists. Preliminary data showed that NBQX, an AMPA/KA antagonist, appeared to have an anabolic effect as it induced PINP synthesis in non-loaded 3D co-cultures (Figure 7.2A) to levels equal to those induced by loading, 5 days after treatment (Figure 7.1B). Whereas, the A_{2A} antagonist SCH 442416 had an additive effect on bone formation in loaded cultures (Figure 7.2B). In loaded cultures, at day 1, the A_{2A} antagonist increased osteoblast ALP mRNA expression to levels which were double of those observed in untreated loaded cultures (Figure 7.1B). Moreover, at day 5, the antagonist further increased PINP release by 1.9-fold (Figure 7.2B), when compared to untreated control cultures.

Both NBQX and SCH 442416 seemed to evoke similar osteogenic responses on the 3D co-culture. Therefore, it could be hypothesised that both AMPA/KA and A_{2A} receptors work in a similar manner in bone cells. As previously stated, A_{2A} is a metabotropic receptor (Jacobson and Gao, 2006) whereas AMPA/KA receptors are ionotropic (Wisden and Seeburg, 1993, Hollmann and Heinemann, 1994) (pages 36 and 40). However, AMPA/KA receptors have also been shown to act as

metabotropic receptors as they can instigate intracellular signalling cascades involving G-proteins (Rao and Finkbeiner, 2007, Rodriguez-Moreno and Sihra, 2007, Sihra and Rodriguez-Moreno, 2011). The A_{2A} receptor has been shown to work through the phosphoinositide-3-kinase–protein kinase B/Akt (PI3K-PKB/Akt) pathway; by activating MAPK; or the cAMP-protein kinase A-cAMP response element-binding protein (cAMP-PKA-CREB) pathway (Jacobson and Gao, 2006). Whereas, during their metabotropic function, KA receptors can work through the phospholipase C-protein kinase C (PLC-PKC) pathway as well as the adenylate cyclase-cAMP-protein kinase A (AC/cAMP/PKA) pathway and AMPA receptors can activate CREB and MAPK. Although NBQX blocks both AMPA and KA receptors, it has a higher affinity for AMPARs (Herrling, 1997). Therefore, it could be hypothesised that the similar osteogenic responses observed as a result of A_{2A} and AMPAR inhibition could be due to both these receptors acting as metabotropic receptors through MAPK. Usually an ionotropic response deactivates within sub-seconds, whereas metabotropic responses are long-lasting (Rodriguez-Moreno and Sihra, 2007). To confirm a metabotropic action of AMPAR on bone formation markers, the osteogenic response should be assessed whether it is sensitive to inhibitors of the putative metabotropic signalling pathways involved, in this case MAPK.

Nevertheless, this experiment must be repeated in order to confirm the NBQX and SCH 442416 effects. Unfortunately, it was not possible to assess the role of CaSR in mechanotransduction in this thesis, even though CaSR is expressed in the 3D model. As adenosine, calcium-sensing and glutamate signalling pathways have been shown to be synergistic in the CNS (page 43) the effects on mechanically-induced bone formation markers of these antagonists in combination should also be investigated.

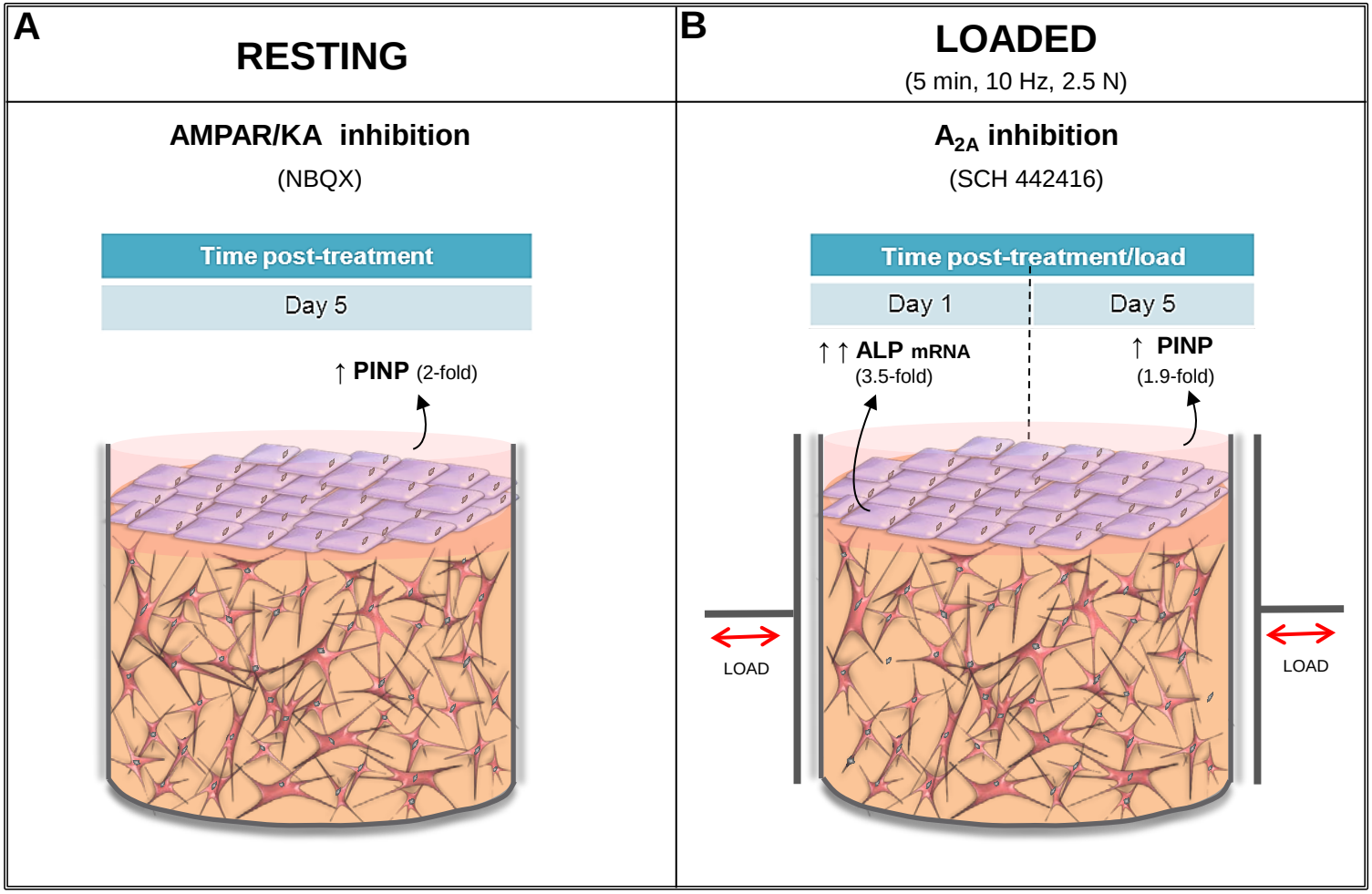

Figure 7.2 *A summary of the results using the 3D model to investigate the role of AMPA/KA and A_{2A} receptors in mechanically-induced bone formation.* A) In a resting state, at day 5 post-treatment, inhibition of AMPA/KA receptors induced a similar anabolic response to that obtained by mechanical loading (Figure 7.1B). B) Mechanical loading and A_{2A} inhibition appeared to have additive effects on bone formation which led to a doubling of ALP mRNA expression at day 1 and a 1.9-fold increase in PINP release at day 5 when compared to untreated control cultures (Figure 7.1B).

7.2.1 Further applications of the 3D model

7.2.1.1 Screening for novel therapeutic targets

Currently there is a lack of effective therapies for common bone diseases and thus there is a great need to search for novel therapeutic targets (section 1.3.3). This thesis showed how the 3D co-culture can be effectively used to test compounds which could influence bone formation (Chapter 6). If the 3D model was to be scaled up it could be used for mass-scale pharmaceutical screening of new therapeutic targets for bone diseases. Anabolic therapies for diseases such as osteoporosis are particularly scarce. Thus the effect of adenosine and glutamate receptor antagonists on mechanically-induced bone formation markers within the 3D model has provided a stepping stone to not only for the delineation of the roles of these signalling pathways in mechanotransduction, but also as possible novel anabolic drug targets which could be used as therapies for not only bone diseases such as osteoporosis, but also for joint diseases such as OA and RA where osteoporosis treatments have already been proven to be useful treatments.

7.2.1.2 Studying bone formation mechanisms

The cell lines used in this 3D model could be replaced by primary cells from rodent genetically modified (GM) models which would, for example, be useful to model bone diseases *in vitro* or determine the effects of deletion of a signalling component of interest. Furthermore, the addition of other cell types to the 3D model could also be of great interest in revealing new mechanisms underlying bone remodelling. Osteocytes orchestrate bone remodelling by regulating the activity of both osteoblasts and osteoclasts (Klein-Nulend et al., 2013) (page 13 and 1.5), thus, if osteoclasts or BMSCs were to be added, making the 3D model a tri-culture, it could also be used for the investigation of bone remodelling, by essentially modelling the BMU (Frost, 1990b). Furthermore, vascular endothelial cells and/or nerve cells could also be added to the 3D model as bone is a highly vascular and innervated tissue (section 1.1) and both cell types have been shown to produce factors that influence bone remodelling (Collin-Osdoby, 1994, Beckman, 2002,

Persson and Lerner, 2011, Clarkin and Gerstenfeld, 2013, Ma et al., 2013, Maes, 2013). This would allow the *in vitro* 3D co-culture model to be adapted into a highly physiological representation of the *in vivo* bone environment enabling the accurate investigation of the role of each of the aforementioned cell types in the remodelling process.

7.3 Concluding remarks

This thesis has provided evidence to support the hypothesis that a 3D osteocyte-osteoblast co-culture model represents a useful *in vitro* model for the investigation of the osteocyte-osteoblast interactions that lead to mechanically-induced bone formation. This thesis also provided evidence for the expression of adenosine, calcium-sensing and glutamate signalling components within the model, facilitating future investigations of their roles in mechanically-induced osteogenesis. Preliminary experiments indicated that adenosine and glutamate signalling may each contribute individually to the regulation of mechanically-induced bone formation markers. The model would be improved, in the first instance, by increasing the osteocyte cell density in order to reduce experiment variability and increase osteocyte connectivity, using osteocytes which express mature osteocyte markers, demonstrating the functionality of cell-cell connections, and optimising the ECM by, for example, mineralisation of the 3D collagen gel.

BIBLIOGRAPHY

8. Bibliography

ADAMS, D. J., SPIRT, A. A., BROWN, T. D., FRITTON, S. P., RUBIN, C. T. & BRAND, R. A. (1997) Testing the daily stress stimulus theory of bone adaptation with natural and experimentally controlled strain histories. *Journal of biomechanics,* 30**,** 671-8.

AGUIRRE, J. I., PLOTKIN, L. I., STEWART, S. A., WEINSTEIN, R. S., PARFITT, A. M., MANOLAGAS, S. C. & BELLIDO, T. (2006) Osteocyte Apoptosis Is Induced by Weightlessness in Mice and Precedes Osteoclast Recruitment and Bone Loss. *Journal of Bone and Mineral Research,* 21**,** 605-615.

AJUBI, N. E., KLEIN-NULEND, J., ALBLAS, M. J., BURGER, E. H. & NIJWEIDE, P. J. (1999) Signal transduction pathways involved in fluid flow-induced PGE2 production by cultured osteocytes. *The American journal of physiology,* 276**,** E171-8.

AJUBI, N. E., KLEIN-NULEND, J., NIJWEIDE, P. J., VRIJHEID-LAMMERS, T., ALBLAS, M. J. & BURGER, E. H. (1996) Pulsating fluid flow increases prostaglandin production by cultured chicken osteocytes--a cytoskeleton-dependent process. *Biochemical and biophysical research communications,* 225**,** 62-8.

ANDERSEN, C. L., JENSEN, J. L. & ORNTOFT, T. F. (2004) Normalization of real-time quantitative reverse transcription-PCR data: a model-based variance estimation approach to identify genes suited for normalization, applied to bladder and colon cancer data sets. *Cancer research,* 64**,** 5245-50.

ANDERSON, H. C. (2003) Matrix vesicles and calcification. *Curr Rheumatol Rep,* 5**,** 222-6.

APSELOFF, G., GIRTEN, B., WALKER, M., SHEPARD, D. R., KRECIC, M. E., STERN, L. S. & GERBER, N. (1993) Aminohydroxybutane bisphosphonate and clenbuterol prevent bone changes and retard muscle atrophy respectively in tail-suspended rats. *The Journal of pharmacology and experimental therapeutics,* 264**,** 1071-8.

ARNETT, T., HENDERSON, B., MEGHJI, S., HILL, P. & HARRIS, M. (1998) Bone organ cultures. *Methods in Bone Biology.* Springer US.

ARRIZA, J. L., ELIASOF, S., KAVANAUGH, M. P. & AMARA, S. G. (1997) Excitatory amino acid transporter 5, a retinal glutamate transporter coupled to a chloride conductance. *Proc Natl Acad Sci U S A,* 94**,** 4155-60.

ARRIZA, J. L., FAIRMAN, W. A., WADICHE, J. I., MURDOCH, G. H., KAVANAUGH, M. P. & AMARA, S. G. (1994) Functional comparisons of three glutamate transporter subtypes cloned from human motor cortex. *J Neurosci,* 14**,** 5559-69.

ATKINS, G. J., KOSTAKIS, P., PAN, B., FARRUGIA, A., GRONTHOS, S., EVDOKIOU, A., HARRISON, K., FINDLAY, D. M. & ZANNETTINO, A. C. (2003) RANKL expression is related to the differentiation state of human osteoblasts. *J Bone Miner Res,* 18**,** 1088-98.

ATKINS, G. J., WELLDON, K. J., HOLDING, C. A., HAYNES, D. R., HOWIE, D. W. & FINDLAY, D. M. (2009) The induction of a catabolic phenotype in human primary osteoblasts and osteocytes by polyethylene particles. *Biomaterials,* 30**,** 3672-81.

AUBIN, J. E., LAIN, J. B. & STEIN, G. S. (2006) Bone formation: maturation and functional activities of osteoblast lineage cells. *Primer on the metabolic bone diseases and disorders of mineral metabolism.* 6th ed. Washington, DC, American Society for Bone and Mineral Research.

AW, M. S., KHALID, K. A., GULATI, K., ATKINS, G. J., PIVONKA, P., FINDLAY, D. M. & LOSIC, D. (2012) Characterization of drug-release kinetics in trabecular bone from titania nanotube implants. *International journal of nanomedicine,* 7**,** 4883-92.

BAILEY, D. A., FAULKNER, R. A. & MCKAY, H. A. (1996) Growth, physical activity, and bone mineral acquisition. *Exerc Sport Sci Rev,* 24**,** 233-66.

BAIN, S. D. & RUBIN, C. T. (1990) Metabolic modulation of disuse osteopenia: Endocrine-dependent site specificity of bone remodeling. *Journal of Bone and Mineral Research,* 5**,** 1069-1075.

BAKKER, A., KLEIN-NULEND, J. & BURGER, E. (2004) Shear stress inhibits while disuse promotes osteocyte apoptosis. *Biochemical and biophysical research communications,* 320**,** 1163-8.

BALDOCK, P. A., THOMAS, G. P., HODGE, J. M., BAKER, S. U., DRESSEL, U., O'LOUGHLIN, P. D., NICHOLSON, G. C., BRIFFA, K. H., EISMAN, J. A. & GARDINER, E. M. (2006) Vitamin D action and regulation of bone remodeling: suppression of osteoclastogenesis by the mature osteoblast. *J Bone Miner Res,* 21**,** 1618-26.

BALDWIN, K. M., WHITE, T. P., ARNAUD, S. B., EDGERTON, V. R., KRAEMER, W. J., KRAM, R., RAAB-CULLEN, D. & SNOW, C. M. (1996) Musculoskeletal adaptations to weightlessness and development of effective countermeasures. *Med Sci Sports Exerc,* 28**,** 1247-53.

BALEMANS, W., EBELING, M., PATEL, N., VAN HUL, E., OLSON, P., DIOSZEGI, M., LACZA, C., WUYTS, W., VAN DEN ENDE, J., WILLEMS, P., PAES-ALVES, A. F., HILL, S., BUENO, M., RAMOS, F. J., TACCONI, P., DIKKERS, F. G., STRATAKIS, C., LINDPAINTNER, K., VICKERY, B., FOERNZLER, D. & VAN HUL, W. (2001) Increased bone density in sclerosteosis is due to the deficiency of a novel secreted protein (SOST). *Hum Mol Genet,* 10**,** 537-43.

BALEMANS, W., PATEL, N., EBELING, M., VAN HUL, E., WUYTS, W., LACZA, C., DIOSZEGI, M., DIKKERS, F. G., HILDERING, P., WILLEMS, P. J., VERHEIJ, J. B., LINDPAINTNER, K., VICKERY, B., FOERNZLER, D. & VAN HUL, W. (2002) Identification of a 52 kb deletion downstream of the SOST gene in patients with van Buchem disease. *Journal of medical genetics,* 39**,** 91-7.

BALEMANS, W., VAN DEN ENDE, J., FREIRE PAES-ALVES, A., DIKKERS, F. G., WILLEMS, P. J., VANHOENACKER, F., DE ALMEIDA-MELO, N., ALVES, C. F., STRATAKIS, C. A., HILL, S. C. & VAN HUL, W. (1999) Localization of the gene for sclerosteosis to the van Buchem disease-gene region on chromosome 17q12-q21. *Am J Hum Genet,* 64**,** 1661-9.

BANNAI, S. & KITAMURA, E. (1980) Transport interaction of L-cystine and L-glutamate in human diploid fibroblasts in culture. *J Biol Chem,* 255**,** 2372-6.

BANNAI, S. & KITAMURA, E. (1981) Role of proton dissociation in the transport of cystine and glutamate in human diploid fibroblasts in culture. *J Biol Chem,* 256**,** 5770-2.

BARBOSA, A. A., DEL CARLO, R. J., GALVÃO, S. R., VILELA, M. J., LOUZADA, M. J. Q., BRITO, A. F. S. & NATALI, A. J. (2011) Bone

mineral density of rat femurs after hindlimb unloading and different physical rehabilitation programs. *Revista Ceres,* 58**,** 407-412.

BARKER, D. J. & GARDNER, M. J. (1974) Distribution of Paget's disease in England, Wales and Scotland and a possible relationship with vitamin D deficiency in childhood. *Br J Prev Soc Med,* 28**,** 226-32.

BARRANGER, Y., DOUMALIN, P., DUPRÉ, J. C. & GERMANEAU, A. (2012) Strain Measurement by Digital Image Correlation: Influence of Two Types of Speckle Patterns Made from Rigid or Deformable Marks. *Strain,* 48**,** 357-365.

BARRON, M. J., TSAI, C. J. & DONAHUE, S. W. (2010) Mechanical stimulation mediates gene expression in MC3T3 osteoblastic cells differently in 2D and 3D environments. *Journal of biomechanical engineering,* 132**,** 041005.

BARTHELEMI, S., ROBINET, J., GARNOTEL, R., ANTONICELLI, F., SCHITTLY, E., HORNEBECK, W. & LORIMIER, S. (2012) Mechanical forces-induced human osteoblasts differentiation involves MMP-2/MMP-13/MT1-MMP proteolytic cascade. *Journal of cellular biochemistry,* 113**,** 760-72.

BAUD, C. A. (1968) Submicroscopic structure and functional aspects of the osteocyte. *Clin Orthop Relat Res,* 56**,** 227-36.

BECKMAN, M. (2002) No Bones About It: Nerve cell protein controls bone formation (Osteoporosis; Neuropeptide Y). *Sci. Aging Knowl. Environ.,* 2002**,** nw44-.

BELLIDO, T., ALI, A. A., GUBRIJ, I., PLOTKIN, L. I., FU, Q., O'BRIEN, C. A., MANOLAGAS, S. C. & JILKA, R. L. (2005) Chronic elevation of parathyroid hormone in mice reduces expression of sclerostin by osteocytes: a novel mechanism for hormonal control of osteoblastogenesis. *Endocrinology,* 146**,** 4577-83.

BEMEUR, C., STE-MARIE, L., DESJARDINS, P., HAZELL, A. S., VACHON, L., BUTTERWORTH, R. & MONTGOMERY, J. (2004) Decreased beta-actin mRNA expression in hyperglycemic focal cerebral ischemia in the rat. *Neuroscience letters,* 357**,** 211-4.

BISSELL, M. J., HALL, H. G. & PARRY, G. (1982) How does the extracellular matrix direct gene expression? *J Theor Biol,* 99**,** 31-68.

BIVI, N., CONDON, K. W., ALLEN, M. R., FARLOW, N., PASSERI, G., BRUN, L. R., RHEE, Y., BELLIDO, T. & PLOTKIN, L. I. (2012) Cell autonomous requirement of connexin 43 for osteocyte survival: consequences for endocortical resorption and periosteal bone formation. *J Bone Miner Res,* 27**,** 374-89.

BLAIR, H. C. & ATHANASOU, N. A. (2004) Recent advances in osteoclast biology and pathological bone resorption. *Histol Histopathol,* 19**,** 189-99.

BLAIR, H. C., TEITELBAUM, S. L., GROSSO, L. E., LACEY, D. L., TAN, H. L., MCCOURT, D. W. & JEFFREY, J. J. (1993) Extracellular-matrix degradation at acid pH. Avian osteoclast acid collagenase isolation and characterization. *Biochem J,* 290 (Pt 3)**,** 873-84.

BONEWALD, L. F. (1999) Establishment and characterization of an osteocyte-like cell line, MLO-Y4. *Journal of bone and mineral metabolism,* 17**,** 61-5.

BONEWALD, L. F. (2010) The Osteocyte Network as a Source and Reservoir of Signaling Factors. *Endocrinol Metab,* 25**,** 161-165.

BONEWALD, L. F. (2011) The amazing osteocyte. *Journal of bone and mineral research : the official journal of the American Society for Bone and Mineral Research,* 26**,** 229-38.

BOO, Y. C. & JO, H. (2003) Flow-dependent regulation of endothelial nitric oxide synthase: role of protein kinases. *Am J Physiol Cell Physiol,* 285**,** C499-508.

BORD, S., BEAVAN, S., IRELAND, D., HORNER, A. & COMPSTON, J. E. (2001) Mechanisms by which high-dose estrogen therapy produces anabolic skeletal effects in postmenopausal women: role of locally produced growth factors. *Bone,* 29**,** 216-222.

BOUKHECHBA, F., BALAGUER, T., MICHIELS, J. F., ACKERMANN, K., QUINCEY, D., BOULER, J. M., PYERIN, W., CARLE, G. F. & ROCHET, N. (2009) Human primary osteocyte differentiation in a 3D culture system. *Journal of bone and mineral research : the official journal of the American Society for Bone and Mineral Research,* 24**,** 1927-35.

BOURNE, G. H. (1972) The biochemistry and physiology of bone. 2nd ed. New York, Academic Press.

BOUTAHAR, N., GUIGNANDON, A., VICO, L. & LAFAGE-PROUST, M. H. (2004) Mechanical strain on osteoblasts activates autophosphorylation of focal adhesion kinase and proline-rich tyrosine kinase 2 tyrosine sites involved in ERK activation. *J Biol Chem,* 279**,** 30588-99.

BOYLE, W. J., SIMONET, W. S. & LACEY, D. L. (2003) Osteoclast differentiation and activation. *Nature,* 423**,** 337-42.

BRAKSPEAR, K. (2010) Glutamate regulation for bone repair. *School of Biosciences.* Cardiff, Cardiff University.

BRAKSPEAR, K. & MASON, D. (2012) Glutamate signalling in bone. *Frontiers in Endocrinology,* 3.

BRENNAN, T. C., RYBCHYN, M. S., GREEN, W., ATWA, S., CONIGRAVE, A. D. & MASON, R. S. (2009) Osteoblasts play key roles in the mechanisms of action of strontium ranelate. *Br J Pharmacol,* 157**,** 1291-300.

BROMLEY, M. & WOOLLEY, D. E. (1984) Chondroclasts and osteoclasts at subchondral sites of erosion in the rheumatoid joint. *Arthritis Rheum,* 27**,** 968-75.

BROOKES, M. (1961) The vascular architecture of the mammalian bone cortex. *Journal of Anatomy,* 95**,** 615.

BROWN, E. M. (2003) Is the calcium receptor a molecular target for the actions of strontium on bone? *Osteoporos Int,* 14 Suppl 3**,** S25-34.

BROWN, E. M., GAMBA, G., RICCARDI, D., LOMBARDI, M., BUTTERS, R., KIFOR, O., SUN, A., HEDIGER, M. A., LYTTON, J. & HEBERT, S. C. (1993) Cloning and characterization of an extracellular Ca(2+)-sensing receptor from bovine parathyroid. *Nature,* 366**,** 575-80.

BROWN, T. D. (2000) Techniques for mechanical stimulation of cells in vitro: a review. *Journal of Biomechanics,* 33**,** 3-14.

BRUNKOW, M. E., GARDNER, J. C., VAN NESS, J., PAEPER, B. W., KOVACEVICH, B. R., PROLL, S., SKONIER, J. E., ZHAO, L., SABO, P. J., FU, Y., ALISCH, R. S., GILLETT, L., COLBERT, T., TACCONI, P., GALAS, D., HAMERSMA, H., BEIGHTON, P. & MULLIGAN, J. (2001) Bone dysplasia sclerosteosis results from loss of the SOST gene product, a novel cystine knot-containing protein. *Am J Hum Genet,* 68**,** 577-89.

BRUNS, R. F., LU, G. H. & PUGSLEY, T. A. (1986) Characterization of the A2 adenosine receptor labeled by [3H]NECA in rat striatal membranes. *Mol Pharmacol,* 29**,** 331-46.

BUCARO, M. A., FERTALA, J., ADAMS, C. S., STEINBECK, M., AYYASWAMY, P., MUKUNDAKRISHNAN, K., SHAPIRO, I. M. & RISBUD, M. V. (2004) Bone cell survival in microgravity: evidence that modeled microgravity increases osteoblast sensitivity to apoptogens. *Annals of the New York Academy of Sciences,* 1027**,** 64-73.

BURFORD, J. H., PERRIEN, D. S., HORNER, A., BOWE, E. A., NOTOMI, T., SUVA, L. J. & SKERRY, T. M. (2004) Glutamate signalling regulates skeletogenesis and bone growth. *Journal of Bone and Mineral Research,* 19**,** S212-S213.

BURGER, E. H. & KLEIN-NULEN, J. (1999) Responses of bone cells to biomechanical forces in vitro. *Advances in dental research,* 13**,** 93-8.

BURGER, E. H., KLEIN-NULEND, J. & SMIT, T. H. (2003) Strain-derived canalicular fluid flow regulates osteoclast activity in a remodelling osteon--a proposal. *J Biomech,* 36**,** 1453-9.

BURR, D. B. & RADIN, E. L. (2003) Microfractures and microcracks in subchondral bone: are they relevant to osteoarthrosis? *Rheum Dis Clin North Am,* 29**,** 675-85.

BUSTIN, S. A. (2000) Absolute quantification of mRNA using real-time reverse transcription polymerase chain reaction assays. *Journal of molecular endocrinology,* 25**,** 169-93.

BUSTIN, S. A. (2002) Quantification of mRNA using real-time reverse transcription PCR (RT-PCR): trends and problems. *Journal of molecular endocrinology,* 29**,** 23-39.

BUSTIN, S. A., BENES, V., GARSON, J. A., HELLEMANS, J., HUGGETT, J., KUBISTA, M., MUELLER, R., NOLAN, T., PFAFFL, M. W., SHIPLEY, G. L., VANDESOMPELE, J. & WITTWER, C. T. (2009) The MIQE guidelines: minimum information for publication of quantitative real-time PCR experiments. *Clin Chem,* 55**,** 611-22.

CARMELIET, G., VICO, L. & BOUILLON, R. (2001) Space flight: a challenge for normal bone homeostasis. *Crit Rev Eukaryot Gene Expr,* 11**,** 131-44.

CARROLL, S. H., WIGNER, N. A., KULKARNI, N., JOHNSTON-COX, H., GERSTENFELD, L. C. & RAVID, K. (2012) A2B adenosine receptor promotes mesenchymal stem cell differentiation to osteoblasts and bone formation in vivo. *J Biol Chem,* 287**,** 15718-27.

CARVALHO, R. S., SCOTT, J. E. & YEN, E. H. (1995) The effects of mechanical stimulation on the distribution of beta 1 integrin and expression of beta 1-integrin mRNA in TE-85 human osteosarcoma cells. *Archives of oral biology,* 40**,** 257-64.

CASTANEDA, S., ROMAN-BLAS, J. A., LARGO, R. & HERRERO-BEAUMONT, G. (2012) Subchondral bone as a key target for osteoarthritis treatment. *Biochem Pharmacol,* 83**,** 315-23.

CHAMBERS, T. J., EVANS, M., GARDNER, T. N., TURNER-SMITH, A. & CHOW, J. W. (1993) Induction of bone formation in rat tail vertebrae by mechanical loading. *Bone and mineral,* 20**,** 167-78.

CHAN, M., LU, X., HUO, B., BAIK, A., CHIANG, V., GULDBERG, R., LU, H. & GUO, X. E. (2009) A Trabecular Bone Explant Model of

Osteocyteâ€“Osteoblast Co-Culture for Bone Mechanobiology. *Cellular and molecular bioengineering,* 2**,** 405-415.

CHANG, J. K., CHANG, L. H., HUNG, S. H., WU, S. C., LEE, H. Y., LIN, Y. S., CHEN, C. H., FU, Y. C., WANG, G. J. & HO, M. L. (2009) Parathyroid hormone 1-34 inhibits terminal differentiation of human articular chondrocytes and osteoarthritis progression in rats. *Arthritis Rheum,* 60**,** 3049-60.

CHANG, W., TU, C., CHEN, T.-H., BIKLE, D. & SHOBACK, D. (2008a) The Extracellular Calcium-Sensing Receptor (CaSR) Is a Critical Modulator of Skeletal Development. *Sci. Signal.,* 1**,** ra1-.

CHANG, W., TU, C., CHEN, T. H., BIKLE, D. & SHOBACK, D. (2008b) The extracellular calcium-sensing receptor (CaSR) is a critical modulator of skeletal development. *Science signaling,* 1**,** ra1.

CHANG, W., TU, C., CHEN, T. H., KOMUVES, L., ODA, Y., PRATT, S. A., MILLER, S. & SHOBACK, D. (1999) Expression and signal transduction of calcium-sensing receptors in cartilage and bone. *Endocrinology,* 140**,** 5883-93.

CHATTERJEE, K., LIN-GIBSON, S., WALLACE, W. E., PAREKH, S. H., LEE, Y. J., CICERONE, M. T., YOUNG, M. F. & SIMON, C. G., JR. (2010) The effect of 3D hydrogel scaffold modulus on osteoblast differentiation and mineralization revealed by combinatorial screening. *Biomaterials,* 31**,** 5051-62.

CHATTOPADHYAY, N., LEGRADI, G., BAI, M., KIFOR, O., YE, C., VASSILEV, P. M., BROWN, E. M. & LECHAN, R. M. (1997) Calcium-sensing receptor in the rat hippocampus: a developmental study. *Brain Res Dev Brain Res,* 100**,** 13-21.

CHATTOPADHYAY, N., YANO, S., TFELT-HANSEN, J., ROONEY, P., KANUPARTHI, D., BANDYOPADHYAY, S., REN, X., TERWILLIGER, E. & BROWN, E. M. (2004) Mitogenic Action of Calcium-Sensing Receptor on Rat Calvarial Osteoblasts. *Endocrinology,* 145**,** 3451-3462.

CHEN, X., YANG, L. & TIAN, W. (2003) [Heterotopic osteogenesis of autogenous marrow stromal cells with recombinant human bone morphogenetic protein 2 gene transfection and porous calcium phosphate ceramic as a scaffold]. *Hua xi kou qiang yi xue za zhi = Huaxi kouqiang yixue zazhi = West China journal of stomatology,* 21**,** 419-21.

CHENG, B., KATO, Y., ZHAO, S., LUO, J., SPRAGUE, E., BONEWALD, L. F. & JIANG, J. X. (2001a) PGE(2) is essential for gap junction-mediated intercellular communication between osteocyte-like MLO-Y4 cells in response to mechanical strain. *Endocrinology,* 142**,** 3464-73.

CHENG, B., ZHAO, S., LUO, J., SPRAGUE, E., BONEWALD, L. F. & JIANG, J. X. (2001b) Expression of functional gap junctions and regulation by fluid flow in osteocyte-like MLO-Y4 cells. *Journal of bone and mineral research : the official journal of the American Society for Bone and Mineral Research,* 16**,** 249-59.

CHENG, M. Z., RAWLINSON, S. C., PITSILLIDES, A. A., ZAMAN, G., MOHAN, S., BAYLINK, D. J. & LANYON, L. E. (2002) Human osteoblasts' proliferative responses to strain and 17beta-estradiol are mediated by the estrogen receptor and the receptor for insulin-like growth factor I. *Journal of bone and mineral research : the official journal of the American Society for Bone and Mineral Research,* 17**,** 593-602.

CHENG, M. Z., ZAMAN, G. & LANYON, L. E. (1994) Estrogen enhances the stimulation of bone collagen synthesis by loading and exogenous prostacyclin, but not prostaglandin E2, in organ cultures of rat ulnae. *Journal of bone and mineral research : the official journal of the American Society for Bone and Mineral Research,* 9**,** 805-16.

CHENU, C., SERRE, C. M., RAYNAL, C., BURT-PICHAT, B. & DELMAS, P. D. (1998) Glutamate receptors are expressed by bone cells and are involved in bone resorption. *Bone,* 22**,** 295-9.

CHERIAN, P. P., CHENG, B., GU, S., SPRAGUE, E., BONEWALD, L. F. & JIANG, J. X. (2003) Effects of Mechanical Strain on the Function of Gap Junctions in Osteocytes Are Mediated through the Prostaglandin EP2 Receptor. *Journal of Biological Chemistry,* 278**,** 43146-43156.

CHERIAN, P. P., SILLER-JACKSON, A. J., GU, S., WANG, X., BONEWALD, L. F., SPRAGUE, E. & JIANG, J. X. (2005) Mechanical strain opens connexin 43 hemichannels in osteocytes: a novel mechanism for the release of prostaglandin. *Mol Biol Cell,* 16**,** 3100-6.

CHO, Y. & BANNAI, S. (1990) Uptake of glutamate and cysteine in C-6 glioma cells and in cultured astrocytes. *J Neurochem,* 55**,** 2091-7.

CHOI, K.-Y., KIM, H.-J., LEE, M.-H., KWON, T.-G., NAH, H.-D., FURUICHI, T., KOMORI, T., NAM, S.-H., KIM, Y.-J., KIM, H.-J. & RYOO, H.-M. (2005) Runx2 regulates FGF2-induced Bmp2 expression during cranial bone development. *Developmental Dynamics,* 233**,** 115-121.

CHOW, J. W., FOX, S. W., LEAN, J. M. & CHAMBERS, T. J. (1998a) Role of nitric oxide and prostaglandins in mechanically induced bone formation. *Journal of bone and mineral research : the official journal of the American Society for Bone and Mineral Research,* 13**,** 1039-44.

CHOW, J. W., JAGGER, C. J. & CHAMBERS, T. J. (1993) Characterization of osteogenic response to mechanical stimulation in cancellous bone of rat caudal vertebrae. *The American journal of physiology,* 265**,** E340-7.

CHOW, J. W., WILSON, A. J., CHAMBERS, T. J. & FOX, S. W. (1998b) Mechanical loading stimulates bone formation by reactivation of bone lining cells in 13-week-old rats. *Journal of bone and mineral research : the official journal of the American Society for Bone and Mineral Research,* 13**,** 1760-7.

CHU, T., RANSON, W. & SUTTON, M. (1985) Applications of digital-image-correlation techniques to experimental mechanics. *Experimental Mechanics,* 25**,** 232-244.

CILLO, J. E., JR., GASSNER, R., KOEPSEL, R. R. & BUCKLEY, M. J. (2000) Growth factor and cytokine gene expression in mechanically strained human osteoblast-like cells: implications for distraction osteogenesis. *Oral surgery, oral medicine, oral pathology, oral radiology, and endodontics,* 90**,** 147-54.

CIRUELA, F., ESCRICHE, M., BURGUENO, J., ANGULO, E., CASADO, V., SOLOVIEV, M. M., CANELA, E. I., MALLOL, J., CHAN, W. Y., LLUIS, C., MCILHINNEY, R. A. & FRANCO, R. (2001) Metabotropic glutamate 1alpha and adenosine A1 receptors assemble into functionally interacting complexes. *J Biol Chem,* 276**,** 18345-51.

CLARKE, B. (2008) Normal bone anatomy and physiology. *Clinical journal of the American Society of Nephrology : CJASN,* 3 Suppl 3**,** S131-9.

CLARKIN, C. E. & GERSTENFELD, L. C. (2013) VEGF and bone cell signalling: an essential vessel for communication? *Cell Biochem Funct,* 31**,** 1-11.

COHEN, S. B., DORE, R. K., LANE, N. E., ORY, P. A., PETERFY, C. G., SHARP, J. T., VAN DER HEIJDE, D., ZHOU, L., TSUJI, W. & NEWMARK, R. (2008) Denosumab treatment effects on structural damage, bone mineral density, and bone turnover in rheumatoid arthritis: a twelve-month, multicenter, randomized, double-blind, placebo-controlled, phase II clinical trial. *Arthritis Rheum,* 58**,** 1299-309.

COLLIN-OSDOBY, P. (1994) Role of vascular endothelial cells in bone biology. *Journal of cellular biochemistry,* 55**,** 304-9.

COLLIN, P., NEFUSSI, J. R., WETTERWALD, A., NICOLAS, V., BOY-LEFEVRE, M. L., FLEISCH, H. & FOREST, N. (1992) Expression of collagen, osteocalcin, and bone alkaline phosphatase in a mineralizing rat osteoblastic cell culture. *Calcified tissue international,* 50**,** 175-83.

COMPSTON, J. E. (2001) Sex steroids and bone. *Physiol Rev,* 81**,** 419-447.

COMPSTON, J. E. (2002) Bone marrow and bone: a functional unit. *J Endocrinol,* 173**,** 387-94.

CONIGRAVE, A. D., QUINN, S. J. & BROWN, E. M. (2000) l-Amino acid sensing by the extracellular Ca2+-sensing receptor. *Proceedings of the National Academy of Sciences,* 97**,** 4814-4819.

CONN, P. J. & PIN, J. P. (1997) Pharmacology and functions of metabotropic glutamate receptors. *Annu Rev Pharmacol Toxicol,* 37**,** 205-37.

COOPER, C., REGINSTER, J. Y., CHAPURLAT, R., CHRISTIANSEN, C., GENANT, H., BELLAMY, N., BENSEN, W., NAVARRO, F., BADURSKI, J., NASONOV, E., CHEVALIER, X. & SAMBROOK, P. N. (2012) Efficacy and safety of oral strontium ranelate for the treatment of knee osteoarthritis: rationale and design of randomised, double-blind, placebo-controlled trial. *Curr Med Res Opin,* 28**,** 231-9.

CORMACK, D. H. & HAM, A. W. (1987) *Ham's Histology,* Univeristy of Michigan, Lippincott Williams & Wilkins.

COSTA, M. A., BARBOSA, A., NETO, E., SA-E-SOUSA, A., FREITAS, R., NEVES, J. M., MAGALHAES-CARDOSO, T., FERREIRINHA, F. & CORREIA-DE-SA, P. (2011) On the role of subtype selective adenosine receptor agonists during proliferation and osteogenic differentiation of human primary bone marrow stromal cells. *J Cell Physiol,* 226**,** 1353-66.

COULOMBE, J., FAURE, H., ROBIN, B. & RUAT, M. (2004) In vitro effects of strontium ranelate on the extracellular calcium-sensing receptor. *Biochemical and Biophysical Research Communications,* 323**,** 1184-1190.

COWAN, R. W., SEIDLITZ, E. P. & SINGH, G. (2012) Glutamate signaling in healthy and diseased bone. *Front Endocrinol (Lausanne),* 3**,** 89.

CROCKETT, J. C., ROGERS, M. J., COXON, F. P., HOCKING, L. J. & HELFRICH, M. H. (2011) Bone remodelling at a glance. *J Cell Sci,* 124**,** 991-8.

CUMMINGS, S. R., SAN MARTIN, J., MCCLUNG, M. R., SIRIS, E. S., EASTELL, R., REID, I. R., DELMAS, P., ZOOG, H. B., AUSTIN, M., WANG, A., KUTILEK, S., ADAMI, S., ZANCHETTA, J., LIBANATI, C., SIDDHANTI, S. & CHRISTIANSEN, C. (2009) Denosumab for prevention of fractures in postmenopausal women with osteoporosis. *N Engl J Med,* 361**,** 756-65.

CUNDY, T. & REID, I. R. (2012) Reprint: Paget's disease of bone. *Clin Biochem,* 45**,** 970-5.

CURREY, J. D. (1984) What should bones be designed to do? *Calcified tissue international,* 36 Suppl 1**,** S7-10.

CZEKANSKA, E. M., STODDART, M. J., RICHARDS, R. G. & HAYES, J. S. (2012) In search of an osteoblast cell model for in vitro research. *Eur Cell Mater,* 24**,** 1-17.

DANBOLT, N. C. (2001) Glutamate uptake. *Prog Neurobiol,* 65**,** 1-105.

DASSOULI, A., SULPICE, J. C., ROUX, S. & CROZATIER, B. (1993) Stretch-induced inositol trisphosphate and tetrakisphosphate production in rat cardiomyocytes. *J Mol Cell Cardiol,* 25**,** 973-82.

DAVIES, C. M., JONES, D. B., STODDART, M. J., KOLLER, K., SMITH, E., ARCHER, C. W. & RICHARDS, R. G. (2006) Mechanically loaded ex vivo bone culture system 'Zetos': systems and culture preparation. *European cells & materials,* 11**,** 57-75; discussion 75.

DAVIS, M. E., CAI, H., DRUMMOND, G. R. & HARRISON, D. G. (2001) Shear stress regulates endothelial nitric oxide synthase expression through c-Src by divergent signaling pathways. *Circ Res,* 89**,** 1073-80.

DELAISSE, J. M., ANDERSEN, T. L., ENGSIG, M. T., HENRIKSEN, K., TROEN, T. & BLAVIER, L. (2003) Matrix metalloproteinases (MMP) and cathepsin K contribute differently to osteoclastic activities. *Microsc Res Tech,* 61**,** 504-13.

DELAISSE, J. M., EECKHOUT, Y., NEFF, L., FRANCOIS-GILLET, C., HENRIET, P., SU, Y., VAES, G. & BARON, R. (1993) (Pro)collagenase (matrix metalloproteinase-1) is present in rodent osteoclasts and in the underlying bone-resorbing compartment. *J Cell Sci,* 106 (Pt 4)**,** 1071-82.

DELAISSE, J. M., LEDENT, P. & VAES, G. (1991) Collagenolytic cysteine proteinases of bone tissue. Cathepsin B, (pro)cathepsin L and a cathepsin L-like 70 kDa proteinase. *Biochem J,* 279 (Pt 1)**,** 167-74.

DEMPSTER, D. W., COSMAN, F., KURLAND, E. S., ZHOU, H., NIEVES, J., WOELFERT, L., SHANE, E., PLAVETIC, K., MULLER, R., BILEZIKIAN, J. & LINDSAY, R. (2001) Effects of daily treatment with parathyroid hormone on bone microarchitecture and turnover in patients with osteoporosis: a paired biopsy study. *J Bone Miner Res,* 16**,** 1846-53.

DEMPSTER, D. W., COSMAN, F., PARISIEN, M. A. Y., SHEN, V. & LINDSAY, R. (1993) Anabolic Actions of Parathyroid Hormone on Bone. *Endocrine Reviews,* 14**,** 690-709.

DEODHAR, A., DORE, R. K., MANDEL, D., SCHECHTMAN, J., SHERGY, W., TRAPP, R., ORY, P. A., PETERFY, C. G., FUERST, T., WANG, H., ZHOU, L., TSUJI, W. & NEWMARK, R. (2010) Denosumab-mediated increase in hand bone mineral density associated with decreased progression of bone erosion in rheumatoid arthritis patients. *Arthritis Care Res (Hoboken),* 62**,** 569-74.

DEYAMA, Y., TAKEYAMA, S., KOSHIKAWA, M., SHIRAI, Y., YOSHIMURA, Y., NISHIKATA, M., SUZUKI, K. & MATSUMOTO, A. (2000) Osteoblast maturation suppressed osteoclastogenesis in coculture with bone marrow cells. *Biochemical and biophysical research communications,* 274**,** 249-54.

DI PALMA, F., DOUET, M., BOACHON, C., GUIGNANDON, A., PEYROCHE, S., FOREST, B., ALEXANDRE, C., CHAMSON, A. & RATTNER, A. (2003) Physiological strains induce differentiation in human osteoblasts cultured on orthopaedic biomaterial. *Biomaterials,* 24**,** 3139-51.

DIAZ-CABIALE, Z., VIVO, M., DEL ARCO, A., O'CONNOR, W. T., HARTE, M. K., MULLER, C. E., MARTINEZ, E., POPOLI, P., FUXE, K. & FERRE, S. (2002) Metabotropic glutamate mGlu5 receptor-mediated modulation of the ventral striopallidal GABA pathway in rats. Interactions with adenosine A(2A) and dopamine D(2) receptors. *Neurosci Lett,* 324**,** 154-8.

DOBNIG, H. & TURNER, R. T. (1995) Evidence that intermittent treatment with parathyroid hormone increases bone formation in adult rats by activation of bone lining cells. *Endocrinology,* 136**,** 3632-8.

DODDS, R. A., ALI, N., PEAD, M. J. & LANYON, L. E. (1993) Early loading-related changes in the activity of glucose 6-phosphate dehydrogenase and alkaline phosphatase in osteocytes and periosteal osteoblasts in rat fibulae in vivo. *J Bone Miner Res,* 8**,** 261-7.

DOMASCHKE, H., GELINSKY, M., BURMEISTER, B., FLEIG, R., HANKE, T., REINSTORF, A., POMPE, W. & ROSEN-WOLFF, A. (2006) In vitro ossification and remodeling of mineralized collagen I scaffolds. *Tissue engineering,* 12**,** 949-58.

DOSCHAK, M. R., WOHL, G. R., HANLEY, D. A., BRAY, R. C. & ZERNICKE, R. F. (2004) Antiresorptive therapy conserves some periarticular bone and ligament mechanical properties after anterior cruciate ligament disruption in the rabbit knee. *J Orthop Res,* 22**,** 942-8.

DOTY, S. B. (1981) Morphological evidence of gap junctions between bone cells. *Calcified tissue international,* 33**,** 509-12.

DOTY, S. B., ROBINSON, R. A. & SCHOFIELD, B. (1976) Morphology of bone and histochemical staining characteristics of bone cells. . *Handbook of Physiology.* Washington DC, American Physiological Society.

DRURY, A. N. & SZENT-GYÖGYI, A. (1929) The physiological activity of adenine compound with special reference to their action upon the mammalian heart. *Journal of Physiology,* 68**,** 213-237.

DUBE, S., QIN, J. & RAMAKRISHNAN, R. (2008) Mathematical analysis of copy number variation in a DNA sample using digital PCR on a nanofluidic device. *PLoS One,* 3**,** e2876.

DUCY, P., ZHANG, R., GEOFFROY, V., RIDALL, A. L. & KARSENTY, G. (1997) Osf2/Cbfa1: a transcriptional activator of osteoblast differentiation. *Cell,* 89**,** 747-54.

DUDLEY, H. R. & SPIRO, D. (1961) THE FINE STRUCTURE OF BONE CELLS. *J Biophys Biochem Cytol,* 11**,** 627-49.

DUMAS, V., PERRIER, A., MALAVAL, L., LAROCHE, N., GUIGNANDON, A., VICO, L. & RATTNER, A. (2009) The effect of dual frequency cyclic compression on matrix deposition by osteoblast-like cells grown in 3D scaffolds and on modulation of VEGF variant expression. *Biomaterials,* 30**,** 3279-88.

DUNCAN, R. L. & TURNER, C. H. (1995) Mechanotransduction and the functional response of bone to mechanical strain. *Calcif Tissue Int,* 57**,** 344-58.

DUNSTAN, C. R., EVANS, R. A., HILLS, E., WONG, S. Y. & HIGGS, R. J. (1990) Bone death in hip fracture in the elderly. *Calcif Tissue Int,* 47**,** 270-5.

DVORAK-EWELL, M. M., CHEN, T. H., LIANG, N., GARVEY, C., LIU, B., TU, C., CHANG, W., BIKLE, D. D. & SHOBACK, D. M. (2011) Osteoblast extracellular Ca2+ -sensing receptor regulates bone development, mineralization, and turnover. *Journal of bone and mineral research : the*

official journal of the American Society for Bone and Mineral Research, 26**,** 2935-47.

DVORAK, M. M., SIDDIQUA, A., WARD, D. T., CARTER, D. H., DALLAS, S. L., NEMETH, E. F. & RICCARDI, D. (2004) Physiological changes in extracellular calcium concentration directly control osteoblast function in the absence of calciotropic hormones. *Proceedings of the National Academy of Sciences of the United States of America,* 101**,** 5140-5145.

EL-FOULY, M. H., TROSKO, J. E. & CHANG, C. C. (1987) Scrape-loading and dye transfer. A rapid and simple technique to study gap junctional intercellular communication. *Exp Cell Res,* 168**,** 422-30.

ENDRES, S., KRATZ, M., WUNSCH, S. & JONES, D. B. (2009) Zetos: a culture loading system for trabecular bone. Investigation of different loading signal intensities on bovine bone cylinders. *Journal of musculoskeletal & neuronal interactions,* 9**,** 173-83.

ERIKSEN, E. F. (1986) Normal and pathological remodeling of human trabecular bone: three dimensional reconstruction of the remodeling sequence in normals and in metabolic bone disease. *Endocr Rev,* 7**,** 379-408.

EVANS, B. & HAM, J. (2012) An emerging role for adenosine and its receptors in bone homeostasis. *Frontiers in Endocrinology,* 3.

EVENTOV, I., FRISCH, B., COHEN, Z. & HAMMEL, I. (1991) Osteopenia, hematopoiesis, and bone remodelling in iliac crest and femoral biopsies: a prospective study of 102 cases of femoral neck fractures. *Bone,* 12**,** 1-6.

FAIRMAN, W. A., VANDENBERG, R. J., ARRIZA, J. L., KAVANAUGH, M. P. & AMARA, S. G. (1995) An excitatory amino-acid transporter with properties of a ligand-gated chloride channel. *Nature,* 375**,** 599-603.

FARZANEH-FAR, A., PROUDFOOT, D., WEISSBERG, P. L. & SHANAHAN, C. M. (2000) Matrix gla protein is regulated by a mechanism functionally related to the calcium-sensing receptor. *Biochem Biophys Res Commun,* 277**,** 736-40.

FELIX, R., CECCHINI, M. G. & FLEISCH, H. (1990) MACROPHAGE COLONY STIMULATING FACTOR RESTORES IN VIVO BONE RESORPTION IN THE OP/OP OSTEOPETROTIC MOUSE. *Endocrinology,* 127**,** 2592-2594.

FENG, J. Q., HUANG, H., LU, Y., YE, L., XIE, Y., TSUTSUI, T. W., KUNIEDA, T., CASTRANIO, T., SCOTT, G., BONEWALD, L. B. & MISHINA, Y. (2003) The Dentin matrix protein 1 (Dmp1) is specifically expressed in mineralized, but not soft, tissues during development. *J Dent Res,* 82**,** 776-80.

FENG, J. Q., WARD, L. M., LIU, S., LU, Y., XIE, Y., YUAN, B., YU, X., RAUCH, F., DAVIS, S. I., ZHANG, S., RIOS, H., DREZNER, M. K., QUARLES, L. D., BONEWALD, L. F. & WHITE, K. E. (2006) Loss of DMP1 causes rickets and osteomalacia and identifies a role for osteocytes in mineral metabolism. *Nat Genet,* 38**,** 1310-5.

FERRAGUTI, F., CONQUET, F., CORTI, C., GRANDES, P., KUHN, R. & KNOPFEL, T. (1998) Immunohistochemical localization of the mGluR1β metabotropic glutamate receptor in the adult rodent forebrain: Evidence for a differential distribution of mGluR1 splice variants. *The Journal of Comparative Neurology,* 400**,** 391-407.

FERRE, S., KARCZ-KUBICHA, M., HOPE, B. T., POPOLI, P., BURGUENO, J., GUTIERREZ, M. A., CASADO, V., FUXE, K., GOLDBERG, S. R., LLUIS, C., FRANCO, R. & CIRUELA, F. (2002) Synergistic interaction between

adenosine A2A and glutamate mGlu5 receptors: implications for striatal neuronal function. *Proc Natl Acad Sci U S A,* 99**,** 11940-5.

FERRETTI, J. L., FROST, H. M., GASSER, J. A., HIGH, W. B., JEE, W. S., JEROME, C., MOSEKILDE, L. & THOMPSON, D. D. (1995) Perspectives on osteoporosis research: its focus and some insights from a new paradigm. *Calcif Tissue Int,* 57**,** 399-404.

FERRY, S., TRAIFFORT, E., STINNAKRE, J. & RUAT, M. (2000) Developmental and adult expression of rat calcium-sensing receptor transcripts in neurons and oligodendrocytes. *Eur J Neurosci,* 12**,** 872-84.

FORWOOD, M. R. (1996) Inducible cyclo-oxygenase (COX-2) mediates the induction of bone formation by mechanical loading in vivo. *Journal of Bone and Mineral Research,* 11**,** 1688-1693.

FOX, S. W., CHAMBERS, T. J. & CHOW, J. W. (1996) Nitric oxide is an early mediator of the increase in bone formation by mechanical stimulation. *Am J Physiol,* 270**,** E955-60.

FRIEDRICHS, W. E., REDDY, S. V., SINGER, F. J. & ROODMAN, G. D. (2002) The Pro and Con of Measles Virus in Paget's Disease: Pro. *Journal of Bone and Mineral Research,* 17**,** 2293-2293.

FRITTON, S. P., J. MCLEOD, K. & RUBIN, C. T. (2000) Quantifying the strain history of bone: spatial uniformity and self-similarity of low-magnitude strains. *Journal of Biomechanics,* 33**,** 317-325.

FROST, H. M. (1960) In Vivo Osteocyte Death. *The Journal of Bone & Joint Surgery,* 42**,** 138-143.

FROST, H. M. (1987a) Bone "mass" and the "mechanostat": a proposal. *Anat Rec,* 219**,** 1-9.

FROST, H. M. (1987b) The mechanostat: a proposed pathogenic mechanism of osteoporoses and the bone mass effects of mechanical and nonmechanical agents. *Bone Miner,* 2**,** 73-85.

FROST, H. M. (1990a) Skeletal structural adaptations to mechanical usage (SATMU): 1. Redefining Wolff's law: the bone modeling problem. *Anat Rec,* 226**,** 403-13.

FROST, H. M. (1990b) Skeletal structural adaptations to mechanical usage (SATMU): 2. Redefining Wolff's Law: The remodeling problem. *The Anatomical Record,* 226**,** 414-422.

FROST, H. M. (1996) Perspectives: a proposed general model of the "mechanostat" (suggestions from a new skeletal-biologic paradigm). *Anat Rec,* 244**,** 139-47.

FROST, H. M. (1998) From Wolff's law to the mechanostat: a new "face" of physiology. *J Orthop Sci,* 3**,** 282-6.

FUJITA, T., IZUMO, N., FUKUYAMA, R., MEGURO, T., NAKAMUTA, H., KOHNO, T. & KOIDA, M. (2001) Phosphate provides an extracellular signal that drives nuclear export of Runx2/Cbfa1 in bone cells. *Biochem Biophys Res Commun,* 280**,** 348-52.

GALEA, G. L., SUNTERS, A., MEAKIN, L. B., ZAMAN, G., SUGIYAMA, T., LANYON, L. E. & PRICE, J. S. (2011) Sost down-regulation by mechanical strain in human osteoblastic cells involves PGE2 signaling via EP4. *FEBS letters,* 585**,** 2450-4.

GAMA, L., WILT, S. G. & BREITWIESER, G. E. (2001) Heterodimerization of Calcium Sensing Receptors with Metabotropic Glutamate Receptors in Neurons. *Journal of Biological Chemistry,* 276**,** 39053-39059.

GAUGAIN, B., BARBET, J., CAPELLE, N., ROQUES, B. P., LEPECQ, J. B. & LEBRET, M. (1978a) DNA Bifunctional Intercalators .2. Fluorescence Properties and DNA Binding Interaction of an Ethidium Homodimer and an Acridine Ethidium Heterodimer. *Biochemistry,* 17**,** 5078-5088.

GAUGAIN, B., BARBET, J., OBERLIN, R., ROQUES, B. P. & LEPECQ, J. B. (1978b) DNA Bifunctional Intercalators .1. Synthesis and Conformational Properties of an Ethidium Homodimer and of an Acridine Ethidium Heterodimer. *Biochemistry,* 17**,** 5071-5078.

GEILER, J., BUCH, M. & MCDERMOTT, M. F. (2011) Anti-TNF treatment in rheumatoid arthritis. *Current pharmaceutical design,* 17**,** 3141-54.

GENETOS, D. C., GEIST, D. J., LIU, D., DONAHUE, H. J. & DUNCAN, R. L. (2005) Fluid shear-induced ATP secretion mediates prostaglandin release in MC3T3-E1 osteoblasts. *J Bone Miner Res,* 20**,** 41-9.

GENETOS, D. C., KEPHART, C. J., ZHANG, Y., YELLOWLEY, C. E. & DONAHUE, H. J. (2007) Oscillating fluid flow activation of gap junction hemichannels induces atp release from MLO-Y4 osteocytes. *Journal of Cellular Physiology,* 212**,** 207-214.

GENEVER, P. G., WILKINSON, D. J., PATTON, A. J., PEET, N. M., HONG, Y., MATHUR, A., ERUSALIMSKY, J. D. & SKERRY, T. M. (1999) Expression of a functional N-methyl-D-aspartate-type glutamate receptor by bone marrow megakaryocytes. *Blood,* 93**,** 2876-83.

GHARIBI, B., ABRAHAM, A. A., HAM, J. & EVANS, B. A. (2011) Adenosine receptor subtype expression and activation influence the differentiation of mesenchymal stem cells to osteoblasts and adipocytes. *J Bone Miner Res,* 26**,** 2112-24.

GHARIBI, B., ABRAHAM, A. A., HAM, J. & EVANS, B. A. (2012) Contrasting effects of A1 and A2b adenosine receptors on adipogenesis. *Int J Obes (Lond),* 36**,** 397-406.

GILBERT, L., HE, X., FARMER, P., RUBIN, J., DRISSI, H., VAN WIJNEN, A. J., LIAN, J. B., STEIN, G. S. & NANES, M. S. (2002) Expression of the Osteoblast Differentiation Factor RUNX2 (Cbfa1/AML3/Pebp2αA) Is Inhibited by Tumor Necrosis Factor-α. *Journal of Biological Chemistry,* 277**,** 2695-2701.

GLAZER, A. N., PECK, K. & MATHIES, R. A. (1990) A stable double-stranded DNA-ethidium homodimer complex: application to picogram fluorescence detection of DNA in agarose gels. *Proceedings of the National Academy of Sciences of the United States of America,* 87**,** 3851-5.

GLIMCHER, M. J. (1981) On the form and function of bone: from molecules to organs. Wolff's law revisited. *The Chemistry and Biology of Mineralised Connective Tissues***,** 618-673.

GLIMCHER, M. J. (1992) The nature of the mineral component of bone and the emchnism of calcification. *Disorders of Bone and Mineral Metabolism***,** 265-286.

GLÜCKSMANN, A. (1939) Studies on bone mechanics in vitro. II. The role of tension and pressure in chondrogenesis. *The Anatomical Record,* 73**,** 39-55.

GLUHAK-HEINRICH, J., YE, L., BONEWALD, L. F., FENG, J. Q., MACDOUGALL, M., HARRIS, S. E. & PAVLIN, D. (2003) Mechanical loading stimulates dentin matrix protein 1 (DMP1) expression in osteocytes in vivo. *J Bone Miner Res,* 18**,** 807-17.

GOLDRING, S. R. (2003) Pathogenesis of bone and cartilage destruction in rheumatoid arthritis. *Rheumatology (Oxford),* 42 Suppl 2**,** ii11-6.

GOODSHIP, A. E., CUNNINGHAM, J. L., OGANOV, V., DARLING, J., MILES, A. W. & OWEN, G. W. (1998) Bone loss during long term space flight is prevented by the application of a short term impulsive mechanical stimulus. *Acta Astronaut,* 43**,** 65-75.

GOODSHIP, A. E., LANYON, L. E. & MCFIE, H. (1979) Functional adaptation of bone to increased stress. An experimental study. *J Bone Joint Surg Am,* 61**,** 539-46.

GOTO, T., TSUKUBA, T., KIYOSHIMA, T., NISHIMURA, Y., KATO, K., YAMAMOTO, K. & TANAKA, T. (1993) Immunohistochemical localization of cathepsins B, D and L in the rat osteoclast. *Histochemistry,* 99**,** 411-4.

GRAVALLESE, E. M., HARADA, Y., WANG, J. T., GORN, A. H., THORNHILL, T. S. & GOLDRING, S. R. (1998) Identification of cell types responsible for bone resorption in rheumatoid arthritis and juvenile rheumatoid arthritis. *Am J Pathol,* 152**,** 943-51.

GRAY, C., MARIE, H., ARORA, M., TANAKA, K., BOYDE, A., JONES, S. & ATTWELL, D. (2001) Glutamate does not play a major role in controlling bone growth. *J Bone Miner Res,* 16**,** 742-9.

GREGORY, C. D. & POUND, J. D. (2011) Cell death in the neighbourhood: direct microenvironmental effects of apoptosis in normal and neoplastic tissues. *The Journal of Pathology,* 223**,** 178-195.

GRIGORIADIS, A. E., WANG, Z. Q., CECCHINI, M. G., HOFSTETTER, W., FELIX, R., FLEISCH, H. A. & WAGNER, E. F. (1994) c-Fos: a key regulator of osteoclast-macrophage lineage determination and bone remodeling. *Science,* 266**,** 443-8.

GRIMAUD, E., SOUBIGOU, L., COUILLAUD, S., COIPEAU, P., MOREAU, A., PASSUTI, N., GOUIN, F., REDINI, F. & HEYMANN, D. (2003) Receptor activator of nuclear factor kappaB ligand (RANKL)/osteoprotegerin (OPG) ratio is increased in severe osteolysis. *Am J Pathol,* 163**,** 2021-31.

GROSS, T. S., MCLEOD, K. J. & RUBIN, C. T. (1992) Characterizing bone strain distributions in vivo using three triple rosette strain gages. *Journal of biomechanics,* 25**,** 1081-7.

GROSS, T. S. & RUBIN, C. T. (1995) Uniformity of resorptive bone loss induced by disuse. *J Orthop Res,* 13**,** 708-14.

GU, G., NARS, M., HENTUNEN, T. A., METSIKKO, K. & VAANANEN, H. K. (2006) Isolated primary osteocytes express functional gap junctions in vitro. *Cell and tissue research,* 323**,** 263-71.

GU, Y. & PUBLICOVER, S. J. (2000) Expression of functional metabotropic glutamate receptors in primary cultured rat osteoblasts. Cross-talk with N-methyl-D-aspartate receptors. *J Biol Chem,* 275**,** 34252-9.

GUDI, S., HUVAR, I., WHITE, C. R., MCKNIGHT, N. L., DUSSERRE, N., BOSS, G. R. & FRANGOS, J. A. (2003) Rapid activation of Ras by fluid flow is mediated by Galpha(q) and Gbetagamma subunits of heterotrimeric G proteins in human endothelial cells. *Arterioscler Thromb Vasc Biol,* 23**,** 994-1000.

HAAPASALO, H., KONTULAINEN, S., SIEVANEN, H., KANNUS, P., JARVINEN, M. & VUORI, I. (2000) Exercise-induced bone gain is due to enlargement in bone size without a change in volumetric bone density: a

peripheral quantitative computed tomography study of the upper arms of male tennis players. *Bone,* 27**,** 351-7.

HADDAWAY, M. J., DAVIE, M. W., MCCALL, I. W. & HOWDLE, S. (2007) Effect of age and gender on the number and distribution of sites in Paget's disease of bone. *Br J Radiol,* 80**,** 532-6.

HADJIARGYROU, M., RIGHTMIRE, E. P., ANDO, T. & LOMBARDO, F. T. (2001) The E11 osteoblastic lineage marker is differentially expressed during fracture healing. *Bone,* 29**,** 149-54.

HALLEUX, C., KRAMER, I., ALLARD, C. & KNEISSEL, M. (2012) Isolation of mouse osteocytes using cell fractionation for gene expression analysis. *Methods Mol Biol,* 816**,** 55-66.

HAM, K. D., LOESER, R. F., LINDGREN, B. R. & CARLSON, C. S. (2002) Effects of long-term estrogen replacement therapy on osteoarthritis severity in cynomolgus monkeys. *Arthritis Rheum,* 46**,** 1956-64.

HAN, Y., COWIN, S. C., SCHAFFLER, M. B. & WEINBAUM, S. (2004) Mechanotransduction and strain amplification in osteocyte cell processes. *Proc Natl Acad Sci U S A,* 101**,** 16689-94.

HANSEN, A., CHEN, Y., INMAN, J. M., PHAN, Q. N., QI, Z. Q., XIANG, C. C., PALKOVITS, M., CHERMAN, N., KUZNETSOV, S. A., ROBEY, P. G., MEZEY, E. & BROWNSTEIN, M. J. (2007) Sensitive and specific method for detecting G protein-coupled receptor mRNAs. *Nature methods,* 4**,** 35-7.

HARRIS, S. E., GLUHAK-HEINRICH, J., HARRIS, M. A., YANG, W., BONEWALD, L. F., RIHA, D., ROWE, P. S., ROBLING, A. G., TURNER, C. H., FENG, J. Q., MCKEE, M. D. & NICOLLELA, D. (2007) DMP1 and MEPE expression are elevated in osteocytes after mechanical loading in vivo: theoretical role in controlling mineral quality in the perilacunar matrix. *J Musculoskelet Neuronal Interact,* 7**,** 313-5.

HAYAMI, T., PICKARSKI, M., WESOLOWSKI, G. A., MCLANE, J., BONE, A., DESTEFANO, J., RODAN, G. A. & DUONG LE, T. (2004) The role of subchondral bone remodeling in osteoarthritis: reduction of cartilage degeneration and prevention of osteophyte formation by alendronate in the rat anterior cruciate ligament transection model. *Arthritis Rheum,* 50**,** 1193-206.

HEINO, T. J., HENTUNEN, T. A. & VAANANEN, H. K. (2004) Conditioned medium from osteocytes stimulates the proliferation of bone marrow mesenchymal stem cells and their differentiation into osteoblasts. *Experimental cell research,* 294**,** 458-68.

HENRIKSEN, Z., HIKEN, J. F., STEINBERG, T. H. & JORGENSEN, N. R. (2006) The predominant mechanism of intercellular calcium wave propagation changes during long-term culture of human osteoblast-like cells. *Cell calcium,* 39**,** 435-44.

HERRLING, P. L. (1997) The NBQX story. *Excitatory amino acids: Clinical results with antagonists.* London, UK, Academic Press, Ltd.

HILLAM, R. A., JACKSON, M., GOODSHIP, A. E. & SKERRY, T. M. (1996) O4. Comparison of physiological strains in the human skull and tibia. *Bone,* 19**,** 686.

HILLAM, R. A. & SKERRY, T. M. (1995) Inhibition of bone resorption and stimulation of formation by mechanical loading of the modeling rat ulna in vivo. *Journal of Bone and Mineral Research,* 10**,** 683-689.

HINOI, E., FUJIMORI, S., TAKEMORI, A., KURABAYASHI, H., NAKAMURA, Y. & YONEDA, Y. (2002) Demonstration of expression of mRNA for

particular AMPA and kainate receptor subunits in immature and mature cultured rat calvarial osteoblasts. *Brain Res,* 943**,** 112-6.

HINOI, E., FUJIMORI, S. & YONEDA, Y. (2003) Modulation of cellular differentiation by N-methyl-D-aspartate receptors in osteoblasts. *FASEB J,* 17**,** 1532-4.

HINOI, E., TAKARADA, T., UNO, K., INOUE, M., MURAFUJI, Y. & YONEDA, Y. (2007) Glutamate suppresses osteoclastogenesis through the cystine/glutamate antiporter. *Am J Pathol,* 170**,** 1277-90.

HIPSKIND, R. A. & BILBE, G. (1998) MAP kinase signaling cascades and gene expression in osteoblasts. *Front Biosci,* 3**,** d804-16.

HO, M. L., TSAI, T. N., CHANG, J. K., SHAO, T. S., JENG, Y. R. & HSU, C. (2005) Down-regulation of N-methyl D-aspartate receptor in rat-modeled disuse osteopenia. *Osteoporos Int,* 16**,** 1780-8.

HO, T. Y., SANTORA, K., CHEN, J. C., FRANKSHUN, A. L. & BAGNELL, C. A. (2011) Effects of relaxin and estrogens on bone remodeling markers, receptor activator of NF-kB ligand (RANKL) and osteoprotegerin (OPG), in rat adjuvant-induced arthritis. *Bone,* 48**,** 1346-53.

HOCKING, L. J., LUCAS, G. J., DAROSZEWSKA, A., MANGION, J., OLAVESEN, M., CUNDY, T., NICHOLSON, G. C., WARD, L., BENNETT, S. T., WUYTS, W., VAN HUL, W. & RALSTON, S. H. (2002) Domain-specific mutations in sequestosome 1 (SQSTM1) cause familial and sporadic Paget's disease. *Hum Mol Genet,* 11**,** 2735-9.

HOEY, D. A., KELLY, D. J. & JACOBS, C. R. (2011) A role for the primary cilium in paracrine signaling between mechanically stimulated osteocytes and mesenchymal stem cells. *Biochem Biophys Res Commun,* 412**,** 182-7.

HOLLIDAY, L. S., WELGUS, H. G., FLISZAR, C. J., VEITH, G. M., JEFFREY, J. J. & GLUCK, S. L. (1997) Initiation of osteoclast bone resorption by interstitial collagenase. *J Biol Chem,* 272**,** 22053-8.

HOLLMANN, M. & HEINEMANN, S. (1994) Cloned glutamate receptors. *Annu Rev Neurosci,* 17**,** 31-108.

HOLLMANN, M., O'SHEA-GREENFIELD, A., ROGERS, S. W. & HEINEMANN, S. (1989) Cloning by functional expression of a member of the glutamate receptor family. *Nature,* 342**,** 643-8.

HOUSE, M. G., KOHLMEIER, L., CHATTOPADHYAY, N., KIFOR, O., YAMAGUCHI, T., LEBOFF, M. S., GLOWACKI, J. & BROWN, E. M. (1997) Expression of an extracellular calcium-sensing receptor in human and mouse bone marrow cells. *J Bone Miner Res,* 12**,** 1959-70.

HSIEH, Y. F., ROBLING, A. G., AMBROSIUS, W. T., BURR, D. B. & TURNER, C. H. (2001) Mechanical loading of diaphyseal bone in vivo: the strain threshold for an osteogenic response varies with location. *J Bone Miner Res,* 16**,** 2291-7.

HUGGETT, J. F., MUSTAFA, A., O'NEAL, L. & MASON, D. J. (2002) The glutamate transporter GLAST-1 (EAAT-1) is expressed in the plasma membrane of osteocytes and is responsive to extracellular glutamate concentration. *Biochem Soc Trans,* 30**,** 890-3.

IGNATIUS, A., BLESSING, H., LIEDERT, A., SCHMIDT, C., NEIDLINGER-WILKE, C., KASPAR, D., FRIEMERT, B. & CLAES, L. (2005) Tissue engineering of bone: effects of mechanical strain on osteoblastic cells in type I collagen matrices. *Biomaterials,* 26**,** 311-318.

IMHOF, H., SULZBACHER, I., GRAMPP, S., CZERNY, C., YOUSSEFZADEH, S. & KAINBERGER, F. (2000) Subchondral bone and cartilage disease: a rediscovered functional unit. *Invest Radiol,* 35**,** 581-8.

IRIE, K., EJIRI, S., SAKAKURA, Y., SHIBUI, T. & YAJIMA, T. (2008) Matrix mineralization as a trigger for osteocyte maturation. *J Histochem Cytochem,* 56**,** 561-7.

ISHIHARA, Y., KAMIOKA, H., HONJO, T., UEDA, H., TAKANO-YAMAMOTO, T. & YAMASHIRO, T. (2008) Hormonal, pH, and calcium regulation of connexin 43-mediated dye transfer in osteocytes in chick calvaria. *J Bone Miner Res,* 23**,** 350-60.

ISHIJIMA, M., EZURA, Y., TSUJI, K., RITTLING, S. R., KUROSAWA, H., DENHARDT, D. T., EMI, M., NIFUJI, A. & NODA, M. (2006) Osteopontin is associated with nuclear factor ÎºB gene expression during tail-suspension-induced bone loss. *Experimental cell research,* 312**,** 3075-3083.

ISHIJIMA, M., RITTLING, S. R., YAMASHITA, T., TSUJI, K., KUROSAWA, H., NIFUJI, A., DENHARDT, D. T. & NODA, M. (2001) Enhancement of osteoclastic bone resorption and suppression of osteoblastic bone formation in response to reduced mechanical stress do not occur in the absence of osteopontin. *The Journal of experimental medicine,* 193**,** 399-404.

ITZSTEIN, C., ESPINOSA, L., DELMAS, P. D. & CHENU, C. (2000) Specific antagonists of NMDA receptors prevent osteoclast sealing zone formation required for bone resorption. *Biochemical and biophysical research communications,* 268**,** 201-9.

JACKSON, R. A., KUMARASURIYAR, A., NURCOMBE, V. & COOL, S. M. (2006) Long-term loading inhibits ERK1/2 phosphorylation and increases FGFR3 expression in MC3T3-E1 osteoblast cells. *J Cell Physiol,* 209**,** 894-904.

JACOBSON, K. A. & GAO, Z. G. (2006) Adenosine receptors as therapeutic targets. *Nat Rev Drug Discov,* 5**,** 247-64.

JAGGER, C. J., CHOW, J. W. & CHAMBERS, T. J. (1996) Estrogen suppresses activation but enhances formation phase of osteogenic response to mechanical stimulation in rat bone. *The Journal of clinical investigation,* 98**,** 2351-7.

JAGODZINSKI, M., DRESCHER, M., ZEICHEN, J., HANKEMEIER, S., KRETTEK, C., BOSCH, U. & VAN GRIENSVEN, M. (2004) Effects of cyclic longitudinal mechanical strain and dexamethasone on osteogenic differentiation of human bone marrow stromal cells. *European cells & materials,* 7**,** 35-41; discussion 41.

JAHN, K., RICHARDS, R. G., ARCHER, C. W. & STODDART, M. J. (2010) Pellet culture model for human primary osteoblasts. *European cells & materials,* 20**,** 149-61.

JANDE, S. S. & BELANGER, L. F. (1973) The life cycle of the osteocyte. *Clin Orthop Relat Res***,** 281-305.

JIANG, J. X. & CHENG, B. (2001) Mechanical stimulation of gap junctions in bone osteocytes is mediated by prostaglandin E2. *Cell Commun Adhes,* 8**,** 283-8.

JIANG, J. X. & CHERIAN, P. P. (2003) Hemichannels formed by connexin 43 play an important role in the release of prostaglandin E(2) by osteocytes in response to mechanical strain. *Cell Commun Adhes,* 10**,** 259-64.

JILKA, R. L. (1998) Cytokines, bone remodeling, and estrogen deficiency: a 1998 update. *Bone,* 23**,** 75-81.

JIN, X., SHEPHERD, R. K., DULING, B. R. & LINDEN, J. (1997) Inosine binds to A3 adenosine receptors and stimulates mast cell degranulation. *J Clin Invest,* 100**,** 2849-57.

JONES, H. H., PRIEST, J. D., HAYES, W. C., TICHENOR, C. C. & NAGEL, D. A. (1977) Humeral hypertrophy in response to exercise. *The Journal of bone and joint surgery. American volume,* 59**,** 204-8.

JONES, S. J. & BOYDE, A. (1976) Experimental study of changes in osteoblastic shape induced by calcitonin and parathyroid extract in an organ culture system. *Cell Tissue Res,* 169**,** 499-65.

KADRI, A., FUNCK-BRENTANO, T., LIN, H., EA, H. K., HANNOUCHE, D., MARTY, C., LIOTE, F., GEOFFROY, V. & COHEN-SOLAL, M. E. (2010) Inhibition of bone resorption blunts osteoarthritis in mice with high bone remodelling. *Ann Rheum Dis,* 69**,** 1533-8.

KALARITI, N., LEMBESSIS, P. & KOUTSILIERIS, M. (2004) Characterization of the glutametergic system in MG-63 osteoblast-like osteosarcoma cells. *Anticancer Res,* 24**,** 3923-9.

KAMEDA, T., MANO, H., YAMADA, Y., TAKAI, H., AMIZUKA, N., KOBORI, M., IZUMI, N., KAWASHIMA, H., OZAWA, H., IKEDA, K., KAMEDA, A., HAKEDA, Y. & KUMEGAWA, M. (1998) Calcium-sensing receptor in mature osteoclasts, which are bone resorbing cells. *Biochemical and biophysical research communications,* 245**,** 419-22.

KAMIOKA, H., HONJO, T. & TAKANO-YAMAMOTO, T. (2001) A three-dimensional distribution of osteocyte processes revealed by the combination of confocal laser scanning microscopy and differential interference contrast microscopy. *Bone,* 28**,** 145-9.

KAMIOKA, H., ISHIHARA, Y., RIS, H., MURSHID, S. A., SUGAWARA, Y., TAKANO-YAMAMOTO, T. & LIM, S. S. (2007) Primary cultures of chick osteocytes retain functional gap junctions between osteocytes and between osteocytes and osteoblasts. *Microsc Microanal,* 13**,** 108-17.

KANAI, Y. & HEDIGER, M. A. (1992) Primary structure and functional characterization of a high-affinity glutamate transporter. *Nature,* 360**,** 467-71.

KANATANI, M., SUGIMOTO, T., KANZAWA, M., YANO, S. & CHIHARA, K. (1999) High Extracellular Calcium Inhibits Osteoclast-like Cell Formation by Directly Acting on the Calcium-Sensing Receptor Existing in Osteoclast Precursor Cells. *Biochemical and biophysical research communications,* 261**,** 144-148.

KANIS, J., ODEN, A. & JOHNELL, O. (2001) Acute and long-term increase in fracture risk after hospitalization for stroke. *Stroke,* 32**,** 702-6.

KANIS, J. A. (1998) *Pathophysiology and Treatment of Paget's Disease of the Bone,* London, Martin Dunitz Limited.

KAPUR, S., BAYLINK, D. J. & LAU, K. H. (2003) Fluid flow shear stress stimulates human osteoblast proliferation and differentiation through multiple interacting and competing signal transduction pathways. *Bone,* 32**,** 241-51.

KAPUSCINSKI, J. (1995) DAPI: a DNA-specific fluorescent probe. *Biotechnic & histochemistry : official publication of the Biological Stain Commission,* 70**,** 220-33.

KARA, F. M., CHITU, V., SLOANE, J., AXELROD, M., FREDHOLM, B. B., STANLEY, E. R. & CRONSTEIN, B. N. (2010a) Adenosine A1 receptors (A1Rs) play a critical role in osteoclast formation and function. *FASEB J,* 24**,** 2325-33.

KARA, F. M., DOTY, S. B., BOSKEY, A., GOLDRING, S., ZAIDI, M., FREDHOLM, B. B. & CRONSTEIN, B. N. (2010b) Adenosine A1 receptors regulate bone resorption in mice: Adenosine A1 receptor blockade or deletion increases bone density and prevents ovariectomy-induced bone loss in adenosine A1 receptor–knockout mice. *Arthritis & Rheumatism,* 62**,** 534-541.

KARSDAL, M. A., BYRJALSEN, I., LEEMING, D. J. & CHRISTIANSEN, C. (2008) Tibolone inhibits bone resorption without secondary positive effects on cartilage degradation. *BMC Musculoskeletal Disorders,* 9**,** 153.

KARTSOGIANNIS, V., ZHOU, H., HORWOOD, N. J., THOMAS, R. J., HARDS, D. K., QUINN, J. M., NIFORAS, P., NG, K. W., MARTIN, T. J. & GILLESPIE, M. T. (1999) Localization of RANKL (receptor activator of NF kappa B ligand) mRNA and protein in skeletal and extraskeletal tissues. *Bone,* 25**,** 525-34.

KASPAR, D., SEIDL, W., NEIDLINGER-WILKE, C., BECK, A., CLAES, L. & IGNATIUS, A. (2002) Proliferation of human-derived osteoblast-like cells depends on the cycle number and frequency of uniaxial strain. *J Biomech,* 35**,** 873-80.

KASPAR, D., SEIDL, W., NEIDLINGER-WILKE, C., IGNATIUS, A. & CLAES, L. (2000) Dynamic cell stretching increases human osteoblast proliferation and CICP synthesis but decreases osteocalcin synthesis and alkaline phosphatase activity. *Journal of Biomechanics,* 33**,** 45-51.

KATO, Y., BOSKEY, A., SPEVAK, L., DALLAS, M., HORI, M. & BONEWALD, L. F. (2001) Establishment of an osteoid preosteocyte-like cell MLO-A5 that spontaneously mineralizes in culture. *Journal of bone and mineral research : the official journal of the American Society for Bone and Mineral Research,* 16**,** 1622-33.

KATO, Y., WINDLE, J. J., KOOP, B. A., MUNDY, G. R. & BONEWALD, L. F. (1997) Establishment of an osteocyte-like cell line, MLO-Y4. *Journal of bone and mineral research : the official journal of the American Society for Bone and Mineral Research,* 12**,** 2014-23.

KHAN, S. A., KANIS, J. A., VASIKARAN, S., KLINE, W. F., MATUSZEWSKI, B. K., MCCLOSKEY, E. V., BENETON, M. N., GERTZ, B. J., SCIBERRAS, D. G., HOLLAND, S. D., ORGEE, J., COOMBES, G. M., ROGERS, S. R. & PORRAS, A. G. (1997) Elimination and biochemical responses to intravenous alendronate in postmenopausal osteoporosis. *J Bone Miner Res,* 12**,** 1700-7.

KITASE, Y., BARRAGAN, L., QING, H., KONDOH, S., JIANG, J. X., JOHNSON, M. L. & BONEWALD, L. F. (2010) Mechanical induction of PGE2 in osteocytes blocks glucocorticoid-induced apoptosis through both the beta-catenin and PKA pathways. *Journal of bone and mineral research : the official journal of the American Society for Bone and Mineral Research,* 25**,** 2657-68.

KLEIN-NULEND, J., BAKKER, A. D., BACABAC, R. G., VATSA, A. & WEINBAUM, S. (2013) Mechanosensation and transduction in osteocytes. *Bone,* 54**,** 182-90.

KLEIN-NULEND, J., HELFRICH, M. H., STERCK, J. G., MACPHERSON, H., JOLDERSMA, M., RALSTON, S. H., SEMEINS, C. M. & BURGER, E. H. (1998) Nitric oxide response to shear stress by human bone cell cultures is endothelial nitric oxide synthase dependent. *Biochem Biophys Res Commun,* 250**,** 108-14.

KLEIN-NULEND, J., ROELOFSEN, J., STERCK, J. G., SEMEINS, C. M. & BURGER, E. H. (1995a) Mechanical loading stimulates the release of transforming growth factor-beta activity by cultured mouse calvariae and periosteal cells. *J Cell Physiol,* 163**,** 115-9.

KLEIN-NULEND, J., SEMEINS, C. M., AJUBI, N. E., NIJWEIDE, P. J. & BURGER, E. H. (1995b) Pulsating fluid flow increases nitric oxide (NO) synthesis by osteocytes but not periosteal fibroblasts--correlation with prostaglandin upregulation. *Biochemical and biophysical research communications,* 217**,** 640-8.

KLEIN-NULEND, J., VAN DER PLAS, A., SEMEINS, C. M., AJUBI, N. E., FRANGOS, J. A., NIJWEIDE, P. J. & BURGER, E. H. (1995b) Sensitivity of osteocytes to biomechanical stress in vitro. *FASEB J,* 9**,** 441-5.

KLEIN-NULEND, J., VAN DER PLAS, A., SEMEINS, C. M., AJUBI, N. E., FRANGOS, J. A., NIJWEIDE, P. J. & BURGER, E. H. (1995a) Sensitivity of osteocytes to biomechanical stress in vitro. *The FASEB journal : official publication of the Federation of American Societies for Experimental Biology,* 9**,** 441-5.

KNOTHE TATE, M. L., ADAMSON, J. R., TAMI, A. E. & BAUER, T. W. (2004) The osteocyte. *Int J Biochem Cell Biol,* 36**,** 1-8.

KOBAYASHI, S., TAKAHASHI, H. E., ITO, A., SAITO, N., NAWATA, M., HORIUCHI, H., OHTA, H., ITO, A., IORIO, R., YAMAMOTO, N. & TAKAOKA, K. (2003) Trabecular minimodeling in human iliac bone. *Bone,* 32**,** 163-9.

KODAMA, H., YAMASAKI, A., NOSE, M., NIIDA, S., OHGAME, Y., ABE, M., KUMEGAWA, M. & SUDA, T. (1991) Congenital osteoclast deficiency in osteopetrotic (op/op) mice is cured by injections of macrophage colony-stimulating factor. *J Exp Med,* 173**,** 269-72.

KOMORI, T. (2010) Regulation of osteoblast differentiation by Runx2. *Advances in experimental medicine and biology,* 658**,** 43-9.

KOMORI, T., YAGI, H., NOMURA, S., YAMAGUCHI, A., SASAKI, K., DEGUCHI, K., SHIMIZU, Y., BRONSON, R. T., GAO, Y. H., INADA, M., SATO, M., OKAMOTO, R., KITAMURA, Y., YOSHIKI, S. & KISHIMOTO, T. (1997) Targeted disruption of Cbfa1 results in a complete lack of bone formation owing to maturational arrest of osteoblasts. *Cell,* 89**,** 755-64.

KONTULAINEN, S., SIEVANEN, H., KANNUS, P., PASANEN, M. & VUORI, I. (2003) Effect of long-term impact-loading on mass, size, and estimated strength of humerus and radius of female racquet-sports players: a peripheral quantitative computed tomography study between young and old starters and controls. *J Bone Miner Res,* 18**,** 352-9.

KOZLOWSKI, M., GAJEWSKA, M., MAJEWSKA, A., JANK, M. & MOTYL, T. (2009) Differences in growth and transcriptomic profile of bovine mammary epithelial monolayer and three-dimensional cell cultures. *J Physiol Pharmacol,* 60 Suppl 1**,** 5-14.

KREMPIEN, B., LEMMINGER, F. M., RITZ, E. & WEBER, E. (1978) The reactionof different skeletal sites to metabolic bone disease – a micromorphometric study. *Klinische Wochenschrift,* 56**,** 755-759.

KRUM, S. A., MIRANDA-CARBONI, G. A., HAUSCHKA, P. V., CARROLL, J. S., LANE, T. F., FREEDMAN, L. P. & BROWN, M. (2008) Estrogen

protects bone by inducing Fas ligand in osteoblasts to regulate osteoclast survival. *Embo Journal,* 27**,** 535-545.

KULKARNI, R. N., BAKKER, A. D., EVERTS, V. & KLEIN-NULEND, J. (2010) Inhibition of osteoclastogenesis by mechanically loaded osteocytes: involvement of MEPE. *Calcif Tissue Int,* 87**,** 461-8.

KULKARNI, R. N., BAKKER, A. D., GRUBER, E. V., CHAE, T. D., VELDKAMP, J. B., KLEIN-NULEND, J. & EVERTS, V. (2012) MT1-MMP modulates the mechanosensitivity of osteocytes. *Biochem Biophys Res Commun,* 417**,** 824-9.

KURATA, K., HEINO, T. J., HIGAKI, H. & VAANANEN, H. K. (2006) Bone marrow cell differentiation induced by mechanically damaged osteocytes in 3D gel-embedded culture. *Journal of bone and mineral research : the official journal of the American Society for Bone and Mineral Research,* 21**,** 616-25.

LACEY, D. L., TIMMS, E., TAN, H. L., KELLEY, M. J., DUNSTAN, C. R., BURGESS, T., ELLIOTT, R., COLOMBERO, A., ELLIOTT, G., SCULLY, S., HSU, H., SULLIVAN, J., HAWKINS, N., DAVY, E., CAPPARELLI, C., ELI, A., QIAN, Y. X., KAUFMAN, S., SAROSI, I., SHALHOUB, V., SENALDI, G., GUO, J., DELANEY, J. & BOYLE, W. J. (1998) Osteoprotegerin ligand is a cytokine that regulates osteoclast differentiation and activation. *Cell,* 93**,** 165-76.

LAM, F. F. & NG, E. S. (2010) Substance P and glutamate receptor antagonists improve the anti-arthritic actions of dexamethasone in rats. *Br J Pharmacol,* 159**,** 958-69.

LAMBERS, F. M., SCHULTE, F. A., KUHN, G., WEBSTER, D. J. & MULLER, R. (2011) Mouse tail vertebrae adapt to cyclic mechanical loading by increasing bone formation rate and decreasing bone resorption rate as shown by time-lapsed in vivo imaging of dynamic bone morphometry. *Bone,* 49**,** 1340-50.

LANDIS, W. J. (1995) The strength of a calcified tissue depends in part on the molecular structure and organization of its constituent mineral crystals in their organic matrix. *Bone,* 16**,** 533-44.

LANGSTON, A. L., CAMPBELL, M. K., FRASER, W. D., MACLENNAN, G., SELBY, P. & RALSTON, S. H. (2007) Clinical determinants of quality of life in Paget's disease of bone. *Calcif Tissue Int,* 80**,** 1-9.

LANYON, L. E. (1973) Analysis of surface bone strain in the calcaneus of sheep during normal locomotion. Strain analysis of the calcaneus. *Journal of biomechanics,* 6**,** 41-9.

LANYON, L. E. (1993) Osteocytes, strain detection, bone modeling and remodeling. *Calcif Tissue Int,* 53 Suppl 1**,** S102-6; discussion S106-7.

LANYON, L. E., HAMPSON, W. G., GOODSHIP, A. E. & SHAH, J. S. (1975) Bone deformation recorded in vivo from strain gauges attached to the human tibial shaft. *Acta orthopaedica Scandinavica,* 46**,** 256-68.

LANYON, L. E. & RUBIN, C. T. (1984) Static vs dynamic loads as an influence on bone remodelling. *J Biomech,* 17**,** 897-905.

LANYON, L. E., RUBIN, C. T. & BAUST, G. (1986) Modulation of bone loss during calcium insufficiency by controlled dynamic loading. *Calcif Tissue Int,* 38**,** 209-16.

LANYON, L. E. & SMITH, R. N. (1970) Bone strain in the tibia during normal quadrupedal locomotion. *Acta Orthop Scand,* 41**,** 238-48.

LAURIN, N., BROWN, J. P., MORISSETTE, J. & RAYMOND, V. (2002) Recurrent mutation of the gene encoding sequestosome 1 (SQSTM1/p62) in Paget disease of bone. *Am J Hum Genet,* 70**,** 1582-8.

LAVANDERO, S., CARTAGENA, G., GUARDA, E., CORBALAN, R., GODOY, I., SAPAG-HAGAR, M. & JALIL, J. E. (1993) Changes in cyclic AMP dependent protein kinase and active stiffness in the rat volume overload model of heart hypertrophy. *Cardiovasc Res,* 27**,** 1634-8.

LEAFFER, D., SWEENEY, M., KELLERMAN, L. A., AVNUR, Z., KRSTENANSKY, J. L., VICKERY, B. H. & CAULFIELD, J. P. (1995) Modulation of osteogenic cell ultrastructure by RS-23581, an analog of human parathyroid hormone (PTH)-related peptide-(1-34), and bovine PTH-(1-34). *Endocrinology,* 136**,** 3624-31.

LECANDA, F., WARLOW, P. M., SHEIKH, S., FURLAN, F., STEINBERG, T. H. & CIVITELLI, R. (2000) Connexin43 deficiency causes delayed ossification, craniofacial abnormalities, and osteoblast dysfunction. *J Cell Biol,* 151**,** 931-44.

LERNER, U. H., SAHLBERG, K. & FREDHOLM, B. B. (1987) Characterization of adenosine receptors in bone. Studies on the effect of adenosine analogues on cyclic AMP formation and bone resorption in cultured mouse calvaria. *Acta Physiol Scand,* 131**,** 287-96.

LEUSHNER, J. R. (1983) Heterogeneity in the collagens extracted from human embryonic calvaria. *Canadian journal of biochemistry and cell biology = Revue canadienne de biochimie et biologie cellulaire,* 61**,** 1012-7.

LI, C. Y., PRICE, C., DELISSER, K., NASSER, P., LAUDIER, D., CLEMENT, M., JEPSEN, K. J. & SCHAFFLER, M. B. (2005a) Long-term disuse osteoporosis seems less sensitive to bisphosphonate treatment than other osteoporosis. *J Bone Miner Res,* 20**,** 117-24.

LI, J., LIU, D., KE, H. Z., DUNCAN, R. L. & TURNER, C. H. (2005b) The P2X7 nucleotide receptor mediates skeletal mechanotransduction. *J Biol Chem,* 280**,** 42952-9.

LI, J., ROSE, E., FRANCES, D., SUN, Y. & YOU, L. (2012a) Effect of oscillating fluid flow stimulation on osteocyte mRNA expression. *Journal of Biomechanics,* 45**,** 247-251.

LI, L., YANG, Z., ZHANG, H., CHEN, W., CHEN, M. & ZHU, Z. (2012b) Low-intensity pulsed ultrasound regulates proliferation and differentiation of osteoblasts through osteocytes. *Biochem Biophys Res Commun,* 418**,** 296-300.

LI, P., SCHWARZ, E. M., O'KEEFE, R. J., MA, L., BOYCE, B. F. & XING, L. (2004a) RANK signaling is not required for TNFalpha-mediated increase in CD11(hi) osteoclast precursors but is essential for mature osteoclast formation in TNFalpha-mediated inflammatory arthritis. *J Bone Miner Res,* 19**,** 207-13.

LI, X., LIU, P., LIU, W., MAYE, P., ZHANG, J., ZHANG, Y., HURLEY, M., GUO, C., BOSKEY, A., SUN, L., HARRIS, S. E., ROWE, D. W., KE, H. Z. & WU, D. (2005c) Dkk2 has a role in terminal osteoblast differentiation and mineralized matrix formation. *Nat Genet,* 37**,** 945-52.

LI, X., OMINSKY, M. S., NIU, Q. T., SUN, N., DAUGHERTY, B., D'AGOSTIN, D., KURAHARA, C., GAO, Y., CAO, J., GONG, J., ASUNCION, F., BARRERO, M., WARMINGTON, K., DWYER, D., STOLINA, M., MORONY, S., SAROSI, I., KOSTENUIK, P. J., LACEY, D. L., SIMONET,

W. S., KE, H. Z. & PASZTY, C. (2008) Targeted deletion of the sclerostin gene in mice results in increased bone formation and bone strength. *Journal of bone and mineral research : the official journal of the American Society for Bone and Mineral Research,* 23**,** 860-9.

LI, X., OMINSKY, M. S., WARMINGTON, K. S., MORONY, S., GONG, J., CAO, J., GAO, Y., SHALHOUB, V., TIPTON, B., HALDANKAR, R., CHEN, Q., WINTERS, A., BOONE, T., GENG, Z., NIU, Q. T., KE, H. Z., KOSTENUIK, P. J., SIMONET, W. S., LACEY, D. L. & PASZTY, C. (2009) Sclerostin antibody treatment increases bone formation, bone mass, and bone strength in a rat model of postmenopausal osteoporosis. *Journal of bone and mineral research : the official journal of the American Society for Bone and Mineral Research,* 24**,** 578-88.

LI, X., PILBEAM, C. C., PAN, L., BREYER, R. M. & RAISZ, L. G. (2002) Effects of prostaglandin E2 on gene expression in primary osteoblastic cells from prostaglandin receptor knockout mice. *Bone,* 30**,** 567-73.

LI, X., ZHANG, X. L., SHEN, G. & TANG, G. H. (2012c) Effects of tensile forces on serum deprivation-induced osteoblast apoptosis: expression analysis of caspases, Bcl-2, and Bax. *Chinese medical journal,* 125**,** 2568-73.

LI, Y. J., BATRA, N. N., YOU, L., MEIER, S. C., COE, I. A., YELLOWLEY, C. E. & JACOBS, C. R. (2004b) Oscillatory fluid flow affects human marrow stromal cell proliferation and differentiation. *Journal of orthopaedic research : official publication of the Orthopaedic Research Society,* 22**,** 1283-9.

LIAN, J. B., STEIN, G. S., CANALIS, E., ROBEY, P. G. & BOSKEY, A. L. (1999) Bone formation: osteoblast lineage cells, growth factors, matrix proteins and the mineralization process. *Primer on the metabolic bone diseases and disorders of mineral metabolism.* Philadelphia, American Society for Bone and Mineral Research.

LIEGIBEL, U. M., SOMMER, U., BUNDSCHUH, B., SCHWEIZER, B., HILSCHER, U., LIEDER, A., NAWROTH, P. & KASPERK, C. (2004) Fluid shear of low magnitude increases growth and expression of TGFbeta1 and adhesion molecules in human bone cells in vitro. *Experimental and clinical endocrinology & diabetes : official journal, German Society of Endocrinology [and] German Diabetes Association,* 112**,** 356-63.

LIN, J. H. (1996) Bisphosphonates: a review of their pharmacokinetic properties. *Bone,* 18**,** 75-85.

LIN, T.-H., YANG, R.-S., TANG, C.-H., WU, M.-Y. & FU, W.-M. (2008) Regulation of the maturation of osteoblasts and osteoclastogenesis by glutamate. *European journal of pharmacology,* 589**,** 37-44.

LINDSAY, R., COSMAN, F., ZHOU, H., BOSTROM, M. P., SHEN, V. W., CRUZ, J. D., NIEVES, J. W. & DEMPSTER, D. W. (2006) A Novel Tetracycline Labeling Schedule for Longitudinal Evaluation of the Short-Term Effects of Anabolic Therapy With a Single Iliac Crest Bone Biopsy: Early Actions of Teriparatide. *Journal of Bone and Mineral Research,* 21**,** 366-373.

LITZENBERGER, J. B., KIM, J. B., TUMMALA, P. & JACOBS, C. R. (2010) Beta1 integrins mediate mechanosensitive signaling pathways in osteocytes. *Calcif Tissue Int,* 86**,** 325-32.

LIU, C., ZHAO, Y., CHEUNG, W. Y., GANDHI, R., WANG, L. & YOU, L. (2010) Effects of cyclic hydraulic pressure on osteocytes. *Bone,* 46**,** 1449-56.

LIU, D., GENETOS, D. C., SHAO, Y., GEIST, D. J., LI, J., KE, H. Z., TURNER, C. H. & DUNCAN, R. L. (2008) Activation of extracellular-signal regulated

kinase (ERK1/2) by fluid shear is Ca(2+)- and ATP-dependent in MC3T3-E1 osteoblasts. *Bone,* 42**,** 644-52.

LIU, X., ZHANG, X. & LUO, Z. P. (2005) Strain-related collagen gene expression in human osteoblast-like cells. *Cell Tissue Res,* 322**,** 331-4.

LIVAK, K. J. & SCHMITTGEN, T. D. (2001) Analysis of relative gene expression data using real-time quantitative PCR and the 2(-Delta Delta C(T)) Method. *Methods,* 25**,** 402-8.

LOOTS, G. G., KNEISSEL, M., KELLER, H., BAPTIST, M., CHANG, J., COLLETTE, N. M., OVCHARENKO, D., PLAJZER-FRICK, I. & RUBIN, E. M. (2005) Genomic deletion of a long-range bone enhancer misregulates sclerostin in Van Buchem disease. *Genome Res,* 15**,** 928-35.

LOWIK, C. W. & VAN BEZOOIJEN, R. L. (2006) Wnt signaling is involved in the inhibitory action of sclerostin on BMP-stimulated bone formation. *J Musculoskelet Neuronal Interact,* 6**,** 357.

LU, H. F., MAI, Z. H., XU, Y., WANG, W. & AI, H. (2012) Mechanical loading induced expression of bone morphogenetic protein-2, alkaline phosphatase activity, and collagen synthesis in osteoblastic MC3T3-E1 cells. *Chin Med J (Engl),* 125**,** 4093-7.

MA, W., ZHANG, X., SHI, S. & ZHANG, Y. (2013) Neuropeptides stimulate human osteoblast activity and promote gap junctional intercellular communication. *Neuropeptides,* 47**,** 179-86.

MACIONE, J., KAVUKCUOGLU, N. B., NESBITT, R. S. A., MANN, A. B., GUZELSU, N. & KOTHA, S. P. (2011) Hierarchies of damage induced loss of mechanical properties in calcified bone after in vivo fatigue loading of rat ulnae. *Journal of the mechanical behavior of biomedical materials,* 4**,** 841-848.

MAENO, S., NIKI, Y., MATSUMOTO, H., MORIOKA, H., YATABE, T., FUNAYAMA, A., TOYAMA, Y., TAGUCHI, T. & TANAKA, J. (2005) The effect of calcium ion concentration on osteoblast viability, proliferation and differentiation in monolayer and 3D culture. *Biomaterials,* 26**,** 4847-55.

MAES, C. (2013) Role and regulation of vascularization processes in endochondral bones. *Calcif Tissue Int,* 92**,** 307-23.

MALONE, A. M., ANDERSON, C. T., STEARNS, T. & JACOBS, C. R. (2007) Primary cilia in bone. *J Musculoskelet Neuronal Interact,* 7**,** 301.

MANN, V., HUBER, C., KOGIANNI, G., COLLINS, F. & NOBLE, B. (2007) The antioxidant effect of estrogen and Selective Estrogen Receptor Modulators in the inhibition of osteocyte apoptosis in vitro. *Bone,* 40**,** 674-684.

MANTILA ROOSA, S. M., LIU, Y. & TURNER, C. H. (2011) Gene expression patterns in bone following mechanical loading. *J Bone Miner Res,* 26**,** 100-12.

MARIE, P. J. (2007) Strontium ranelate: New insights into its dual mode of action. *Bone,* 40**,** S5-S8.

MARTIN, R. B. (1991) Determinants of the mechanical properties of bones. *J Biomech,* 24 Suppl 1**,** 79-88.

MARTIN, R. B. & BURR, D. B. (1989) *Structure, function, and adaptation of compact bone,* Raven Press.

MARTINI, F. H., NATH, J. L. & BARTHOLOMEW, E. F. (2011) *Fundamentals of Anatomy and Physiology*, Pearson Education, Limited.

MARX, R. E. (2003) Pamidronate (Aredia) and zoledronate (Zometa) induced avascular necrosis of the jaws: a growing epidemic. *J Oral Maxillofac Surg,* 61**,** 1115-7.

MARX, R. E., SAWATARI, Y., FORTIN, M. & BROUMAND, V. (2005) Bisphosphonate-induced exposed bone (osteonecrosis/osteopetrosis) of the jaws: risk factors, recognition, prevention, and treatment. *J Oral Maxillofac Surg,* 63**,** 1567-75.

MASON D., D. C., EVANS B., BRAKSPEAR K., WILLIAMS S., JAEHN K., RALPHS J. (2009) Interactions between osteocytes and osteoblasts in a novel 3D co-culture system. *Bio reconstruction de l'os a la peau.* Universite de Franche Comte, Saraumps Medical.

MASON, D. J. (2004) Glutamate signalling and its potential application to tissue engineering of bone. *Eur Cell Mater,* 7**,** 12-25; discussion 25-6.

MASON, D. J., DILLINGHAM, C. H., WILLIAMS, S., EVANS, B., BRAKSPEAR, K. & RALPHS, J. (2009) Interactions between osteocytes and osteoblasts in a novel 3D co-culture system. *International Journal of Experimental Pathology,* 90**,** A104-A104.

MASON, D. J., EVANS, B. A. J., BURLEIGH, A., DUGGAN, K., LORRAINE, O., PEXA, A., DEUSSEN, A. & HAM, J. (2006) Do adenosine and glutamate-mediated signalling pathways interact in osteoblasts and osteocytes? *Bone,* 38**,** 15-16.

MASON, D. J., HILLAM, R. A. & SKERRY, T. M. (1996) Constitutive in vivo mRNA expression by osteocytes of beta-actin, osteocalcin, connexin-43, IGF-I, c-fos and c-jun, but not TNF-alpha nor tartrate-resistant acid phosphatase. *Journal of bone and mineral research : the official journal of the American Society for Bone and Mineral Research,* 11**,** 350-7.

MASON, D. J., SUVA, L. J., GENEVER, P. G., PATTON, A. J., STEUCKLE, S., HILLAM, R. A. & SKERRY, T. M. (1997) Mechanically regulated expression of a neural glutamate transporter in bone: a role for excitatory amino acids as osteotropic agents? *Bone,* 20**,** 199-205.

MASU, M., TANABE, Y., TSUCHIDA, K., SHIGEMOTO, R. & NAKANISHI, S. (1991) Sequence and expression of a metabotropic glutamate receptor. *Nature,* 349**,** 760-5.

MATSUO, K. & IRIE, N. (2008) Osteoclast-osteoblast communication. *Archives of biochemistry and biophysics,* 473**,** 201-9.

MATTINZOLI, D., EVANS, B. A. J., ELFORD, C., RASALDI, M. P., MESSA, P. G., MASON, D. & RICCARDI, D. (2009) World Congress of Nephrology. Cell signalling and cell growth control - 2: Metabolic signals regulate cell proliferation and production of interleukin 6 (IL-6) in the osteocyte-like cell line, MLO-Y4. *NDT Plus,* 2**,** ii1.

MAZZON, E., ESPOSITO, E., IMPELLIZZERI, D., R, D. I. P., MELANI, A., BRAMANTI, P., PEDATA, F. & CUZZOCREA, S. (2011) CGS 21680, an agonist of the adenosine (A2A) receptor, reduces progression of murine type II collagen-induced arthritis. *J Rheumatol,* 38**,** 2119-29.

MCALLISTER, T. N. & FRANGOS, J. A. (1999) Steady and transient fluid shear stress stimulate NO release in osteoblasts through distinct biochemical pathways. *J Bone Miner Res,* 14**,** 930-6.

MCCLUNG, M. R., LEWIECKI, E. M., COHEN, S. B., BOLOGNESE, M. A., WOODSON, G. C., MOFFETT, A. H., PEACOCK, M., MILLER, P. D., LEDERMAN, S. N., CHESNUT, C. H., LAIN, D., KIVITZ, A. J.,

HOLLOWAY, D. L., ZHANG, C., PETERSON, M. C. & BEKKER, P. J. (2006) Denosumab in postmenopausal women with low bone mineral density. *N Engl J Med,* 354**,** 821-31.

MCENTEE, W. J. & CROOK, T. H. (1993) Glutamate: its role in learning, memory, and the aging brain. *Psychopharmacology (Berl),* 111**,** 391-401.

MCGARRY, J. G., KLEIN-NULEND, J. & PRENDERGAST, P. J. (2005) The effect of cytoskeletal disruption on pulsatile fluid flow-induced nitric oxide and prostaglandin E2 release in osteocytes and osteoblasts. *Biochem Biophys Res Commun,* 330**,** 341-8.

MCINNES, I. B. & SCHETT, G. (2011) The Pathogenesis of Rheumatoid Arthritis. *New England Journal of Medicine,* 365**,** 2205-2219.

MCNEARNEY, T., BAETHGE, B. A., CAO, S., ALAM, R., LISSE, J. R. & WESTLUND, K. N. (2004) Excitatory amino acids, TNF-alpha, and chemokine levels in synovial fluids of patients with active arthropathies. *Clin Exp Immunol,* 137**,** 621-7.

MCNEARNEY, T., SPEEGLE, D., LAWAND, N., LISSE, J. & WESTLUND, K. N. (2000) Excitatory amino acid profiles of synovial fluid from patients with arthritis. *J Rheumatol,* 27**,** 739-45.

MEDIERO, A. & CRONSTEIN, B. N. (2013) Adenosine and bone metabolism. *Trends Endocrinol Metab.*

MEDIERO, A., KARA, F. M., WILDER, T. & CRONSTEIN, B. N. (2012) Adenosine A(2A) receptor ligation inhibits osteoclast formation. *Am J Pathol,* 180**,** 775-86.

MENG, Y., QIN, Y. X., DIMASI, E., BA, X., RAFAILOVICH, M. & PERNODET, N. (2009) Biomineralization of a self-assembled extracellular matrix for bone tissue engineering. *Tissue Eng Part A,* 15**,** 355-66.

MENTAVERRI, R., KAMEL, S., WATTEL, A., PROUILLET, C., SEVENET, N., PETIT, J. P., TORDJMANN, T. & BRAZIER, M. (2003) Regulation of bone resorption and osteoclast survival by nitric oxide: possible involvement of NMDA-receptor. *Journal of cellular biochemistry,* 88**,** 1145-56.

MENTAVERRI, R., YANO, S., CHATTOPADHYAY, N., PETIT, L., KIFOR, O., KAMEL, S., TERWILLIGER, E. F., BRAZIER, M. & BROWN, E. M. (2006) The calcium sensing receptor is directly involved in both osteoclast differentiation and apoptosis. *The FASEB journal : official publication of the Federation of American Societies for Experimental Biology,* 20**,** 2562-4.

MENTON, D. N., SIMMONS, D. J., CHANG, S. L. & ORR, B. Y. (1984) From bone lining cell to osteocyte--an SEM study. *The Anatomical record,* 209**,** 29-39.

MERLOTTI, D., GENNARI, L., GALLI, B., MARTINI, G., CALABRO, A., DE PAOLA, V., CECCARELLI, E., NARDI, P., AVANZATI, A. & NUTI, R. (2005) Characteristics and familial aggregation of Paget's disease of bone in Italy. *J Bone Miner Res,* 20**,** 1356-64.

MIKUNI-TAKAGAKI, Y., KAKAI, Y., SATOYOSHI, M., KAWANO, E., SUZUKI, Y., KAWASE, T. & SAITO, S. (1995) Matrix mineralization and the differentiation of osteocyte-like cells in culture. *J Bone Miner Res,* 10**,** 231-42.

MILES, R. R., TURNER, C. H., SANTERRE, R., TU, Y., MCCLELLAND, P., ARGOT, J., DEHOFF, B. S., MUNDY, C. W., ROSTECK, P. R., JR., BIDWELL, J., SLUKA, J. P., HOCK, J. & ONYIA, J. E. (1998) Analysis of differential gene expression in rat tibia after an osteogenic stimulus in vivo:

mechanical loading regulates osteopontin and myeloperoxidase. *Journal of cellular biochemistry,* 68**,** 355-65.

MILLER, S. C., DE SAINT-GEORGES, L., BOWMAN, B. M. & JEE, W. S. (1989) Bone lining cells: structure and function. *Scanning Microsc,* 3**,** 953-60; discussion 960-1.

MILLS, B. G., SINGER, F. R., WEINER, L. P., SUFFIN, S. C., STABILE, E. & HOLST, P. (1984) Evidence for both respiratory syncytial virus and measles virus antigens in the osteoclasts of patients with Paget's disease of bone. *Clin Orthop Relat Res***,** 303-11.

MIZUNO, A., AMIZUKA, N., IRIE, K., MURAKAMI, A., FUJISE, N., KANNO, T., SATO, Y., NAKAGAWA, N., YASUDA, H., MOCHIZUKI, S., GOMIBUCHI, T., YANO, K., SHIMA, N., WASHIDA, N., TSUDA, E., MORINAGA, T., HIGASHIO, K. & OZAWA, H. (1998) Severe osteoporosis in mice lacking osteoclastogenesis inhibitory factor/osteoprotegerin. *Biochem Biophys Res Commun,* 247**,** 610-5.

MOLOSTVOV, G., JAMES, S., FLETCHER, S., BENNETT, J., LEHNERT, H., BLAND, R. & ZEHNDER, D. (2007) Extracellular calcium-sensing receptor is functionally expressed in human artery. *Am J Physiol Renal Physiol,* 293**,** F946-55.

MORALES-PIGA, A. A., REY-REY, J. S., CORRES-GONZALEZ, J., GARCIA-SAGREDO, J. M. & LOPEZ-ABENTE, G. (1995) Frequency and characteristics of familial aggregation of Paget's disease of bone. *J Bone Miner Res,* 10**,** 663-70.

MOREAU, M., RIALLAND, P., PELLETIER, J.-P., MARTEL-PELLETIER, J., LAJEUNESSE, D., BOILEAU, C., CARON, J., FRANK, D., LUSSIER, B., DEL CASTILLO, J., BEAUCHAMP, G., GAUVIN, D., BERTAIM, T., THIBAUD, D. & TRONCY, E. (2011) Tiludronate treatment improves structural changes and symptoms of osteoarthritis in the canine anterior cruciate ligament model. *Arthritis Research & Therapy,* 13**,** R98.

MOREY-HOLTON, E. R. & GLOBUS, R. K. (1998) Hindlimb Unloading of Growing Rats: A Model for Predicting Skeletal Changes During Space Flight. *Bone,* 22**,** 83S-88S.

MORIMOTO, R., UEHARA, S., YATSUSHIRO, S., JUGE, N., HUA, Z., SENOH, S., ECHIGO, N., HAYASHI, M., MIZOGUCHI, T., NINOMIYA, T., UDAGAWA, N., OMOTE, H., YAMAMOTO, A., EDWARDS, R. H. & MORIYAMA, Y. (2006) Secretion of L-glutamate from osteoclasts through transcytosis. *The EMBO journal,* 25**,** 4175-86.

MORNET, E., STURA, E., LIA-BALDINI, A. S., STIGBRAND, T., MENEZ, A. & LE DU, M. H. (2001) Structural evidence for a functional role of human tissue nonspecific alkaline phosphatase in bone mineralization. *J Biol Chem,* 276**,** 31171-8.

MOSLEY, J. R. & LANYON, L. E. (1998) Strain rate as a controlling influence on adaptive modeling in response to dynamic loading of the ulna in growing male rats. *Bone,* 23**,** 313-8.

MULARI, M. T., ZHAO, H., LAKKAKORPI, P. T. & VAANANEN, H. K. (2003) Osteoclast ruffled border has distinct subdomains for secretion and degraded matrix uptake. *Traffic,* 4**,** 113-25.

MULLENDER, M., EL HAJ, A. J., YANG, Y., VAN DUIN, M. A., BURGER, E. H. & KLEIN-NULEND, J. (2004) Mechanotransduction of bone cells in vitro:

mechanobiology of bone tissue. *Medical & biological engineering & computing,* 42**,** 14-21.

MULLENDER, M. G. & HUISKES, R. (1997) Osteocytes and bone lining cells: which are the best candidates for mechano-sensors in cancellous bone? *Bone,* 20**,** 527-32.

MULLENDER, M. G., VAN DER MEER, D. D., HUISKES, R. & LIPS, P. (1996) Osteocyte density changes in aging and osteoporosis. *Bone,* 18**,** 109-13.

MURSHID, S. A., KAMIOKA, H., ISHIHARA, Y., ANDO, R., SUGAWARA, Y. & TAKANO-YAMAMOTO, T. (2007) Actin and microtubule cytoskeletons of the processes of 3D-cultured MC3T3-E1 cells and osteocytes. *Journal of bone and mineral metabolism,* 25**,** 151-8.

NAKAGAWA, K., ABUKAWA, H., SHIN, M. Y., TERAI, H., TROULIS, M. J. & VACANTI, J. P. (2004) Osteoclastogenesis on tissue-engineered bone. *Tissue engineering,* 10**,** 93-100.

NAKAGAWA, N., KINOSAKI, M., YAMAGUCHI, K., SHIMA, N., YASUDA, H., YANO, K., MORINAGA, T. & HIGASHIO, K. (1998) RANK is the essential signaling receptor for osteoclast differentiation factor in osteoclastogenesis. *Biochem Biophys Res Commun,* 253**,** 395-400.

NAKAMURA, H. (2007) Morphology, Function, and Differentiation of Bone Cells. *Journal of hard tissue biology,* 16**,** 15-22.

NAKAMURA, T., IMAI, Y., MATSUMOTO, T., SATO, S., TAKEUCHI, K., IGARASHI, K., HARADA, Y., AZUMA, Y., KRUST, A., YAMAMOTO, Y., NISHINA, H., TAKEDA, S., TAKAYANAGI, H., METZGER, D., KANNO, J., TAKAOKA, K., MARTIN, T. J., CHAMBON, P. & KATO, S. (2007) Estrogen prevents bone loss via estrogen receptor alpha and induction of Fas ligand in osteoclasts. *Cell,* 130**,** 811-823.

NAKANISHI, S. (1998) [Glutamate receptors and brain function]. *Seikagaku,* 70**,** 1145-58.

NAKASHIMA, K., ZHOU, X., KUNKEL, G., ZHANG, Z., DENG, J. M., BEHRINGER, R. R. & DE CROMBRUGGHE, B. (2002) The novel zinc finger-containing transcription factor osterix is required for osteoblast differentiation and bone formation. *Cell,* 108**,** 17-29.

NAKASHIMA, T., HAYASHI, M., FUKUNAGA, T., KURATA, K., OH-HORA, M., FENG, J. Q., BONEWALD, L. F., KODAMA, T., WUTZ, A., WAGNER, E. F., PENNINGER, J. M. & TAKAYANAGI, H. (2011) Evidence for osteocyte regulation of bone homeostasis through RANKL expression. *Nat Med,* 17**,** 1231-4.

NAUMAN, E. A., SATCHER, R. L., KEAVENY, T. M., HALLORAN, B. P. & BIKLE, D. D. (2001) Osteoblasts respond to pulsatile fluid flow with short-term increases in PGE2 but no change in mineralization. *Journal of Applied Physiology,* 90**,** 1849-1854.

NEER, R. M., ARNAUD, C. D., ZANCHETTA, J. R., PRINCE, R., GAICH, G. A., REGINSTER, J. Y., HODSMAN, A. B., ERIKSEN, E. F., ISH-SHALOM, S., GENANT, H. K., WANG, O. & MITLAK, B. H. (2001) Effect of parathyroid hormone (1-34) on fractures and bone mineral density in postmenopausal women with osteoporosis. *N Engl J Med,* 344**,** 1434-41.

NEIDLINGER-WILKE, C., WURTZ, K., LIEDERT, A., SCHMIDT, C., BORM, W., IGNATIUS, A., WILKE, H. J. & CLAES, L. (2005) A three-dimensional collagen matrix as a suitable culture system for the comparison of cyclic

strain and hydrostatic pressure effects on intervertebral disc cells. *J Neurosurg Spine,* 2**,** 457-65.

NGUYEN, A. M. & JACOBS, C. R. (2013) Emerging role of primary cilia as mechanosensors in osteocytes. *Bone,* 54**,** 196-204.

NIJWEIDE, P. J., VAN DER PLAS, A., ALBLAS, M. J. & KLEIN-NULEND, J. (2003) Osteocyte isolation and culture. *Methods in molecular medicine,* 80**,** 41-50.

NING, J., BRAXTON, V. G., WANG, Y., SUTTON, M. A., WANG, Y. & LESSNER, S. M. (2011) Speckle Patterning of Soft Tissues for Strain Field Measurement Using Digital Image Correlation: Preliminary Quality Assessment of Patterns. *Microscopy and Microanalysis,* 17**,** 81-90.

NOBLE, B. (2003) Bone microdamage and cell apoptosis. *Eur Cell Mater,* 6**,** 46-55; discusssion 55.

NOBLE, B. S., PEET, N., STEVENS, H. Y., BRABBS, A., MOSLEY, J. R., REILLY, G. C., REEVE, J., SKERRY, T. M. & LANYON, L. E. (2003) Mechanical loading: biphasic osteocyte survival and targeting of osteoclasts for bone destruction in rat cortical bone. *American Journal of Physiology - Cell Physiology,* 284**,** C934-C943.

NOBLE, B. S., STEVENS, H., LOVERIDGE, N. & REEVE, J. (1997) Identification of apoptotic changes in osteocytes in normal and pathological human bone. *Bone,* 20**,** 273-82.

NOMURA, S. & TAKANO-YAMAMOTO, T. (2000) Molecular events caused by mechanical stress in bone. *Matrix biology : journal of the International Society for Matrix Biology,* 19**,** 91-6.

NOSE, K., SAITO, H. & KUROKI, T. (1990) Isolation of a gene sequence induced later by tumor-promoting 12-O-tetradecanoylphorbol-13-acetate in mouse osteoblastic cells (MC3T3-E1) and expressed constitutively in ras-transformed cells. *Cell Growth Differ,* 1**,** 511-8.

O'CONNOR, J. A., LANYON, L. E. & MACFIE, H. (1982) The influence of strain rate on adaptive bone remodelling. *Journal of biomechanics,* 15**,** 767-781.

OGATA, T. (2003) Increase in epidermal growth factor receptor protein induced in osteoblastic cells after exposure to flow of culture media. *American journal of physiology. Cell physiology,* 285**,** C425-32.

OGATA, T., NAKAMURA, Y., TSUJI, K., SHIBATA, T., KATAOKA, K. & SCHUBERT, P. (1994) Adenosine enhances intracellular Ca2+ mobilization in conjunction with metabotropic glutamate receptor activation by t-ACPD in cultured hippocampal astrocytes. *Neurosci Lett,* 170**,** 5-8.

OTTO, F., THORNELL, A. P., CROMPTON, T., DENZEL, A., GILMOUR, K. C., ROSEWELL, I. R., STAMP, G. W., BEDDINGTON, R. S., MUNDLOS, S., OLSEN, B. R., SELBY, P. B. & OWEN, M. J. (1997) Cbfa1, a candidate gene for cleidocranial dysplasia syndrome, is essential for osteoblast differentiation and bone development. *Cell,* 89**,** 765-71.

PACIFICI, R. (1999) Aging and cytokine production. *Calcified tissue international,* 65.

PALUMBO, C. (1986) A three-dimensional ultrastructural study of osteoid-osteocytes in the tibia of chick embryos. *Cell Tissue Res,* 246**,** 125-31.

PALUMBO, C., PALAZZINI, S. & MAROTTI, G. (1990) Morphological study of intercellular junctions during osteocyte differentiation. *Bone,* 11**,** 401-6.

PAPADIMITROPOULOS, A., RIBOLDI, S. A., TONNARELLI, B., PICCININI, E., WOODRUFF, M. A., HUTMACHER, D. W. & MARTIN, I. (2011a) A

collagen network phase improves cell seeding of open-pore structure scaffolds under perfusion. *Journal of tissue engineering and regenerative medicine*.

PAPADIMITROPOULOS, A., SCHERBERICH, A., GUVEN, S., THEILGAARD, N., CROOIJMANS, H. J., SANTINI, F., SCHEFFLER, K., ZALLONE, A. & MARTIN, I. (2011b) A 3D in vitro bone organ model using human progenitor cells. *European cells & materials,* 21**,** 445-58; discussion 458.

PAPANICOLAOU, S. E., PHIPPS, R. J., FYHRIE, D. P. & GENETOS, D. C. (2009) Modulation of sclerostin expression by mechanical loading and bone morphogenetic proteins in osteogenic cells. *Biorheology,* 46**,** 389-99.

PAPAPOULOS, S. E. (2011) Targeting sclerostin as potential treatment of osteoporosis. *Annals of the rheumatic diseases,* 70**,** i119-i122.

PAPAPOULOS, S. E. & CREMERS, S. C. (2007) Prolonged bisphosphonate release after treatment in children. *N Engl J Med,* 356**,** 1075-6.

PARFITT, A. M. (1977) The cellular basis of bone turnover and bone loss: a rebuttal of the osteocytic resorption--bone flow theory. *Clinical orthopaedics and related research***,** 236-47.

PARFITT, A. M. (1983) Recent developments in bone physiology. *Henry Ford Hosp Med J,* 31**,** 209-10.

PARFITT, A. M. (1987) Bone remodeling and bone loss: understanding the pathophysiology of osteoporosis. *Clin Obstet Gynecol,* 30**,** 789-811.

PARFITT, A. M. (1994) Osteonal and hemi-osteonal remodeling: the spatial and temporal framework for signal traffic in adult human bone. *Journal of cellular biochemistry,* 55**,** 273-86.

PARFITT, A. M. (2000) The mechanism of coupling: a role for the vasculature. *Bone,* 26**,** 319-23.

PARFITT, A. M., MUNDY, G. R., ROODMAN, G. D., HUGHES, D. E. & BOYCE, B. F. (1996) A new model for the regulation of bone resorption, with particular reference to the effects of bisphosphonates. *J Bone Miner Res,* 11**,** 150-9.

PAVLIN, D., DOVE, S. B., ZADRO, R. & GLUHAK-HEINRICH, J. (2000) Mechanical loading stimulates differentiation of periodontal osteoblasts in a mouse osteoinduction model: effect on type I collagen and alkaline phosphatase genes. *Calcif Tissue Int,* 67**,** 163-72.

PAVLIN, D., ZADRO, R. & GLUHAK-HEINRICH, J. (2001) Temporal Pattern of Stimulation of Osteoblast-Associated Genes During Mechanically-Induced Osteogenesis In Vivo: Early Responses of Osteocalcin and Type I Collagen. *Connective Tissue Research,* 42**,** 135-148.

PEAD, M. J., SUSWILLO, R., SKERRY, T. M., VEDI, S. & LANYON, L. E. (1988) Increased 3H-uridine levels in osteocytes following a single short period of dynamic bone loading in vivo. *Calcif Tissue Int,* 43**,** 92-6.

PECK, R., OLSEN, C. & DEVORE, J. L. (2012) *Introduction to statistics and data analysis : infancy through adulthood,* Boston, MA, Brooks/Cole, CENGAGE Learning.

PEET, N. M., GRABOWSKI, P. S., LAKETIC-LJUBOJEVIC, I. & SKERRY, T. M. (1999) The glutamate receptor antagonist MK801 modulates bone resorption in vitro by a mechanism predominantly involving osteoclast differentiation. *The FASEB journal : official publication of the Federation of American Societies for Experimental Biology,* 13**,** 2179-85.

PELLEGATTI, P., FALZONI, S., DONVITO, G., LEMAIRE, I. & DI VIRGILIO, F. (2011) P2X7 receptor drives osteoclast fusion by increasing the extracellular adenosine concentration. *FASEB J,* 25**,** 1264-74.

PERIS, J. & DUNWIDDIE, T. V. (1985) Inhibitory neuromodulation of release of amino acid neurotransmitters. *Alcohol Drug Res,* 6**,** 253-64.

PERSSON, E. & LERNER, U. H. (2011) The neuropeptide VIP regulates the expression of osteoclastogenic factors in osteoblasts. *J Cell Biochem,* 112**,** 3732-41.

PETERS, W. H. & RANSON, W. F. (1982) Digital Imaging Techniques In Experimental Stress Analysis. *Optical Engineering,* 21**,** 213427-213427.

PETERSEN, D. N., TKALCEVIC, G. T., MANSOLF, A. L., RIVERA-GONZALEZ, R. & BROWN, T. A. (2000) Identification of osteoblast/osteocyte factor 45 (OF45), a bone-specific cDNA encoding an RGD-containing protein that is highly expressed in osteoblasts and osteocytes. *J Biol Chem,* 275**,** 36172-80.

PETTIT, A. R., JI, H., VON STECHOW, D., MULLER, R., GOLDRING, S. R., CHOI, Y., BENOIST, C. & GRAVALLESE, E. M. (2001) TRANCE/RANKL knockout mice are protected from bone erosion in a serum transfer model of arthritis. *Am J Pathol,* 159**,** 1689-99.

PHILLIS, J. W. & WU, P. H. (1981) The role of adenosine and its nucleotides in central synaptic transmission. *Prog Neurobiol,* 16**,** 187-239.

PINES, G., DANBOLT, N. C., BJORAS, M., ZHANG, Y., BENDAHAN, A., EIDE, L., KOEPSELL, H., STORM-MATHISEN, J., SEEBERG, E. & KANNER, B. I. (1992) Cloning and expression of a rat brain L-glutamate transporter. *Nature,* 360**,** 464-7.

PINTOR, A., PEZZOLA, A., REGGIO, R., QUARTA, D. & POPOLI, P. (2000) The mGlu5 receptor agonist CHPG stimulates striatal glutamate release: possible involvement of A2A receptors. *Neuroreport,* 11**,** 3611-4.

PITSILLIDES, A. A. & RAWLINSON, S. C. (2012) Using cell and organ culture models to analyze responses of bone cells to mechanical stimulation. *Methods in molecular biology,* 816**,** 593-619.

PLAITAKIS, A., BERL, S. & YAHR, M. D. (1982) Abnormal glutamate metabolism in an adult-onset degenerative neurological disorder. *Science,* 216**,** 193-196.

PLOTKIN, L. I., MANOLAGAS, S. C. & BELLIDO, T. (2002) Transduction of cell survival signals by connexin-43 hemichannels. *The Journal of biological chemistry,* 277**,** 8648-57.

PLOTKIN, L. I., MATHOV, I., AGUIRRE, J. I., PARFITT, A. M., MANOLAGAS, S. C. & BELLIDO, T. (2005) Mechanical stimulation prevents osteocyte apoptosis: requirement of integrins, Src kinases, and ERKs. *American journal of physiology. Cell physiology,* 289**,** C633-43.

POGODA, P., PRIEMEL, M., RUEGER, J. M. & AMLING, M. (2005) Bone remodeling: new aspects of a key process that controls skeletal maintenance and repair. *Osteoporosis international : a journal established as result of cooperation between the European Foundation for Osteoporosis and the National Osteoporosis Foundation of the USA,* 16 Suppl 2**,** S18-24.

PONIK, S. M. & PAVALKO, F. M. (2004) Formation of focal adhesions on fibronectin promotes fluid shear stress induction of COX-2 and PGE2 release in MC3T3-E1 osteoblasts. *Journal of Applied Physiology,* 97**,** 135-142.

POOLE, K. E., VAN BEZOOIJEN, R. L., LOVERIDGE, N., HAMERSMA, H., PAPAPOULOS, S. E., LOWIK, C. W. & REEVE, J. (2005) Sclerostin is a delayed secreted product of osteocytes that inhibits bone formation. *The FASEB journal : official publication of the Federation of American Societies for Experimental Biology,* 19**,** 1842-4.

POPOLI, P., PEZZOLA, A., TORVINEN, M., REGGIO, R., PINTOR, A., SCARCHILLI, L., FUXE, K. & FERRE, S. (2001) The selective mGlu(5) receptor agonist CHPG inhibits quinpirole-induced turning in 6-hydroxydopamine-lesioned rats and modulates the binding characteristics of dopamine D(2) receptors in the rat striatum: interactions with adenosine A(2a) receptors. *Neuropsychopharmacology,* 25**,** 505-13.

POSNER, A. S. (1987) Bone mineral and the mineralisation process. *Bone and Mineral Research***,** 65-116.

PRICE, C., ZHOU, X., LI, W. & WANG, L. (2011) Real-time measurement of solute transport within the lacunar-canalicular system of mechanically loaded bone: direct evidence for load-induced fluid flow. *Journal of bone and mineral research : the official journal of the American Society for Bone and Mineral Research,* 26**,** 277-85.

PRIDEAUX, M., LOVERIDGE, N., PITSILLIDES, A. A. & FARQUHARSON, C. (2012) Extracellular Matrix Mineralization Promotes E11/gp38 Glycoprotein Expression and Drives Osteocytic Differentiation. *PLoS ONE,* 7**,** e36786.

QI, J., CHI, L., FABER, J., KOLLER, B. & BANES, A. J. (2007) ATP reduces gel compaction in osteoblast-populated collagen gels. *Journal of applied physiology,* 102**,** 1152-60.

RADIN, E. L. & ROSE, R. M. (1986) Role of subchondral bone in the initiation and progression of cartilage damage. *Clin Orthop Relat Res***,** 34-40.

RAISZ, L. G. (1997) The osteoporosis revolution. *Ann Intern Med,* 126**,** 458-62.

RAISZ, L. G. (2005) Pathogenesis of osteoporosis: concepts, conflicts, and prospects. *J Clin Invest,* 115**,** 3318-25.

RALSTON, S. H., AFZAL, M. A., HELFRICH, M. H., FRASER, W. D., GALLAGHER, J. A., MEE, A. & RIMA, B. (2007) Multicenter blinded analysis of RT-PCR detection methods for paramyxoviruses in relation to Paget's disease of bone. *J Bone Miner Res,* 22**,** 569-77.

RALSTON, S. H. & LAYFIELD, R. (2012) Pathogenesis of Paget disease of bone. *Calcif Tissue Int,* 91**,** 97-113.

RANTAKOKKO, J., UUSITALO, H., JAMSA, T., TUUKKANEN, J., ARO, H. T. & VUORIO, E. (1999) Expression profiles of mRNAs for osteoblast and osteoclast proteins as indicators of bone loss in mouse immobilization osteopenia model. *J Bone Miner Res,* 14**,** 1934-42.

RAO, V. R. & FINKBEINER, S. (2007) NMDA and AMPA receptors: old channels, new tricks. *Trends Neurosci,* 30**,** 284-91.

RATH-WOLFSON, L., BAR-YEHUDA, S., MADI, L., OCHAION, A., COHEN, S., ZABUTTI, A. & FISHMAN, P. (2006) IB-MECA, an A3 adenosine receptor agonist prevents bone resorption in rats with adjuvant induced arthritis. *Clin Exp Rheumatol,* 24**,** 400-6.

RATH, B., NAM, J., KNOBLOCH, T. J., LANNUTTI, J. J. & AGARWAL, S. (2008) Compressive forces induce osteogenic gene expression in calvarial osteoblasts. *Journal of Biomechanics,* 41**,** 1095-1103.

RAWADI, G., VAYSSIERE, B., DUNN, F., BARON, R. & ROMAN-ROMAN, S. (2003) BMP-2 controls alkaline phosphatase expression and osteoblast mineralization by a Wnt autocrine loop. *J Bone Miner Res,* 18**,** 1842-53.

RAWLINSON, S. C. F., MOSLEY, J. R., SUSWILLO, R. F. L., PITSILLIDES, A. A. & LANYON, L. E. (1995) Calvarial and limb bone cells in organ and monolayer culture do not show the same early responses to dynamic mechanical strain. *Journal of Bone and Mineral Research,* 10**,** 1225-1232.

REDDY, S. V. (2004) Regulatory mechanisms operative in osteoclasts. *Crit Rev Eukaryot Gene Expr,* 14**,** 255-70.

REDLICH, K., HAYER, S., RICCI, R., DAVID, J. P., TOHIDAST-AKRAD, M., KOLLIAS, G., STEINER, G., SMOLEN, J. S., WAGNER, E. F. & SCHETT, G. (2002) Osteoclasts are essential for TNF-alpha-mediated joint destruction. *J Clin Invest,* 110**,** 1419-27.

REGINSTER, J. Y., BADURSKI, J., BELLAMY, N., BENSEN, W., CHAPURLAT, R., CHEVALIER, X., CHRISTIANSEN, C., GENANT, H., NAVARRO, F., NASONOV, E., SAMBROOK, P. N., SPECTOR, T. D. & COOPER, C. (2013) Efficacy and safety of strontium ranelate in the treatment of knee osteoarthritis: results of a double-blind, randomised placebo-controlled trial. *Ann Rheum Dis,* 72**,** 179-86.

REICH, K. & FRANGOS, J. (1993) Protein kinase C mediates flow-induced prostaglandin E2 production in osteoblasts. *Calcified Tissue International,* 52**,** 62-66.

REID, I. R., MILLER, P., LYLES, K., FRASER, W., BROWN, J. P., SAIDI, Y., MESENBRINK, P., SU, G., PAK, J., ZELENAKAS, K., LUCHI, M., RICHARDSON, P. & HOSKING, D. (2005) Comparison of a single infusion of zoledronic acid with risedronate for Paget's disease. *N Engl J Med,* 353**,** 898-908.

REIJNDERS, C. M., BRAVENBOER, N., HOLZMANN, P. J., BHOELAN, F., BLANKENSTEIN, M. A. & LIPS, P. (2007a) In vivo mechanical loading modulates insulin-like growth factor binding protein-2 gene expression in rat osteocytes. *Calcif Tissue Int,* 80**,** 137-43.

REIJNDERS, C. M., BRAVENBOER, N., TROMP, A. M., BLANKENSTEIN, M. A. & LIPS, P. (2007b) Effect of mechanical loading on insulin-like growth factor-I gene expression in rat tibia. *J Endocrinol,* 192**,** 131-40.

REYNOLDS, I. J. & MILLER, R. J. (1988) [3H]MK801 binding to the NMDA receptor/ionophore complex is regulated by divalent cations: evidence for multiple regulatory sites. *Eur J Pharmacol,* 151**,** 103-12.

RHEE, Y., ALLEN, M. R., CONDON, K., LEZCANO, V., RONDA, A. C., GALLI, C., OLIVOS, N., PASSERI, G., O'BRIEN, C. A., BIVI, N., PLOTKIN, L. I. & BELLIDO, T. (2011) PTH receptor signaling in osteocytes governs periosteal bone formation and intracortical remodeling. *Journal of bone and mineral research : the official journal of the American Society for Bone and Mineral Research,* 26**,** 1035-46.

RICCARDI, D. & BROWN, E. M. (2010) Physiology and pathophysiology of the calcium-sensing receptor in the kidney. *Am J Physiol Renal Physiol,* 298**,** F485-99.

RIDDLE, R. C., TAYLOR, A. F., ROGERS, J. R. & DONAHUE, H. J. (2007) ATP release mediates fluid flow-induced proliferation of human bone marrow stromal cells. *J Bone Miner Res,* 22**,** 589-600.

RIGGS, B. L., WAHNER, H. W., MELTON, L. J., 3RD, RICHELSON, L. S., JUDD, H. L. & OFFORD, K. P. (1986) Rates of bone loss in the appendicular and axial skeletons of women. Evidence of substantial vertebral bone loss before menopause. *J Clin Invest,* 77**,** 1487-91.

RIMA, B. K., GASSEN, U., HELFRICH, M. H. & RALSTON, S. H. (2002) The pro and con of measles virus in Paget's disease: con. *J Bone Miner Res,* 17**,** 2290-2; author reply 2293.

ROBEY, P. G., BIANCO, P. & TERMINE, J. D. (1992) The cellular biology and biochemistry of bone formation. *Disorders of Bone and Mineral Metabolism***,** 241-263.

ROBEY, P. G., FISHER, L. W., YOUNG, M. F. & TERMINE, J. D. (1988) The biochemistry of bone. *Osteoporosis: Etiology, Diagnosis and Management***,** 95-109.

ROBLING, A. G., BURR, D. B. & TURNER, C. H. (2000) Partitioning a daily mechanical stimulus into discrete loading bouts improves the osteogenic response to loading. *J Bone Miner Res,* 15**,** 1596-602.

ROBLING, A. G., DUIJVELAAR, K. M., GEEVERS, J. V., OHASHI, N. & TURNER, C. H. (2001) Modulation of appositional and longitudinal bone growth in the rat ulna by applied static and dynamic force. *Bone,* 29**,** 105-113.

ROBLING, A. G., NIZIOLEK, P. J., BALDRIDGE, L. A., CONDON, K. W., ALLEN, M. R., ALAM, I., MANTILA, S. M., GLUHAK-HEINRICH, J., BELLIDO, T. M., HARRIS, S. E. & TURNER, C. H. (2008) Mechanical Stimulation of Bone in Vivo Reduces Osteocyte Expression of Sost/Sclerostin. *Journal of Biological Chemistry,* 283**,** 5866-5875.

RODAN, G. A. (1997) Bone mass homeostasis and bisphosphonate action. *Bone,* 20**,** 1-4.

RODRIGUEZ-MORENO, A. & SIHRA, T. S. (2007) Metabotropic actions of kainate receptors in the CNS. *J Neurochem,* 103**,** 2121-35.

ROGERS, K. V., DUNN, C. K., HEBERT, S. C. & BROWN, E. M. (1997) Localization of calcium receptor mRNA in the adult rat central nervous system by in situ hybridization. *Brain Res,* 744**,** 47-56.

ROMANELLO, M., PANI, B., BICEGO, M. & D'ANDREA, P. (2001) Mechanically Induced ATP Release from Human Osteoblastic Cells. *Biochemical and Biophysical Research Communications,* 289**,** 1275-1281.

ROODMAN, G. D. (1999) Cell biology of the osteoclast. *Exp Hematol,* 27**,** 1229-41.

ROSEN, C. J., COMPSTON, J. E. & LIAN, J. B. (2008) *Primer on the metabolic bone diseases and disorders of mineral metabolism,* Washington, D.C., The American Society for Bone and Mineral Research.

ROSZEK, B., WEINANS, H., VAN LOON, P. & HUISKES, R. (1993) In vivo measurements of the loading conditions on the tibia of the goat. *Acta Anat (Basel),* 146**,** 188-92.

ROWE, P. S., KUMAGAI, Y., GUTIERREZ, G., GARRETT, I. R., BLACHER, R., ROSEN, D., CUNDY, J., NAVVAB, S., CHEN, D., DREZNER, M. K., QUARLES, L. D. & MUNDY, G. R. (2004) MEPE has the properties of an osteoblastic phosphatonin and minhibin. *Bone,* 34**,** 303-19.

RUBIN, A. (2010) *Statistics for evidence-based practice and evaluation,* Belmont, Calif., Brooks/Cole.

RUBIN, C., GROSS, T., QIN, Y. X., FRITTON, S., GUILAK, F. & MCLEOD, K. (1996) Differentiation of the bone-tissue remodeling response to axial and torsional loading in the turkey ulna. *J Bone Joint Surg Am,* 78**,** 1523-33.

RUBIN, C. & LANYON, L. (1985) Regulation of bone mass by mechanical strain magnitude. *Calcified tissue international,* 37**,** 411-417.

RUBIN, C., TURNER, A. S., BAIN, S., MALLINCKRODT, C. & MCLEOD, K. (2001a) Anabolism. Low mechanical signals strengthen long bones. *Nature,* 412**,** 603-4.

RUBIN, C. T. & LANYON, L. E. (1982) Limb mechanics as a function of speed and gait: a study of functional strains in the radius and tibia of horse and dog. *J Exp Biol,* 101**,** 187-211.

RUBIN, C. T. & LANYON, L. E. (1984a) Dynamic strain similarity in vertebrates; an alternative to allometric limb bone scaling. *J Theor Biol,* 107**,** 321-7.

RUBIN, C. T. & LANYON, L. E. (1984b) Regulation of bone formation by applied dynamic loads. *The Journal of bone and joint surgery. American volume,* 66**,** 397-402.

RUBIN, C. T., MCLEOD, K. J. & BAIN, S. D. (1990) Functional strains and cortical bone adaptation: epigenetic assurance of skeletal integrity. *J Biomech,* 23 Suppl 1**,** 43-54.

RUBIN, C. T., SOMMERFELDT, D. W., JUDEX, S. & QIN, Y.-X. (2001b) Inhibition of osteopenia by low magnitude, high-frequency mechanical stimuli. *Drug Discovery Today,* 6**,** 848-858.

RUBIN, J., MURPHY, T. C., FAN, X., GOLDSCHMIDT, M. & TAYLOR, W. R. (2002) Activation of Extracellular Signal–Regulated Kinase Is Involved in Mechanical Strain Inhibition of RANKL Expression in Bone Stromal Cells. *Journal of Bone and Mineral Research,* 17**,** 1452-1460.

RUBIN, J., RUBIN, C. & JACOBS, C. R. (2006) Molecular pathways mediating mechanical signaling in bone. *Gene,* 367**,** 1-16.

RUBIN, M. R. & BILEZIKIAN, J. P. (2003) The anabolic effects of parathyroid hormone therapy. *Clin Geriatr Med,* 19**,** 415-32.

RUGGIERO, S. L., MEHROTRA, B., ROSENBERG, T. J. & ENGROFF, S. L. (2004) Osteonecrosis of the jaws associated with the use of bisphosphonates: a review of 63 cases. *J Oral Maxillofac Surg,* 62**,** 527-34.

RUSSELL, J., STEPHENSON, G., YELLOWLEY, C. & BENTON, H. (2007) Adenosine Inhibition of Lipopolysaccharide-Induced Interleukin-6 Secretion by the Osteoblastic Cell Line MG-63. *Calcified Tissue International,* 81**,** 316-326.

RUSSELL, R. G. (2007) Bisphosphonates: mode of action and pharmacology. *Pediatrics,* 119 Suppl 2**,** S150-62.

SAINI, V., YADAV, S. & MCCORMICK, S. (2011) Low-intensity pulsed ultrasound modulates shear stress induced PGHS-2 expression and PGE2 synthesis in MLO-Y4 osteocyte-like cells. *Ann Biomed Eng,* 39**,** 378-93.

SANCHEZ, C., GABAY, O., SALVAT, C., HENROTIN, Y. E. & BERENBAUM, F. (2009) Mechanical loading highly increases IL-6 production and decreases OPG expression by osteoblasts. *Osteoarthritis Cartilage,* 17**,** 473-81.

SANTOS, M. I., UNGER, R. E., SOUSA, R. A., REIS, R. L. & KIRKPATRICK, C. J. (2009) Crosstalk between osteoblasts and endothelial cells co-cultured on a polycaprolactone-starch scaffold and the in vitro development of vascularization. *Biomaterials,* 30**,** 4407-15.

SARRAMEGNA, V., TALMONT, F., DEMANGE, P. & MILON, A. (2003) Heterologous expression of G-protein-coupled receptors: comparison of expression systems from the standpoint of large-scale production and purification. *Cell Mol Life Sci,* 60**,** 1529-46.

SATO, M., WESTMORE, M., MA, Y. L., SCHMIDT, A., ZENG, Q. Q., GLASS, E. V., VAHLE, J., BROMMAGE, R., JEROME, C. P. & TURNER, C. H. (2004) Teriparatide [PTH(1-34)] strengthens the proximal femur of ovariectomized nonhuman primates despite increasing porosity. *J Bone Miner Res,* 19**,** 623-9.

SCHMITTGEN, T. D. & LIVAK, K. J. (2008) Analyzing real-time PCR data by the comparative C(T) method. *Nat Protoc,* 3**,** 1101-8.

SCHMITTGEN, T. D. & ZAKRAJSEK, B. A. (2000) Effect of experimental treatment on housekeeping gene expression: validation by real-time, quantitative RT-PCR. *Journal of biochemical and biophysical methods,* 46**,** 69-81.

SCHNEIDER, A., KALIKIN, L. M., MATTOS, A. C., KELLER, E. T., ALLEN, M. J., PIENTA, K. J. & MCCAULEY, L. K. (2005) Bone turnover mediates preferential localization of prostate cancer in the skeleton. *Endocrinology,* 146**,** 1727-36.

SCHOUSBOE, A. & DIVAC, I. (1979) Difference in glutamate uptake in astrocytes cultured from different brain regions. *Brain Res,* 177**,** 407-9.

SCHRODER, H. C., WANG, X. H., WIENS, M., DIEHL-SEIFERT, B., KROPF, K., SCHLOSSMACHER, U. & MULLER, W. E. (2012) Silicate modulates the cross-talk between osteoblasts (SaOS-2) and osteoclasts (RAW 264.7 cells): inhibition of osteoclast growth and differentiation. *Journal of cellular biochemistry,* 113**,** 3197-206.

SCHULZE, E., WITT, M., KASPER, M., LOWIK, C. W. & FUNK, R. H. (1999) Immunohistochemical investigations on the differentiation marker protein E11 in rat calvaria, calvaria cell culture and the osteoblastic cell line ROS 17/2.8. *Histochemistry and cell biology,* 111**,** 61-9.

SCULLY, N. E. E., EVANS, S. L., MASON, D. J. & EVANS, B. A. J. (2013a) Development of a novel 3D mineralising culture system to investigate the differentiation of osteoblasts to osteocytes. *Presented at the European Calcified Tissue Society Conference ECTS 2013 , Lisbon, Portugal. Bone Abstracts.,* 1**,** PP246.

SCULLY, N. E. E., EVANS, S. L., MASON, D. J. & EVANS, B. A. J. (2013b) Mimicking osteocytes in vivo using 3D collagen gels: development of a novel tool to study osteocyte biology. *Presented at Society for Endocrinology BES 2007, Birmingham, UK. Endocrine Abstracts,* 31**,** P5.

SEIREG, A. & KEMPKE, W. (1969) Behavior of in vivo bone under cyclic loading. *Journal of biomechanics,* 2**,** 455-61.

SELYE, H. (1932) ON THE STIMULATION OF NEW BONE-FORMATION WITH PARATHYROID EXTRACT AND IRRADIATED ERGOSTEROL. *Endocrinology,* 16**,** 547-558.

SEMENOV, M., TAMAI, K. & HE, X. (2005) SOST is a ligand for LRP5/LRP6 and a Wnt signaling inhibitor. *J Biol Chem,* 280**,** 26770-5.

SEMENOV, M. V. & HE, X. (2006) LRP5 mutations linked to high bone mass diseases cause reduced LRP5 binding and inhibition by SOST. *J Biol Chem,* 281**,** 38276-84.

SHALHOUB, V., SHATZEN, E., HENLEY, C., BOEDIGHEIMER, M., MCNINCH, J., MANOUKIAN, R., DAMORE, M., FITZPATRICK, D., HAAS, K., TWOMEY, B., KIAEI, P., WARD, S., LACEY, D. L. & MARTIN, D. (2006) Calcification inhibitors and Wnt signaling proteins are

implicated in bovine artery smooth muscle cell calcification in the presence of phosphate and vitamin D sterols. *Calcif Tissue Int,* 79**,** 431-42.

SHI, S., KIRK, M. & KAHN, A. J. (1996) The role of type I collagen in the regulation of the osteoblast phenotype. *Journal of bone and mineral research : the official journal of the American Society for Bone and Mineral Research,* 11**,** 1139-45.

SHIGERI, Y., SEAL, R. P. & SHIMAMOTO, K. (2004) Molecular pharmacology of glutamate transporters, EAATs and VGLUTs. *Brain Res Brain Res Rev,* 45**,** 250-65.

SHIN, C. S., LECANDA, F., SHEIKH, S., WEITZMANN, L., CHENG, S. L. & CIVITELLI, R. (2000) Relative abundance of different cadherins defines differentiation of mesenchymal precursors into osteogenic, myogenic, or adipogenic pathways. *J Cell Biochem,* 78**,** 566-77.

SHIN, H. I., DIVIETI, P., SIMS, N. A., KOBAYASHI, T., MIAO, D., KARAPLIS, A. C., BARON, R., BRINGHURST, R. & KRONENBERG, H. M. (2004) Gp130-mediated signaling is necessary for normal osteoblastic function in vivo and in vitro. *Endocrinology,* 145**,** 1376-85.

SIHRA, T. S. & RODRIGUEZ-MORENO, A. (2011) Metabotropic actions of kainate receptors in the control of GABA release. *Adv Exp Med Biol,* 717**,** 1-10.

SILVER, I. A., MURRILLS, R. J. & ETHERINGTON, D. J. (1988) Microelectrode studies on the acid microenvironment beneath adherent macrophages and osteoclasts. *Exp Cell Res,* 175**,** 266-76.

SINGH, P. P., VAN DER KRAAN, A. G., XU, J., GILLESPIE, M. T. & QUINN, J. M. (2012) Membrane-bound receptor activator of NFkappaB ligand (RANKL) activity displayed by osteoblasts is differentially regulated by osteolytic factors. *Biochem Biophys Res Commun,* 422**,** 48-53.

SIRIS, E. S. (1994) Epidemiological aspects of Paget's disease: family history and relationship to other medical conditions. *Semin Arthritis Rheum,* 23**,** 222-5.

SITTICHOCKECHAIWUT, A., SCUTT, A. M., RYAN, A. J., BONEWALD, L. F. & REILLY, G. C. (2009) Use of rapidly mineralising osteoblasts and short periods of mechanical loading to accelerate matrix maturation in 3D scaffolds. *Bone,* 44**,** 822-829.

SITTICHOKECHAIWUT, A., EDWARDS, J. H., SCUTT, A. M. & REILLY, G. C. (2010) Short bouts of mechanical loading are as effective as dexamethasone at inducing matrix production by human bone marrow mesenchymal stem cell. *Eur Cell Mater,* 20**,** 45-57.

SKERRY, T. M. (2008a) The response of bone to mechanical loading and disuse: Fundamental principles and influences on osteoblast/osteocyte homeostasis. *Archives of Biochemistry and Biophysics,* 473**,** 117-123.

SKERRY, T. M. (2008b) The role of glutamate in the regulation of bone mass and architecture. *Journal of musculoskeletal & neuronal interactions,* 8**,** 166-73.

SKERRY, T. M., BITENSKY, L., CHAYEN, J. & LANYON, L. E. (1989) Early strain-related changes in enzyme activity in osteocytes following bone loading in vivo. *J Bone Miner Res,* 4**,** 783-8.

SLUKA, K. A., JORDAN, H. H., WILLIS, W. D. & WESTLUND, K. N. (1994) Differential effects of N-methyl-D-aspartate (NMDA) and non-NMDA receptor antagonists on spinal release of amino acids after development of acute arthritis in rats. *Brain Res,* 664**,** 77-84.

SMAJILOVIC, S., HANSEN, J. L., CHRISTOFFERSEN, T. E., LEWIN, E., SHEIKH, S. P., TERWILLIGER, E. F., BROWN, E. M., HAUNSO, S. & TFELT-HANSEN, J. (2006) Extracellular calcium sensing in rat aortic vascular smooth muscle cells. *Biochem Biophys Res Commun,* 348**,** 1215-23.

SMALT, R., MITCHELL, F. T., HOWARD, R. L. & CHAMBERS, T. J. (1997) Induction of NO and prostaglandin E2 in osteoblasts by wall-shear stress but not mechanical strain. *Am J Physiol,* 273**,** E751-8.

SPENCER, G. J. & GENEVER, P. G. (2003) Long-term potentiation in bone--a role for glutamate in strain-induced cellular memory? *BMC Cell Biol,* 4**,** 9.

STAEHLING-HAMPTON, K., PROLL, S., PAEPER, B. W., ZHAO, L., CHARMLEY, P., BROWN, A., GARDNER, J. C., GALAS, D., SCHATZMAN, R. C., BEIGHTON, P., PAPAPOULOS, S., HAMERSMA, H. & BRUNKOW, M. E. (2002) A 52-kb deletion in the SOST-MEOX1 intergenic region on 17q12-q21 is associated with van Buchem disease in the Dutch population. *Am J Med Genet,* 110**,** 144-52.

STAINS, J. P. & CIVITELLI, R. (2005) Gap junctions in skeletal development and function. *Biochim Biophys Acta,* 1719**,** 69-81.

STANDRING, S. (2004) Musculoskeletal System. *Gray's Anatomy.* 39th ed. New York, Elseiver.

STERN, A. R., STERN, M. M., VAN DYKE, M. E., JAHN, K., PRIDEAUX, M. & BONEWALD, L. F. (2012) Isolation and culture of primary osteocytes from the long bones of skeletally mature and aged mice. *Biotechniques,* 52**,** 361-73.

STEVENSON, J. C. & LINDSAY, R. (1998) Bone structure and cellular activity. *Osteoporosis* 1-2.

STINEHELFER, S., VRUWINK, M. & BURETTE, A. (2000) Immunolocalization of mGluR1alpha in specific populations of local circuit neurons in the cerebral cortex. *Brain Res,* 861**,** 37-44.

STORCK, T., SCHULTE, S., HOFMANN, K. & STOFFEL, W. (1992) Structure, expression, and functional analysis of a Na(+)-dependent glutamate/aspartate transporter from rat brain. *Proc Natl Acad Sci U S A,* 89**,** 10955-9.

SUDA, T., TAKAHASHI, N. & MARTIN, T. J. (1992) Modulation of Osteoclast Differentiation. *Endocrine Reviews,* 13**,** 66-80.

SUDO, H., KODAMA, H. A., AMAGAI, Y., YAMAMOTO, S. & KASAI, S. (1983) In vitro differentiation and calcification in a new clonal osteogenic cell line derived from newborn mouse calvaria. *The Journal of cell biology,* 96**,** 191-8.

SUGAWARA, Y., ANDO, R., KAMIOKA, H., ISHIHARA, Y., HONJO, T., KAWANABE, N., KUROSAKA, H., TAKANO-YAMAMOTO, T. & YAMASHIRO, T. (2011) The three-dimensional morphometry and cell-cell communication of the osteocyte network in chick and mouse embryonic calvaria. *Calcif Tissue Int,* 88**,** 416-24.

SUGDEN, K., PARIANTE, C. M., MCGUFFIN, P., AITCHISON, K. J. & D'SOUZA, U. M. (2010) Housekeeping gene expression is affected by antidepressant treatment in a mouse fibroblast cell line. *Journal of psychopharmacology,* 24**,** 1253-9.

SUN, Y. Q., MCLEOD, K. J. & RUBIN, C. T. (1995) Mechanically induced periosteal bone formation is paralleled by the upregulation of collagen type one mRNA in osteocytes as measured by in situ reverse transcript-polymerase chain reaction. *Calcif Tissue Int,* 57**,** 456-62.

SUTTON, M. A., ORTEU, J. & SCHREIER, H. W. (2009) Digital Image Correlation (DIC). *Image Correlation for Shape, Motion and Deformation Measurements: Basic Concepts, Theory and Applications.* US, Springer.

SUZUKI, T., HIGGINS, P. J. & CRAWFORD, D. R. (2000) Control selection for RNA quantitation. *BioTechniques,* 29**,** 332-7.

SZCZESNIAK, A. M., GILBERT, R. W., MUKHIDA, M. & ANDERSON, G. I. (2005) Mechanical loading modulates glutamate receptor subunit expression in bone. *Bone,* 37**,** 63-73.

SZOLLAR, S. M., MARTIN, E. M., SARTORIS, D. J., PARTHEMORE, J. G. & DEFTOS, L. J. (1998) Bone mineral density and indexes of bone metabolism in spinal cord injury. *Am J Phys Med Rehabil,* 77**,** 28-35.

TAKARADA-IEMATA, M., TAKARADA, T., NAKAMURA, Y., NAKATANI, E., HORI, O. & YONEDA, Y. (2011) Glutamate preferentially suppresses osteoblastogenesis than adipogenesis through the cystine/glutamate antiporter in mesenchymal stem cells. *J Cell Physiol,* 226**,** 652-65.

TAKARADA, T., HINOI, E., FUJIMORI, S., TSUCHIHASHI, Y., UESHIMA, T., TANIURA, H. & YONEDA, Y. (2004) Accumulation of [3H]glutamate in cultured rat calvarial osteoblasts. *Biochemical Pharmacology,* 68**,** 177-184.

TAKUWA, Y., OHSE, C., WANG, E. A., WOZNEY, J. M. & YAMASHITA, K. (1991) Bone morphogenetic protein-2 stimulates alkaline phosphatase activity and collagen synthesis in cultured osteoblastic cells, MC3T3-E1. *Biochemical and biophysical research communications,* 174**,** 96-101.

TALLAKSEN-GREENE, S. J., KAATZ, K. W., ROMANO, C. & ALBIN, R. L. (1998) Localization of mGluR1a-like immunoreactivity and mGluR5-like immunoreactivity in identified populations of striatal neurons. *Brain Res,* 780**,** 210-7.

TALMAGE, R. V. & ELLIOT, J. R. (1958) REMOVAL OF CALCIUM FROM BONE AS INFLUENCED BY THE PARATHYROIDS. *Endocrinology,* 62**,** 717-722.

TAN, S. D., BAKKER, A. D., SEMEINS, C. M., KUIJPERS-JAGTMAN, A. M. & KLEIN-NULEND, J. (2008) Inhibition of osteocyte apoptosis by fluid flow is mediated by nitric oxide. *Biochemical and Biophysical Research Communications,* 369**,** 1150-1154.

TAN, S. D., DE VRIES, T. J., KUIJPERS-JAGTMAN, A. M., SEMEINS, C. M., EVERTS, V. & KLEIN-NULEND, J. (2007) Osteocytes subjected to fluid flow inhibit osteoclast formation and bone resorption. *Bone,* 41**,** 745-751.

TAN, S. D., KUIJPERS-JAGTMAN, A. M., SEMEINS, C. M., BRONCKERS, A. L. J. J., MALTHA, J. C., VON DEN HOFF, J. W., EVERTS, V. & KLEIN-NULEND, J. (2006) Fluid Shear Stress Inhibits TNFα-induced Osteocyte Apoptosis. *Journal of Dental Research,* 85**,** 905-909.

TANABE, Y., MASU, M., ISHII, T., SHIGEMOTO, R. & NAKANISHI, S. (1992) A family of metabotropic glutamate receptors. *Neuron,* 8**,** 169-79.

TANAKA, J., NAKAGAWA, S., KUSHIYA, E., YAMASAKI, M., FUKAYA, M., IWANAGA, T., SIMON, M. I., SAKIMURA, K., KANO, M. & WATANABE, M. (2000) Gq protein alpha subunits Galphaq and Galpha11 are localized at postsynaptic extra-junctional membrane of cerebellar Purkinje cells and hippocampal pyramidal cells. *Eur J Neurosci,* 12**,** 781-92.

TASHJIAN, A. H., JR. & GAGEL, R. F. (2006) Teriparatide [human PTH(1-34)]: 2.5 years of experience on the use and safety of the drug for the treatment of osteoporosis. *J Bone Miner Res,* 21**,** 354-65.

TAT, S. K., PELLETIER, J. P., MINEAU, F., CARON, J. & MARTEL-PELLETIER, J. (2011) Strontium ranelate inhibits key factors affecting bone remodeling in human osteoarthritic subchondral bone osteoblasts. *Bone,* 49**,** 559-67.

TATA, U., XU, H., RAO, S. M. N., CHUONG, C.-J., NGUYEN, K. T. & CHIAO, J. C. (2011) A Novel Multiwell Device to Study Vascular Smooth Muscle Cell Responses Under Cyclic Strain. *Journal of Nanotechnology in Engineering and Medicine,* 2**,** 021007-021007.

TAYLOR, A. F. (2002) Osteoblastic glutamate receptor function regulates bone formation and resorption. *J Musculoskelet Neuronal Interact,* 2**,** 285-90.

TAYLOR, A. F., SAUNDERS, M. M., SHINGLE, D. L., CIMBALA, J. M., ZHOU, Z. & DONAHUE, H. J. (2007) Mechanically stimulated osteocytes regulate osteoblastic activity via gap junctions. *American journal of physiology. Cell physiology,* 292**,** C545-52.

TESTA, C. M., STANDAERT, D. G., LANDWEHRMEYER, G. B., PENNEY, J. B., JR. & YOUNG, A. B. (1995) Differential expression of mGluR5 metabotropic glutamate receptor mRNA by rat striatal neurons. *J Comp Neurol,* 354**,** 241-52.

THELLIN, O., ZORZI, W., LAKAYE, B., DE BORMAN, B., COUMANS, B., HENNEN, G., GRISAR, T., IGOUT, A. & HEINEN, E. (1999) Housekeeping genes as internal standards: use and limits. *Journal of biotechnology,* 75**,** 291-5.

TOMKINSON, A., GEVERS, E. F., WIT, J. M., REEVE, J. & NOBLE, B. S. (1998) The role of estrogen in the control of rat osteocyte apoptosis. *Journal of bone and mineral research : the official journal of the American Society for Bone and Mineral Research,* 13**,** 1243-50.

TOMKINSON, A., REEVE, J., SHAW, R. W. & NOBLE, B. S. (1997) The death of osteocytes via apoptosis accompanies estrogen withdrawal in human bone. *The Journal of clinical endocrinology and metabolism,* 82**,** 3128-35.

TOMS, N. J. & ROBERTS, P. J. (1999) Group 1 mGlu receptors elevate [Ca2+]i in rat cultured cortical type 2 astrocytes: [Ca2+]i synergy with adenosine A1 receptors. *Neuropharmacology,* 38**,** 1511-7.

TORRANCE, A. G., MOSLEY, J. R., SUSWILLO, R. F. & LANYON, L. E. (1994) Noninvasive loading of the rat ulna in vivo induces a strain-related modeling response uncomplicated by trauma or periostal pressure. *Calcified tissue international,* 54**,** 241-7.

TORTELLI, F. & CANCEDDA, R. (2009) Three-dimensional cultures of osteogenic and chondrogenic cells: a tissue engineering approach to mimic bone and cartilage in vitro. *European cells & materials,* 17**,** 1-14.

TORTELLI, F., PUJIC, N., LIU, Y., LAROCHE, N., VICO, L. & CANCEDDA, R. (2009) Osteoblast and osteoclast differentiation in an in vitro three-dimensional model of bone. *Tissue engineering. Part A,* 15**,** 2373-83.

TORTORA, G. J. & DERRICKSON, B. (2006) *Principles of Anatomy and Physiology,* USA, John Wiley & Sons, Inc.

TRACY, R. P., STENNER, D. D. & MINTZ, K. P. (1987) Calcium regulation and bone metabolism: basic and clinical aspects. *Journal of Cell Physiology,* 127**,** 373-387.

TRICARICO, C., PINZANI, P., BIANCHI, S., PAGLIERANI, M., DISTANTE, V., PAZZAGLI, M., BUSTIN, S. A. & ORLANDO, C. (2002) Quantitative real-time reverse transcription polymerase chain reaction: normalization to rRNA

or single housekeeping genes is inappropriate for human tissue biopsies. *Analytical biochemistry,* 309**,** 293-300.

TU, X., RHEE, Y., CONDON, K. W., BIVI, N., ALLEN, M. R., DWYER, D., STOLINA, M., TURNER, C. H., ROBLING, A. G., PLOTKIN, L. I. & BELLIDO, T. (2012) Sost downregulation and local Wnt signaling are required for the osteogenic response to mechanical loading. *Bone,* 50**,** 209-17.

TURNER, A. S., ATHANASIOU, K. A., ZHU, C. F., ALVIS, M. R. & BRYANT, H. U. (1997) Biochemical effects of estrogen on articular cartilage in ovariectomized sheep. *Osteoarthritis Cartilage,* 5**,** 63-9.

TURNER, C. H., AKHTER, M. P., RAAB, D. M., KIMMEL, D. B. & RECKER, R. R. (1991) A noninvasive, in vivo model for studying strain adaptive bone modeling. *Bone,* 12**,** 73-79.

TURNER, C. H., ROBLING, A. G., DUNCAN, R. L. & BURR, D. B. (2002) Do bone cells behave like a neuronal network? *Calcified tissue international,* 70**,** 435-42.

UBARA, Y., FUSHIMI, T., TAGAMI, T., SAWA, N., HOSHINO, J., YOKOTA, M., KATORI, H., TAKEMOTO, F. & HARA, S. (2003) Histomorphometric features of bone in patients with primary and secondary hypoparathyroidism. *Kidney Int,* 63**,** 1809-1816.

UBARA, Y., TAGAMI, T., NAKANISHI, S., SAWA, N., HOSHINO, J., SUWABE, T., HIDEYUKI, K., TAKEMOTO, F., HARA, S. & TAKAICHI, K. (2005) Significance of minimodeling in dialysis patients with adynamic bone disease. *Kidney international,* 68**,** 833-839.

UNO, K., TAKARADA, T., HINOI, E. & YONEDA, Y. (2007) Glutamate is a determinant of cellular proliferation through modulation of nuclear factor E2 p45-related factor-2 expression in osteoblastic MC3T3-E1 cells. *J Cell Physiol,* 213**,** 105-14.

UNO, K., TAKARADA, T., TAKARADA-IEMATA, M., NAKAMURA, Y., FUJITA, H., HINOI, E. & YONEDA, Y. (2011) Negative regulation of osteoblastogenesis through downregulation of runt-related transcription factor-2 in osteoblastic MC3T3-E1 cells with stable overexpression of the cystine/glutamate antiporter xCT subunit. *J Cell Physiol,* 226**,** 2953-64.

VAANANEN, H. K., ZHAO, H., MULARI, M. & HALLEEN, J. M. (2000) The cell biology of osteoclast function. *J Cell Sci,* 113 (Pt 3)**,** 377-81.

VAHLE, J. L., LONG, G. G., SANDUSKY, G., WESTMORE, M., MA, Y. L. & SATO, M. (2004) Bone neoplasms in F344 rats given teriparatide [rhPTH(1-34)] are dependent on duration of treatment and dose. *Toxicol Pathol,* 32**,** 426-38.

VAN BEZOOIJEN, R. L., DERUITER, M. C., VILAIN, N., MONTEIRO, R. M., VISSER, A., VAN DER WEE-PALS, L., VAN MUNSTEREN, C. J., HOGENDOORN, P. C., AGUET, M., MUMMERY, C. L., PAPAPOULOS, S. E., TEN DIJKE, P. & LOWIK, C. W. (2007) SOST expression is restricted to the great arteries during embryonic and neonatal cardiovascular development. *Developmental dynamics : an official publication of the American Association of Anatomists,* 236**,** 606-12.

VAN BEZOOIJEN, R. L., ROELEN, B. A., VISSER, A., VAN DER WEE-PALS, L., DE WILT, E., KARPERIEN, M., HAMERSMA, H., PAPAPOULOS, S. E., TEN DIJKE, P. & LOWIK, C. W. (2004) Sclerostin is an osteocyte-expressed negative regulator of bone formation, but not a classical BMP antagonist. *The Journal of experimental medicine,* 199**,** 805-14.

VAN BEZOOIJEN, R. L., TEN DIJKE, P., PAPAPOULOS, S. E. & LOWIK, C. W. (2005) SOST/sclerostin, an osteocyte-derived negative regulator of bone formation. *Cytokine & growth factor reviews,* 16**,** 319-27.

VAN DER PLAS, A. & NIJWEIDE, P. J. (2005) JBMR anniversary classic. Isolation and purification of osteocytes. A van der Plas A, PJ Nijweide. Originally published in Volume 7, Number 4, pp 389-96 (1992). *Journal of bone and mineral research : the official journal of the American Society for Bone and Mineral Research,* 20**,** 706-14.

VAN STAA, T. P., DENNISON, E. M., LEUFKENS, H. G. & COOPER, C. (2001) Epidemiology of fractures in England and Wales. *Bone,* 29**,** 517-22.

VAN STAA, T. P., SELBY, P., LEUFKENS, H. G., LYLES, K., SPRAFKA, J. M. & COOPER, C. (2002) Incidence and natural history of Paget's disease of bone in England and Wales. *J Bone Miner Res,* 17**,** 465-71.

VERBORGT, O., TATTON, N. A., MAJESKA, R. J. & SCHAFFLER, M. B. (2002) Spatial distribution of Bax and Bcl-2 in osteocytes after bone fatigue: complementary roles in bone remodeling regulation? *J Bone Miner Res,* 17**,** 907-14.

VOGELSTEIN, B. & KINZLER, K. W. (1999) Digital PCR. *Proc Natl Acad Sci U S A,* 96**,** 9236-41.

WANG, B., DU, T., WANG, Y., YANG, C., ZHANG, S. & CAO, X. (2011) Focal adhesion kinase signaling pathway is involved in mechanotransduction in MG-63 cells. *Biochemical and biophysical research communications,* 410**,** 671-6.

WANG, B., ZHOU, X., PRICE, C., LI, W., PAN, J. & WANG, L. (2013) Quantifying load-induced solute transport and solute-matrix interaction within the osteocyte lacunar-canalicular system. *J Bone Miner Res,* 28**,** 1075-86.

WANG, C. M., CHEN, Y., DEVIVO, M. J. & HUANG, C. T. (2001) Epidemiology of extraspinal fractures associated with acute spinal cord injury. *Spinal Cord,* 39**,** 589-94.

WANG, D., CHRISTENSEN, K., CHAWLA, K., XIAO, G., KREBSBACH, P. H. & FRANCESCHI, R. T. (1999) Isolation and characterization of MC3T3-E1 preosteoblast subclones with distinct in vitro and in vivo differentiation/mineralization potential. *Journal of bone and mineral research : the official journal of the American Society for Bone and Mineral Research,* 14**,** 893-903.

WANIEWSKI, R. A. & MARTIN, D. L. (1984) Characterization of L-glutamic acid transport by glioma cells in culture: evidence for sodium-independent, chloride-dependent high affinity influx. *J Neurosci,* 4**,** 2237-46.

WARK, J. D. (1993) Osteoporosis: pathogenesis, diagnosis, prevention and management. *Baillieres Clin Endocrinol Metab,* 7**,** 151-81.

WARRINGTON, J. A., NAIR, A., MAHADEVAPPA, M. & TSYGANSKAYA, M. (2000) Comparison of human adult and fetal expression and identification of 535 housekeeping/maintenance genes. *Physiological genomics,* 2**,** 143-7.

WASSERMAN, E., WEBSTER, D., KUHN, G., ATTAR-NAMDAR, M., MULLER, R. & BAB, I. (2013) Differential load-regulated global gene expression in mouse trabecular osteocytes. *Bone,* 53**,** 14-23.

WEBSTER, D., WASSERMAN, E., EHRBAR, M., WEBER, F., BAB, I. & MULLER, R. (2010) Mechanical loading of mouse caudal vertebrae

increases trabecular and cortical bone mass-dependence on dose and genotype. *Biomechanics and modeling in mechanobiology,* 9**,** 737-47.

WEBSTER, D. J., MORLEY, P. L., VAN LENTHE, G. H. & MULLER, R. (2008) A novel in vivo mouse model for mechanically stimulated bone adaptation--a combined experimental and computational validation study. *Computer methods in biomechanics and biomedical engineering,* 11**,** 435-41.

WEINER, S. (1986) Organization of extracellularly mineralized tissues: a comparative study of biological crystal growth. *CRC critical reviews in biochemistry,* 20**,** 365-408.

WEINER, S. & TRAUB, W. (1986) Organization of hydroxyapatite crystals within collagen fibrils. *FEBS letters,* 206**,** 262-6.

WEINREB, M., RODAN, G. A. & THOMPSON, D. D. (1989) Osteopenia in the immobilized rat hind limb is associated with increased bone resorption and decreased bone formation. *Bone,* 10**,** 187-94.

WEINSTEIN, R. S., NICHOLAS, R. W. & MANOLAGAS, S. C. (2000) Apoptosis of Osteocytes in Glucocorticoid-Induced Osteonecrosis of the Hip. *Journal of Clinical Endocrinology & Metabolism,* 85**,** 2907-2912.

WETTERWALD, A., HOFFSTETTER, W., CECCHINI, M. G., LANSKE, B., WAGNER, C., FLEISCH, H. & ATKINSON, M. (1996) Characterization and cloning of the E11 antigen, a marker expressed by rat osteoblasts and osteocytes. *Bone,* 18**,** 125-32.

WHITE, T. D. & FOLKENS, P. A. (1999) Gross Anatomy of Bones. *Human Osteology.* 2nd ed. Benicia, California, Academic Press.

WHYTE, M. P. (1994) Hypophosphatasia and the role of alkaline phosphatase in skeletal mineralization. *Endocrine reviews,* 15**,** 439-61.

WIJENAYAKA, A. R., KOGAWA, M., LIM, H. P., BONEWALD, L. F., FINDLAY, D. M. & ATKINS, G. J. (2011) Sclerostin stimulates osteocyte support of osteoclast activity by a RANKL-dependent pathway. *PLoS One,* 6**,** e25900.

WINKLER, D. G., SUTHERLAND, M. K., GEOGHEGAN, J. C., YU, C., HAYES, T., SKONIER, J. E., SHPEKTOR, D., JONAS, M., KOVACEVICH, B. R., STAEHLING-HAMPTON, K., APPLEBY, M., BRUNKOW, M. E. & LATHAM, J. A. (2003) Osteocyte control of bone formation via sclerostin, a novel BMP antagonist. *The EMBO journal,* 22**,** 6267-76.

WISDEN, W. & SEEBURG, P. H. (1993) Mammalian ionotropic glutamate receptors. *Curr Opin Neurobiol,* 3**,** 291-8.

WOLFF, J. (1986) *The law of bone remodelling,* Berlin, Springer.

WOO, S. L., KUEI, S. C., AMIEL, D., GOMEZ, M. A., HAYES, W. C., WHITE, F. C. & AKESON, W. H. (1981) The effect of prolonged physical training on the properties of long bone: a study of Wolff's Law. *The Journal of bone and joint surgery. American volume,* 63**,** 780-7.

WOO, S. M., ROSSER, J., DUSEVICH, V., KALAJZIC, I. & BONEWALD, L. F. (2011) Cell line IDG-SW3 replicates osteoblast-to-late-osteocyte differentiation in vitro and accelerates bone formation in vivo. *Journal of bone and mineral research : the official journal of the American Society for Bone and Mineral Research,* 26**,** 2634-46.

WUCHERPFENNIG, A. L., LI, Y. P., STETLER-STEVENSON, W. G., ROSENBERG, A. E. & STASHENKO, P. (1994) Expression of 92 kD type IV collagenase/gelatinase B in human osteoclasts. *J Bone Miner Res,* 9**,** 549-56.

XAUS, J., VALLEDOR, A. F., CARDO, M., MARQUES, L., BELETA, J., PALACIOS, J. M. & CELADA, A. (1999) Adenosine inhibits macrophage colony-stimulating factor-dependent proliferation of macrophages through the induction of p27kip-1 expression. *J Immunol,* 163**,** 4140-9.

XIA, X., BATRA, N., SHI, Q., BONEWALD, L. F., SPRAGUE, E. & JIANG, J. X. (2010) Prostaglandin promotion of osteocyte gap junction function through transcriptional regulation of connexin 43 by glycogen synthase kinase 3/beta-catenin signaling. *Mol Cell Biol,* 30**,** 206-19.

XIAO, Z., DALLAS, M., QIU, N., NICOLELLA, D., CAO, L., JOHNSON, M., BONEWALD, L. & QUARLES, L. D. (2011) Conditional deletion of Pkd1 in osteocytes disrupts skeletal mechanosensing in mice. *The FASEB journal : official publication of the Federation of American Societies for Experimental Biology,* 25**,** 2418-32.

XIAO, Z., ZHANG, S., MAHLIOS, J., ZHOU, G., MAGENHEIMER, B. S., GUO, D., DALLAS, S. L., MASER, R., CALVET, J. P., BONEWALD, L. & QUARLES, L. D. (2006) Cilia-like structures and polycystin-1 in osteoblasts/osteocytes and associated abnormalities in skeletogenesis and Runx2 expression. *J Biol Chem,* 281**,** 30884-95.

XING, L. & BOYCE, B. F. (2005) Regulation of apoptosis in osteoclasts and osteoblastic cells. *Biochem Biophys Res Commun,* 328**,** 709-20.

XIONG, J., ONAL, M., JILKA, R. L., WEINSTEIN, R. S., MANOLAGAS, S. C. & O'BRIEN, C. A. (2011) Matrix-embedded cells control osteoclast formation. *Nat Med,* 17**,** 1235-41.

YAMAGUCHI, D. T. & MA, D. (2003) Mechanism of pH regulation of connexin 43 expression in MC3T3-E1 cells. *Biochemical and biophysical research communications,* 304**,** 736-9.

YAMAGUCHI, T., CHATTOPADHYAY, N., KIFOR, O., BUTTERS, R. R., JR., SUGIMOTO, T. & BROWN, E. M. (1998a) Mouse osteoblastic cell line (MC3T3-E1) expresses extracellular calcium (Ca2+o)-sensing receptor and its agonists stimulate chemotaxis and proliferation of MC3T3-E1 cells. *J Bone Miner Res,* 13**,** 1530-8.

YAMAGUCHI, T., CHATTOPADHYAY, N., KIFOR, O., YE, C., VASSILEV, P. M., SANDERS, J. L. & BROWN, E. M. (2001) Expression of extracellular calcium-sensing receptor in human osteoblastic MG-63 cell line. *Am J Physiol Cell Physiol,* 280**,** C382-93.

YAMAGUCHI, T., KIFOR, O., CHATTOPADHYAY, N. & BROWN, E. M. (1998b) Expression of Extracellular Calcium (Ca2+o)-Sensing Receptor in the Clonal Osteoblast-like Cell Lines, UMR-106 and SAOS-2. *Biochemical and Biophysical Research Communications,* 243**,** 753-757.

YAMAUCHI, M., YAMAGUCHI, T., KAJI, H., SUGIMOTO, T. & CHIHARA, K. (2005) Involvement of calcium-sensing receptor in osteoblastic differentiation of mouse MC3T3-E1 cells. *American journal of physiology. Endocrinology and metabolism,* 288**,** E608-16.

YANG, H., WANNER, I. B., ROPER, S. D. & CHAUDHARI, N. (1999) An Optimized Method for In Situ Hybridization with Signal Amplification That Allows the Detection of Rare mRNAs. *Journal of Histochemistry & Cytochemistry,* 47**,** 431-445.

YANG, M., HUANG, L., XIAO, L. & LIAO, E. (2012) [Effects of mechanical stimulation on proliferation and differentiation in MG-63 osteoblast-like cells]. *Sheng Wu Yi Xue Gong Cheng Xue Za Zhi,* 29**,** 894-7.

YANG, W., HARRIS, M. A., HEINRICH, J. G., GUO, D., BONEWALD, L. F. & HARRIS, S. E. (2009) Gene expression signatures of a fibroblastoid preosteoblast and cuboidal osteoblast cell model compared to the MLO-Y4 osteocyte cell model. *Bone,* 44**,** 32-45.

YANG, W., KALAJZIC, I., LU, Y., GUO, D., HARRIS, M. A., GLUHAK-HEINRICH, J., BONEWALD, L. F., FENG, J. Q., ROWE, D. W. & HARRIS, S. E. (2004) In vitro and in vivo study on osteocyte-specific mechanical signaling pathways. *J Musculoskelet Neuronal Interact,* 4**,** 386-7.

YASUDA, H., SHIMA, N., NAKAGAWA, N., MOCHIZUKI, S. I., YANO, K., FUJISE, N., SATO, Y., GOTO, M., YAMAGUCHI, K., KURIYAMA, M., KANNO, T., MURAKAMI, A., TSUDA, E., MORINAGA, T. & HIGASHIO, K. (1998a) Identity of osteoclastogenesis inhibitory factor (OCIF) and osteoprotegerin (OPG): a mechanism by which OPG/OCIF inhibits osteoclastogenesis in vitro. *Endocrinology,* 139**,** 1329-37.

YASUDA, H., SHIMA, N., NAKAGAWA, N., YAMAGUCHI, K., KINOSAKI, M., MOCHIZUKI, S., TOMOYASU, A., YANO, K., GOTO, M., MURAKAMI, A., TSUDA, E., MORINAGA, T., HIGASHIO, K., UDAGAWA, N., TAKAHASHI, N. & SUDA, T. (1998b) Osteoclast differentiation factor is a ligand for osteoprotegerin/osteoclastogenesis-inhibitory factor and is identical to TRANCE/RANKL. *Proc Natl Acad Sci U S A,* 95**,** 3597-602.

YE, C. P., YAMAGUCHI, T., CHATTOPADHYAY, N., SANDERS, J. L., VASSILEV, P. M. & BROWN, E. M. (2000) Extracellular calcium-sensing-receptor (CaR)-mediated opening of an outward K+ channel in murine MC3T3-E1 osteoblastic cells: evidence for expression of a functional CaR. *Bone,* 27**,** 21-27.

YOU, J., YELLOWLEY, C. E., DONAHUE, H. J., ZHANG, Y., CHEN, Q. & JACOBS, C. R. (2000) Substrate deformation levels associated with routine physical activity are less stimulatory to bone cells relative to loading-induced oscillatory fluid flow. *Journal of biomechanical engineering,* 122**,** 387-93.

YOU, L., COWIN, S. C., SCHAFFLER, M. B. & WEINBAUM, S. (2001) A model for strain amplification in the actin cytoskeleton of osteocytes due to fluid drag on pericellular matrix. *J Biomech,* 34**,** 1375-86.

YOU, L., TEMIYASATHIT, S., LEE, P., KIM, C. H., TUMMALA, P., YAO, W., KINGERY, W., MALONE, A. M., KWON, R. Y. & JACOBS, C. R. (2008) Osteocytes as mechanosensors in the inhibition of bone resorption due to mechanical loading. *Bone,* 42**,** 172-9.

YU, L., VAN DER VALK, M., CAO, J., HAN, C. Y., JUAN, T., BASS, M. B., DESHPANDE, C., DAMORE, M. A., STANTON, R. & BABIJ, P. (2011) Sclerostin expression is induced by BMPs in human Saos-2 osteosarcoma cells but not via direct effects on the sclerostin gene promoter or ECR5 element. *Bone,* 49**,** 1131-40.

ZAIDI, M., INZERILLO, A. M., MOONGA, B. S., BEVIS, P. J. R. & HUANG, C. L. H. (2002) Forty years of calcitonin - Where are we now? A tribute to the work of Iain Macintyre, FRS. *Bone,* 30**,** 655-663.

ZAIDI, M., KERBY, J., HUANG, C. L. H., ALAM, A. S. M. T., RATHOD, H., CHAMBERS, T. J. & MOONGA, B. S. (1991) Divalent cations mimic the inhibitory effect of extracellular ionised calcium on bone resorption by isolated rat osteoclasts: Further evidence for a “calcium receptor”. *Journal of cellular physiology,* 149**,** 422-427.

ZAMAN, G., PITSILLIDES, A. A., RAWLINSON, S. C. F., SUSWILLO, R. F. L., MOSLEY, J. R., CHENG, M. Z., PLATTS, L. A. M., HUKKANEN, M., POLAK, J. M. & LANYON, L. E. (1999) Mechanical Strain Stimulates Nitric Oxide Production by Rapid Activation of Endothelial Nitric Oxide Synthase in Osteocytes. *Journal of Bone and Mineral Research,* 14**,** 1123-1131.

ZAMAN, G., SAXON, L. K., SUNTERS, A., HILTON, H., UNDERHILL, P., WILLIAMS, D., PRICE, J. S. & LANYON, L. E. (2010) Loading-related regulation of gene expression in bone in the contexts of estrogen deficiency, lack of estrogen receptor Î± and disuse. *Bone,* 46**,** 628-642.

ZAMBONIN ZALLONE, A., TETI, A. & PRIMAVERA, M. V. (1984) Resorption of vital or devitalized bone by isolated osteoclasts in vitro. The role of lining cells. *Cell Tissue Res,* 235**,** 561-4.

ZARRINKALAM, M. R., MULAIBRAHIMOVIC, A., ATKINS, G. J. & MOORE, R. J. (2012) Changes in osteocyte density correspond with changes in osteoblast and osteoclast activity in an osteoporotic sheep model. *Osteoporosis international : a journal established as result of cooperation between the European Foundation for Osteoporosis and the National Osteoporosis Foundation of the USA,* 23**,** 1329-36.

ZERWEKH, J. E., RUML, L. A., GOTTSCHALK, F. & PAK, C. Y. (1998) The effects of twelve weeks of bed rest on bone histology, biochemical markers of bone turnover, and calcium homeostasis in eleven normal subjects. *J Bone Miner Res,* 13**,** 1594-601.

ZHANG, K., BARRAGAN-ADJEMIAN, C., YE, L., KOTHA, S., DALLAS, M., LU, Y., ZHAO, S., HARRIS, M., HARRIS, S. E., FENG, J. Q. & BONEWALD, L. F. (2006) E11/gp38 selective expression in osteocytes: regulation by mechanical strain and role in dendrite elongation. *Molecular and cellular biology,* 26**,** 4539-52.

ZHANG, Y., PAUL, E. M., SATHYENDRA, V., DAVISON, A., SHARKEY, N., BRONSON, S., SRINIVASAN, S., GROSS, T. S. & DONAHUE, H. J. (2011) Enhanced osteoclastic resorption and responsiveness to mechanical load in gap junction deficient bone. *PLoS One,* 6**,** e23516.

ZHAO, S., ZHANG, Y. K., HARRIS, S., AHUJA, S. S. & BONEWALD, L. F. (2002) MLO-Y4 osteocyte-like cells support osteoclast formation and activation. *Journal of bone and mineral research : the official journal of the American Society for Bone and Mineral Research,* 17**,** 2068-79.

ZHOU, H., CHOONG, P., MCCARTHY, R., CHOU, S. T., MARTIN, T. J. & NG, K. W. (1994) In situ hybridization to show sequential expression of osteoblast gene markers during bone formation in vivo. *Journal of bone and mineral research : the official journal of the American Society for Bone and Mineral Research,* 9**,** 1489-99.

APPENDIX

9. Appendix

9.1 Serum batch test results (page 51)

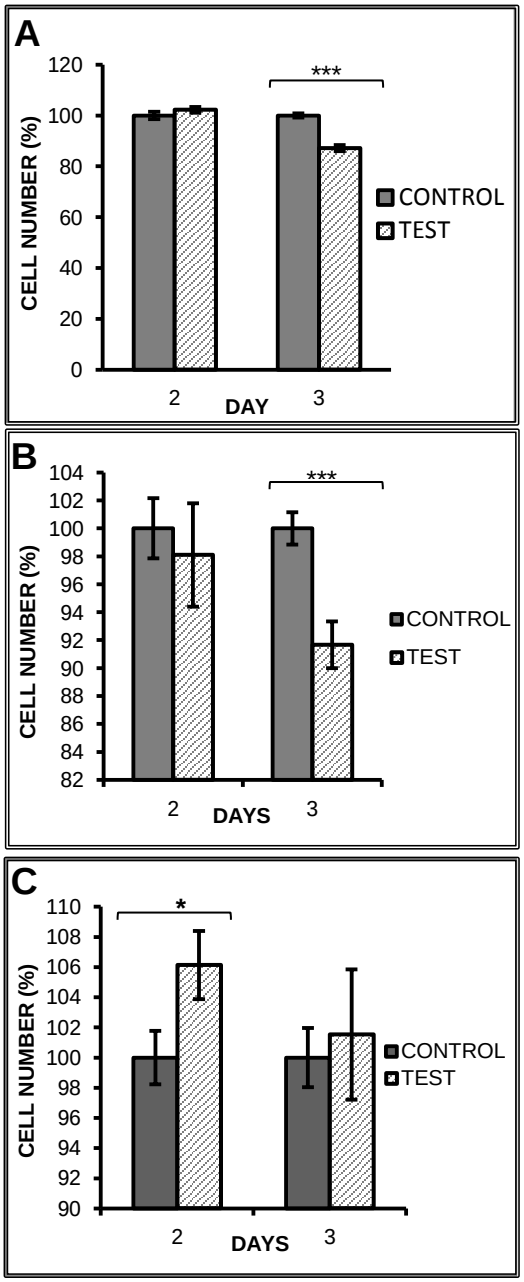

Figure 9.1 *Effect of new batches of FCS and NCS on MC3T3-E1(14) and MLO-Y4 cell number.* A) MC3T3-E1(14) cell number significantly decreased 12.85 % on day 3 when cultured with test FCS. B) MLO-Y4 cell number significantly increased 8.3 % on day 3 when cultured with test FCS. C) MLO-Y4 cell number significantly increased 6 % on day 2 when cultured with test NCS. Significant differences were obtained by t-test and are denoted by *$P<0.05$, ***$P<0.001$.

9.2 Solutions

1X TBE

10X TBE was obtained from Promega and diluted 1:10 in dH_2O.

LB agar

LB agar tablets were dissolved in dH_2O (50 ml/tablet) by autoclaving twice. The solution was cooled to rt before adding ampicillin (100 µg/ml), IPTG (0.5 mM) and X-gal (40 µg/ml). The agar was then poured into 10 cm agar petri dishes and allowed to solidify aseptically. Plates were stored at 4°C until needed.

LB broth

LB broth tablets were dissolved in dH_2O (50 ml/tablet) by autoclaving once. The solution was cooled to rt before adding ampicillin (100 µg/ml) and stored at 4°C until needed.

Phosphate Buffered Saline (PBS)

1.42 g/L di-sodium orthophosphate anhydrous (Na_2HPO_4)

0.32 g/L sodium phosphate monobasic anhydrous (NaH_2PO_4)

8 g/L sodium chloride (NaCl)

Dissolved in 1 L of distilled water (dH_2O). Solution was sterilised by autoclaving for tissue culture use only.

4 % PFA

4 g of PFA powder was diluted in 100 ml of PBS with continuous stirring whilst heated up to 60°C forming a milky solution. At 60°C NaOH (1 M) was added until the milky solution became clear. The solution was then adjusted to pH 7.4, aliquoted and stored at -20°C until needed. For specimen fixation, PFA was diluted to 1 % using PBS.

9.3 Low molecular weight DNA ladder (page 55)

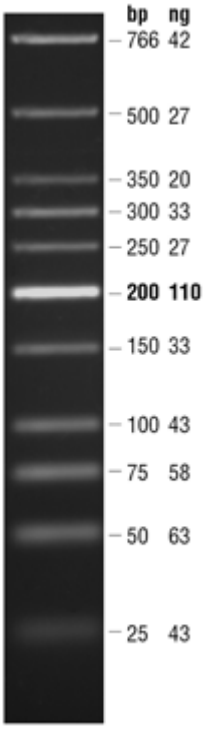

9.4 Example RT-qPCR cDNA standard curve (page 56)

GAPDH (0.1 µM Primers, 3.5 mM $MgCl_2$)

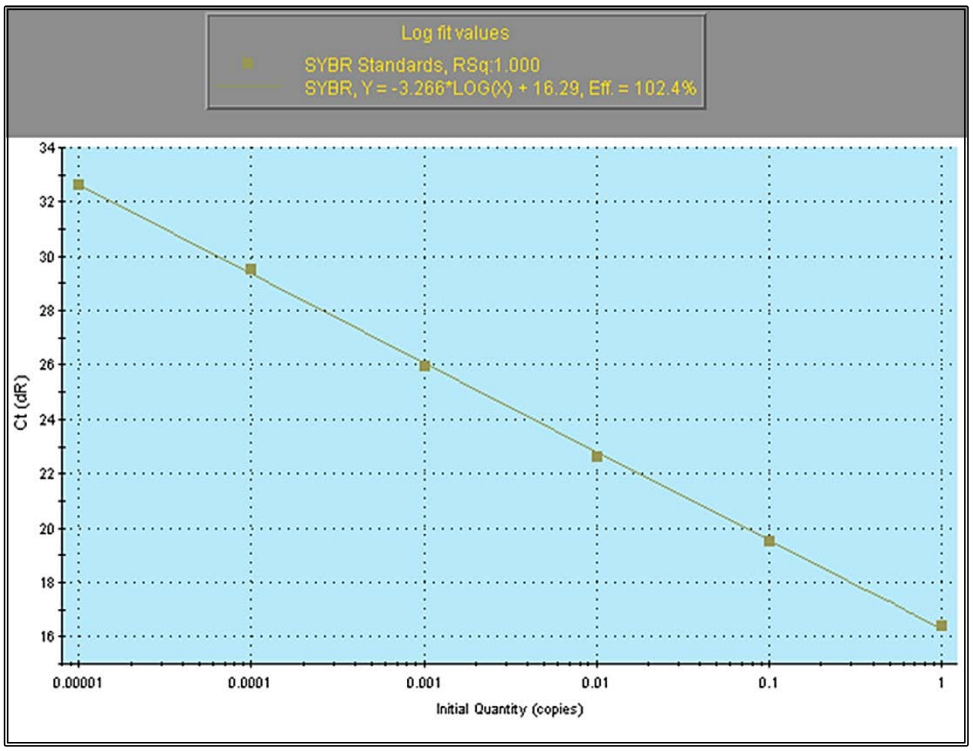

9.5 pGEM®-T vector map and sequence reference points (page 61)

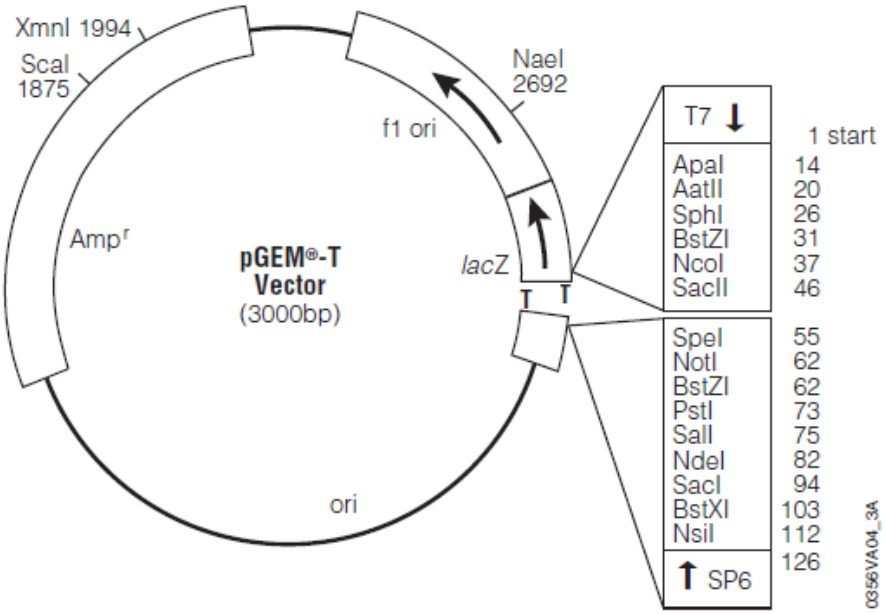

pGEM®-T Vector sequence reference points:

T7 RNA polymerase transcription initiation site	1
multiple cloning region	10–113
SP6 RNA polymerase promoter (–17 to +3)	124–143
SP6 RNA polymerase transcription initiation site	126
pUC/M13 Reverse Sequencing Primer binding site	161–177
*lac*Z start codon	165
lac operator	185–201
β-lactamase coding region	1322–2182
phage f1 region	2365–2820
lac operon sequences	2821–2981, 151–380
pUC/M13 Forward Sequencing Primer binding site	2941–2957
T7 RNA polymerase promoter (–17 to +3)	2984–3

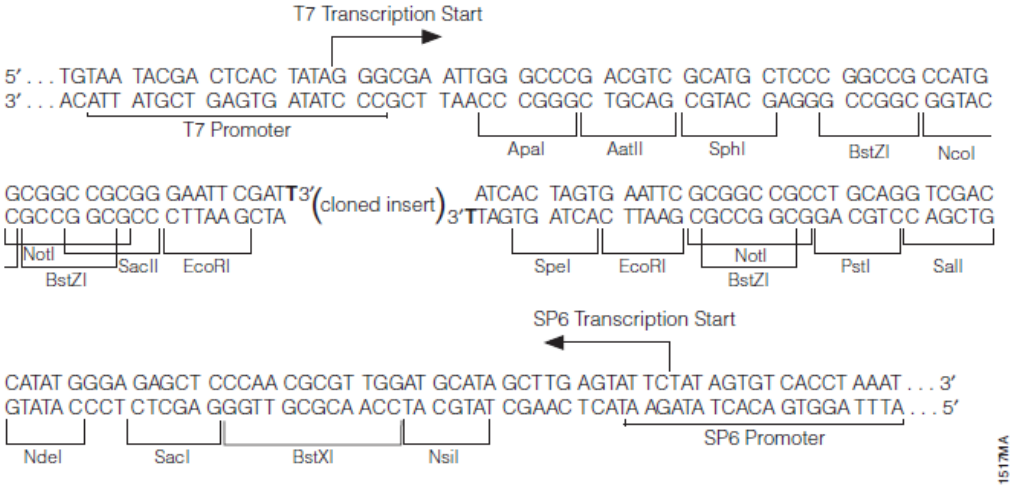

9.6 Examples of microplate assays standard curves

Quant-iT™ dsDNA High-Sensitivity Assay Kit standard curve (page 54, fluorescence measured at 510/527 nm fluorescein wavelength)

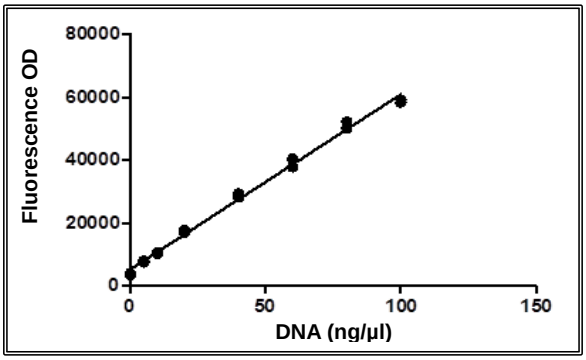

ELISAs 4 Parameter Logistic (4PL) standard curves (page 74)

PGE$_2$ (absorbance measured at 405 nm wavelength with correction between 570 and 590 nm).

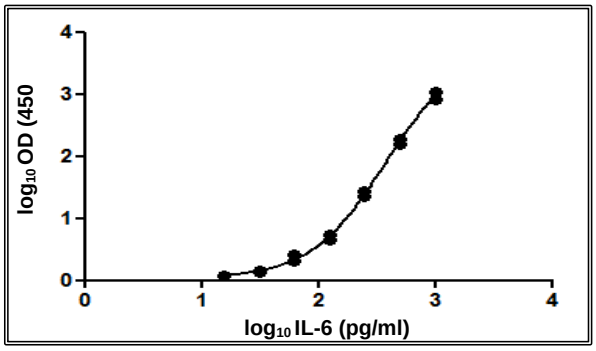

IL-6 (absorbance measured at 450 nm wavelength with correction at 540 nm and 570 nm).

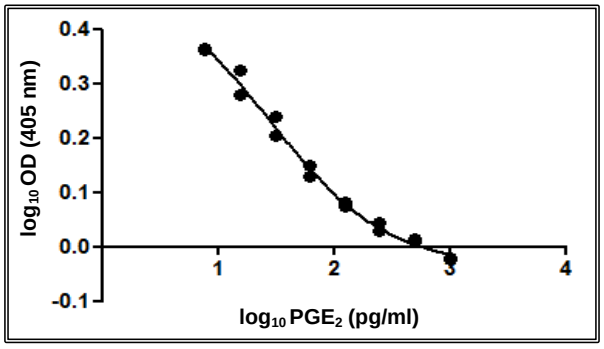

PINP (absorbance measured at 450 nm wavelength with correction at 650 nm).

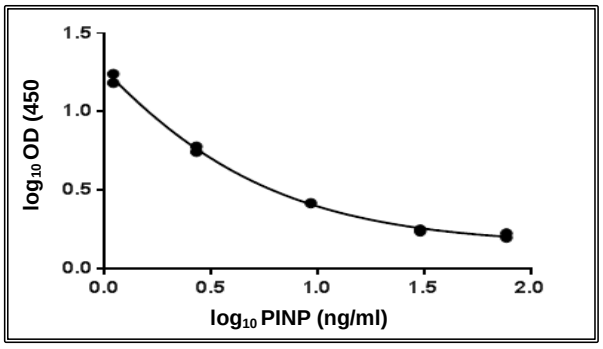

9.7 Immunofluorescence controls for ColI staining (Figure 3.1)

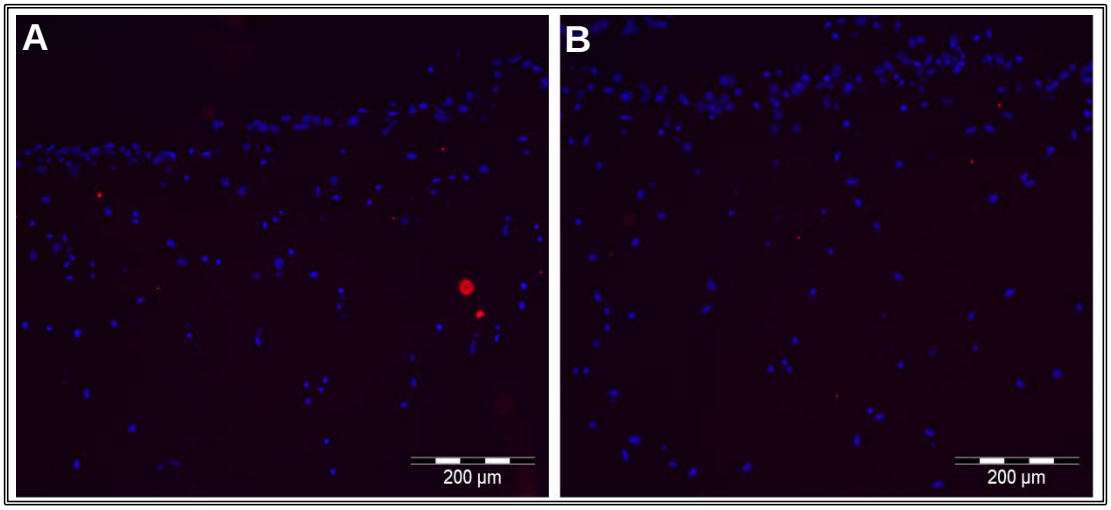

Figure 9.2 *Type I collagen immunofluorescence controls.* IgG (A) and PBST (B) controls showed no labelling. Scale bars: 200 µm.

9.8 MC3T3-E1(14) cells cultured on an empty 3D collagen gel (page 113)

Toluidine blue staining

Rings were drawn around cryosections on poly-lysine coated slides using an ImmEdge pen. Sections were washed in tap water (5 min), stained in toluidine blue solution (5 min), washed in tap water (5 min) and dried before mounting with DPX mounting medium. Slides were left to dry o/n before imaging with a digital camera attached to a light microscope (page 48). 4-6 sections were observed for each replicate.

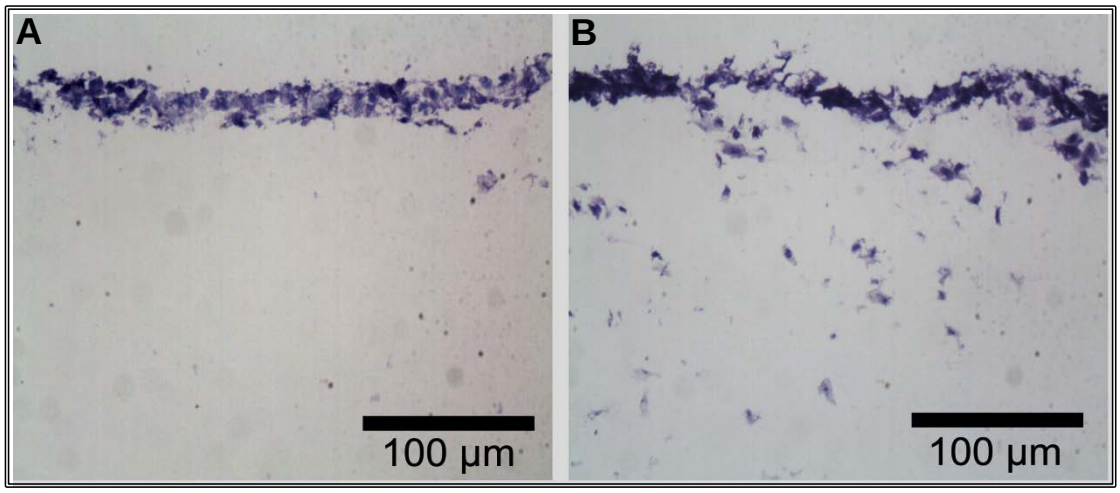

Figure 9.3 *Osteoblasts cultured on empty 3D type I collagen gels.* A) Light microscope image of a day 7 transverse cryosection stained with toluidine blue to reveal MC3T3-E1(14) cell bodies and nuclei. Image shows no invasion of MC3T3-E1(14) cells into the empty 3D collagen gel. B) Light microscope image of a day 7 transverse cryosection stained with toluidine blue to reveal MG63 cell bodies and nuclei. Image shows extensive invasion of MG63 cells into the empty 3D collagen gel as previously shown by (Mason et al., 2009, Mason D., 2009). Images are representative of 2 independent experiments, n=3 per experiment. Scale bars: 100 µm.

9.9 MLO-Y4 total cell number raw data (page 114)

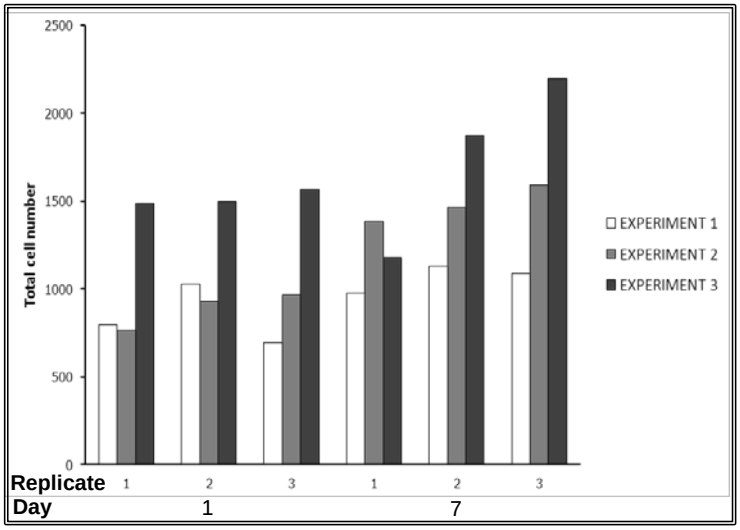

Figure 9.4 Graph shows variation in total cell number counted for each replicate gel at day 1 and day 7 in all 3 independent experiments.

9.10 mGluR5 (NM_001081414.2) RT-PCR (page 119)

Primers (5'-3')	Amplicon size (bp)	PCR conditions			qPCR conditions		Source
		[Primers] & [$MgCl_2$]	Cycle Nº	Tm (ºC)	[Primers] & [$MgCl_2$]	Tm (ºC)	
Fwd - CAATTGATGGACGGAAACT	179	0.2 µM Primers 2.5 mM $MgCl_2$	40	60	NI	NI	Dr Cleo Bonnet
Rev - CCATTGTCCCAACTTCCAAC							

Optimised conditions for brain cDNA (positive control) only; NI: not investigated.

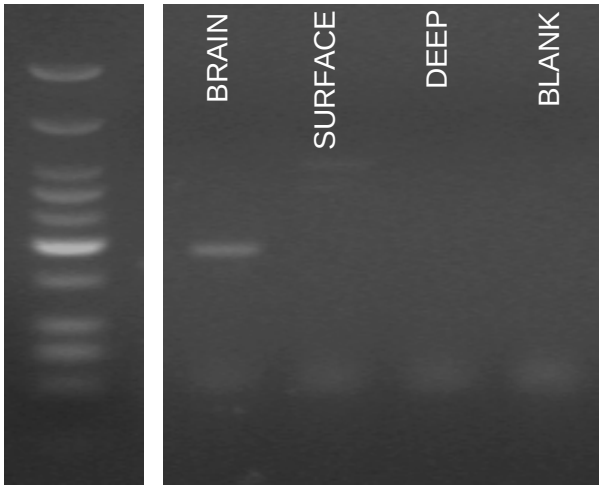

Figure 9.5 *mGluR5 mRNA expression in 3D co-cultures after 7 days.* Gel electrophoresis showing expression of mGluR5 (179 bp) by RT-PCR in mouse brain (positive control), but absence of expression in the surface and deep zones of the model. Negative control (blank) was clean. Gel is representative of 3 independent experiments, n=3 for both surface and deep zones.

9.11 PGE_2 release raw data (Chapter 5)

For all tables in this section: ABS- absorbance; W/O- without; NSB- non-specific binding; STDEV- standard deviation; SEM- standard error or the mean. Outliers are highlighted in yellow.

Pilot experiment (24 hr time pre-load time)

	TIME POST-LOAD (hr)	ABS	W/O BLANK	pg/ml	x64	AVERAGE	STDEV	SEM
CONTROL	0	0.58	0.395	33.47	2142.13	1862.02	396.14	280.11
		0.634	0.449	24.71	1581.90			
	0.5	0.688	0.503	18.26	1169.23	1206.55	52.78	37.32
		0.677	0.492	19.43	1243.88			
	1	0.679	0.494	19.21	1229.98	1258.22	39.93	28.23
		0.671	0.486	20.10	1286.46			
	3	0.572	0.387	35.02	2241.81	2430.22	266.44	188.40
		0.545	0.36	40.91	2618.62			
	6	0.601	0.416	29.73	1902.72	1691.07	299.31	211.64
		0.646	0.461	23.11	1479.43			
	12	0.438	0.253	79.75	5104.16	3564.23	2177.78	1539.92
		0.59	0.405	31.62	2024.30			
	24	0.503	0.318	52.52	3361.34	2788.88	809.57	572.45
		0.574	0.389	34.63	2216.42			
LOADED	0	0.657	0.472	21.73	1391.29	2306.44	1294.21	915.14
		0.51	0.325	50.33	3221.58			
	0.5	0.406	0.221	100.10	6406.70	4632.91	2508.51	1773.78
		0.53	0.345	44.67	2859.12			
	1	0.543	0.358	41.39	2649.29	2458.41	269.94	190.88
		0.57	0.385	35.43	2267.53			
	3	0.726	0.541	14.71	941.57	3558.54	3700.95	2616.96
		0.411	0.226	96.49	6175.51			
	6	0.461	0.276	68.40	4378.18	3799.88	817.83	578.29
		0.51	0.325	50.33	3221.58			
	12	0.531	0.346	44.41	2842.31	4696.73	2622.54	1854.42
		0.403	0.218	102.36	6551.15			
	24	0.406	0.221	100.10	6406.70	4118.05	3236.62	2288.64
		0.608	0.423	28.58	1829.41			

BLANKS	ABS	NSB	ABS	W/O BLANK
1	0.19	1	0.187	0.002
2	0.18	2	0.181	-0.004
AVERAGE	0.185	AVERAGE		-0.001

24 hr time pre-load time experiments

	TIME POST-LOAD (hr)	ABS	W/O BLANK	W/O NSB	pg/ml	x64	NORMALISED TO CELL NUMBER	AVERAGE 0.5 hr CONTROL	W/O AVERAGE 0.5 hr CONTROL	AVERAGE	STDEV	SEM
CONTROL	0.5	0.581	0.353	0.34	10.35	662.51	1417.64	1311.30	106.34	-7.572E-14	320.31	184.93
		0.617	0.389	0.376	6.87	439.83	951.34		-359.95			
		0.571	0.343	0.33	11.47	734.46	1564.91		253.61			
LOADED	0.5	0.601	0.373	0.36	8.31	532.30	1103.59		-207.70	-231.53	110.88	64.01
		0.601	0.373	0.36	8.31	532.30	1176.79		-134.50			
		0.619	0.391	0.378	6.70	428.94	958.89		-352.40			

	TIME POST-LOAD (hr)	ABS	W/O BLANK	W/O NSB	pg/ml	x64	NORMALISED TO CELL NUMBER	AVERAGE 0.5 hr CONTROL	W/O AVERAGE 0.5 hr CONTROL	AVERAGE	STDEV	SEM
CONTROL	0.5	0.538	0.31	0.297	15.78	1010.51	2505.40	3136.84	-631.44	0	1605.71	927.05
		0.557	0.329	0.316	13.18	843.83	1942.83		-1194			
		0.497	0.269	0.256	22.82	1460.56	4962.29		1825.44			
LOADED	0.5	0.574	0.346	0.333	11.13	712.36	2016.13		-1120.71	-261.41	832.67	480.74
		0.532	0.304	0.291	16.68	1068.04	2931.50		-205.33			
		0.501	0.273	0.26	22.03	1410.14	3678.64		541.80			

BLANKS	ABS	NSB	ABS	W/O BLANK
1	0.224	1	0.234	0.006
2	0.232	2	0.248	0.02
AVERAGE	0.228	AVERAGE		0.013

48 hr time pre-load time experiment

	TIME POST-LOAD (hr)	ABS	W/O BLANK	W/O NSB	pg/ml	x16	NORMALISED TO CELL NUMBER	AVERAGE 0.5 hr CONTROL	W/O AVERAGE 0.5 hr CONTROL	AVERAGE	STDEV	SEM
CONTROL	0.5	0.332	0.157	0.139	195.66	3130.65	38970.94	36086.32	2884.61	-1.21E-12	5383.80	3108.34
		0.352	0.177	0.159	157.46	2519.43	29874.88		-6211.44			
		0.364	0.189	0.171	138.76	2220.26	39413.14		3326.82			
LOADED	0.5	0.354	0.179	0.161	154.15	2466.43	49002.38		12916.05	36120.75	23135.11	13357.06
		0.295	0.12	0.102	299.93	4798.98	72346.90		36260.58			
		0.279	0.104	0.086	365.20	5843.31	95271.96		59185.63			

72 hr time pre-load time experiment

	TIME POST-LOAD (hr)	ABS	W/O BLANK	W/O NSB	pg/ml	x16	NORMALISED TO CELL NUMBER	AVERAGE 0.5 hr CONTROL	W/O AVERAGE 0.5 hr CONTROL	AVERAGE	STDEV	SEM
CONTROL	0.5	0.374	0.199	0.181	125.14	2002.34	16502.86	20676.18	-4173.31	0	8073.61	4661.30
		0.384	0.209	0.191	113.05	1808.92	29982.31		9306.13			
		0.458	0.283	0.265	55.69	891.14	15543.36		-5132.82			
LOADED	0.5	0.379	0.204	0.186	118.92	1902.78	37067.39		16391.21	15896.88	4090.89	2361.87
		0.389	0.214	0.196	107.52	1720.38	32257.46		11581.27			
		0.385	0.21	0.192	111.92	1790.80	40394.32		19718.14			

BLANKS	ABS	NSB	ABS	W/O BLANK
1	0.171	1	0.19	0.015
2	0.179	2	0.196	0.021
AVERAGE	0.175	AVERAGE		0.018

7 days time pre-load time experiment

	TIME POST-LOAD (hr)	ABS	W/O BLANK	W/O NSB	pg/ml	x40	NORMALISED TO CELL NUMBER	AVERAGE	STDEV	SEM	AVERAGE W/O OUTLIER	STDEV	SEM
CONTROL	0.5	0.303	0.119	0.107	22.38	895.32	1305.13	3613.08	4188.97	2418.50	1195.40	155.18	109.72
		0.317	0.133	0.121	17.12	685.06	1085.67						
		0.236	0.052	0.040	139.39	5575.96	8448.43						
LOADED	0.5	0.28	0.096	0.084	37.05	1482.04	2322.95	3152.26	753.79	435.20	3152.26	753.79	435.20
		0.26	0.076	0.064	62.72	2509.02	3795.79						
		0.264	0.080	0.068	55.99	2239.82	3338.04						

BLANKS	ABS	NSB	ABS	W/O BLANK
1	0.186	**1**	0.2	0.016
2	0.181	**2**	0.191	0.007
AVERAGE	0.183	**AVERAGE**		0.012

9.12 IL-6 release raw data (Chapter 5)

For all tables in this section: ABS- absorbance; W/O- without; STDEV- standard deviation; SEM- standard error or the mean.

Pilot experiment (24 hr time pre-load time)

	TIME POST-LOAD (hr)	ABS	W/O BLANK	pg/ml	AVERAGE	STDEV	SEM
CONTROL	0	2.455	2.333	531.85	522.33	13.46	9.52
		2.414	2.292	512.81			
	0.5	1.646	1.5245	259.80	356.19	136.31	96.39
		2.272	2.1505	452.58			
	1	2.185	2.0635	419.48	368.46	72.15	51.01
		1.867	1.7455	317.44			
	3	1.13	1.0085	152.92	249.99	137.27	97.06
		1.968	1.8465	347.06			
	6	2.277	2.1555	454.56	368	122.42	86.56
		1.733	1.6115	281.43			
	12	1.764	1.6425	289.45	260.02	41.62	29.43
		1.52	1.3985	230.59			
	24	1.834	1.7125	308.25	338.95	43.42	30.70
		2.04	1.9185	369.66			
LOADED	0	1.389	1.2675	202.57	173.50	41.10	29.06
		1.082	0.9605	144.44			
	0.5	1.701	1.5795	273.32	235.49	53.49	37.82
		1.365	1.2435	197.66			
	1	1.075	0.9535	143.21	133.46	13.79	9.75
		0.96	0.8385	123.71			
	3	1.101	0.9795	147.77	114.76	46.68	33.01
		0.692	0.5705	81.75			
	6	1.012	0.8905	132.40	130.89	2.14	1.51
		0.994	0.8725	129.37			
	12	1.067	0.9455	141.82	138.22	5.10	3.60
		1.025	0.9035	134.61			
	24	1.257	1.1355	176.40	145.57	43.60	30.83
		0.905	0.7835	114.73			

BLANKS	ABS
1	0.116
2	0.127
AVERAGE	0.121

24 hr time pre-load time experiments

	TIME POST-LOAD (hr)	ABS	W/O BLANK	pg/ml	NORMALISED TO CELL NUMBER	AVERAGE 0 hr CONTROL	W/O AVERAGE 0 hr CONTROL	AVERAGE	STDEV	SEM
CONTROL	0	1.977	1.855	349.82	185.94	188.05	-2.11	0	3.68	2.12
		1.984	1.862	351.97	185.90		-2.14			
		2.07	1.948	379.47	192.30		4.25			
	0.5	2.533	2.411	570.43	305.154		117.10	107.32	9.53	5.50
		2.483	2.361	545.33	294.88		106.83			
		2.466	2.344	537.10	286.10		98.05			
	6	2.571	2.449	590.45	287.55		99.50	173.08	80.31	46.36
		2.695	2.573	662.21	349.02		160.97			
		2.871	2.749	785.18	446.80		258.75			
	24	2.737	2.615	689.05	385.09		197.04	279.45	79.99	46.18
		3.146	3.024	1053.37	544.85		356.80			
		2.821	2.699	747.28	472.56		284.51			
LOADED	0.5	2.426	2.304	518.30	268.64		80.59	101.12	17.79	10.27
		2.478	2.356	542.89	300.05		112.01			
		2.461	2.339	534.71	298.83		110.78			
	6	2.668	2.546	645.67	349.13		161.08	212.68	53.68	30.99
		2.838	2.716	759.88	456.29		268.24			
		2.735	2.613	687.74	396.77		208.72			
	24	3.286	3.164	1248.10	740.56		552.51	424.45	181.87	105.01
		3.268	3.146	1219.94	692.62		504.57			
		2.965	2.843	864.19	404.33		216.28			

BLANKS	ABS
1	0.116
2	0.127
AVERAGE	0.121

	TIME POST-LOAD (hr)	ABS	W/O BLANK	pg/ml	NORMALISED TO CELL NUMBER	AVERAGE 0 hr CONTROL	W/O AVERAGE 0 hr CONTROL	AVERAGE	STDEV	SEM
CONTROL	0	2.066	1.944	378.15	199.23	218.38	-19.14	1.89E-14	22.37	12.91
		2.01	1.888	360.08	242.97		24.58			
		1.982	1.860	351.35	212.94		-5.44			
	0.5	2.331	2.209	476.60	294.56		76.17	161.01	193.20	111.54
		2.196	2.074	423.52	243.12		24.74			
		2.768	2.646	709.80	600.51		382.12			
	6	2.707	2.585	669.73	404.92		186.53	255.13	95.74	55.28
		2.821	2.699	747.28	582.90		364.52			
		2.714	2.592	674.18	432.72		214.33			
	24	2.996	2.874	892.77	495.43		277.05	247.56	140.18	80.93
		3.252	3.130	1195.77	589.04		370.66			
		2.913	2.791	819.15	313.37		94.98			
LOADED	0.5	2.018	1.896	362.61	255.72		37.33	113.80	73.37	42.36
		2.566	2.444	587.76	402.03		183.64			
		2.432	2.310	521.07	338.80		120.41			
	6	2.839	2.717	760.63	474.80		256.41	292.34	58.04	33.50
		2.984	2.862	881.54	577.68		359.30			
		2.879	2.757	791.50	479.69		261.31			
	24	2.841	2.719	762.13	390.03		171.65	174.68	18.79	10.85
		2.74	2.618	691.02	375.96		157.58			
		2.741	2.619	691.68	413.19		194.80			

BLANKS	ABS
1	0.116
2	0.127
AVERAGE	0.121

48 hr time pre-load time experiment

	TIME POST-LOAD (hr)	ABS	W/O BLANK	pg/ml	x10	NORMALISED TO CELL NUMBER	AVERAGE 0 hr CONTROL	W/O AVERAGE 0 hr CONTROL	AVERAGE	STDEV	SEM
CONTROL	0	0.44	0.322	60.42	604.22	10725.92	7980.21	2745.71	0	3111.01	1796.14
		0.4	0.282	53.69	536.90	8613.41		633.20			
		0.27	0.152	30.52	305.21	4601.30		-3378.91			
	0.5	0.712	0.594	104.89	1048.91	13057.09		5076.88	3989.93	3732.66	2155.05
		0.473	0.355	65.90	659.03	7814.65		-165.55			
		0.588	0.470	84.71	847.17	15038.69		7058.47			
	6	0.651	0.533	94.95	949.56	21913.11		13932.89	7935.85	5387.06	3110.22
		0.67	0.552	98.04	980.46	14348.32		6368.11			
		0.691	0.573	101.46	1014.66	11486.77		3506.55			
	24	0.747	0.629	110.61	1106.17	14304.08		6323.87	12351.79	6916.40	3993.18
		1.252	1.134	198.89	1988.97	27883.01		19902.79			
		0.707	0.589	104.07	1040.75	18808.92		10828.70			
LOADED	0.5	0.58	0.462	83.41	834.16	16572.91		8592.69	6524.94	2595.09	1498.27
		0.54	0.422	76.90	769	11593.03		3612.81			
		0.646	0.528	94.14	941.43	15349.53		7369.31			
	6	0.59	0.472	85.04	850.42	13219.13		5238.91	7036.80	1557.03	898.952
		0.648	0.530	94.46	944.68	15921.72		7941.51			
		0.628	0.510	91.21	912.18	15910.21		7929.99			
	24	0.673	0.555	98.53	985.34	16607.06		8626.84	6506.74	3229.09	1864.31
		0.644	0.526	93.81	938.18	16083.20		8102.99			
		0.566	0.448	81.13	811.38	10770.60		2790.38			

BLANKS	ABS
1	0.117
2	0.118
AVERAGE	0.1175

72 hr time pre-load time experiment

	TIME POST-LOAD (hr)	ABS	W/O BLANK	pg/ml	x10	NORMALISED TO CELL NUMBER	AVERAGE 0 hr CONTROL	W/O AVERAGE 0 hr CONTROL	AVERAGE	STDEV	SEM
CONTROL	0	0.358	0.240	46.47	464.73	7223.96	7902.09	-678.13	-6.06E-13	889.58	513.60
		0.364	0.246	47.51	475.16	8909.34		1007.25			
		0.332	0.214	41.90	419.03	7572.97		-329.12			
	0.5	0.604	0.486	87.31	873.18	7196.57		-705.52	2080.43	2429.49	1402.66
		0.5	0.382	70.35	703.51	11660.58		3758.48			
		0.459	0.341	63.58	635.84	11090.43		3188.33			
	6	0.583	0.465	83.90	839.04	13906.87		6004.78	8898.65	6668.14	3849.85
		0.938	0.820	142.48	1424.89	24426.94		16524.84			
		0.515	0.397	72.81	728.12	12068.41		4166.32			
	24	0.47	0.352	65.40	654.07	8799.22		897.12	7192.60	5867.99	3387.88
		0.693	0.575	101.79	1017.92	16072.52		8170.42			
		0.786	0.668	117.03	1170.30	20412.36		12510.26			
LOADED	0.5	0.43	0.312	58.74	587.49	11444.79		3542.70	5532.48	1932.90	1115.96
		0.569	0.451	81.62	816.26	15305.08		7402.98			
		0.438	0.320	60.08	600.88	13553.85		5651.75			
	6	0.498	0.380	70.02	700.23	9173.38		1271.28	1425.86	452.01	260.97
		0.674	0.556	98.69	986.97	9836.98		1934.88			
		0.549	0.431	78.36	783.68	8973.50		1071.41			
	24	1.095	0.977	169.90	1699.07	15261.16		7359.06	3672.36	4470.89	2581.27
		0.866	0.748	130.32	1303.22	12860.82		4958.72			
		0.483	0.365	67.55	675.54	6601.40		-1300.68			

BLANKS	ABS
1	0.117
2	0.118
AVERAGE	0.1175

9.13 Cell death raw data (Chapter 5)

For all tables in this section: ABS- absorbance; W/O- without.

Pilot experiment (24 hr time pre-load time)

	TIME POST-LOAD (hr)	ABS	W/O BLANK
CONTROL	0	0.19	-0.020
		0.184	-0.026
	0.5	0.203	-0.007
		0.196	-0.014
	1	0.182	-0.028
		0.186	-0.024
	3	0.201	-0.009
		0.194	-0.016
	6	0.187	-0.023
		0.181	-0.029
	12	0.203	-0.007
		0.198	-0.012
	24	0.19	-0.020
		0.193	-0.017
LOADED	0	0.193	-0.017
		0.196	-0.014
	0.5	0.192	-0.018
		0.197	-0.013
	1	0.193	-0.017
		0.2	-0.010
	3	0.194	-0.016
		0.202	-0.008
	6	0.196	-0.014
		0.195	-0.015
	12	0.199	-0.011
		0.199	-0.011
	24	0.193	-0.017
		0.199	-0.011

BLANKS	ABS
1	0.207
2	0.209
3	0.216
AVERAGE	0.210

24 hr time pre-load time experiments

	TIME POST-LOAD (hr)	ABS	W/O BLANK
CONTROL	0	0.201	-0.009
		0.215	0.004
		0.213	0.002
	0.5	0.222	0.011
		0.21	-0.001
		0.205	-0.005
	6	0.198	-0.012
		0.206	-0.004
		0.208	-0.002
	24	0.222	0.011
		0.192	-0.018
		0.194	-0.016
LOADED	0.5	0.209	-0.001
		0.214	0.003
		0.198	-0.012
	6	0.21	-0.001
		0.213	0.002
		0.211	0.001
	24	0.208	-0.002
		0.208	-0.002
		0.206	-0.004

BLANKS	ABS
1	0.207
2	0.209
3	0.216
AVERAGE	0.210

	TIME POST-LOAD (hr)	ABS	W/O BLANK
CONTROL	0	0.2	-0.010
		0.202	-0.008
		0.202	-0.008
	0.5	0.205	-0.005
		0.211	0.001
		0.209	-0.001
	6	0.191	-0.019
		0.196	-0.014
		0.205	-0.005
	24	0.212	0.001
		0.201	-0.009
		0.204	-0.006
LOADED	0.5	0.208	-0.002
		0.214	0.003
		0.192	-0.018
	6	0.202	-0.008
		0.201	-0.009
		0.204	-0.006
	24	0.212	0.001
		0.215	0.004
		0.224	0.013

BLANKS	ABS
1	0.207
2	0.209
3	0.216
AVERAGE	0.210

48 hr time pre-load time experiment

	TIME POST-LOAD (hr)	ABS	W/O BLANK
CONTROL	0	0.196	-0.036
		0.194	-0.038
		0.197	-0.035
	0.5	0.198	-0.034
		0.200	-0.032
		0.194	-0.038
	6	0.187	-0.045
		0.192	-0.04
		0.198	-0.034
	24	0.199	-0.033
		0.193	-0.039
		0.192	-0.04
LOADED	0.5	0.201	-0.031
		0.205	-0.027
		0.191	-0.041
	6	0.200	-0.032
		0.198	-0.034
		0.192	-0.04
	24	0.198	-0.034
		0.195	-0.037
		0.210	-0.022

BLANKS	ABS
1	0.230
2	0.232
3	0.234
AVERAGE	0.232

72 hr time pre-load time experiment

	TIME POST-LOAD (hr)	ABS	W/O BLANK
CONTROL	0	0.195	-0.037
		0.192	-0.04
		0.204	-0.028
	0.5	0.199	-0.033
		0.194	-0.038
		0.195	-0.037
	6	0.189	-0.043
		0.190	-0.042
		0.200	-0.032
	24	0.198	-0.034
		0.186	-0.046
		0.192	-0.04
LOADED	0.5	0.206	-0.026
		0.197	-0.035
		0.192	-0.04
	6	0.199	-0.033
		0.197	-0.035
		0.201	-0.031
	24	0.192	-0.04
		0.199	-0.033
		0.203	-0.029

BLANKS	ABS
1	0.230
2	0.232
3	0.234
AVERAGE	0.232

7 days time pre-load time experiment

	TIME POST-LOAD (hr)	ABS	W/O BLANK
CONTROL	0	0.237	-0.001
		0.227	-0.010
		0.251	0.013
	0.5	0.21	-0.027
		0.214	-0.023
		0.203	-0.034
LOADED	0.5	0.226	-0.011
		0.223	-0.014
		0.209	-0.028

BLANKS	ABS
1	0.231
2	0.229
3	0.253
AVERAGE	0.237

9.14 Cell death and PGE_2 raw data (Chapter 6)

For all tables in this section: ABS- absorbance; W/O- without.

Cell death

TIME POST-LOAD		TREATMENT	ABS	W/O BLANK
DAY 1	CONTROL	NBQX	0.217	-0.019333
			0.24	0.003667
			0.232	-0.004333
	LOADED		0.334	0.097667
			0.269	0.032667
			0.25	0.013667
	CONTROL	SCH 442416	0.241	0.004667
			0.254	0.017667
			0.227	-0.009333
	LOADED		0.27	0.033667
			0.33	0.093667
			0.298	0.061667
	CONTROL	UNTREATED	0.233	-0.003333
			0.23	-0.006333
	LOADED		0.225	-0.011333
			0.332	0.095667
DAY 5	CONTROL	NBQX	0.246	0.009667
			0.222	-0.014333
	LOADED		0.223	-0.013333
			0.235	-0.001333
	CONTROL	SCH 442416	0.241	0.004667
			0.232	-0.004333
			0.229	-0.007333
	LOADED		0.276	0.039667
			0.229	-0.007333
			0.222	-0.014333
	CONTROL	UNTREATED	0.244	0.007667
			0.242	0.005667
	LOADED		0.231	-0.005333
			0.259	0.022667

BLANKS	ABS
1	0.231
2	0.237
3	0.241
AVERAGE	0.236333

PGE_2 (0.5 hr post-load)

	ABS	W/O BLANK	pg/ml	NORMALISED TO ng DNA	AVERAGE	STDEV	SEM
CONTROL	0.3	0.107	38.60	0.040	0.030	0.008	0.004
	0.331	0.138	17.12	0.025			
	0.331	0.138	17.12	0.027			
LOADED	0.325	0.132	20.14	0.033	0.023	0.011	0.006
	0.334	0.141	15.75	0.023			
	0.318	0.125	24.25	0.011			

BLANKS	ABS	NSB	ABS	W/O BLANK
1	0.194	1	0.195	0.002
2	0.192	2	0.188	-0.005
AVERAGE	0.193	AVERAGE		-0.0015

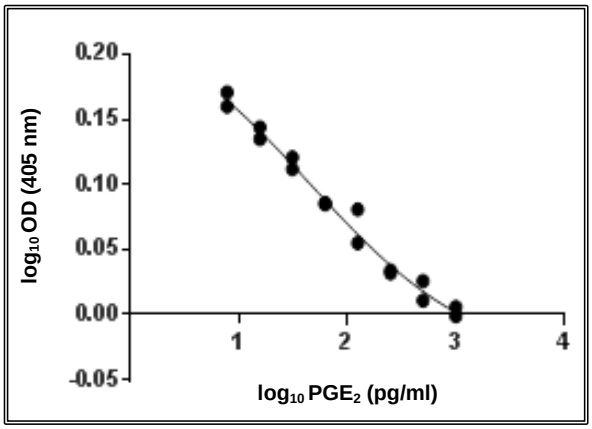

PRESENTATIONS,

PUBLICATIONS,

AND

PRIZES

ORAL PRESENTATIONS (speaker)

September, 2012 - 2nd South West Regional Regenerative Medicine Meeting, Bristol, UK. Talk title: '*In vitro* 3D osteoblast-osteocyte co-culture model'.

June, 2012 - eCM Bone Fixation, Repair and Regeneration, Davos, Switzerland. Talk title: '*In vitro* 3D osteoblast-osteocyte co-culture model'.

September, 2011 - 1st South West Regional Regenerative Medicine Meeting, Bristol University, UK. Talk title: 'Bone *in vitro* 3D osteocyte-osteoblast co-culture model'.

July, 2011 - Arthritis Research UK Biomechanics and Bioengineering Centre Symposium, Cardiff University, UK. Talk title: 'Growing bone in the lab: 3D modelling for therapeutic testing'.

June, 2011 - Bone Research Society and British Orthopaedic Research Society 3rd Joint Meeting, Cambridge University, UK. Talk title: 'Bone *in vitro* 3D osteocyte-osteoblast co-culture model'.

May, 2011 - Speaking of Science Conference, Cardiff University. Talk title: 'Growing bone in the lab: 3D modelling for therapeutic testing'.

February, 2011 - Connective Tissue Biology Laboratories Seminar Series, Cardiff University, UK. Talk title: 'Investigating the roles of adenosine, glutamate and calcium signalling in mechanically-induced bone formation'.

December, 2010 - Connective Tissue Biology Laboratories Seminar Series, Cardiff University, UK. Talk title: 'Bone 3D co-culture of the future: to boldly go where no scientist has gone before'.

POSTER PRESENTATIONS (presenting author)

November, 2012 – Arthritis Research UK Meeting of the Centres, Loughborough University, UK. Poster title: '*In vitro* 3D osteoblast-osteocyte co-culture mechanical loading model'.

July, 2012 – Osteoporosis and Bone Conference 2012, Manchester, UK. Poster title: '*In vitro* 3D osteoblast-osteocyte co-culture mechanical loading model'.

January, 2012 – Arthritis Research UK Biomechanics and Bioengineering Centre Advisory Board Meeting, Cardiff University, UK. Poster title: 'Bone *in vitro* 3D osteoblast-osteocyte co-culture model'.

November, 2011 - UK Purine Club Meeting, Cardiff, UK. Poster title: 'Bone *in vitro* 3D osteoblast-osteocyte co-culture model'.

May, 2011 - School of Bioscience Year 2 PhD Poster Evening, Cardiff University, UK. Poster title: 'Bone *in vitro* 3D osteoblast-osteocyte co-culture model'.

April, 2011 – British Society for Matrix Biology Spring Meeting 'Advances in Musculoskeletal Repair and Regeneration', Bristol University, UK. Poster title: 'Bone *in vitro* 3D osteoblast-osteocyte co-culture model'.

September, 2010 - Cardiff Institute of Tissue Engineering and Repair and Arthritis Research UK Biomechanics and Bioengineering Centre Joint Annual Scientific Meeting, Gloucestershire, UK. Poster title: 'Investigating the roles of adenosine, glutamate and calcium signalling in mechanically-induced bone formation'.

July, 2010 - Arthritis Research UK Biomechanics and Bioengineering Centre Symposium and Advisory Board Meeting, Cardiff University, UK. Poster title: 'Investigating the roles of adenosine, glutamate and calcium signalling in mechanically-induced bone formation'.

January, 2010 – School of Bioscience Year 1 PhD Poster Evening, Cardiff University, UK. Poster title: 'Investigating the roles of adenosine, glutamate and calcium signalling in mechanically-induced bone formation'.

POSTER PRESENTATIONS (non-presenting author)

May, 2013 - European Calcified Tissue Society 50th Anniversary, Lisbon, Portugal. Poster title: '*In vitro* 3D osteoblast-osteocyte co-culture mechanical loading model'.

PUBLISHED ABSTRACTS

Vazquez, M., Evans, B.A.J., Ralphs, J.R., Riccardi, D., Mason, D.J. 2012. eCM XIII - Bone Fixation, Repair & Regeneration: *In vitro* 3D osteoblast-osteocyte co-culture model. *European Cells and Materials*, 24, supplement 1, 7.

Vazquez, M., Evans, B.A.J., Ralphs, J.R., Riccardi, D., Mason, D.J. 2011. UK Purine Club 2011 Symposium. Bone *in vitro* 3D osteoblast-osteocyte co-culture model. *Purinergic Signalling*. 8, issue 4, 781-800.

Vazquez, M., Evans, B., Ralphs, J., Riccardi, D., Mason, D. 2011. Bone *in vitro* 3D osteoblast-osteocyte co-culture model. *Frontiers in Endocrinology*. Conference Abstract: 2011 joint meeting of the Bone Research Society & the British Orthopaedic Research Society.

Vazquez, M., Evans, B.A.J., Ralphs, J.R., Riccardi, D., Mason, D.J. 2011. British Society for Matrix Biology – Spring 2011 Meeting Report: Bone in vitro 3D osteoblast-osteocyte co-culture model. *International Journal of Experimental Pathology*, 92, A21.

PRIZES

September, 2011 - Best Presentation Prize at 1st South West Regional Regenerative Medicine Meeting, Bristol University, UK. Talk title: 'Bone *in vitro* 3D osteocyte-osteoblast co-culture model'.

June, 2011 - Best Oral Communication Prize (Basic Science) at Bone Research Society and British Orthopaedic Research Society 3rd Joint Meeting, Cambridge University, UK. Talk title: 'Bone *in vitro* 3D osteocyte-osteoblast co-culture model'.

May, 2011 - 1st Prize for a talk at Speaking of Science Conference, Cardiff University. Talk title: 'Growing bone in the lab: 3D modelling for therapeutic testing'.

May, 2011 - Joint 1st Prize School of Bioscience Year 2 PhD Poster Evening, Cardiff University, UK. Poster title: 'Bone *in vitro* 3D osteoblast-osteocyte co-culture model'.

SCHOLARSHIPS

June, 2012 - Gillian Powell Memorial Travel Scholarship, Cardiff University, UK.